Fabrication of Anisotropic Polymer Colloid Particles

By

Attyah Alzhrani

A thesis submitted in fulfilment of the requirements for the degree of Doctor of Philosophy in Chemistry

University of Warwick, Department of Chemistry

September 2011

Table of contents

Acknowledgement

Declaration

Abstract

Abbreviations

Table of Contents

Acknowledgment

"In Arabic expression says that, if you don't show gratitude to people, you will not show appreciation to God".

First of all, it was amazing time here at Warwick to do a PhD and particularly with supervision of Prof. Stefan Bon. Many thanks to my supervisor for his assistance during my research. His support, guidance and ideas are valuable. I still remember his statement when I do some progress that (you are getting there) which makes me persevere to do research. I would like also to thank all members of the Bon group the precedent and the current members.

A lot of staff at Warwick University assisted me; particularly I want to thank Mr. Portman Ian for his help for taking together the Cryo-TEM images.

Many thanks to my father, mother, Kids and wife for their magnificent support which makes me focus more in my study. And I would like to thank my sponsor (SABIC) for financial support during my study.

Declaration

I hereby declare that this thesis consists of my own work, and that it has not previously been submitted for any previous degree at any institution.

Other sources of information have been used; they have been acknowledged and referenced.

Signature: Date:

Abstract

The fabrication of complex colloidal particles with anisotropic "patchy" e.g. Janus-like, morphology will be studied. Known approaches towards "Janus particles" focus mostly on the micron-sized domain, with common fabrication routes based on monolayer modification or microfluidic production (restricts scale-up). We operate in the submicron regime (typically 100-500 nm) and use scalable emulsion polymerization strategies, in combination with entropic phase separation of swollen cross-linked latex particles and living radical polymerization, i.e. SET-LRP, to prepare our "patchy" amphiphilic particles.

In this research, various Cross-linked densities (typically from 1 - 8wt%) poly(styrene) latexes (typically 100-500 nm) functionalized with *tert*-bromine functional groups, by batch or shot addition of (2-methacryloxyethyl -2́-bromoisobutyrate) made via soap-free emulsion polymerization used as the precursor particles.

Two synthetic pathways were investigated to make the targeted hairy Janus Particles. Approach one: in which we carried out the domain formation step prior to the fabrication of the polymer brushes, We found out that the effective synthetic way to make Janus hairy dumbbell particles in a reproducible manner is to start the synthesis with light cross-linked density of (1.9 to 3.0 wt% DVB) precursor poly(styrene) latex particles (150-250 nm diameter) made by shot addition method. The direct entropic phase separation from these latex particles leads to the formation of only one new domain with dumbbell shape morphology, when the swelling ratio used between monomer and latex is between 2.0 and 4.0, and with low DVB

concentration in the swelling monomer (between 0.15-1.0wt%) using AIBN as initiator.

Formation of hydrophilic polymer brushes by SET-LRP resulted in targeted hairy Janus particles with sub-micrometer diameter, in a reproducible manner. The length of the polymer brushes can be controlled by addition of water soluble ATRP initiator to produce shorter polymer brushes. The rate of SET-LRP was ultrafast and the rate can be reduced by addition of deactivator $CuBr_2$.

The second approach: water-soluble polymer brushes were grafted onto the surface of latex particles by SET-LRP. These "hairy" cross-linked colloids were swollen with additional monomers and initiator. Elevation of temperature causes entropic phase separation inducing new domains, which were polymerized. This approach leads to mainly popcorn and raspberry particles with some limited cases that are able to make hairy Janus Particles with non reproducible manner.

The obtained complex particles show some interesting application such as a stabilization agent for Carbon Nanotubes (CNTs) in aqueous medium, Pickering emulsion stabilizer, and they self assembled upon addition of dilute electrolyte solution.

Abbreviations

ATRP	Atom Transfer Radical Polymerization
AuNPs	Gold nanoparticles
AGET	Activator Generated by electron transfer
AIBN	Azobisisobutyronitrile
AA	Acrylic Acid
BPEM	2-(2-bromopropionyloxy) ethyl methacrylate
BIEM	2-(2-bromoisobutyryloxy)ethyl methacrylate
BPOEA	2-(2-bromopropionyloxy) ethyl acrylate)
BMA	Butyl methacrylate
Brij-35	Polyoxyethylene Lauryl ether
(bpy)	2,2'-bipyreidine
CTAB	hexadecyl cetyl trimethyl ammonium bromide
Cryo-TEM	Cryogenic-transmission electron microscope
CMS	Chloro methyl styrene
CNTs	Carbon nano-tubes
(L_c)	Contour length
DVB	Divinylbenzene
D_2O	Deuterium monoxide
DLS	Dynamic light scattering
DMAEMA	2-(Dimethyl amino) ethyl methacrylate
DMF	Dimethylformamide
DM	2-(dimethylamino) ethyl methacrylate
Exp	Experiment
EGDMA	Ethylene glycol dimethacrylate
Full-IPN	Full interpenetrating polymer network

FTIR	Fourier Transform Infrared Spectroscopy
FITC	Fluorescein isothiocyanate
HMTETA	1,1,4,7,10,10-hexamethyltriethylenetetramine
HEA	2-Hydroxyethylacrylate
HEMA	hydroxy ethyl methacrylate
HLB	Hydrophilic-Lipophilic balance
ID	Inner diameter
inimer	Initiator for ATRP and monomer for Free radical polymerization
KPS	Potassium persulfate.
K_{dis}	Rate constant of disproportionate
K_p	Rate constant of propagation
k_B	Boltzmann constant
LCST	Lower Critical Solution Temperature
MMA	Methyl methacrylate
[*Mp*]	Monomer concentration in the growing particles
MMA	methyl methacrylate
Me_6TREN	tris [2-(dimethyl amino) ethyl] amine
Me_4cyclam	1,4,8,11-Tetramethyl-1,4,8,11-tetraazacyclotetradecane
MAETACL	2-(methacryloyl-oxy)ethyl trimethyl ammonium chloride
(M/P)	Monomer to polymer ratio
MWCNTS	Multi-walled carbon nanotubes
NaSS	Sodium Styrene Sulfonate
NIPAM	*N*-isopropylacrylamide
NMR	Nuclear Magnetic Resonance.
NMP	Nitroxide Mediated Polymerization
NA	Avogadro's number

NaMA	Sodium methacrylate
Np	Particle number density
(n)	Average number of radicals per particles
OEGMA	Oligo (ethylene glycol) methacrylate
OD	Outer diameter
o/w	Oil in water emulsion
PMMA	poly(methyl methacrylate)
PMDETA	*N, N, N', N'', N''*- Pentamethyl diethylene triamine
PEO	Poly(ethylene oxide)
PDMS	Poly(dimethyl siloxane)
PS	Poly(styrene)
PNA	Poly(*N*-*i*sopropyl acrylamide-*co*-acrylic acid)
PDM	Poly[2-(dimethylamino) ethyl methacrylate]
PAN	Poly(acrylonitrile)
PGMA	Poly(glycidyl methacrylate)
PBA	Poly(butyl acrylate)
PMA	Poly(methyl acrylate)
(PEA)	Poly(ethyl acrylate)
P(S-B)	Poly(styrene-butyl acrylate)
PVA	Poly(vinyl alcohol)
PEM	Poly(electrolyte) multi-layer
PVBC	Poly(4-vinylbenzyl chloride)
PHEMA	Poly(hydroxy ethyl methacrylate)
PVP	Poly(vinyl pyrrolidone)
RAFT	Reversible Addition Fragmentation chain Transfer
Rp	Whole rate of emulsion polymerization

SET-LRP	Single Electron Transfer -Living Radical Polymerization
surfmer	Surfactant and monomer
SDS	Sodium dodecyl sulfate
SEM	Scanning Electron Microscopy
S1	2-methacryloxyethyl -2- bromoisobutyrate
SIP	surface initiated polymerization
SEC	Size exclusion chromatography
SWCNTS	Single-walled carbon nanotubes
SDBS	sodium dodecyl benzene sulfonate
THF	Tetrahydrofuran
TMSPA	Trimethoxysilylpropyl acrylate
(t.s) %	total solid %
TMED	Tetremethyl ethylenediamine
Tg °	Glass transition temperature
V-65B	2,2'-Azobis (2,4- dimethyl valeronitrile)

Chapter 1: JANUS PARTICLES

1.1 Introduction

The term Janus is derived from the name of the Roman God who had two faces. In chemistry, particles that have surfaces in two phases are called Janus particles. De Gennes was one of the first scientists to use the term Janus in his Nobel lecture in 1991 to describe particles that exhibit asymmetric chemical/physical properties [1]. In recent years, attention has shifted to Janus-type materials, attributed to their potential use as building blocks for supracolloidal structures [2], chemical sensors [3], surfactants for emulsion polymerization [4], nano-probes [5] and many other applications (see the applications section of this chapter and also chapter 7 of this thesis). Several reviews have been already published on the synthesis and applications of Janus and patchy particles. For instance, Perro and co-workers reviewed the design and synthesis of Janus micro- and nanoparticles [6]. Kilbinger *et al*, reviewed polymeric Janus particles with a particular focus on the formation of Janus particles by block copolymer self-assembly [7]. Granick and co-workers summarized the recent developments in the synthesis and self-assembly of Janus particles [8]. Kretzschmar and Pawar reviewed the fabrication, assembly and application of patchy particles [9]. Müller and Walther have also reviewed recent progress in the field of Janus particles [10]. Wang and co-workers reviewed the current utilization of self-assembly of anisotropic colloidal particles in different applied areas with their applications that mimic those of ordinary amphiphilic molecules [11]. Moreover, anisotropic Janus particles are classified as smart materials which can respond to external stimuli or their environment; their synthesis and

applications have been reviewed by Yoshida and Lahann [12]. Here, this introductory chapter reviews the current methods that are used to fabricate Janus particles, with a particular focus on those made from latex particles and polymers in general. Some examples of the other types of non-polymeric Janus particles will be described based on the limitations to their methods of synthesis, for example inorganic colloidal particles. Some examples will cover the applications and properties of synthesized Janus particles described in the literature. At the end of this chapter a short summary about our method that will be used to fabricate latex particles with Janus morphology is described.

1.2 Methods used to fabricate Janus particles.

The potential methods that are used to construct Janus particles are categorized. In total, there are ten main methods without taking into consideration the amount of produced Janus particles, which means that some of these methods could be used on a commercial scale. The potential methods are as follow:

1.2.1 Surface modification of a hemisphere of the precursor particle which has at least half of its structure embedded in a flat surface.

1.2.2 Surface modification of a hemisphere of the precursor particle which has at least half of its structure embedded in a curved surface (Pickering system).

1.2.3 Glancing angle deposition

1.2.4 Microfluidics

1.2.5 Microcontact printing

1.2.6 Controlled phase separation

1.2.7 Controlled surface nucleation

1.2.8 Template-assisted self-assembly

1.2.9 Electrified jetting

1.2.10 Particle lithography

Each method will be described and discussed by presenting some current examples.

1.2.1 Surface modification of a hemisphere of the precursor particle which has at least half of its structure embedded in a flat surface

This method is based on the fabrication of Janus particles through the surface modification of particles deposited in a packed monolayer on a flat solid substrate whereby one side of the particle is masked (embedded) and protected by the flat surface template and the other hemisphere is exposed to modification. After completion of the modification, the Janus particles are isolated by removing the flat surface template. One of the main drawbacks of this method is the extremely limited amount of particles that can be produced and the multiple steps that are required in order to isolate the Janus particles from the template. An example of this method is the work performed by Kuo *et al*, who fabricated Janus silica particles (500 nm) from the surface of electro-spun polymer fibers. The electro-spinning of hydrophobic poly(methyl methacrylate) and hydrophilic poly(4-vinyl pyridine) blends produced polymer fibers with a high specific surface area and the desired surface hydrophilicities. The colloidal adsorption and embedding was carried out by using 20 ml of silica colloids with 10 mg of polymer fiber for 4 hours of isothermal treatment at various temperatures (105, 120, 135, and 150ºC) in order to determine the effect upon the polymer fibers before and after their glass transition temperature. Embedded particles underwent surface modification using a silane-based modification. Silica Janus particles were recovered by dissolving the polymer fiber in an appropriate solvent [13-14].

Li and co-workers synthesized gold Janus particles via deposition and immobilization of precursor ammonium ligand-protected gold nanoparticles (6 nm)

on a solid substrate of a single crystal of thiol-terminated poly(ethylene oxide) which could modify the contacting part of the particles to form poly(ethylene oxide) brushes by solid state grafting. The exposed surface of the particles was treated by replacing the ammonium ligand by a thiol-terminated ATRP initiator which served to grow poly(methyl methacrylate) at room temperature using pentyl acetate as the solvent, and with a catalyst system containing CuBr/Me_6TREN. After dissolving the solid substrate the Janus gold nanoparticles were isolated [15].

The gel trapping technique was used to partially mask (2.7 μm) poly(styrene) particles; the exposed surface of the particles was modified by gold sputtering onto the monolayer of trapped particles to form anisotropic particles [16]. Kretzschmar and co-worker synthesized anisotropic poly(styrene) particles (2.4 μm) by selective electroless deposition of silver nanoparticles on one hemisphere of the sulfate poly(styrene) particles. The procedure for deposition consisted of five steps: first, the sulfate poly(styrene) particles are assembled as a monolayer on a silicon wafer substrate via continuous convective assembly, then these particles are pressed onto a pre-cured poly(dimethyl siloxane) mask. This mask is exposed to the silver electrolyte solution. Due to the electrostatic attraction between the negatively charged poly(styrene) particles and the positively charged silver particles (which become positive after the addition of ammonia and formaldehyde), the exposed negatively charged hemisphere is coated with silver particles [17].

Huskens and co-workers made Janus particles by the deposition of silica particles (5 μm) to form a monolayer by spin coating them onto a flat silicon substrate, and then PMMA was spin coated onto this silica particle monolayer. Next, oxygen plasma etching was applied to the sample which led to partial removal of the PMMA layer to generate an exposed area of the silica particles for further chemical modification.

The remaining PMMA layer was further removed by acetone to collect the Janus particles [18]. Amine-modified silica nanoparticles of sub-micrometer size were covalently attached to a styrene-acrylic acid random copolymer film substrate; in the presence of the solvent, the polymer film substrate swelled, which led to the silica particles being embedded in the film. Subsequently, the exposed unimpeded region of the silica particle was coated with gold nanoparticles (15 nm) via electrostatic attraction [19]. In Figure 1 are shown images of Janus Particles that are prepared by this method.

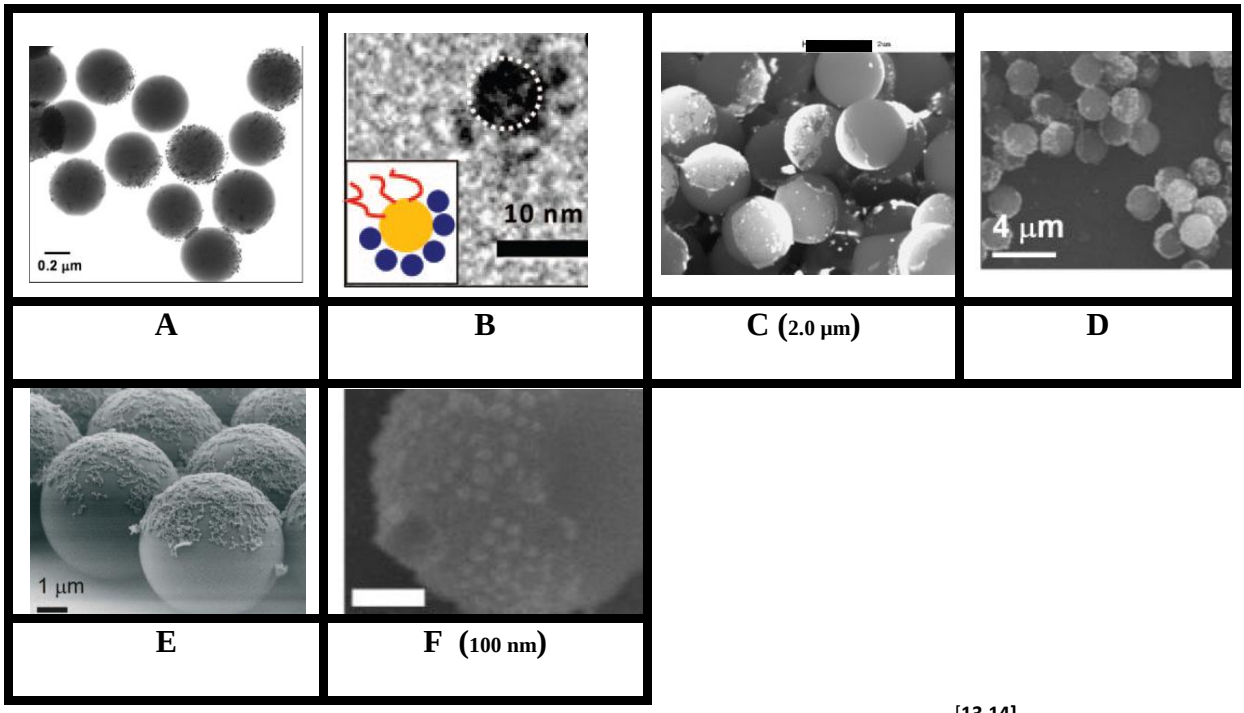

Fig.1. (A) TEM image of silica colloids hemispherically coated with gold nanoparticles [13,14]. **(B)** TEM image of Janus AuNPs: PEO-Au-PMMA, scale bar is 10 nm [15]. **(C)** SEM image of Janus Particles fabricated by gold sputtering on a monolayer of 2.7 µm sulfate poly(styrene) latex particles embedded on the surface of PDMS, scale bar is 2.0 µm [16]. **(D)** SEM image of Surface - anisotropic 2.4 *µm* silver-modified PS spheres released from the sphere/PDMS composite [17]. **(E)** SEM image of anisotropic particle structures formed by attaching 60 nm SiO2 particles to 5 µm amino-functionalized Janus SiO2 particles [18]. **(F)** SEM image of a side view of the 460 nm silica Janus particle, scale bar is 100 nm [19].

1.2.2 Surface modification of a hemisphere of the precursor particle which has at least half of its structure embedded in a curved surface (Pickering system)

This method offers a potential way to increase Janus particles productivity, whereby the precursor particles are adsorbed and embedded into a curved interface which has a larger surface area compared to flat surface. Precursor particles adsorbed into the interface between oil droplets and water form emulsions stabilized by the Pickering mechanism (solid particles instead of ordinary surfactant molecules). Based on this, selective chemical modification can be performed by dissolving the reagents for chemical modification selectively in the water phase or the oil phase. The Janus particles are collected by destruction of the emulsion. Some examples utilizing this method are described below.

Kawaguchi *et al*, prepared microgel particles by using precipitation polymerization of poly(*N*-isopropyl acrylamide-*co*-acrylic acid) (PNA) which has a responsive character, since the particles shrink and swell upon changes in pH or temperature (e.g. 2.8 μm diameter at pH 6.0 and 1.5 μm at pH 4.0). In this method, a Pickering o/w emulsion is formed by stirring hexadecane and water in the presence of the PNA microgel at pH 6.0 and 25ºC. After removing unattached microgel at the oil/water interface, amino groups were introduced through a carbodiimide coupling reaction in water phase at 25ºC using ethylenediamine and 1-ethyl-3-(3-dimethylaminopropyl) carbodiimide hydrochloride . This generated amino/carboxylic acid functional Janus particles which are isolated by destabilization of the emulsion to detach the Janus particles. It was observed that these Janus particles aggregated (self-assembled) at pH 4.0 into string structures [20]. Yang *et al*, synthesized Janus particles through the simultaneous biphasic grafting of different polymer brushes onto the two parts of a

Pickering colloid at a liquid/liquid emulsion interface through atomic transfer radical polymerization (ATRP), whereby monodisperse silica particles (450 nm) were functionalized by 4-(chloro-methyl) phenyl) trichlorosilane to have a chlorine atom on their surface to serve as the ATRP initiator for surface-initiated grafting-from polymerization. These silica particles were able to form a stable water/oil emulsion through a Pickering mechanism. Water droplets with a water-soluble monomer acrylamide and water-soluble ligand 2,2`-bipyridine were dispersed in toluene, which had a styrene monomer and oil-soluble ligand 4,4`-di-5-nonyl-2,2`-bipyridine. CuCl was added to activate the initiator through abstraction of the chlorine atom from the silica particle, followed by the alternating (redox) initiation and growth of the polymer brushes on the two parts of the particles that stabilized the emulsion at 60ºC [21]. Moreover, amphiphilic silica Janus particles (150 nm) with hydrophobic poly(styrene) and hydrophilic poly(sodium methacrylate) brushes were synthesized by adsorbing the precursor silica particles (anchored by a free radical initiator) at the styrene-water interface, then growing the polymer brushes by surface-initiated free radical polymerization upon heating. In this method, one hemisphere of the silica particle forms poly(sodium methacrylate) brushes in water, and the other hemisphere in styrene forms poly(styrene) brushes [22]. A wax-in-water emulsion formed at elevated temperature using 800 nm to 1.5 μm silica particles as the Pickering stabilizer, led to armored wax droplets. Cooling the emulsion to room temperature resulted in solidification of the paraffin wax droplets, thereby partially embedding the adhered silica particles. The exposed surface of the silica particles was modified by (3-aminopropyltriethoxysilane); the silica Janus particles were isolated by dissolving the wax in chloroform [23]. In Figure 2 are images of Janus Particles that are prepared by this method.

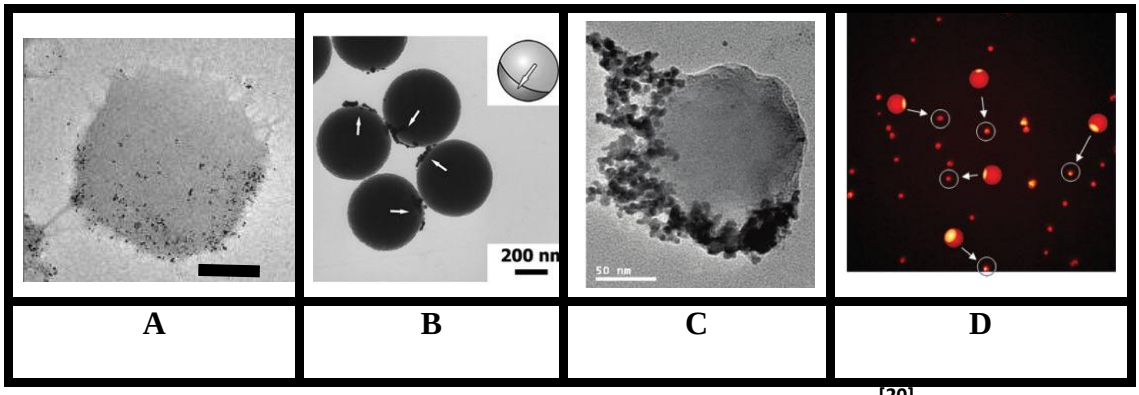

Fig.2. (A) TEM image of AuNP-conjugated PNA microgels, scale bar is 200 nm [20]. **(B)** TEM image of Janus Silica particles with adsorbed Au NPs [21]. **(C)** TEM image of Janus silica particles after complex with poly(2-vinylpyridine) and absorbing of gold nanoparticles [22]. **(D)** Fluorescence images of Janus particles with wax protected area labelled with fluorescent dye [23].

1.2.3. Glancing angle deposition

Hong and Granick synthesized zwitterionic Janus particles used a suspension of poly(styrene) particles with a diameter of 1.0 μm with carboxylic acid groups on their surfaces. These particles were spread onto a cleaned glass substrate and then a monolayer of colloid was formed. After the evaporation of the liquid, a thin gold film (15 nm) was deposited using electron-beam deposition to introduce a positive charge on the surface by monolayers of *N*,*N*,*N*-trimethyl (11-mercaptoundecyl) ammonium chloride which were deposited from an ethanol solution. The untreated side of the hemisphere had a negative charge due to the presence of the carboxylic acid group. The self-assembly of these particles into clusters was observed [24]. Glancing angle deposition was also utilized to prepare multifunctional patchy particles, whereby a 2.5 μm monolayer of sulfate latex poly(styrene) was prepared on the surface of either silicon wafer or glass slides by convective assembly; a vapor of gold or silver was deposited on the poly(styrene) monolayer. The angle of incidence of the metal vapor is referred to as the angle of vapor deposition [25].

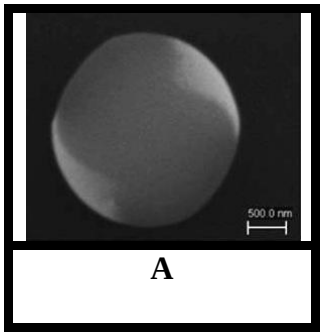

Fig.3. (A) SEM image of 2.5 µm Poly(styrene) particle with two patches [25].

1.2.4. Microfluidics

Microfluidic techniques allow the formation of monodisperse emulsion micro-droplets by co-flowing immiscible fluids at low Reynolds numbers. Based on this principle, a microfluid device has been utilized to synthesize Janus particles. Some existing examples from the literature are described here, for instance the study by Takizawa and co-workers, who used two-dimensional microfluidic technology to generate Janus droplets which were subsequently cured into polymeric Janus particles. Their method involved the use of a Y-shaped channel used to form a two-phase organic stream of white and black isobornyl acrylate after the addition of pigment of titanium oxide and carbon black. This bicolored stream entered the co-flowing aqueous stream to produce biphasic droplets, which were stabilized by the steric stabilizer poly(vinyl alcohol). Next, the Janus droplets were cured for 20 seconds by thermal polymerization at 90°C to form Janus particles with a size of 20-30 µm [26]. Another research group has used microfluidics to synthesize highly monodisperse Janus polymer particles in the size range of 40 to 200 µm, whereby two immiscible monomers are used. Methacryloxypropyl dimethylsiloxane was the first monomer. The second monomer was a mixture of several monomers, including pentaerylthritol triacrylate, poly(ethylene glycol), diacrylate and acrylic acid. Both monomers contained a photo-initiator (4% 1-hydroxycyclohexyl phenyl ketene).

These monomers were passed through a microfluidic channel to the aqueous phase to form monomer droplets which were stabilized by (SDS). Subsequently, the monomer droplets were solidified by photo-polymerization induced by UV irradiation [27]. Additionally, a planar microfluidic system with a Y-shaped channel has been used to fabricate biphasic Janus droplets. The oil phase consisted of two organic liquids, a photo-polymerizable monomer (1,6-hexanediol diacrylate) and a non-polymerizable organic liquid (silicone oil).

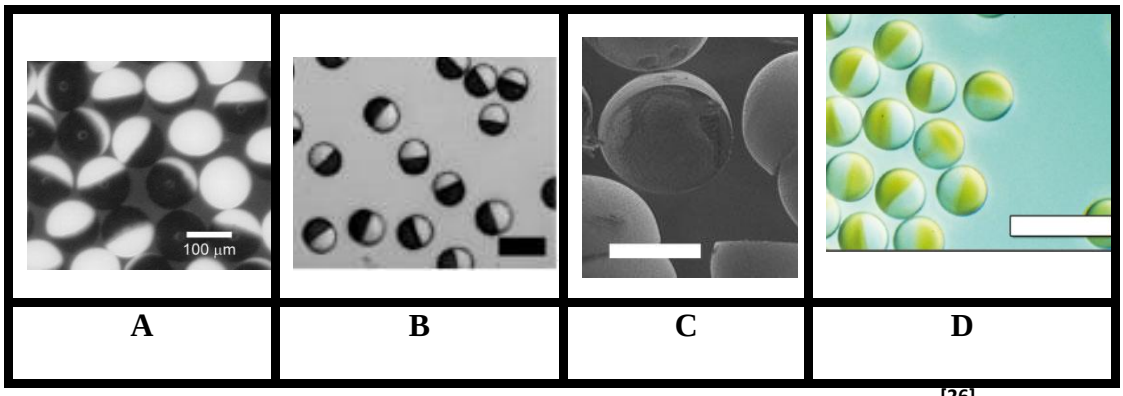

Fig.4. (A) Optical microscopy of monodisperse bicolored polymeric particles [26]**.(B)** Optical microscopy image of Janus Particles, scale bar is 100 µm [27] **.(C)** SEM of hemispheric particles, Scale bar is 100 µm [28] .**(D)** DIC (differential interference contrast microscope) image of magnetic Janus particles generated from coflowing streams of polymer, the scale bar is 100 µm [29]**.**

The stream of the two organic liquids entered into an aqueous phase containing SDS to stabilize the organic oil droplets. The polymerization of the polymerizable side was performed by UV irradiation to produce hemispheric particles [28]. Doyle and co-workers synthesized Janus hydrogel particles with anisotropic super-paramagnetic properties by microfluidics, wherein a Janus droplet of a UV-curable monomer had two sides to form Janus particles with size of 48 µm after exposure to UV irradiation, whereby one side contained poly(ethylene glycol)-diacrylate and the other side contained the same polymer but with magnetic (Fe_3O_4) nanoparticles [29].

1.2.5. Microcontact printing

The microcontact printing technique has been used as a tool for surface modification of precursor particles. Velev and co-workers made dipolar Janus particles by microcontact printing of non-water soluble cationic surfactants onto a monolayer of negatively charged 9.6 µm poly(styrene) particles; after dispersing these dipolar particles in water and after the addition of a high concentration of salt, the particles assembled as linear aggregates [30].

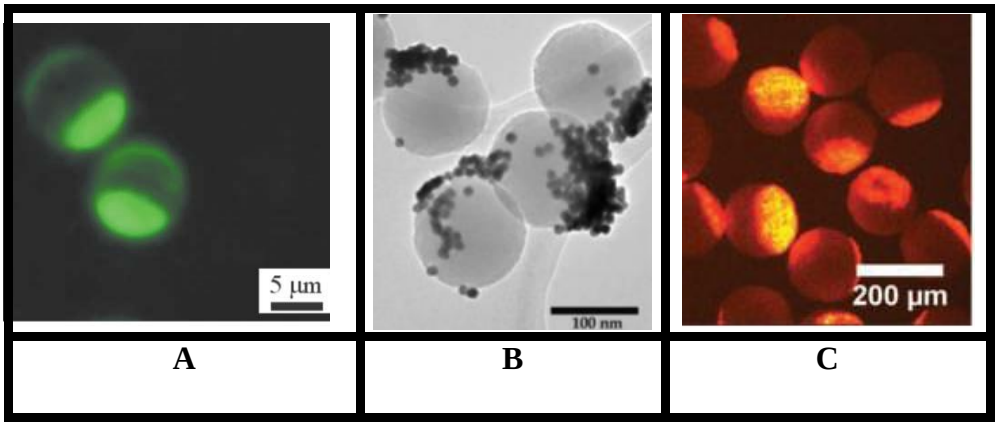

Fig.5.(A) High magnification fluorescent microscopy image of 9.6 µm sulfate PS latex particles stamped with a film of Neuro Dio (hydrophobic fluorescent cationic dye) deposited on an elastomer stamp and redispersed in water **[30]. (B)** TEM image of Janus particles labeled with Au nanoparticles **[31]. (C)** Fluorescent microscopy image Janus polymer particles obtained by printing rhodamine ethylenediamine dye **[32].**

1.0 µm trivalent silica patchy Janus particles were synthesized in two steps by the microcontact printing method. The first step is the formation of a monolayer of the monodisperse silica particles on a solid substrate; the exposed surface is stamped by a PDMS stamp which contains an amino silane. The second step involves stamping the unmodified side of the silica particles with a PDMS stamp which contains on another type of chemical functionality [31].Microcontact printing was also used to fabricate Janus trivalent porous micro-particles (160 µm) carrying epoxy moieties by adsorbing them between two stamps loaded with different inks. These inks contained

different types of amine which reacted with the epoxy groups on the surface of the particles [32].

1.2.6. Controlled phase separation

Several methods have been investigated to design Janus particles by utilizing controlled-phase separation phenomena. Okubo and co-workers made a solution of poly(styrene) and poly(methyl methacylate-*co*-(chloro methyl) styrene) in toluene, and then emulsified the solution using a membrane emulsification device to yield micron-sized monodisperse droplets. Upon toluene evaporation, phase-separated Janus microspheres were obtained. Subsequently, selective grafting-from by ATRP (atom transfer radical polymerization) was performed in water at 5°C under a nitrogen atmosphere to grow poly[2-(dimethylamino) ethyl methacrylate] brushes; the catalyst system for ATRP consisted of $CuBr_2$, ascorbic acid and PMDETA [33]. Recently, the same research group synthesized monodisperse mushroom-like Janus polymer particles using the same strategy that they proposed earlier, but with the use of (PMMA)/poly(styrene-2-(2-bromoisobutyryloxy)ethyl methacrylate) (S-BIEM), with the same grafted polymer brushes and under the same ATRP conditions [34]. (PMMA) and poly(styrene) particles with Janus properties were synthesized via internal phase separation, whereby emulsion droplets of PMMA/PS/hexadecane and dichloromethane were formed in water with a high shear rate of 500 rpm and stabilized by sodium dodecylbenzyl sulfate. Subsequently, the dichloromethane was evaporated to form hexadecane/PS-PMMA microparticles. The hexadecane was further removed by extraction with hexane to produce Janus particles with sizes between 1-6 μm [35]. Seeded emulsion polymerization was used to synthesize sub-micrometer Janus particles, whereby cross-linked poly(acrylonitrile)(PAN) hollow particles with a size of 400 nm were used as the seed for the emulsion

polymerization of styrene and divinylbenzene which were slowly fed during polymerization. The phase separation of the poly(styrene) from the poly(acrylonitrile) was driven by the elastic-retractile force due to the presence of a cross-linked network [36].

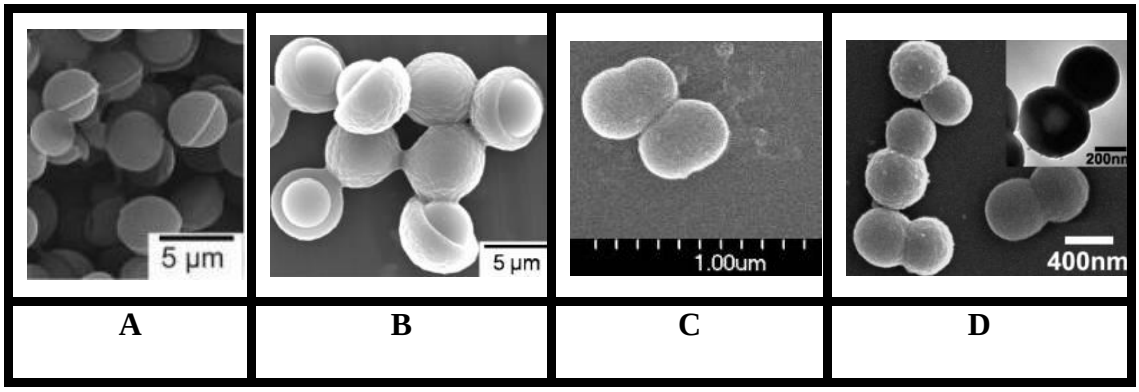

Fig.6. (A) SEM of PS/P(MMA-CMS)-b-PDM brushes composite particles **[33]. (B)** SEM of PMMA/P(S-BIEM)-g-PDM Janus particles prepared by surface initiated ARGET-ATRP of DM in the aqueous medium **[34]**. **(C)** SEM image of charge anisotropic particles **[37]. (D)** SEM and inset TEM image Janus PAN/PS polymer colloids prepared by one-step batch seeded emulsion polymerization **[36].**

Zukoski synthesized chemically and spatially anisotropic semi-interpenetrating poly(styrene) latex particles by seeded emulsion polymerization. Their strategy was based on using the low cross-linked density poly(styrene) (0.68%, DVB) particles which carry a negative charges comes from the sulfate group of KPS initiator and also from the co-monomer 2-(diethylamino)ethylmethacrylate) at high pH . These seed particles swell styrene with a (monomer/polymer) ratio of (1.2:1) were incubated at room temperature and low pH (2.0) for 21 h, and then heated to 80°C for 3 h, followed by the addition of CTAB as the cationic surfactant and hydroquinone to prevent secondary nucleation in the aqueous phase. After 1 hour, AIBN (the initiator) dissolved in 4.0 mL of styrene was added to the polymerization mixture to initiate polymerization. Subsequently, at the end of polymerization and after increasing the pH to around 8.0, dumbbell particles were formed with a

positively charged side in the new domain as result of adsorbing the CTAB in this region and a negative charge on the original seed side due to sulfate groups and deprotonation of the co-polymer. However, the author does not suggest that the CTAB should cover both sides and not just the new domain, which is clear as a result of the electrostatic attraction between the CTAB and the sulfate group in the original domain of the seed particles [37].

1.2.7. Controlled surface nucleation

This method depends upon the controlled nucleation and growth of a single particle on the surface of precursor particles. An example of this process is the synthesis of hybrid Janus nanoparticles through the controlled surface nucleation of poly(styrene) latex particles on the surface of inorganic nanoparticles. This method is derived from the growth-seeded emulsion polymerization process, but differs from the phase-separation method in seeded emulsion polymerization, in which the controlled surface nucleation method depends upon using inorganic seed nanoparticles, such as silica particles, as a precursor. The silica particles were initially chemically modified and then an emulsion polymerization of styrene performed in the presence of the modified silica particles, the formation of the poly(styrene) nodules being highly favored at the silica surface to form ultimately snowman or dumbbell like particles [38]. Dumbbell-like Janus [Au-Fe_3O_4] nanoparticles with sizes around 20 nm were synthesized by decomposition of [$Fe(CO)_5$] (iron pentacarbonyl) on the surface of gold nanoparticles followed by oxidation. These Janus particles showed dual properties in terms of surface plasmon absorption as a result of the gold as well as the magnetic properties due to the presence of iron oxide [39].

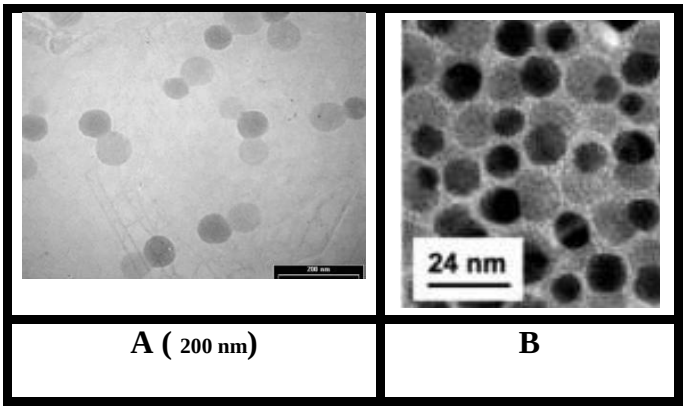

Fig.7. (A) Dissymmetrical particles of silica-Poly(styrene), scale bar is 200 nm [38]**. (B)** TEM image of the dumbbell-like Au-Fe3O4 nanoparticles [39]**.**

1.2.8. Template-assisted self-assembly

This approach is based on self-assembly of the precursor particles on the surface of another particle by using a template with defined dimensions which allows for self-assembly by confinement geometry. For instance, asymmetric dimmers were formed from the two types of spherical monodispersed particles, whereby the two particles are self-assembled by geometrical confinement and attractive capillary forces. The method is based on the use of two glass substrates parallel to each other followed by flow of particle dispersion through the two glass substrates. The surface of the bottom glass substrate contains a two-dimensional array of cylindrical holes which are bigger than the particles, and during the flow of the colloidal particles, some of the particles are physically trapped in the holes, with only one 2.8 μm poly(styrene) particle trapped in each hole. The poly(styrene) particle in each hole tends to be in physical contact with the wall of the hole because of the attractive capillary forces during the evaporation of the dispersed phase. Subsequently, the position of the poly(styrene) particles inside the holes is fixed by heating above the glass transition temperature of the poly(styrene). After that, another self-assembly step using different particles (1.6 μm silica particles) fills the remaining voids in the holes, with

two particles now in physical contact because of the attractive capillary forces due to dispersed phase evaporation. The two particles are welded together as single snowman particle by heating above the Tg° of poly(styrene) [40]. Müller *et al*. synthesized disc-shaped Janus structures through a so-called template-assisted pathway, using well-defined lamellar microphase-segregated block terpolymer films of poly(styrene)-*block*-poly(butadiene)-*block*-poly(methylmethacrylate) (PS-PB-PMMA). Upon cross-linking of the butadiene phase, fracturing the film into small fragments via sonication and hydrolysis of the PMMA to poly(methacrylic acid) yielded disc-shaped Janus particles [41].

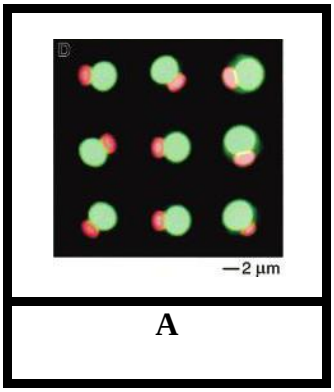

Fig.8. (A) Fluorescence microscopy image of a 2D array of dimers poly(styrene)-silica beads **[40]**.

1.2.9. Electrified jetting

Electrohydrodynamic jetting of parallel polymer solutions of poly(ethylene oxide) and poly(styrene sulfonate) or poly(ethylene oxide) and poly(ethylene imine), each of which contains a different fluorescent dye, has been used to fabricate biphasic Janus particles of sub-micrometer size under the influence of an electrical field. Lahann and co-workers used this method, whereby a laminar flow of two distinct polymer solutions was pumped through a nozzle with side by side geometry. The polymer solution droplets at the tip of the nozzle were distorted into a narrow cone

by applying an electrical field (5-15 Kv) [42]. Moreover, the same research group made triphasic Janus particles by electrified jetting, wherein a laminar flow of three distinct polymer solutions containing three different dyes was pumped through a nozzle with side by side geometry; an electrical field was applied to form triphasic nanocolloids [43].

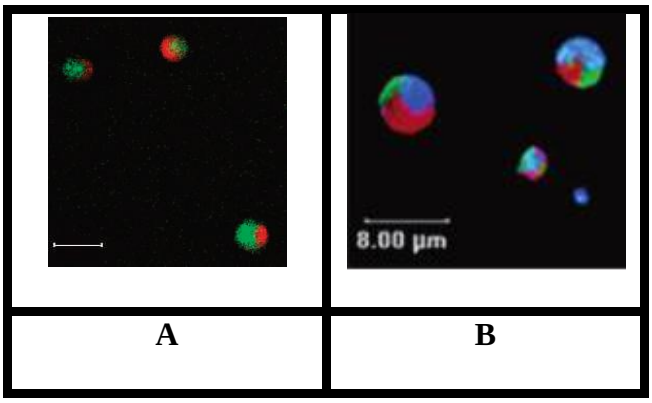

Fig.9. (A) Confocal micrograph of biphasic particles, scale bar is 4.0 µm **[42]. (B)** Confocal laser scanning microscopy image of triphasic nanocolloids **[43].**

1.2.10. Particle lithography

This method has been used to induce anisotropy on the surface of poly(styrene) latex particles (1.5 µm), whereby positively charged poly(styrene) latex particles adhered to a negatively charged flat glass substrate, and then negatively charged poly(styrene sulfonate) was added to cover the entire particle surface except at the sites which adhered to the glass. Subsequently, the particles were sonicated from the glass. These anisotropic particles were used to form doublet particles by adhering negatively charged silica or sulfated latex particles to the small positively charged region [44]. Anisotropic melamine formaldehyde particles (4.0 µm) with two patches were fabricated by the particle lithography technique, whereby the melamine formaldehyde particles were aggregated to form doublet particles by the salting out/quenching technique. The melamine formaldehyde particles were aggregated

with 2.0 M KCl for 15 minutes, the concentration of KCl was later reduced to 20 mM by dilution with water. The doublet melamine formaldehyde particles were transferred to a Petri dish where they bound electrostatically to the glass surface. The doublet particles were then coated with 60 nm poly(styrene) particles. Subsequently, the Petri dish was sonicated and the doublets were removed from the glass and broken into singlets; each singlet consisted of two uncoated patches. These two patches were used as bonding regions for other particles, and indeed 4.0 μm sulfate functionalized poly(styrene) particles were added selectively to the patchy regions of melamine formaldehyde particles via electrostatic attraction to form trimer particles with the morphology of colloidal water molecules [45].

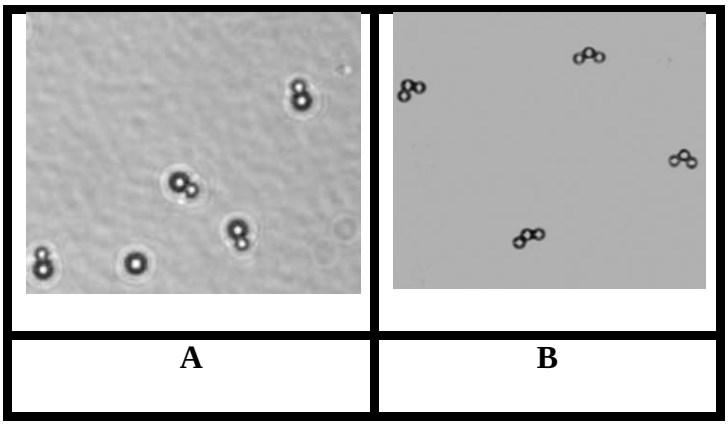

Fig.10. (A) Optical microscopy image of doublet 1.5 μm amidine PS latex and 2.4 μm sulfate PS Latex particles [44]**. (B)** Confocal microscopy image of polystyrene-melamine formaldehyde triplet particles [45].

1.3. Properties and application of Janus Particles

The unique anisotropic structure of Janus particles makes this type of particle useful in many applications. The existing current applications of Janus particles will be discussed and listed here, providing examples for each particular application.

1.3.1. As a Pickering stabilizer (surfactant)

This application was inspired by the pioneering work of Casagrande and co-workers in 1989 when they synthesized spherical glass particles with sizes from 50 to 90 μm with one hemisphere hydrophilic and the other hydrophobic [46]. These Janus particles were synthesized by protecting one hemisphere on the surface so that side remained hydrophilic and chemically modifying the exposed surface with aliphatic chains to make that side hydrophobic. They studied the differences between completely hydrophilic particles, hydrophobic particles and Janus (amphiphilic particles) at an oil/water interface, and found that the most of the completely hydrophilic particles partitioned in water and most of the hydrophobic particles partitioned in the oil phase, whereas Janus particles partitioned in both phases equally. A theoretical study was performed to study the activity of amphiphilic particles (Janus particles) and the homogenous counterpart particles on adsorption at an oil-water interface. The calculations showed that the amphiphilic particles were more surface active by three orders of magnitude compared to homogenous particles [47]. Krausch and co-workers compared the interfacial activity of iron oxide particles containing one ligand of either oleic acid or oleylamine to render them hydrophilic, and gold particles with dodecanethiol and octadecanethiol attached to make them hydrophobic, with amphiphilic gold-iron oxide Janus particles to form a water-in-hexane emulsion. The surface activity of the particles was tested by a pendant drop method tensiometer. It was observed that the lowest interfacial tension was found when the Janus particles were used [48]. Moreover, 500 nm amphiphilic silica Janus particles were used as a Pickering stabilizer to form a stable water-in-toluene emulsion after mixing with speed of 18000 rpm for 1 minute [8]. Weitz and co-workers synthesized amphiphilic dimer particles via phase separation upon seeded

polymerization, whereby 800 nm linear poly(styrene) seed particles were swollen with styrene, 1% DVB,10% 3-(trimethoxysilyl) propyl acrylate, and 0.5 wt% of an oil-soluble initiator (V-65B). The monomer to seed particles swelling ratio was 4 to 1. Polymerization was carried out at 70°C for 8 hours to make cross-linked seed poly(styrene) latex particles containing one trimethoxysilane group. These cross-linked particles were further swelled with styrene, 1%DVB and V-65B; phase separation occurred upon heating due to elastic stress to form snowman dimer particles. The original seed domain containing trimethoxysilane was chemically modified by reacting with *N*-[3-(trimethoxysilyl) propyl] ethyleneamine] to make that domain hydrophilic, consequently 2.0 µm amphiphilic snowman particles were formed. It was observed that these amphiphilic dimer particles were surface active and adsorbed strongly at the hexadecane:water interface [49].

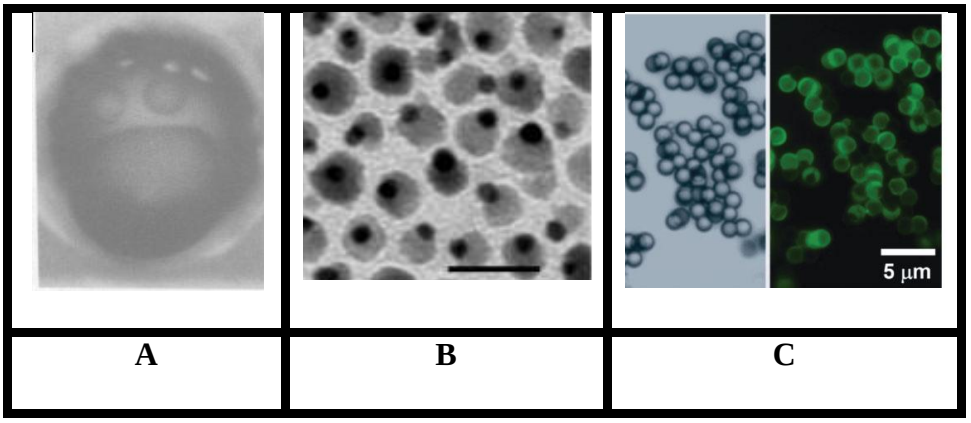

Fig.1.3.1 (A) Microphotography of a Janus glass bead, the water spreads on the hydrophilic part and makes a film, whereas on the hydrophobic part one observes small droplets as water does not wet completely **[46]**. **(B)** TEM image of Janus particles consisting of gold (darker spheres) and iron oxide (brighter spheres), scale bar 25 nm **[48]. (C)** Bright field microscope image (left) and a fluorescence microscope image (right) of polystyrene dimer, Hydrophilic bulbs are labelled with fluorescein isothiocyanate **[49]**.

Moreover, 5.0 µm mushroom-like Janus polymer particles prepared by phase separation upon solvent evaporation were used to stabilize droplets of 1-octanol in water [50]. Furthermore, Janus particles can be used in conventional emulsion polymerization as the Pickering agent with disc-shaped Janus particles [51].

1.3.2. Compatible agent for blending two polymers.

Due to the anisotropic nature of Janus particles, they could potentially be used as compatible agents to maximize dispersing between two immiscible phases. Axel Müller and co-workers used Janus particles to make a mixture of two immiscible polymers compatible in a twin screw mini-mixer. They observed that Janus particles were located at the interface of the two polymer phases and the efficiency of these particles was superior as compared to ordinary block copolymer compatible agents. These Janus particles had one side containing poly(styrene) and the other side containing poly(methyl methacrylate) and were used as a compatible agent to blend PS and PMMA [52].

1.3.3. Water-repellent textiles.

As amphiphilic Janus particles have hydrophilic one side and another hydrophobic side, they can be used as textile modifiers. As a result of the chemically immobilized hydrophilic side facing towards the textile and the hydrophobic side directed towards the outer environment, the surface of the textile becomes hydrophobic instead of its original state which was hydrophilic and, consequently, becomes water-repellent. Bellmann and co-workers synthesized Janus particles and used them for this purpose, wherein 1.0 μm silica particles were used as a Pickering stabilizer to form wax colloidosomes. The exposed surface of the silica particles was chemically modified, then the wax was dissolved and the silica Janus particles were collected. To selectively immobilize silica Janus particles on the surface of the textile, first the textile was chemically modified to contain poly(glycidyl methacrylate) (PGMA) which provides reactive epoxy groups that react with the hydrophilic amine side of silica Janus particles. After Janus particle adsorption, the textile had a higher contact

angle with water, which showed that the hydrophobic side of Janus particles was positioned toward the outer environment whereas the hydrophilic part was linked to the textile surface [53].

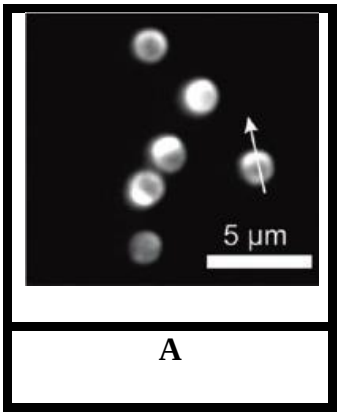

Fig.1.3.3. (A) Fluorescence microscopy images for Silica Janus particles after labelling with FITC **[53]**.

1.3.4. Electronic and optical applications.

In this section, some examples of the use of Janus particles in electrical and optical applications will be discussed. Latex Janus particles made of poly(styrene) (20 µm) were prepared by selective modification from a flat surface whereby one side was coated with gold. This was followed by chemisorption of thiol-modified ionizable groups 2-aminoethanethiol which converted these Janus particles to be pH-dependent electric dipole moments; this led them to orient under an electric field at a certain pH [5].

Conversely, using the same preparation method with thermal evaporation of gold on a monolayer of poly(styrene) latex particles, but with a smaller particle size (110 nm), Janus particles were used as an optical biosensor which exhibited a large extinction coefficient of optical density of 2.4 with a bandwidth of 100 nm in the visible region [54]. Janus particles have also been used an antireflection coating for optical applications. These Janus particles were synthesized by deposition of a poly(electrolyte) multilayer on a glass substrate with the cationic layer on top;

anionic poly(styrene) particles with a size of 100 nm adhered to that layer by electrostatic attraction, and then the surface of the anionic particles was made positive by contact printing of cationic PDMS on the surface of the latex particles followed by removal of the PDMS stamp. Anionic 50 nm poly(styrene) latex particles attached to the cationic particles to form a film of snowman Janus particles which worked as an antireflection coating [3].

1.3.5. Selective adhesion to a specifically targeted surface.

Janus particles can selectively orient themselves to adhere to a specific surface and subsequently modify the properties of that surface. For example, 132 nm latex Janus particles have one side consisting of poly(n-butyl acrylate), which is soft, while the other side is hard poly(methyl methacrylate) prepared by emulsion polymerization.

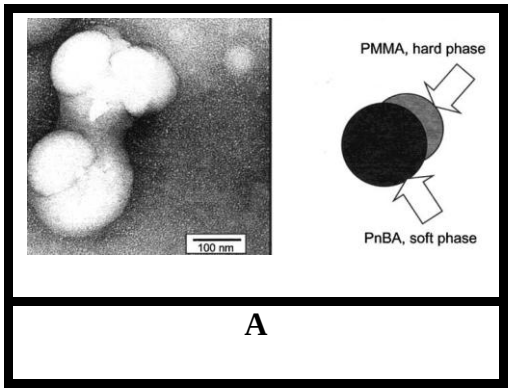

Fig.1.3.5. (A) TEM image (left) and schematic representation (right) of the particle morphology of Janus particles with PMMA hard phase and PBA soft phase **[55].**

These particles selectively adhere to a targeted surface on a particular side based on the hydrophilicity of that surface, whereby on hydrophilic surfaces, the hard side preferentially orients to that surface, but the soft domain adheres to a hydrophobic surface [55].

1.3.6. Self-motile colloidal particles.

When chemical reactions are catalyzed on the surface of spherical colloidal particles with an asymmetric distribution of catalyst on their surface (Janus characteristic), the reaction products propels the particles by a process of self-diffusion phoresis which transforms chemical energy into mechanical energy. As an example of this, 1.62 μm monodispersed spherical poly(styrene) particles with one side coated with platinum and the other side kept as non-conducting poly(styrene) have been used with hydrogen peroxide (the fuel). Hydrogen peroxide is reduced on the platinum side to produce oxygen and water in large quantities compared to the fuel; consequently, the Janus particles move and this movement can be detected by particle tracking [56].

1.3.7. Gene delivery.

Multi-segment bimetallic nano-rods (with Janus characteristics) can simultaneously bind compacted DNA plasmids. In this method, bifunctional Au/Ni nanorods were prepared by template synthesis, and then incubated with a 3-[(2-aminoethyl) dithio] propionic acid linker. The plasmids were then bound by electrostatic interactions to protonated amines on a nickel surface; $CaCl_2$ then compacted the surface and immobilized the plasmids. The evaluation of gene delivery by these dual functionalized Janus nanorods was assessed by *in vitro* transfection experiments on human embryonic kidney cells [57].

1.4. Our proposed approach to make Janus particles

The proposed method in this research is summarized in scheme 1.4.1.

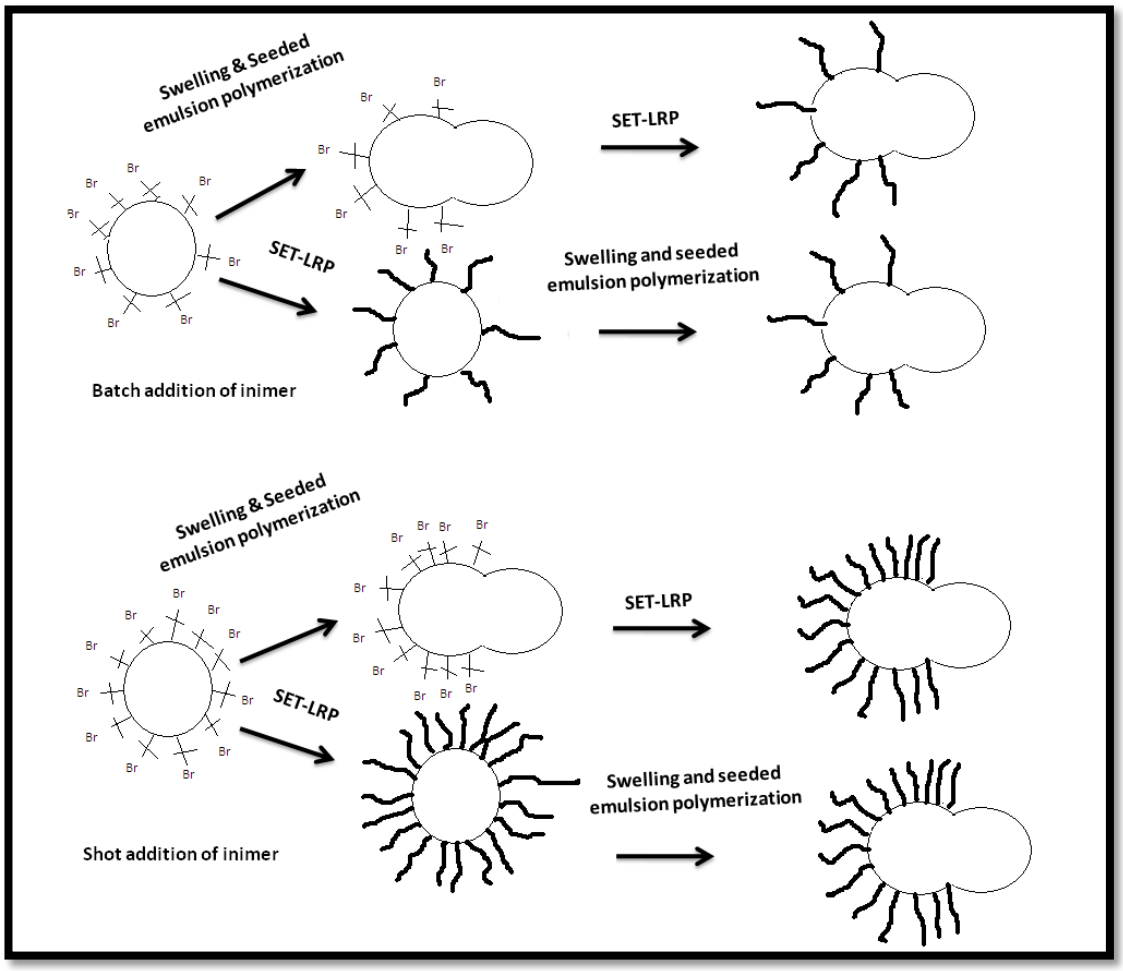

Scheme.1.4.1. Proposed method to fabricate hairy dumbbell shape Janus Particles by utilization of both seeded emulsion polymerization and SET-LRP.

As it can be seen from the scheme 1.4.1, two synthetic pathways were investigated. Cross-linked polymer latexes (150-260 nm) with various cross-linked densities (1-8wt% DVB) grafted with *tert*-bromine functional groups were made via soap-free emulsion polymerization and incorporated a functional methacrylic monomer (2-methacryloxyethyl -2[']- bromoisobutyrate) containing *tert*-bromine functional groups by batch addition from the beginning of the polymerization or by shot addition at elevated conversion, approximately above 50% monomer conversion. It is expected

that based on the time of addition of the *tert*-bromine functional, that both the entropic phase separation after swelling and seeded emulsion polymerization and SET-LRP (Single Electron Transfer-Living Radical Polymerization) to grow hydrophilic polymer brushes will be different as a result of different concentration of *tert*-bromine which will alter the hydrophilicity of the particles as well as the density of the polymer brushes. There are two routes for each latex (batch and shot addition) in order to fabricate Janus Particles, (i) induce entropic phase separation to form a new single domain followed by formation of hydrophilic polymer brushes from the original seed domain, (ii) or the vise versa, the formation of the hydrophilic polymer brushes by SET-LRP and then induce entropic phase separation via swelling and seeded emulsion polymerization.

Based on the two approaches, the thesis contains seven chapters, the **first chapter** as described above, general review of Janus particles and demonstration of our approach to make sub-micrometer hairy Janus latex particles, the **second chapter** describes the formation of the precursor latex particles that contain a *tert*-bromine functional group via soap-free emulsion polymerization. **Chapter three** covers a fundamental study of performing SET-LRP of several hydrophilic monomers in a completely aqueous condition. **Chapter four,** studies the formation of the different type of hydrophilic polymer brushes from latex particles contain tert-bromine functional group made via batch and shot addition method by utilizing SET-LRP as a synthesis mechanism. **Chapter five** describes the fabrication of hairy Janus particles form non-hairy and hairy precursor particles made by batch addition. **Chapter six** describes the fabrication of hairy Janus particles form non-hairy and hairy precursor particles made by shot addition. **Chapter seven**, studies the potential application of the synthesized complex particles in different areas such as carbon nano tubes

(CNTs) stabilizer in aqueous phase, Pickering stabilizer for emulsion, this chapter also involve the study of the interaction among the non-hairy Janus particles in aqueous phase upon addition of dilute electrolyte solution. **Chapter eight** describes the final conclusions of the thesis and possible future work.

1.5. References

1- De Gennes, P. G. *Rev. Mod. Phys.* **1992**, *64*, 645-648.

2- Chen, Q.; Whitmer, J. K.; Jiang, S.; Bae, S. C.; Luijten, E.; Granick, S. *Science*. **2011**, *331*, 199-202.

3- Koo, H. Y.; Yi, D. K.; Yoo, S. J.; Kim, D.-Y. *Adv. Mater*. **2004**, *16*, 274-277.

4- Walther, A.; Hoffmann, M.; Mueller, A. H. E. *Angew. Chem., Int. Ed.* **2008**, *47*, 711-714.

5- Takei, H.; Shimizu, N. *Langmuir*. **1997**, *13*, 1865-1868.

6- Perro, A.; Reculusa, S.; Ravaine, S.; Bourgeat-Lami, E.; Duguet, E. *J. Mater. Chem.* **2005**, *15*, 3745-3760.

7- Wurm, F.; Kilbinger Andreas, F. M. *Angew. Chem.* **2009**, *48*, 8412-8421.

8- Jiang, S.; Chen, Q.; Tripathy, M.; Luijten, E.; Schweizer, K. S.; Granick, S. *Adv. Mater*. **2010**, *22*, 1060-1071.

9- Pawar, A. B.; Kretzschmar, I. *Macromol. Rapid Commun*.**2010**, *31*, 150-168.

10- Walther, A.; Mueller, A. H. E. *Soft matter* .**2008**, *4*, 663-668.

11- Mao, Z.; Xu, H.; Wang, D. *Adv. Funct. Mater*.**2010**, *20*, 1053-1074.

12- Yoshida, M.; Lahann, J. *ACS Nano* .**2008**, *2*, 1101-1107.

13- Ho, C.-C.; Chen, W.-S.; Shie, T.-Y.; Lin, J.-N.; Kuo, C .*Langmuir*. **2008**, *24*, 5663-5666.

14- Lin, C.-C.; Liao, C.-W.; Chao, Y.-C.; Kuo, C. *ACS Appl. Mater. Interfaces*. **2010**, *2* , 3185-3191.

15- Wang, B.; Li, B.; Zhao, B.; Li, C. Y. *J. Am. Chem. Soc.* **2008**, *130*, 11594-11595.

16- Paunov, V. N.; Cayre, O. J. *Adv. Mater* .**2004**, *16*, 788-791.

17- Cui, J.-Q.; Kretzschmar, I. *Langmuir* .**2006**, *22*, 8281-8284.

18- Ling Xing, Y.; Phang In, Y.; Acikgoz, C.; Yilmaz, M. D.; Hempenius Mark, A.; Vancso, G. J.; Huskens, J. *Angew Chem.* **2009**, *48*, 7677-82.

19- McConnell, M. D.; Kraeutler, M. J.; Yang, S.; Composto, R. J. *Nano Lett.* **2010**,*10*, 603-609.

20- Suzuki, D.; Tsuji, S.; Kawaguchi, H. *J. Am. Chem. Soc.* **2007**, *129*, 8088-8089.

21- Liu, B.; Wei, W.; Qu, X.; Yang, Z. *Angew. Chem.* **2008**, *47*, 3973-3975.

22- Zhang, J.; Jin, J.; Zhao, H. *Langmuir* .**2009**, *25*, 6431-6437.

23- Hong, L.; Jiang, S.; Granick, S. *Langmuir* .**2006**, *22*, 9495-9499.

24- Hong, L.; Cacciuto, A.; Luijten, E.; Granick, S. *Nano Lett.* **2006**, *6*, 2510-2514.

25- Pawar, A. B.; Kretzschmar, I. *Langmuir* .**2009**, *25*, 9057-9063.

26- Nisisako, T.; Torii, T.; Takahashi, T.; Takizawa, Y. *Adv. Mater.* **2006**, *18*, 1152-1156.

27- Nie, Z.; Li, W.; Seo, M.; Xu, S.; Kumacheva, E. *J. Am. Chem. Soc.* **2006**, *128*, 9408-9412.

28- Nisisako, T.; Torii, T. *Adv. Mater.* **2007**, *19*, 1489-1493.

29- Yuet, K. P.; Hwang, D. K.; Haghgooie, R.; Doyle, P. S. *Langmuir.* **2010**, *26*, 4281-4287.

30- Cayre, O.; Paunov, V. N.; Velev, O. D. *J. Mater. Chem.* **2003**, *13*, 2445-2450.

31- Jiang, S.; Granick, S. *Langmuir* .**2009**, *25*, 8915-8918.

32- Kaufmann, T.; Gokmen, M. T.; Wendeln, C.; Schneiders, M.; Rinnen, S.; Arlinghaus, H. F.; Bon, S. A. F.; Du Prez, F. E.; Ravoo, B. J. *Adv. Mater.* **2011,** *23*, 79-83.

33- Ahmad, H.; Saito, N.; Kagawa, Y.; Okubo, M. *Langmuir* .**2008**, *24*, 688-691.

34- Tanaka, T.; Okayama, M.; Kitayama, Y.; Kagawa, Y.; Okubo, M. *Langmuir*. **2010**, *26*, 7843-7847.

35- Wang, Y.; Guo, B.-H.; Wan, X.; Xu, J.; Wang, X.; Zhang, Y.-P. *Polymer* .**2009**, *50*, 3361-3369.

36- Tang, C.; Zhang, C.; Liu, J.; Qu, X.; Li, J.; Yang, Z. *Macromolecules*. **2010**, *43*, 5114-5120.

37- Mock, E. B.; Zukoski, C. F. *Langmuir.* **2010**, *26*, 13747-13750.

38- Reculusa, S.; Poncet-Legrand, C.; Perro, A.; Duguet, E.; Bourgeat-Lami, E.; Mingotaud, C.; Ravaine, S. *Chem. Mater.* **2005**, *17*, 3338-3344.

39- Yu, H.; Chen, M.; Rice, P. M.; Wang, S. X.; White, R. L.; Sun, S. *Nano Lett.* **2005**, *5*, 379-382.

40- Yin, Y.; Lu, Y.; Xia, Y. *J. Am. Chem .Soc* .**2001**, *123*, 771-772.

41- Walther, A.; Hoffmann, M.; Mueller, A. H. E. *Angew. Chem.***2008**, *47*, 711-714.

42- Roh, K.-H.; Martin, D. C.; Lahann, J. *Nat. Mater.* **2005**, *4*, 759-763.

43- Roh, K.-H.; Martin, D. C.; Lahann, J. *J. Am. Chem. Soc.***2006**, *128*, 6796-6797.

44- Snyder, C. E.; Yake, A. M.; Feick, J. D.; Velegol, D. *Langmuir* .**2005**, *21*, 4813-4815.

45- Snyder, C. E.; Ong, M.; Velegol, D. *Soft Matter* .**2009**, *5*, 1263-1268.

46- Casagrande, C.; Fabre, P.; Raphael, E.; Veyssie, M. *Europhys. Lett.* **1989**, *9*, 251-255.

47- Binks, B. P.; Fletcher, P. D. I. *Langmuir* .**2001**, *17*, 4708-4710.

48- Glaser, N.; Adams, D. J.; Boeker, A.; Krausch, G. *Langmuir* .**2006**, *22*, 5227-5229.

49- Kim, J.-W.; Lee, D.; Shum, H. C.; Weitz, D. A. *Adv. Mater.* **2008**, *20*, 3239-3243.

50- Tanaka, T.; Okayama, M.; Minami, H.; Okubo, M. *Langmuir.***2010**, *26*, 11732-11736.

51- Walther, A.; Hoffmann, M.; Mueller, A. H. E. *Angew. Chem.***2008**, *47*, 711-714.

52- Walther, A.; Matussek, K.; Mueller, A. H. E. *ACS. Nano.***2008**, *2*, 1167-1178.

53- Synytska, A.; Khanum, R.; Ionov, L.; Cherif, C.; Bellmann, C. *ACS Appl. Mater. Interfaces.***2011**, *3*, 1216-1220.

54- Himmelhaus, M.; Takei, H. *Sens. Actuators, B* .**2000**, *B63*, 24-30.

55- Pfau, A.; Sander, R.; Kirsch, S. *Langmuir* .**2002**, *18*, 2880-2887

56- Howse, J. R.; Jones, R. A. L.; Ryan, A. J.; Gough, T.; Vafabakhsh, R.; Golestanian, R. *Phys. Rev. Lett.* **2007**, *99*, 048102/1-048102/4.

57- Salem, A. K.; Searson, P. C.; Leong, K. W. *Nat. Mater.***2003**, *2*, 668-671.

Chapter 2: Synthesis of 2-bromoisobutyrate functionalized crosslinked latex particles by soap-free emulsion polymerization

2.1. Summary

Monodisperse negatively charged crosslinked poly(styrene) latex particles with variable crosslinked densities are functionalized with a 2-bromoisobutyrate moiety, to later serve as an initiator for atom transfer radical polymerization (ATRP), and are synthesised by soap-free emulsion polymerization. The incorporation of the ATRP initiator sites is accomplished by copolymerization of styrene with a functional methacrylic monomer (2-methacryloxyethyl-2'-bromoisobutyrate). This inimer is added either at the start of the polymerization (batch conditions) or through shot addition at later stages of the overall monomer conversion. The incorporation of the ATRP initiator sites is verified by FTIR spectroscopy by monitoring the absorption of the carbonyl functional group, which is present in the ATRP initiator. The polymer latexes that are made using both the batch and shot addition methods show incorporation of the functional monomer. The particle size distribution is controlled with the aid of the ionic comonomer sodium styrene sulfonate (NaSS) as a surfmer. The fabricated 2-bromosiobutyrate polymer latexes are to be used as colloidal macroinitiators for single electron-transfer living radical polymerization (SET-LRP), and to form the basis for the preparation of anisotropic latex particles, which have a complex particle morphology (hairy Janus particles).

2.2. Introduction

Soap-free emulsion polymerization is the chosen method to synthesis the precursor crosslinked poly(styrene) particles, which are subsequently used to fabricate more complex particle morphology; of particular interest is the Janus type morphology. Sub-micrometer, monodisprese and crosslinked poly(styrene) latex particles are intended to be the main characteristics of our particles as these properties will have a major influence on the both the synthesis and the applications of our targeted Janus particles.

Two types of precursor particles are synthesized based on the time of the addition of the co-monomer (2-methacryloxyethyl-2'- bromoisobutyrate), which will be referred to as the inimer, whereby -*ini* is a prefix meaning initiator, in this case for atom transfer radical polymerization (ATRP), and –*mer* stands for a monomer for free radical polymerization. Its dual functionality is employed first to serve as a comonomer in soap-free emulsion free radical polymerization (this is to prepare polymer colloids) and subsequently as an initiator for single electron transfer-living radical polymerization (SET-LRP) (this is to graft polymer brushes onto the particles). This inimer is based on ATRP mechanism, which we selected based on the wide range of types of monomers that can be polymerized by ATRP and the fact that a limited free polymer can be generated due to the absence of an ordinary free radical initiator.

Inimers are based on the other controlled radical polymerization. For example, in the case of RAFT two different methods are used: either the surface immobilization of the conventional free radical initiator or the surface immobilization of the RAFT agent. The drawbacks of RAFT are the usage of the ordinary free radical initiator,

which leads to the formation of a huge amount of free polymers instead of polymer brushes, and the immobilizing of the RAFT agent approach, which is limited to particular surfaces that can be covalently linked with a RAFT agent such as silica, gold and clay mineral surfaces, and also the anchored RAFT agent undergoes surface detachment [1].

Soap-free emulsion polymerization is chosen as the method to prepare the precursor polymer particles as this technique (1) generally affords particles with a monodisperse particle size distribution and (2) does not have large amounts of water soluble or amphiphilic entity impurities that can complicate further seeded polymerization steps. In situ produced oligomeric species of such a nature are easily removed by a simple dialysis step. The absence of a surfactant makes the colloidal stability of the latex particles poor even in the presence of ionic groups such as sulfate, which originates from the water-soluble initiator (potassium persulfate) on the surface of the particles, which aids the electrostatic stabilization.

Hence, small amounts of the ionic water-soluble comonomer (sodium styrene sulfonate) are used to enhance the electrostatic barrier towards coagulation. The additional benefit is that smaller average particle diameters of around 200 nm will be obtained; ordinary soap-free emulsion polymerization gives bigger particles above 400 nm without the usage of the co-ionic monomer [2, 3, 4].

The soap-free emulsion polymerization without a surfmer usually gives a poor colloidal stable latex, and requires more concentration of the per-sulfate initiator to enhance the stability; the rate of the polymerization is slow with only 40% monomer conversion after 10 hours from the commencing of the polymerization, and the rate is enhanced by the addition of $CaSO_4$ as a reducing agent [5, 6, 7].

The emulsion copolymerization of sodium styrene sulfonate with styrene under the normal emulsion polymerization condition in the presence of surfactant has also been studied. It is observed that a very fast copolymerization reaction between styrene and (NaSS) and this is verified by the disappearance rate of (NaSS); the particle size of the latex obtained is very small, around 40 nm, with broad particle size distribution due to the high ratio of (NaSS) used, but it is relatively narrower than the homopolymerization of styrene alone [8].

From the kinetic perspective, Jana and co-workers determined the reactivity ratios for copolymerization of styrene (1) and sodium styrene sulfonate (2), which are r_1 = 0.5 and r_2 = 10, respectively. Based on this the styrene prefers to form the copolymer, but the styrene sulfonate favours the formation of the hompolymer. They found, in addition, that the styrene copolymerization rate is only twice as fast as the homo-polymerization; in contrast, the homo-polymerization rate of styrene sulfonate is 10 times that of the copolymerization with the styrene monomer [9].

From soap-free emulsion polymerization studies of styrene in the presence of sodium styrene sulfonate it is known that the total solid content has to be kept below ca. 20 wt% to prevent coagulation. Moreover, from these studies [8, 9], it appears that the amount of ionic comonomer used needs to be kept low, typically below 2 wt% of the total amount of monomer, in order to obtain a monodisperse particle size distribution. Increasing the amount broadens the particle size distribution due to longer particle formation periods. The use of large relative quantities leads to the formation of amphiphilic polymers that will induce bridging and depletion flocculation/coagulation.

The application of another type of anionic surfmer with soap-free emulsion polymerization has been studied as well; (sodium 1-allyloxy-2- hydroxyl propane sulfonate) is used as a surfmer and is copolymerized with styrene and crosslinked with divinylbenzene (DVB) [2]. The final particle size obtained is in the range of 500-600 nm when this particular surfmer is used. The rate of polymerization increases with similar behaviour as in the case of the presence of the sodium styrene sulfonate; this indicates the surfmer works as the locus of the polymerization.

Moreover, oleic acid is used as a surfmer in soap-free emulsion polymerization of styrene with DVB to obtain monodisperse crosslinked poly(styrene) particles with the carboxyl group on their surfaces [10]. As the concentration of oleic acid increases, the particle size goes down as in typical soap-free emulsion polymerization in the presence of the surfmer.

Xu and co-workers prepared monodisperse thermo-sensitive particles by the soap-free emulsion polymerization of styrene and *N*-isopropyl acrylamide [11]. The particle size decreased as the concentration of water soluble monomer NIPAM increased; similar trends observed in this particular case were when the concentration of KPS increased the particle size decreased and the particle size went down when heated above the LCST, which indicates the thermo responsive character of these particles.

Our goal is to synthesize polymer particles that could be post-modified by grafting water-soluble polymer brushes from their surface. The *tert*-bromine functionality on the precursor latex particles serves as an initiator for second polymerization (surface initiated polymerization). The inimer (2-methacryloxyethyl-2'-bromoisobutyrate) copolymerizes with styrene to incorporate the tertiary bromine functional group with a covalent bond onto the surface of the poly(styrene) particles, which creates a strong

attachment to the particles instead of simply coating the active sites, which might lead to the migration of the initiator sites as in the case of the adsorption of the polymer or surfactant that is contained in a tertiary bromine functional group. The chemical structure of the inimer (**S1**) is depicted below in Scheme 1.

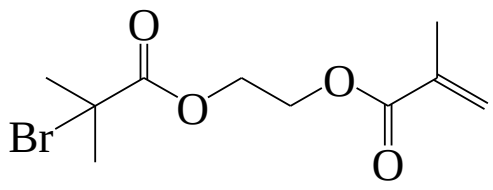

2-methacryloxyethyl-2'-bromoisobutyrate

Scheme.1. Chemical structure of the inimer (S1) (2-methacryloxyethyl-2′-bromoisobutyrate).

This strategy, to incorporate a tertiary or secondary bromine functional group on the surface of the latex particles and then use the latex particles as a surface-initiator for ATRP, has been investigated by several research groups. Guerrini *et al*, functionalized crosslinked polymer latex through the emulsion polymerization of styrene in the presence of typically 20 wt% (on the basis of the total monomer) of 2-(2-bromopropionyloxy) ethyl methacrylate (BPEM). Emulsion polymerizations were carried out using a cationic surfactant, nonionic surfactant and cationic initiator with DVB as a crosslinker [12]. The BPEM was mixed with small amount of DVB and added by the shot addition method after 90 minutes from the onset of the polymerization at which the particle size was 92 nm. The final particle size reached was 104 nm, with no secondary nucleation observed; this indicated that most of the BPEM was copolymerized in the surface regions of the latex particles and the total conversion of the polymerization was 89%. The reason behind their use of a cationic system is their claim that ionic attraction between the anionic latex and positively charged ATRP catalyst is prevented as this will improve the control of the living polymerization and the colloidal stability. The functional latex was used as the

initiator for the surface initiated ATRP of several hydrophilic monomers to form core-shell latex particles, whereby the core was the hydrophobic crosslinked poly (styrene), and the formed water soluble polymer was the shell.

Brooks and coworkers functionalized latex particles with ATRP initiator moieties that contained a chloro-functional group to form poly(*N*,*N*-dimethylacrylamide) brushes in an aqueous medium at room temperature [13]. They synthesized negatively charged latex particles employing 2-(methyl-2-chloropropionato) ethyl acrylate as a functional comonomer in a seeded emulsion polymerization using a poly(styrene) seed 550 nm in diameter. Despite the electrostatic interaction between the ATRP catalyst and the negatively charged latex particles the surface initiated living radical polymerization was successful as a narrow molecular weight distribution was obtained. They extended their investigation by using functionalized latex particles as an initiator for surface initiated polymerization to form hydrophilic block copolymer brushes by aqueous ATRP [14].

Mittal and coworkers investigated several conditions for the incorporation of an acrylic monomer that contained ATRP initiator moiety, which was (BPOEA) (2-(2-bromopropionyloxy) ethyl acrylate) in cross- and non-crosslinked particles prepared by soap-free emulsion polymerization, and without the usage of ionic comonomers [15]. In this study two strategies for the addition of the inimer were studied. The first one was a two-step method wherein initially seed latex particles were formed reaching near complete conversion, after which an inimer was added to polymerize in the surface of the latex particles in a second-step seeded polymerization. As a second approach the inimer was added after approximately 70% monomer conversion, which was referred to as the shot addition method. They observed that in the case of emulsion polymerization of the inimer alone led to coagulation. They

observed that the inimer was not compatible with poly(styrene) latex particles; this indicates that the inimer was not able to swell the latex particles. They suggested that the best condition under which to incorporate the inimer in the surface of the crosslinked particles was the shot addition method of the inimer and with DVB at a high conversion, around 70% monomer conversions. The *tert*-bromine functional particles were also used as a macro-ATRP initiator to grow poly(*N*-isopropylacrylamide) (NIPAM) brushes from the latex particles through ATRP providing the hairy particles with thermoresponsive behaviour [16].

Besides the application of poly(styrene) latex particles as an ATRP initiator, crosslinked poly(methyl methacrylate) latex particles with ATRP initiator moieties were synthesized by soap-free emulsion polymerization and subsequently used as an initiator in surface-initiated polymerization of styrene to form a poly(styrene) shell on the surface of these (PMMA) microgels in toluene as a dispersion medium [17]. It is worth mentioning that in the previous work the inimer was added as a batch addition from the beginning of the soap-free emulsion polymerization; the concentration of the inimer was 5% with respect to MMA concentration.

Conversely, poly(styrene) latex particles grafted with an ATRP initiator were used as a core to grow a shell of poly(methyl methacrylate) and poly(methyl acrylate) to form core-shell latex particles [18]. The core crosslinked poly(styrene) latex particles were prepared by soap-free emulsion polymerization and the formation of an ATRP initiator moiety attained by using the chloromethylation method in THF. The latex that is made by ordinary emulsion polymerization of styrene with the presence of surfactant sodium dodecyl sulfate (SDS) has also been used as an ATRP initiator; the incorporation of inimer (2-(2-bromoisobutyryloxy) ethyl methacrylate) was achieved separately in another polymerization in the presence of crosslinker DVB [19].

Furthermore, a miniemulsion polymerization has been used to functionalize poly (styrene) latex particles with α-chloroester group as an ATRP initiator moiety as a result of the polymerization of styrene and 2-chloropropionyloxyethyl methacrylate in the presence of a reactive surfactant (surfmer) (*N*,*N*-dimethyl-*N*-dodecyl-*N*-2-methacryloyloxyethylammonium bromide) and cationic initiator [20]. This method incorporated the inimer by batch addition as all the monomers were mixed from the beginning of the polymerization and the nucleation of the particles was homogenous since the miniemulsion process was used.

Our particular inimer (**S1**) is used as an initiator for surface initiated polymerization from the surface of silicon wafer substrate to grow poly(styrene), P(MMA) and hydroxyl ethylmethacrylate (HEMA) in typical ATRP conditions. Besides the successful usage of the (**S1**) as an inimer, the synthesis of (**S1**) is straightforward and easy; the presence of the ethylene oxide group in (**S1**) makes its formed copolymer on the surface of the latex as an additional source of colloidal stability as non-ionic moieties are present on the surface.

As the latex particles need to be crosslinked because of the synthesis and application reasons for the ultimate Janus particles, with regards to the synthesis, the latex has to be crosslinked to induce phase separation to generate the Janus particles, and with regards to the application the particles will be used in the organic solvent environment; therefore, the particles have to be stable and not soluble in this solvent.

In our research a crosslinker DVB (divinylbenzene) been used at various concentrations from almost 8% to 1% based on the total styrene concentration. The usage of high concentrations of DVB in emulsion polymerization leads to gel formation and this cause the latex particles to coagulate; consequently, a small

amount of DVB is usually used as this small amount is sufficient to crosslink most of the particles [21,22]. Here soap-free emulsion polymerization is used to fabricate several types of monodisperse poly(styrene) latex particles, based on the time of the addition of the inimer, crosslinked density (DVB concentration) and comonomer (sodium styrene sulfonate), in order to find the best latex particles that can be served to synthesize our targeted Janus particles.

2.3. Experimental Section

2.3.1. Materials

Tetrahydrofuran (99.9% inhibitor free, Aldrich), 2-HEMA (2-hydroxy ethyl methacrylate (97%, Aldrich) is purified by passing it through a column of basic alumina, Triethylamine,(anhydrous, Fisher Scientific), 2-bromoisobutyryl bromide, (98%, Aldrich), dichloromethane (Fisher Scientific), Sodium sulphate, (Anhydrous, fisher Scientific), Styrene (99%, Fluka) is purified by passing it through a column of basic alumina, DVB (mixture of isomers 80%, Aldrich) is purified by passing it through a column of basic alumina, 4-Styrene sulfonic acid, sodium salt (NaSS, Aldrich), Potassium persulfate (KPS, 99%, Fluka)

2.3.2. Synthesis of (2-Methacryloyloxyethyl- 2´- bromoisobutyrate) (inimer).

2-Methacryloxyethyl-2´-bromoisobutyrate (inimer) is synthesized according to the procedure in the literature [23]. 200 mL of anhydrous THF is placed in a dry one-neck round bottom glass flask that contains a magnetic stir bar. 4.24 g (32.6 mmol) of 2-HEMA and 3.30 g (32.6 mmol) of triethylamine are added to the flask. The glass flask is closed with a rubber stopper, and the mixture is cooled to 0 ºC using a water/ice bath. 8.74 g (38mmol) of 2-bromoisobutyryl bromide is added dropwise using a syringe. After the addition, the mixture is allowed to warm to room temperature overnight. The mixture is washed with water and no phase separation is

observed; based on this, in order to collect the product the organic layer is separated by washing the mixture three times with 100 mL of dichloromethane or diethyl ether. The organic layer is dried over anhydrous $NaSO_4$, and then the solvent mixture is evaporated at 40°C by using a rotary vapour. A viscous yellowish liquid with a yield of 95% is obtained. The inimer is characterized by NMR: ^{1}H NMR (300 MHz, $CDCl_3$) δ (ppm) 1.85 (S,3H), 1.90 (S,6H), 4.35 (S,4H), 5.55 (S,1H), 6.15(S,1H).^{13}C NMR (300 MHz) in $CDCl_3$ δ (ppm) 170.8 (2C, C = O), 135.18 (1C, **C**= C), 125.65 (1C, C = **C**), 62.9 (1C,O-CH_2-**C**H_2-O-), 62.5 (1C,O-**C**H_2-CH_2-O), 54.72 (1C,Br-**C**), 29.68 (2C, **C**H_3-C-**C**H_3), 17.58 (1C, **C**H_3-C=C). Mass spectrum: m/z = 303.0, the theoretical value is 301.8 g.moL^{-1}.

2.3.3. General procedure for the synthesis of 2-bromoisobutyrate functionalized crosslinked poly (styrene) latex particles

Soap-free emulsion polymerizations are performed in a 250-mL glass reactor, which is connected to the water thermostat to control the temperature inside the reactor via the water circulation. The reactor is equipped with a Teflon stirrer and two inlets, which are closed by using rubber stoppers to allow the system to be degassed with nitrogen and samples to be withdrawn during the polymerization. 180 g of distilled degassed water is placed in the reactor, followed by the addition of a mixture of 20 g of styrene; various amounts of DVB and 4-styrene sulfonate sodium salt are added based on the required crosslinked density, particle size and colloidal stability. This mixture is mixed at a speed of 250 rpm for 30 min under degassing and then heated to 70ºC. When the temperature becomes stable at 70ºC, 0.075 g of KPS (potassium per sulfate) is dissolved in 10 mL of degassed water added using a syringe. The polymerization time varies from latex to latex from 4 to 24 hours. 1.0 or 2.0 g of the inimer is added using the addition method; if it is the batch addition method, it is

added at the beginning along with styrene, and, if it is the shot addition method, it is added with DVB and 5.0 g of water as a degassed emulsion usually after 150 min from the beginning of the polymerization. White milky latex is obtained and no huge amount of coagulation is observed in the reactor. The conversion is determined gravimetrically by withdrawing samples at certain times from the onset of the polymerization. The latexes are dialysized by placing the latex inside a dialysis tube for two weeks with daily replacing of the water phase.

In the case of the latex (PS-31) a seeded emulsion polymerization is performed as follows: 100 g of seed latex (PS-23) is placed in one neck round bottom flask, and then 0.523 g of styrene, 0.150 g of DVB, 1.25 g of (S1) and 10 mL of water. Next the mixture is degassed for 30 min and after that the temperature of the flask is increased to 70°C and, when the temperature becomes constant at around 70°C, 0.0231 g of KPS is added, which is dissolved prior to the addition in 5.0 mL of degassed water.

2.3.4. Apparatus

Particle size determination by dynamic light scattering (DLS): (Zetasizer Nano model number ZEN 3600) is used to determine the particle sizes and particle size distribution. The laser is the light source (red laser 633 nm) and the detector position is at 173º (backscatter detection). The data is analyzed as intensity particle size distribution. The measurement is performed by putting one or two drops of the concentrated sample in 10 to 15 ml of water; after this 2 to 3 ml of this dispersion is transferred to the polystyrene cell to perform the measurement at 25ºC.

Zeta potential and mobility measurements: (Zetasizer Nano model number ZEN 3600) is used to measure the zeta potential and mobility of the latex particles by placing the dilute latex emulsion in the zeta cell and then the measurement is carried out.

Scanning Electron Microscopy (SEM): Zeiss Supra-55VP SEM is used. The sample is prepared by placing a drop of diluted latex onto the surface of a silicon wafer and then it is kept to dry for one day. After this the samples are coated with either gold or platinum by using a sputter coater. The accelerating voltage used is between 5 to15 KV.

2.4. Results and discussion

Two strategies are employed to provide latex particles with initiator moieties suitable for ATRP, namely the introduction of the inimer from the start of the emulsion polymerization process (batch addition) versus the addition of the inimer, preferentially with a small amount of crosslinker monomer, after the intermediate overall monomer conversion, typically of around 70%, a method we refer to as the shot addition method.

We, therefore, carry out two series of emulsion polymerizations in which (**S1**) is employed as an inimer. The effect of the presence of sodium styrene sulfonate in the soap-free emulsion of styrene has been studied by several research groups in extensive detail, such as El-Aasser *et al*, studied the effect of sodium styrene sulfonate on the kinetics of the soap-free emulsion polymerization of styrene. They observed that the rate of the polymerization increases in the presence of sodium styrene sulfonate; this is attributed to the increase in the number of particles when sodium styrene sulfonate is used. At lower concentrations of sodium styrene sulfonate a monodisperse latex particle size is obtained and a broader particle size distribution at higher concentrations of sodium styrene sulfonate. Based on this, it

was proposed that at lower concentrations of styrene sulfonate the mechanism is a homogenous nucleation, and at higher concentrations of (NaSS), the free water soluble poly(styrene sulfonate) functions as the locus of the polymerization; therefore, both mechanisms of nucleation observed homogeneity and heterogeneity at higher concentrations of styrene sulfonate [3,24].

It is important to point out here that in their study a redox initiation system of sulfate/bisulfate was used, and in our study a thermal decomposition of potassium persulfate at 70ºC is the source of the free radicals. The increase in the rate of emulsion polymerization is explained by the mechanism proposed by Smith-Ewart, whereby the rate of the emulsion polymerization increases with particle number density as follows in equation (1) [25, 26]:

$$R_p = k_p N_p [M_p] \frac{n}{NA} \qquad (1)$$

Where R_p = the whole rate of the polymerization, k_p = the rate constant of the propagation, N_p = the particle number density, $[M_p]$ = the monomer concentration in the growing particles, n = the average number of radicals per particles and *NA* = Avogadro's number. Based on this the rate of the emulsion polymerization of styrene depends on the total concentration of the monomer-swollen latex particles and hence the number of particles.

In typical emulsion polymerization, there are three regions or intervals to describe the rate of polymerization. The first one is at the beginning of the polymerization when the nucleation of the particles takes place and the rate of the polymerization is high. As all the particles are formed, the rate stays constant due to the constant

concentration of monomer inside the latex particles; this is the second region when the growth of the particle occurs and the third region is when the monomer concentration inside the latex particles declines and then the rate of polymerization decreases. There is another factor behind the higher rate of the polymerization in the presence of sodium styrene sulfonate, which is the gel effect, which occurs early in soap-free emulsion polymerization. Let us consider, for example, one latex particle: when the conversion increases, the molecular weight and the viscosity inside the latex particles become high and this leads to a decrease in the number of termination reactions inside the latex particle due to the slow diffusion of the polymeric radicals inside the latex particles. This phenomenon is enhanced by the ionic association of sulfate groups, which make the diffusion slower and, therefore, there is a lower rate of termination and this leads to an increase in the rate of propagation, which leads to the overall rate increasing in the polymerization, as shown in equation (1).

The proposed mechanism for particle growth in soap-free emulsion polymerization of styrene in the presence of sodium styrene sulfonate has three steps [3].

1- Initiation of the water-soluble oligomeric radical of poly(styrene sulfonate) and poly(styrene) and the copolymer.
2- Growth of the oligomeric radicals until they become insoluble and precipitate to form nucleuses (primary particles).
3- Coagulation of primary particles to form the final particles. This step is crucial for determining the final particle size, whereby with a high concentration of sodium styrene sulfonate the primary particles are very stable and, therefore, the rate of coagulation of the primary particle decreases, leading to a smaller particle size and wider particle size distribution; with a lower concentration of sodium styrene sulfonate the

particle size is bigger due do the tendency of the primary particles to coagulate and, therefore, a monodisperse distribution is obtained due to the shorter nucleation period.

Here in our research the obtained latexes, which have been synthesized by soap-free emulsion polymerization, are divided in two categories based on the addition time of the inimer. Table 1 shows a summary of the ingredients used, obtained total solid for each particular polymerization and total polymerizations time for each latex made by the batch addition method of the inimer. Each polymerization attains different monomer conversion, this is recognized as each latex has different overall total solid, since constant amount of styrene and water were used, and it is expected to have a total solid of 11.11% in case of 100% monomer conversion.

Table.1. Summary of the ingredients used in soap-free emulsion polymerization using the batch addition method, and some characteristics of the polymerization such as total solid content (T.S%) and the polymerization time. The amount of KPS used is 0.075 g with the exception of (PS-23) where 0.082 g is used; (S1%) = the inimer concentration relative to the total styrene used**.**

Latex	NaSS %	DVB %	Buffer %	S1 %	T.S%	Polymerization time (min)
PS-10	**0.50**	**6.00**	0.0	0.0	11.4	240
PS-23	**0.295**	**2.87**	0.79	0.0	6.5	300
PS-18	**0.50**	**6.43**	0.0	5.2	5.8	240
PS -21	**0.30**	**7.48**	0.0	5.37	4.2	240
PS-24	**0.257**	**2.60**	0.62	5.12	8.7	240
PS-26	**0.272**	**1.00**	0.49	5.0	7.0	285

Tables 2, 3 and 4 contain summaries of the latexes' characteristic properties, such as particle size, particle size distribution and zeta potentials of the particles produced by using the batch addition method with various degrees of electrolyte concentration in

order to examine the particles' colloidal stability before using them as seeds in further polymerizations, as in SET-LRP and seeded emulsion polymerization.

It is apparent from the tables that when the concentration of surfmer (NaSS%) decreases by half, as in the case of (PS-21), (PS-23), (PS-24) and (PS-26), the particle size increases from around 150 nm, such in the case of (PS-10) and (PS-18) to above 200 nm, and this is attributed to the lower concentration of surfmer used in these cases whereby the primary latex particles are less stable and coagulate to form larger particle sizes during the nucleation period of the soap-free emulsion polymerization. However, when the concentration of surfmer is high the primary nucleus latex particles are stable enough and the growth of these particles leads to the formation of relatively smaller particle sizes and a broader particle size distribution due to the longer nucleation period. Figure 1 shows the growth of the particle size with time during the soap-free emulsion for some polymerizations for both the batch and shot addition methods.

Table.2. Summary of the latexes characteristic properties without the addition of the electrolyte solution of NaCl; the latexes are prepared by soap-free emulsion polymerization using the batch addition method, PDI (particle distribution index).

Latex	Particle (diameter) (nm)	PDI	Zeta potential (mV)	Mobility (µm.cm)/(v.s)	Conductivity (mS/cm)
PS-10	158	0.003	-49.2	-3.90	0.012
PS-23	240	0.011	-44.6	-3.40	0.012
PS-18	148	0.020	-47.7	-3.75	0.015
PS -21	223	0.008	-44.5	-3.50	0.028
PS-24	202	0.024	-41.4	-3.30	0.025
PS-26	261	0.027	-39.8	-3.10	0.044

Table.3. Summary of the latexes characteristic properties with the addition of 0.1M electrolyte solution NaCl; the latexes are prepared by soap-free emulsion polymerization using the batch addition method**,** PDI (particle distribution index).

Latex	Particle (diameter) (nm)	PDI	Zeta potential (mV)	Mobility (µm.cm)/(v.s)	Conductivity (mS/cm)
PS-10	629	0.509	-29.9	-2.35	5.41
PS-23	229	0.046	-43.3	-3.50	5.31
PS-18	175	0.360	-52.5	-4.10	5.52
PS -21	768	0.960	-44.9	-3.50	5.53
PS-24	200	0.024	-35.5	-2.80	5.90
PS-26	259	0.002	-39.1	-3.10	5.16

Table.4. Summary of the latexes characteristic properties with the addition of 0.4M electrolyte solution NaCl; the latexes are prepared by soap-free emulsion polymerization using the batch addition method, PDI (particle distribution index).

Latex	Particle (diameter) (nm)	PDI	Zeta potential (mV)	Mobility (µm.cm)/(v.s)	Conductivity (mS/cm)
PS-10	Coagulation	Coagulation	Coagulation	Coagulation	Coagulation
PS-23	2280	0.607	-28.9	-2.30	18.5
PS-18	5300	0.636	-27.5	-2.20	16.5
PS -21	Coagulation	Coagulation	-23.9	-1.90	18.0
PS-24	2450	0.137	-23.0	-1.80	22.0
PS-26	263	0.018	-23.6	-1.80	18.0

From Figure 1, the latexes (PS-10), (PS-18) and (PS-20) are polymerized with 0.5% concentration of surfmer relative to the total amount of styrene and the particle size is smaller compared to those polymerized with lower concentrations of surfmer at

around 0.25% concentration as in (PS-21, PS-23 and PS-25), which have a bigger particle size.

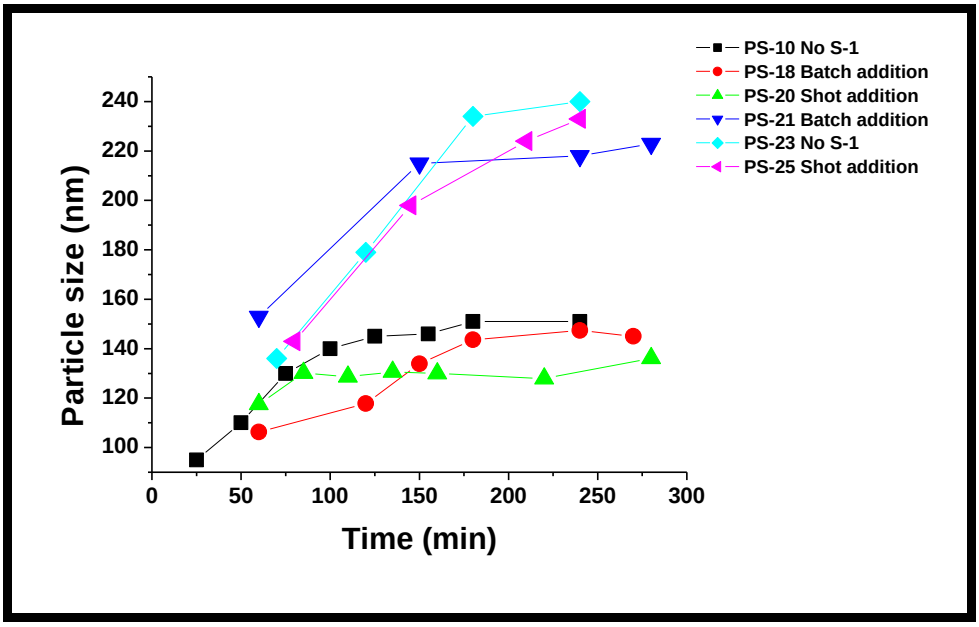

Fig.1. Growth of the particle diameter versus time for the soap-free emulsion co-polymerization of styrene with Sodium Styrene Sulfonate (NaSS), Inimer (S1) and DVB.

The latexes prepared using the batch addition method show good colloidal stability with zeta potential above (-40 mV). The latexes also differ from each other in terms of the concentration of crosslinked density inside each latex particle as the concentration of DVB varies in each polymerization in order to examine the effect of the crosslinked density in the formation of the new domain as a result of the second step polymerization (seeded emulsion polymerization). It is interesting to note that the latex that has a lower crosslinked density shows a huge resistance to coagulation even at a higher concentration of electrolyte, as in the case of (PS-26) at 0.4M NaCl.

The latexes produced using the batch addition method are characterized by SEM to compare the particle size that is gained from DLS to that obtained by SEM; the measurements show a good agreement between the two characterization techniques.

Figure 2 shows the SEM images for all the latexes synthesized by soap-free emulsion polymerization using the batch addition method.

From the SEM images, the latexes produced with 0.5% styrene sulfonate have a polydispersed particle size distribution as in the cases of (PS-10) and (PS-18), and a monodispersed particle size distribution as in the cases of (PS-21), (PS-23), (PS-24) and (PS-26) since lower concentration of sodium styrene sulfonate is used and this gives a bigger particle size.

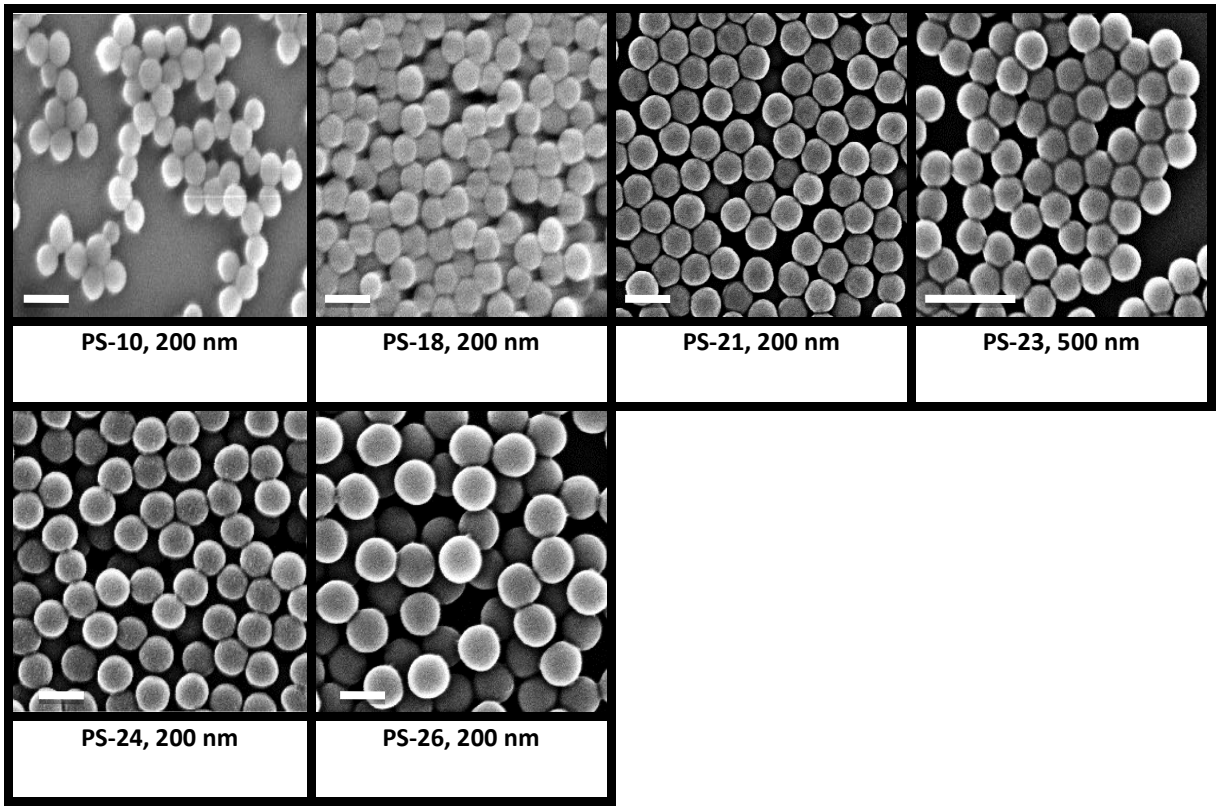

Fig.2. SEM images for all the latexes synthesized by soap-fee emulsion polymerization using the batch addition method; the scale bar in all the images is 200 nm with the exception of PS-23, where the scale bar is 500 nm.

Consequently, the optimum recipe for obtaining monodisperse latex with a smaller particle size, below 300 nm, is a low concentration of styrene sulfonate relative to the concentration of styrene with a fixed amount of KPS. There is no great influence in terms of the concentrations of DVB and inimer on the particle size as in the case

of batch addition, but it might have an effect in terms of obtaining monodisperse latex particles since the presence of the inimer from the inception of the polymerization assists the primary particles to coalesce to form a smaller number of particles, and this cause a bigger particle size and low polydispersity.

It is known from the literature that when the inimer polymerizes alone this forms a coagulum rather than particles [15], and, consequently, in the presence of the primary particles the poly(inimer) will be precipitated on them and this induces the primary latex particles to coalesce [15, 16].

The colloidal stability of the latex that is obtained using the batch addition method is tested with the addition of an electrolyte NaCl to a diluted dispersion of the latex. On the addition of electrolyte with a concentration of 0.1M of NaCl, the latexes (PS-23), (PS-24) and (PS-26) show a very good colloidal stability, whereby the particle size decreases due to the depletion of electrical double layers or stay constant without any remarkable changes; the polydispersity also remains low, below 0.05.

Moreover, this trend is also observed when the latex is treated with 0.4M of NaCl electrolyte; (PS-23) and (PS-24) have a lower coagulation rate in contrast to the other latexes, which show substantial coagulation. (PS-26) has a significant colloidal stability against the addition of electrolyte. The potential reasons behind the good colloidal stability of these latexes are that all of these latexes have 0.25% of surfmer and most of latex particles are monodisperse, and all of them have lower concentrations of DVB. The essential characteristic of these latexes as opposed to the other latexes, which show lower stability, is the presence of the buffer during the polymerization, which decreases the protonation of styrene sulfonate and keeps it

stable with a negatively charged surface; this make the latexes relatively tolerant to the presences of the electrolyte.

FTIR is carried out in the dry solid latex to verify the presence of the copoly(S-NaSS-S1-DVB) (copolymer of styrene–styrene sulfonate- 2-methacryloxyethyl-2́-bromoisobutryrate-DVB). The FTIR absorptions of several latexes without a copolymer and with the copolymer are presented in Figure 3.

The FTIR assists in identifying a particular vibration of a functional group in the sample as a result of the absorption of the FTIR light at a particular wavenumber, and as in our case the carbonyl functional group is one of the significant groups that have apparent absorption in the range of 1710-1750 cm^{-1}; this absorption should appear in the existing copolymer sample. With samples that do not have this copolymer, there is no absorption at this wavenumber, as in the case of (PS-10) and (PS-23). The nature of the carbonyl bond in this copolymer is in an ester environment; therefore, the range of the expected absorption is 1730-1750 cm^{-1}. Each absorption in Figure 3 shows the finger print of the sharp absorption of the aromatic ring of the benzene that comes from the poly(styrene) at 1602, 1494 and 1452 cm^{-1}, and in the sample that contains the copolymer there is an additional significant absorption in each particular sample, as follows: (PS-18) = 1734 cm^{-1} ,(PS-21) = 1736 cm^{-1}, (PS-24) = 1736 cm^{-1} and (PS-26) = 1737 cm^{-1}, the absorption is in the range of the typical absorption of carbonyl group in ester. This verifies the successful incorporation of the inimer in the surface of the latex particles although the batch addition method is used. In addition, after using the latexes that contain the carbonyl absorption in surface initiated polymerization using the SET-LRP mechanism in an aqueous medium of water soluble monomers, theses latexes are able to initiate the polymerization to grow water soluble polymer brushes, which

changes the physical and chemical properties of these particles as will be discussed in Chapter 4.

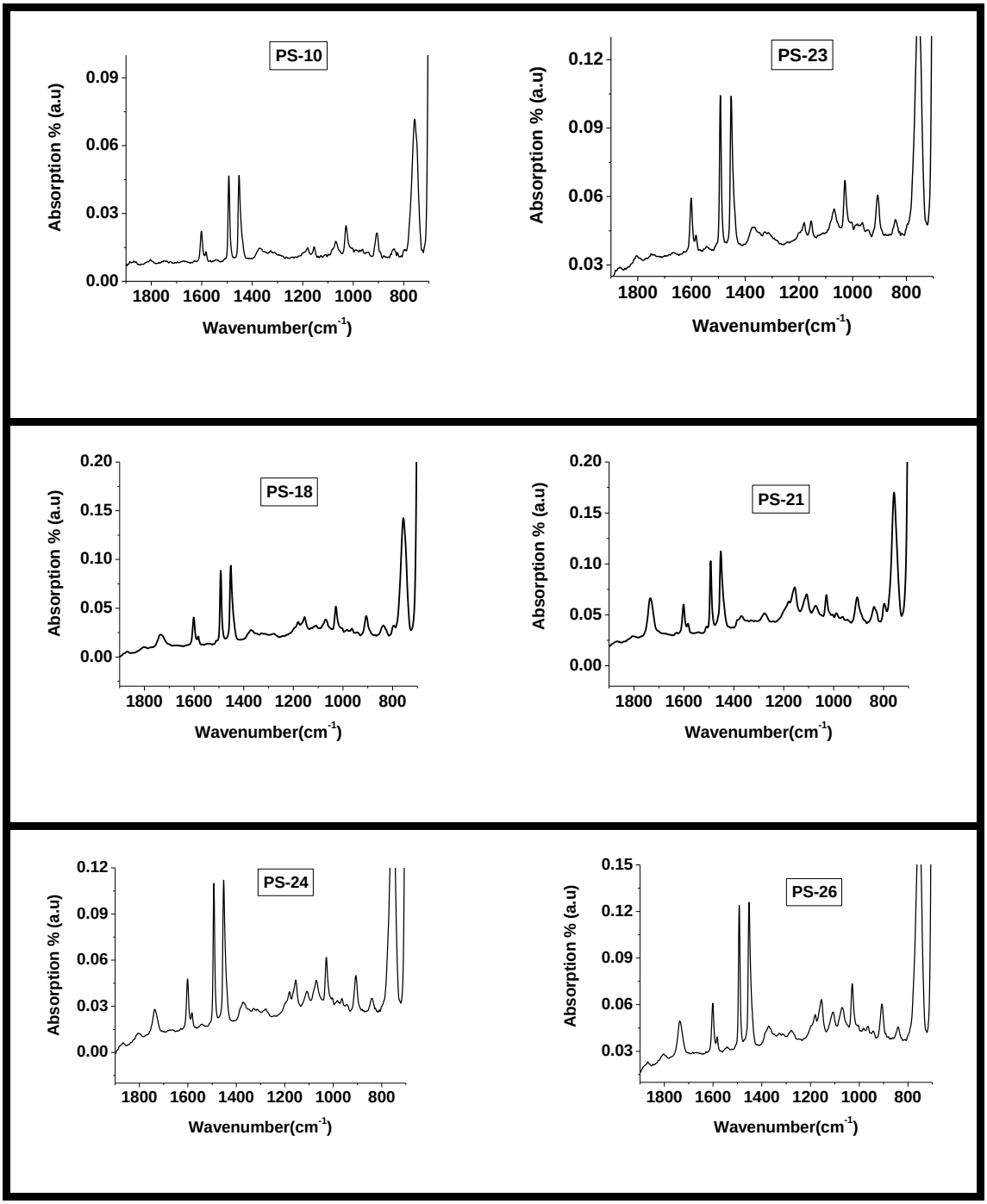

Fig.3. FTIR of the latexes made by soap-free emulsion polymerization in the presence of an inimer in PS-18, PS-21, PS-24 and PS-26 using the batch addition method, and without an inimer as in the case of PS-10 and PS-23.

The second strategy to incorporate the inimer in the surface of the latex particles is when the inimer is added at an elevated conversion when all the particles are formed

and they are at the final stage of their growth. Table 5 gives a summary of the ingredients and the conditions that are used in each particular polymerization using the shot addition method.

Table.5. Summary of the ingredients used in soap-free emulsion polymerization using the shot addition method and some characteristics of the polymerizations such as total solid content (T.S %), time for S1 = time for the addition of S1, PS of S1 = particle size when the inimer is added. The amount of KPS used is 0.075 g with the exceptions of PS-29 = 0.080 g and 0.079 g in PS-30. PS-31* = is a seeded emulsion polymerization by using PS-23 as a seed**.**

Latex	(NaSS) %	(DVB) %	(Buffer) %	(S1)%	Time for S1 (min)	PS of S-1 (nm)	T.S %
PS-20	0.490	**7.49**	0.00	5.00	150	130	8.6
PS-25	0.293	**3.10**	0.58	5.15	150	200	5.0
PS-27	0.284	**1.95**	0.46	5.18	150	150	1.8
PS-29	0.334	**2.55**	0.49	9.74	150	178	5.6
PS-30	0.251	**5.25**	0.62	10.00	160	208	8.0
PS-31*	0.295	**3.62**	0.79	17.8	0.0	0.0	7.8

As in the table above different conditions are used in each polymerization; the major difference in each latex is in the concentration of the DVB. Therefore, each latex has a different crosslinked density.

Additionally, the concentration of styrene sulfonate is extra higher in one position at latex (PS-20). This is the main reason why all the other latexes are bigger in particle size than in the case of (PS-20) with the exception of (PS-27) due to the very low conversion as that indicated by the low total solid content of (PS-27) .

Although there is a low monomer conversion in (PS-27), a particle with a diameter of 156 nm diameter is formed. Therefore, the final diameter of the particles is established at a lower conversion below the 10% monomer conversion, and then the

particle slightly grows to a bigger size. Therefore, the addition of an inimer after 10% conversion is enough to have latex particles with sufficient inimer functionally on the surface of the latex particles, since after this 10% conversion most of the monomer diffuses inside the latex particles and the conversion increases with the polymerization of the styrene inside the latex particles; the inimer will polymerize with itself or copolymerize with styrene and then this polymer attaches to the surface of the latex particles through a covalent bond.

The inimer is added after about 2.0 hours from the beginning of the polymerization after making sure that each entire particle is formed. For instance, in the case of (PS-20) the inimer is added after 150 min, and the particle size of the latex before the addition of the inimer is around 130 nm, and after completing the polymerization the particle size slightly increased to132 nm. The particle size is similar to that before the addition of the inimer at 130 nm and this indicates that most of the remaining styrene is just polymerized inside the latex particles with very small increases in the particle size; the inimer copolymerizes and is precipitated on to the surface of the latex particles with a covalent bond attachment to the latex particles.

In the case of (PS-25), the inimer is added when the latex particle size is 200 nm, and after completing the polymerization, the latex particle size increased to 220 nm with increases of 20 nm after the addition of the inimer. As a low (NaSS) concentration is used, a bigger particle size is produced as in the case of (PS-30), which has a particle size of 230 nm. The latexes particle size, size distribution and surface charge properties (zeta potentials) with different concentrations of electrolyte NaCl are shown in tables 6,7 and 8.

Table.6. Summary of the latexes characteristic properties without the addition of the electrolyte solution NaCl; the latexes are prepared by soap-free emulsion polymerization using the shot addition method, PDI (particle distribution index).

Latex	Particle diameter (nm)	PDI	Zeta potential (mV)	Mobility (µm.cm)/(v.s)	Conductivity mS/cm
PS-20	132	0.029	-41.0	-3.25	0.019
PS-25	220	0.015	-49.9	-3.90	0.030
PS-27	156	0.065	-49.7	-3.90	0.030
PS-29	187	0.013	-45.5	-3.55	0.022
PS-30	230	0.053	-39.5	-3.15	0.013
PS-31*	250+ secondary nucleation	0.003	-37.0	-2.85	0.050

Table.7. Summary of the latexes characteristic properties with the addition of the 0.1M electrolyte solution of NaCl; the latexes are prepared by soap-free emulsion polymerization using the shot addition method, PDI (particle distribution index).

Latex	Particle diameter (nm)	PDI	Zeta potential (mV)	Mobility (µm.cm)/(v.s)	Conductivity mS/cm
PS-20	188	0.402	-39.5	-3.15	5.46
PS-25	215	0.021	-39.2	-3.10	5.13
PS-27	153	0.070	-38.7	-3.00	5.46
PS-29	176	0.033	-37.0	-2.85	5.10
PS-30	1004	1.0	-27.0	-2.65	5.54
PS-31*	245	0.032	-32.8	-2.60	5.04

Table.8. Summary of the latexes characteristic properties with the addition of 0.4M electrolyte solution of NaCl; the latexes are prepared by soap-free emulsion polymerization using the batch addition method, PDI (particle distribution index).

Latex	Particle diameter (nm	PDI	Zeta potential (mV)	Mobility (µm.cm)/(v.s)	Conductivity mS/cm
PS-20	Coagulation	Coagulation	-21.5	-1.70	18.10
PS-25	339	0.205	-28.0	-2.20	17.05
PS-27	158	0.050	-27.5	-2.16	18.25
PS-29	2400	0.555	-25.0	-1.10	18.00
PS-30	Coagulation	Coagulation	-2.10	-0.20	17.0
PS-31*	8900	0.387	-20.9	-1.65	18.0

(PS-25), (PS-27) and (PS-29) show very good colloidal stability with initial zeta potentials of (-49.0 mV) and (-45.0 mV) and, after treating these latexes with the electrolyte solution at a concentration of 0.1M, the particle size just decreases slightly; this suggests that just a small decrease in the electrical double layer occurred. This might be as a result of the lower level of total solid in these latexes, with the exception of (PS-29), which has a higher level of total solid and shows some coagulation when it is treated with the 0.4M electrolyte solution in which its particle size increases to above 2.0 µm. The latex (PS-25) shows a slight increase in the particle size, and the (PS-27) particle size does not change due also to the low level of total solid.

The latexes (PS-20) and (PS-30) have the poorest colloidal stability, whereby both latexes coagulate massively when they are treated with 0.4M electrolyte solution, and they show a substantial increase in their particle size after being treated with 0.1M of electrolyte. The low stability of these latexes might be attributed to the

following: in the case of (PS-20), although the highest concentration of styrene sulfonate is used, a low stability can be explained as a result of three other possible reasons, which are the absence of a buffer in this latex, the polydispersed particle size distribution as shown in the SEM image (see Figure 4) and the high DVB concentration in this latex. In addition, in the case of (PS-30), the fact that it uses the lowest amount of styrene sulfonate, has a bigger latex and a high DVB concentration are the possible reasons for the lowest colloidal stability of this latex.

(PS-31) is prepared by soap-free seeded emulsion polymerization by using (PS-23) as a seed. This seeded soap-free emulsion polymerization shows massive formation of secondary nucleation, and in order to prevent this the seeded polymerization should be performed in the absence of or with a very small concentration of styrene, not as it is used in (PS-31) as described in reference [15, 16]. Despite these secondary nucleation, this latex is further used in this research as in the formation of polymer brushes from their surface and in the swelling and the second stage soap-free emulsion polymerization to see the effect of these small secondary particles and the higher concentration of the inimer on the surface of the latex particles in both the brushes formation and phase separation. Figure 4 shows the SEM images for all the latexes synthesized by soap-free emulsion polymerization using the shot addition method.

From this figure it can be concluded that a monodisperse latex particle that contains an inimer is successfully synthesized by soap-free emulsion polymerization with the exception of (PS-31) when a secondary nucleation takes place. The shot addition of the inimer and DVB after 2.0 hours from the beginning of the polymerization does not cause the formation of a secondary nucleation after polymerizing with the

remaining amount of styrene at this stage of the polymerization at the higher conversion (low styrene concentration) and when all the particles are formed.

FTIR absorptions are performed on dry powdery latexes to verify the incorporation of the inimer in the surface of the latex particles; the FTIR absorptions of these latexes are shown in Figure 5. All the FTIR absorptions show the finger print of the aromatic ring of styrene at 1602, 1494 and 1452 cm^{-1} and the absorption of the carbonyl group as follows: PS-20 = 1734 cm^{-1}, PS-25 = 1736 cm^{-1}, PS-27 = 1737 cm^{-1}, PS-29 = 1735 cm^{-1}, PS-30 = 1737 cm^{-1} and PS-31 = 1735 cm^{-1}.

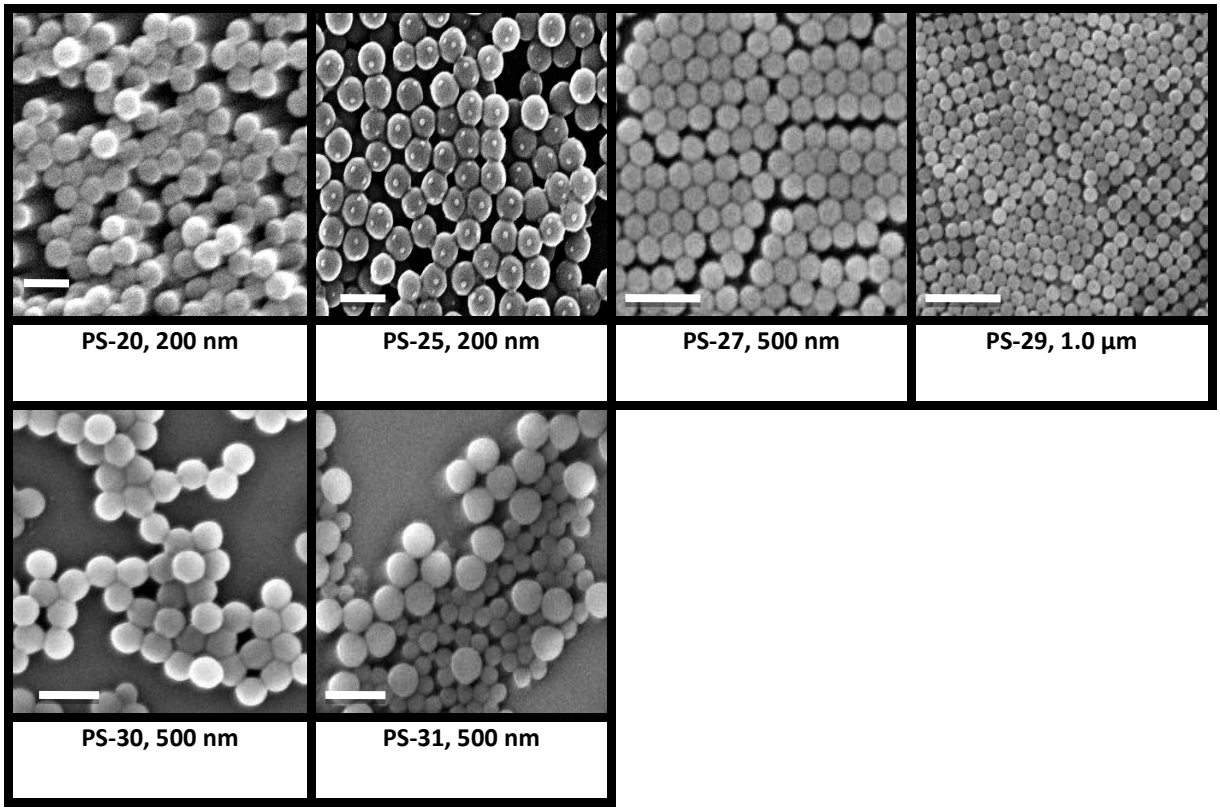

Fig.4. SEM images for all the latexes synthesized by soap-fee emulsion polymerization using the shot addition method; the scale bar is 200 nm in PS-20 and PS-25 images, 1.0 µm in PS-29, 500 nm in PS-27 ,PS-30 and PS-31 images.

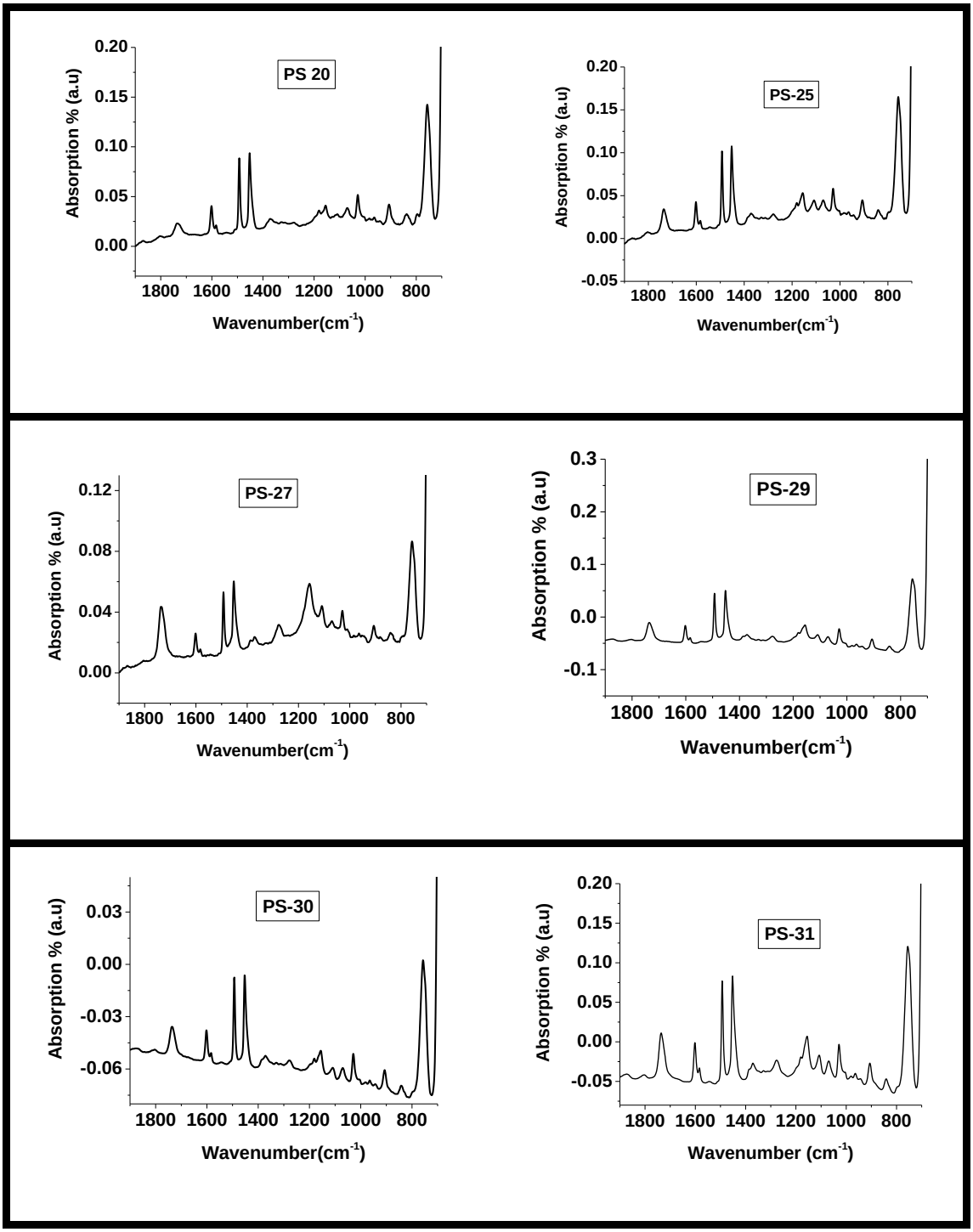

Fig.5. FTIR of the latexes made by soap-free emulsion polymerization in the presence of the inimer using the shot addition method.

2.5. Conclusion

Monodisperse negatively charged poly(styrene) latex particles with different crosslinked network density, which contain a (tertiary bromine) functional group using the batch and shot addition methods, are synthesised by the soap-free emulsion

co-polymerization of styrene, DVB, (2-methacryloxyethyl-2́-bromoisobutryrate), sodium styrene sulfonate and utilizing KPS as an initiator. The optimum level of total solid of the latexes is 11.11%, but due to the non-complete monomer conversion in most of the polymerization the level of total solid is below 11.11%.

The soap-free emulsion polymerization has a moderate rate of polymerization and most of the particles are formed within two hours from the inception of the polymerization. Both the batch and shot addition methods for the inimer show that the (tertiary bromine) functional group is covalently attached to the latex particles, as is verified by FTIR by monitoring the carbonyl group absorption.

Neither method (batch or shot) of inimer has a significant influence on the latex particle size and colloidal stability, in contrast to sodium styrene sulfonate (surfmer), which has a major effect on the latex particle size, particle size distribution and colloidal stability, wherein bigger particle sizes is produced with small concentrations of (NaSS). It is also observed that when the latex has more DVB concentration its colloidal stability decreases and vice versa. The best conditions for having monodisperse latex and good colloidal satiability latex are to use a 0.25% concentration of sodium styrene sulfonate, 0.5% of buffer in the system. The shot addition of (inimer and DVB) should be performed with lowest amount of styrene present in the polymerization mixture to minimize the secondary nucleation. These latexes are ready now to be used as a macro-initiator for SET-LRP as the (tertiary bromine) functional group is present in the outer surface of the latex particles, and for swelling and phase separation experiments to fabricate the targeted hairy Janus particles.

2.6. References

1- Barbey, R.; Lavanant, L.; Paripovic, D.; Schuwer, N.; Sugnaux, C.; Tugulu, S.; Klok, H.-A. *Chem. Rev.***2009**, *109*, 5437-5527.

2- Zhang, L.; Ni, C. *Colloid Polym. Sci.***2007**, *285*, 1637-1643.

3- Kim, J. H.; Chainey, M.; El-Aasser, M. S.; Vanderhoff, J. W. *J. Polym. Sci., Part A: Polym. Chem.* **1992**, *30*, 171-83.

4- Jin, L.; Liu, Z.; Xu, Q.; Li, Y. *J. Appl. Polym. Sci.***2006**, *99*, 1111-1116.

5- Chiu, W. Y.; Shih, C. C. *J. Appl. Polym. Sci.***1986**, *31*, 2117-28.

6- Goodall, A. R.; Wilkinson, M. C.; Hearn, J. *J. Colloid Interface Sci.* **1975**, *53*, 327-31.

7- Goodall, A. R.; Wilkinson, M. C.; Hearn, J. *J. Polym. Sci., Polym. Chem. Ed.* **1977**, *15*, 2193-218.

8- Turner, S. R.; Weiss, R. A.; Lundberg, R. D. *J. Polym. Sci., Polym. Chem. Ed.***1985**, *23*, 535-48.

9- Arunbabu, D.; Sanga, Z.; Seenimeera, K. M.; Jana, T. *Polym. Int.* **2009**, *58*, 88-96.

10- Liu, G.; Liu, P. *Colloids Surf., A, 354*, 377-381

11- Yi, C.; Deng, Z.; Xu, Z. *Colloid Polym. Sci.***2005**, *283*, 1259-1266.

12- Guerrini, M. M.; Charleux, B.; Vairon, J.-P. *Macromol. Rapid Commun.* **2000**, *21*, 669-674.

13- Jayachandran, K. N.; Takacs-Cox, A.; Brooks, D. E. *Macromolecules* .**2002**, *35*, 4247-4257.

14- Kizhakkedathu, J. N.; Kumar, K. R.; Goodman, D.; Brooks, D. E. *Polymer* .**2004**, *45*, 7471-7489.

15- Mittal, V.; Matsko, N. B.; Butte, A.; Morbidelli, M. *Polymer* .**2007**, *48*, 2806-2817.

16- Mittal, V.; Matsko, N. B.; Butte, A.; Morbidelli, M. *Eur. Polym. J.* **2007**, *43*, 4868-4881.

17- Jhaveri, S. B.; Koylu, D.; Maschke, D.; Carter, K. R. *J. Polym. Sci., Part A: Polym. Chem.***2007**, *45*, 1575-1584.

18- Min, K.; Hu, J.; Wang, C.; Elaissari, A. *J. Polym. Sci., Part A: Polym. Chem.* **2002**, *40*, 892-900.

19- Zhang, M.; Liu, L.; Zhao, H.; Yang, Y.; Fu, G.; He, B. *J. Colloid Interface Sci.* **2006**, *301*, 85-91.

20- Taniguchi, T.; Kasuya, M.; Kunisada, Y.; Miyai, T.; Nagasawa, H.; Nakahira, T. *Colloids Surf., B* .**2009**, *71*, 194-199.

21- Funke, W. *Br. Polym. J.* **1989**, *21*, 107-115.

22- Choi, E. C.; Jin, S. M.; Park, Y. J.; Kim, Y. *J. Chin. Inst. Chem. Eng.* **2008**, *39*, 483-488.

23- vonWerne Timothy, A.; Germack David, S.; Hagberg Erik, C.; Sheares Valerie, V.; Hawker Craig, J.; Carter Kenneth, R. *J. Am. Chem.Soc* .**2003**, *125*, 3831-8.

24- Qiu, D.; Cosgrove, T.; Howe, A. M. *Macromol. Chem. Phys.* **2005**, *206*, 2233-2238.

25- Smith, W. V.; Ewart, R. H. *J. Chem. Phys.* **1948**, *16*, 592-9

26- Smith, W. V. *J. Am. Chem. Soc* .**1948**, *70*, 3695-3702.

Chapter 3: Aqueous Solution SET-LRP of water soluble monomers.

3.1. Summary

SET-LRP (Single Electron Transfer-Living Radical Polymerization) of several water soluble monomers such as *N*-isopropyl acrylamide (NIPAM), *N*,*N*-dimethylacrylamide (DMA), poly(ethylene glycol methyl ether acrylate) (PEGMEA) M_n= 454 g/mol, and sodium styrene sulfonate (NaSS) were studied at room temperature in water. Two types of water soluble ATRP initiators with a tertiary bromine functional group identical to the one of our functionalized polymer latex particles were used, (**1**) [2-bromo-2-methylpropionic acid], and (**2**) [1, 2-dihydroxypropane-3-oxy-(2-bromo-2-methylpropionyl)] to examine the effect of the chemical nature of the initiator. PMDETA (*N,N,N',N'',N''*- pentamethyl diethylene triamine) was used predominantly as ligand, in some cases Me_6TREN (tris [2-(dimethyl amino) ethyl] amine) was used. Cu(0) was used in two physical states, i.e. powder and wire, in order to explore the effect on the polymerization. In several cases $CuBr_2$ (Cu(II)) was added to examine its effect and role on the polymerization kinetics. In case of NIPAM, it was found out that the best conditions to obtain on a good agreement between theoretical M_n (number average molecular weight) and experimental values is to use initiator (**2**), PMDETA as ligand, Cu(0) powder and an external amount of Cu(II). In case of (DMA), the obtained experimental M_n is twice larger than theoretical ones. And in case of (PEGMEA), it was found that the best condition that gives very good agreement between theoretical and experimental M_n is when initiator (**2**) was used with PMDETA ligand, and whatever the type of physical states of Cu(0) if the Cu(II) is presented in the polymerization mixture. In

general the polymerizations mixtures do not show very high viscosity, and the polymerization can be performed with usage of Cu(0) wire. Both factors make the colloidal stability not affected and the purification of the hairy latex after SET-LRP much easier.

3.2. Introduction

In this chapter we investigate how SET-LRP (Single Electron Transfer- Living Radical Polymerization) behaves in aqueous system by synthesis of water soluble polymers, before utilizing it as a strategy to modify of latex particles with water soluble polymer brushes. We will look at the mechanism of SET-LRP in water by monitoring the overall rate of polymerization in conjunction with the average molecular weight and its corresponding molecular weight distribution. Catalyst type and concentration (copper/ligand), initiator type and its concentration play a significant role in controlling the polymerization. Understanding how SET-LRP operates in water for the synthesis of water soluble polymers employing a water soluble initiator is crucial to understand some events that may take place in using polymer latex particles as macro-initiator.

Living radical polymerization is based on a free radical polymerization mechanism which at least in relative terms minimizes the amounts of dead polymer chains through radical bimolecular termination (coupling or disproportionation) and chain transfer reactions. The lifetime of chains able to propogate is prolonged by creating a dormant state. This can be done through reversible activation. The three most common technologies are nitroxide mediated radical polymerization, atom transfer radical polymerization (ATRP), and the RAFT (reversible addition fragmentation chain-transfer) process. Control of chain growth (propagation) allows for control of

monomer sequence and chain length. Polymers with narrow molecular weight distributions, variable topologies such as block copolymer, star-polymer, comb-shaped polymers, and chain functionality have been made by applying living radical polymerization methods.

The nature of living radical polymerization methods allows prediction of values for M_n (number average molecular weight) by a simple formula whereby the:

$$M_n = \frac{M_m \times [M]}{[I]} \qquad (1)$$

Whereby M_m = molecular weight of monomer, [M] = monomer concentration, [I] = Initiator concentration. This formula suggests that each initiator molecule is able to initiate and grow one chain of polymer, consequently by manipulating the values on the formula (1) lead to different obtained (M_n), for instance a decrease in the concentration of initiator will decline the average number of growing chains, and as a result of that bigger (M_n) will be gained if good control in the polymerizations was established.

The term living polymer was coined by Szwarc when he performed anionic polymerization of styrene with solution of sodium naphthalenide in THF [1]. The drawbacks of this anionic polymerization are the stringent conditions that should be followed to perform the polymerization, such as the absence of traces of impurities such as water. In the middle of the 1990s, several living polymerizations methods were proposed to be conducted with sensible conditions, for instance, Nitroxide Mediated Radical Polymerization (NMRP), Reversible Addition Fragmentation Polymerization (RAFT) and Atom Transfer Radical Polymerization (ATRP).

The main feature to acquire a control of the molecular weight distribution whereby (M_n) can be predicted and narrow molecular weight distribution is to have a polymerization with rapid activation, and a kinetic chain length which is small relative to the end molar mass; this effectively means that all the polymer chains grow at the same time and with the same rate of propagation keeping termination by combination or disproportionation and chain transfer at low rate. In order to accomplish that the initiation step should be efficient, and the radical concentration should be reduced. Hence, the only possible termination reactions are by addition of species that react with the active radical by reversible termination or reversible transfer to form dormant chain which can be activated later, therefore equilibrium is established among the active radicals and dormant chains, this equilibrium should have more tendencies toward the dormant chains. The living character of the polymerization is determined by the value of the equilibrium constant. In ideal living polymerization the dormant chains concentration is more than the propagating radicals by 6 orders of magnitude in order to shift the equilibrium toward the dormant chain [2].

Based on the type of the species that react with active radicals to form dormant chains, the methods of controlled (living) radical polymerization are categorized into the three main methods which are previously mentioned.

We chose ATRP as the technique to modify the latex particles by grafting from an ATRP initiator moiety on the surface of latex. A short preface of ATRP's principles will be given here. The proposed mechanism for the reversible activation step and propagation in ATRP is illustrated in the scheme 1.

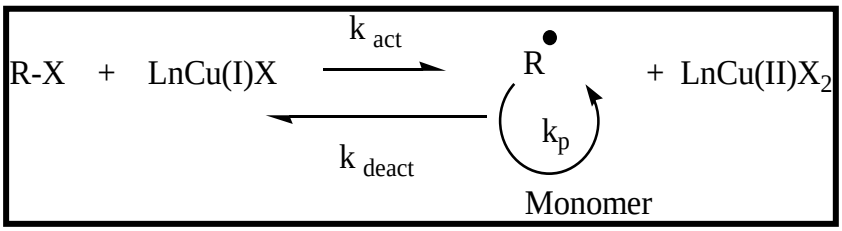

Scheme.1. Basic principle of ATRP.

(R-X) is an alkyl halide (ATRP initiator) which reacts with Cu(I)/ligand complex (LnCu(I)X), the alkyl halid oxidizes the Cu(I) complex to become a Cu(II) complex. This causes the formation of a free radical in the alkyl which can attack the double bond of a vinyl based monomer to undergo monomer addition hereby sequentially forming a polymer chain, intermitted by reversible deactivation placing the growing chain in the dormant state. In the deactivation process, Cu(II) is reduced to Cu(I) by releasing halogen ions which deactivate the polymer chains to be dormant chains, thus this process can be called a (redox) system. The initial term used for ATRP is ATRA (atom transfer radical addition) by Matyjaszewski in 1995 [3], the typical stoichiometry ratios used between the ingredients in that work are as following, alkyl halide with 0.01 equivalent molar ratio to monomer, CuCl with 1.0 equivalent molar ratio to the alkyl halid and ligand with 3.0 equivalent molar ratio to CuCl in order to establish good control for the polymerization. The function of the ligand is to form a coordination complex with the transition metal (Cu), this complex formation changes and often facilitates the position of the redox equilibrium of the transition metal to assist the abstraction of the halogen atom hereby activating the dormant chain. The second role of the ligand is to promote the solubility of the cupper complex in the polymerization medium. The concentration of propagating radical in ATRP is obtained as in equation (2) [2]:

$$[R^{\cdot}] = \frac{K\ [I][Cu(i)]}{[Cu(ii)]} \qquad (2)$$

$$K = \frac{k_{act}}{k_{deact}}$$

K = *equilibrium constant,* k_{act}*= rate constant of activation,* k_{deact} *= rate constant of deactivation*

The rate of propagating (R_p) in normal free radical polymerization is given in equation (3):

$$R_p = k_p\ [M][R^{\cdot}] \qquad (3)$$

k_p *= rate constant of propagation*

By compensation of $[R^{\cdot}]$ in equation 2 into equation 3, the rate of ATRP polymerization is given as in equation (4).

$$R_p = \frac{k_p\ K\ [M][I][Cu\,(i)]}{[Cu(ii)]} \qquad (4)$$

As the rate of the polymerization is expressed as the decrease of the monomer concentration with time as in equation (5):

$$ln\frac{[M]_0}{[M]_t} = \frac{k_p\ K\ [I]\ [Cu(i)]}{[Cu(ii)]}\ t \qquad (5)$$

$[M]_o$ *= initial monomer concentration, and* $[M]_t$ *= monomer concentration at time (t).*

The decrease of monomer concentration in ATRP polymerization should be first-order in monomer concentration, therefore the plot between $ln\frac{[M]_0}{[M]_t}$ and time is linear and that indicates the concentration of propagating radicals is constant during the whole course of the polymerization which means the rate of the termination is suppressed and the dormant chain just grow after certain time of deactivation, and subsequently the molecular weight of the polymer increased linearly with the conversion. The Polydisperseity index (PDI) of ATRP (molecular weight distribution) is given by equation 6:

$$PDI = 1 + \left\{\frac{[I]k_p}{k_{deact}\ [Cu\,(ii)]}\right\}\{\frac{2}{p} - 1\} \qquad (6)$$

From this equation the PDI is narrow with lower initiator concentration, high fractional conversion (p)**,** higher concentration of Cu(II) and rapid deactivation and slower propagation rate. Reverse ATRP involve the presence of ordinary free radical initiator which undergoes decomposition by heat to form free radicals that react with Cu(II) to generate Cu(I) which then reacts with alkyl halide to generate free radicals that react with monomer. ARGET (Atom Regenerated Electron Transfer) ATRP is developed to apply the ATRP in more realistic condition such as the presence of oxygen in the system; it is based on the using of reducing agent such as ascorbic acid which reduces the Cu(II) to form Cu(I) to catalyze the ATRP. In 2006, Percec *et al* [5], proposed a new alternative mechanism for ATRP. They observed that by using Cu(0) in the presence of *N*-containing ligands with an alkyl halide initiator and acrylate, methacrylate monomers in polar solvents, the rate of the polymerization is ultrafast with ultrahigh molecular weight. Scheme 2 illustrates the

proposed mechanism for this polymerization, which was called [single Electron Transfer-Living Radicals Polymerization] (SET-LRP).

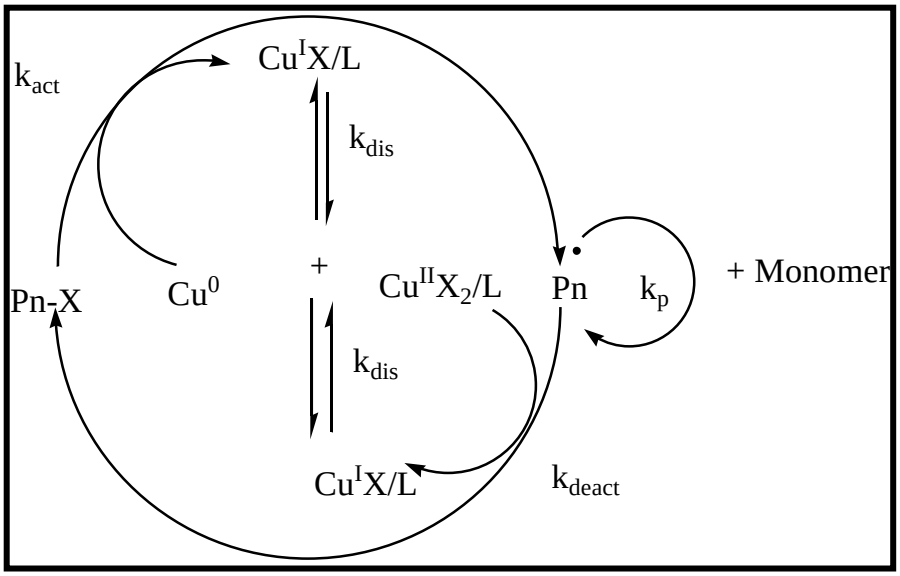

Scheme.2. Proposed mechanism of SET-LRP.

In this polymerization the Cu(0) species complex with the ligand by coordination bonds in the presence of polar solvent and act as electron donors and react with alkyl halide and the dormant chains which both work as electron acceptors. Subsequently the Cu(I) species are formed and spontaneously disproportionate into extremely reactive Cu(II) and Cu(0) atomic species, which mediate the initiation again and the reversible termination to control the polymerization.

The main controversy of (SET-LRP) mechanism is whether the abstraction of a halide atom from the alkyl halide is made by the action of Cu(I) as known in ATRP or by Cu(0) as in case of this new proposed mechanism SET-LRP. Percec *et al*, observed that the SET-LRP occurs under very mild polymerization conditions such as that it can be conducted at room temperature, with the presence of inhibitor and oxygen, using a catalytic amount rather than a stoichiometric amount of catalyst. Cu(0) in wire physical state is used and that enhances the method to remove the

catalyst from the formed polymer. They observed that mixing of Cu(0) with Cu(II) gives better control over the polymerization rather than just using Cu(0) alone, which gives poor control over molecular weight and molecular weight distribution. The higher molecular weight obtained by SET-LRP suggests that a significantly less termination reactions and a much higher rate of polymerization. Another advantage of this process is it can be performed at room temperature which gives fewer side reactions such as chain transfer reaction which lead to branching of the polymer chains.

The use of Cu(0) as metal catalyzed living radical polymerization has been investigated long time before the establishment of the proposed mechanism of SET-LRP. Percec studied that 8 years before of his proposed mechanism of SET-LRP in 2006 [6]. In that work he demonstrated that the usage of Cu(0) with (bpy) (2,2'-bipyridine) and alkylsulfonyl halide, that lead to in situ generation of Cu(I)/Cu(II) catalyst to mediate the polymerization, thus he called it self-regulated living radial polymerization. An induction period was observed in that system which could be removed by addition of a phase transfer catalyst (multidentate acyclic ligand) such as ethylene glycol. This studied system of ATRP is heterogeneous compared to normal catalyst system employing Cu(I) alone. It does give good control of molecular weight and as well as gives high rate of polymerization with smaller amount of required catalyst. Matyjaszewski [7,8] reported the use of Cu(0) in normal ATRP to assist the performing of the polymerization in the presence of air and inhibitor , the action of Cu(0) is to reduce the formed Cu(II) to regenerate the oxidized Cu(I) until all the oxygen and the inhibitor are consumed. These polymerizations show living character such as a low PDI and the first order kinetic of the polymerization whereby a steady decline of monomer concentration with time. In absence of oxygen and/or

inhibitor, the presence of Cu(0) causes the rate of the polymerization to increase due to the decline in the concentration of the deactivator Cu(II). Overall polymerization rate enhancements of up to10 times were observed, maintaining control of the molecular weight distribution. One of the drawbacks of using Cu(0) zerovalent metal is that in the presence of alkyl halide even without the existence of the ligand the polymerization is initiated but by free radical mechanism with uncontrolled molecular weight [9]. The proposed mechanism for the former case is that the metal and the alkyl halide form a complex, and then one-electron transfer from metal to carbon-halogen bond to give the initiating radicals and the halide.

The role of Cu(0) in living polymerization was also studied extensively by Matyjaszewski and coworkers [10]. They observed that the rate of polymerization of Cu(I)/Me_6TREN was significantly faster than systems with Cu(0)/Me_6TREN in DMSO as solvent. Consequently they suggested that the role of Cu(0) is not to initiate the polymerization rather than it works as a reducing agent by regenerating Cu(I) from the accumulated Cu(II). As a result of that the mechanism involving Cu(0) is similar to the (ARGET ATRP).

Percec and Rosen reviewed the SET-LRP and SET-DTLRP (Single-Electron Transfer-Degenerative chain Transfer mediated LRP) [11], the SET-DTLRP is named after the first LRP of vinyl chloride which composed of both SET and DT mechanism, in that review the authors claim that the kinetics of SET-LRP for a given monomer to initiator ratio can be adjusted by solvent concentration, ligand loading level, the surface area of the catalyst Cu(0), change in the initiator structure, addition of deactivator Cu(II) or changing in the temperature. For example, increasing the ratio of monomer concentration to the polar solvent tends to raise the rate of the SET-LRP, same behavior observed with increasing the concentration of the ligand,

and in case of the absence of ligand no polymerization take place. Increasing the surface area of Cu(0) by smaller particles size of Cu(0) particles or with longer Cu(0) wire leads to increase in the rate of the polymerization [12-13].

We are interested in using water as medium (solvent) of polymerization. The underlying reason is that we would like to functionalize waterborne polymer latexes with polymer brushes. Consequently, the SET-LRP process will occur in aqueous environment to functionalize the latex particles by formation of hydrophilic polymer brushes.

The free radical polymerization of water soluble monomers in homogenous aqueous solution has some features compare to that performed in organic solvent, one of these features is that when monomer has an ionizable groups, this monomer polymerizes in aqueous medium with faster rate of the polymerization, in contrast to the normal bulk polymerization and that attributed to increase in the propagation rate constant (k_p) of water soluble monomers in aqueous medium, whereby a water molecule solvates a monomer molecules via hydrogen bond and that alters the electron density of the double bond of the monomer which makes it more reactive [14-15]. Moreover, the electrostatic repulsion between the ionizable growing propagating radicals minimizes the termination reactions which make the polymerization rate faster and instantaneous.

In regard to ATRP, the first attempt to conduct an aqueous solution polymerization of hydrophilic monomer by ATRP was performed with 2-hydroxyethyl acrylate with successful controlled manner [16]. Some side reactions may occur in aqueous ATRP system, for instance, the side reaction of acidic water soluble monomers, such as sodium methacrylate (NaMA), whereby the monomer coordinates with the transition

metal at higher pH or by protonation of the ligand at lower pH which decrease the efficiency of the catalyst. Therefore, optimum pH is necessary for a successful control of the polymerization in aqueous medium [17-18]. Pyridylmethanimine ligand was used in ATRP polymerization of oligo(ethylene glycol) methacrylate (OEGMA)in water at 20 ºC which gives well controlled polymerization under natural pH [19]. Jonsson and coworkers suggested that the faster ATRP kinetics in water of (OEGMA) is due to the higher equilibrium concentration of propagating radicals and to solvent effects as water in this case [20]. Water based ATRP generally tends to show poor living character and that may attributed to polarity effects on the stability of the polymerization intermediates and a competitive coordination of ligand with water molecules to the copper center [21]. Some of the hydrophilic monomers that contain functional group such as (oxyethylene) tend to coordinate with copper as long as the ligand this makes the copper complex more active and therefore a higher polymerization rate [21]. The main side reactions for conducting ATRP in the water is the hydrolysis of the $CuBr_2$, therefore the rate of the polymerization is faster due to the low concentration of the deactivator and subsequently uncontrolled polymer formed .

Here several hydrophilic monomers will be polymerized by SET-LRP condition in aqueous medium, the obtained outcomes from the aqueous polymerization will be used to optimize the conditions that will be used in the surface initiated polymerization from latex particles.

3.3. Experimental section

3.3.1. Materials

2,2-Dimethyl-1,3-dioxolane-4-methanol, 98% (Aldrich), triethylamine anhydrous from (Fisher scientific), KOH pellets (Fisher scientific), anhydrous THF (Aldrich), 2-

bromo-2-methylpropionylbromide, 98% (Aldrich), Na_2CO_3 (BDH), Na_2SO_4 (Fisher scientific), Glacial acetic acid, 60.05wt% (Fisher scientific), Methoxybenzene (anisole), 99% (Aldrich), Diethyl ether, tris (2-aminoethyl) amine, 98% (Aldrich), formic acid, 96% (Sigma-Aldrich), formaldehyde solution, (37%) (Aldrich), chloroform and toluene (Fisher scientific), Copper wire (0.25 mm diameter), 99.999% metals basis, Copper powder for organic synthesis, 99% (Aldrich), Copper bromide, 99% (Aldrich), *N*-isopropyl acryl amide, 97% (Aldrich), *N, N, N′,N″,N″*-pentamethyldiethylenetriamine (PMDETA), 99% (Aldrich), Ethylene glycol, 99% (Aldrich), 2-Hydroxy ethyl acrylate, 96% (Aldrich) was purified by passing it through a column of basic alumina, 4-styrene sulfonic acid sodium salt (Nass, Aldrich), poly(ethylene glycol methyl ether acrylate), Average M_n= 454 g/mol (Aldrich) was purified by passing it through a column of basic alumina), *N, N*-Dimethyl acrylamide, 99% (Aldrich) was purified by passing it through a column of basic alumina, 2-bromo-2-methylpropionic acid (Aldrich).

3.3.2. Synthesis of [1, 2 – dihydroxypropane-3-oxy-(2-bromo-2-methylpropionyl)] (2)

Synthesis of this water-soluble ATRP initiator (**2**) comprised of two steps. The first step synthesized the intermediate compound (**3**) [2, 2-dimethyl-1,3-dioxolane-4-methoxy-(2-bromo-2-methylpropionyl)], and secondly compound (**3**) involved another reaction to create the final compound (**2**). The first step is synthesized the intermediate (**3**). The procedure for the synthesis is described from literature [22]. 2,2-dimethyl-1,3-dioxolane -4-methanol (0.04 mol), and triethylamine (TEA) (0.08 mol) which was dried over KOH pellets prior to use were placed in 100 mL round-bottomed glass flask equipped with a magnetic stirrer. Then, anhydrous THF (50 mL) were placed to the mixture and the flask was cooled to 0°C by using an ice-bath.

2-bromo-2-methylpropionylbromide (0.044 mol) was then added dropwise using a syringe. Then the mixture was stirred for 45 min and allowed to reach to the room temperature. The reaction mixture was then poured into an excess of cold water and extracted using 50 mL of diethylether. The organic layer was subsequently washed with a saturated aqueous solution of Na_2CO_3. The organic layer was then dried over anhydrous Na_2SO_4 .Finally, the Na_2SO_4 was removed by filtration and the solvent was removed by using a rotary evaporator in order to isolate the compound in quantitative yield as slight yellowish oil. ^{1}H NMR (300 MHz , $CDCl_3$) δ 1.30 and 1.38 (s, 6H,OC(**CH$_3$**)$_2$O), 1.90 (s, 6H,C(**CH$_3$**)$_2$Br), 3.75 (dd, 1H,C5**Ha**Hb), 4.05 (dd, 1H,C5Ha**Hb**), 4.15 (dd,1H,C**Ha**Hb), 4.22 (dd, 1H,CHa**Hb**), 4.30 (m, 1H,**C4H**). ^{13}C NMR (300 MHz, $CDCl_3$) δ 24.95 and 26.04 (1C, OC(**CH$_3$**)$_2$O), 30.05 (2C, C(**CH$_3$**)$_2$Br), 54.79 (2C,**C**$(CH_3)_2$Br), 62.36 (1C,**C**5HaHb), 65.55 (1C,**C**HaHb), 72.57 (1C, **C**4H), 109.10 (1C, O**C**$(CH_3)_2$O), 170.79 (1C, C=O). Mass spectrum: m/z = 263.0 and theoretical value is 263.9 g/mol.

The second step is to mix (5.0 g) of compound (**3**) with glacial acetic acid (15 mL) and (40 mL) of water and a catalytic amount of methoxybenzene and stirred for 30 min at 80 ºC. Next the mixture was cooled to room temperature, the aqueous layer was saturated with sodium hydrogen carbonate and 50 mL of diethylether was added. The organic layer was isolated and the aqueous layer was washed with extra 50 mL of diethylether. The crude product, initially yellowish oil, was obtained by removing the diethyl ether from the combined organic layers by rotary evaporation. Crystallization occurred overnight upon standing inside a freezer. The product was recrystallized from toluene. ^{1}H NMR (300 MHz, $CDCl_3$) δ 1.90 (s,6H, C(**CH$_3$**)$_2$Br), 3.60 (dd,1H, C**Ha**OH), 3.65 (dd,1H, C**Hb**OH), 4.27 (m,C**H**OH), 4.20 (dd,1H, C**Ha**Hb), 4.30 (dd,1H, CHa**Hb**), ^{13}C NMR (300 MHz, $CDCl_3$) δ 30.04

(2C,C(**C**H_3)$_2$Br), 62.61 (1C,**C**(CH_3)$_2$Br), 65.8 (1C,**C**H_2OH), 69.3 (1C, **C**H_2OC=O), 76.8 (1C,**C**HOH). Mass spectrum: m/z = 304.9 and theoretical value is 303.9 g/mol.

3.3.3. Synthesis of tris (2-(dimethylamino) ethyl) amine (Me_6TREN)

The modified procedure described in literature was followed [43], as following: In a 250 mL round bottom flask 50.0 mL of tris (2-aminoethyl) amine was added and cooled to 5°C. To this cold mixture 58.0 mL of formic acid was added dropwise by dropping funnel. Note that fumes were observed upon the addition of formic acid. After a waiting period of 10 min the reaction mixture was placed into an oil bath with temperature of 80 °C. Next 54.0 mL of formaldehyde solution (37% aqueous solution) was added to the mixture. The color of mixture turned dark brown and almost black, and after certain period became light brown. The mixture kept at that temperature overnight under reflux. After that the volatile components were removed by rotary evaporation. The pH of the remaining liquid was increased to be above 10 by using aqueous solution of KOH, the oil layer was extracted with chloroform and then dried over $MgSO_4$. The title compound was obtained through rotary evaporation. The product was characterized by ^{1}H NMR (300 MHz, $CDCl_3$) δ 2.15 (s,18H), 2.35 (mt,6H), 2.50 (mt,6H), ^{13}C NMR (300 MHz, $CDCl_3$) δ 45.19, 55.24, 56.98, 76.89. Mass spectrum m/z: 231 and theoretical value is 230 g/mol.

3.3.4. Aqueous solution SET-LRP of several hydrophilic monomers:

Two examples are presented here based on the type of initiator used and the physical state of the Cu(0) that used:

SET-LRP-74: (37.5 mg) of 8.0 cm (0.25 mm diameter) of copper wire was fixed around a magnetic stirrer and placed in a 50 mL round bottom flask, Followed by addition of 0.560 g of *N*-isopropyl acryl amide, 2.3 mg of $CuBr_2$, and 0.20 g of ethylene glycol (to be used

as NMR marker) to the flask. Then 2.0 g of a 0.5 wt% aqueous solution of (2-bromo-2-methyl propionoic acid) (**1**) (equal to 10.0 mg of (**1**)) was added together with 15.0 g of demineralized water. Finally the flask was closed by a rubber stopper and placed on a water bath at 25ºC. The mixture was degassed by purging and bubbling for 30 min by nitrogen gas, the purging was kept during all the whole course of the polymerization with slow rate. Subsequently, 2.0 g of a 2 wt% of degassed aqueous solution of ligand (PMDETA) was added. The samples were withdrawn from the polymerization mixture regularly after specified time to follow monomer conversion.

SET-LRP-179: 21.3 mg of copper powder (platelets shape as seen in SEM image of approximate length and width of 60 and 40 µm respectively) was placed in a 50 mL round bottom flask. Next 0.5417 g of *N*-isopropyl acryl amide was added together with 5.4 mg of $CuBr_2$. Then 0.20 g of ethylene glycol was added to the mixture as ^1H NMR reference for conversion determination. Followed by addition of 0.0212 g of (1,2-dihydroxypropane-3-oxy-(2-bromo-2-methylpropionyl) (**2**) to the flask. After that, 15.0 g of demineralized water was added. Finally the flask was closed by a rubber stopper and placed on a water bath at 25ºC. The mixture was degassed by purging and bubbling for 30 minutes with nitrogen gas, the purging was kept during all the whole course of the polymerization with slow rate. After that 2.0 g of 2 wt% of degassed aqueous solution of ligand (PMDETA) was added. The samples were withdrawn from the polymerization mixture regularly after specified time to follow the conversion.

3.3.5. GPC: Varian 390-LC Gel Permeation Chromatography (GPC) equipped with refractive index as detector and 2X PL gel mixed columns. The mobile phase (Eluent) is 100% chloroform which is a good solvent for Poly(NIPAM), Poly(N,N-dimethylacrylamide) and Poly(PEGMEA). The sample solvent is 95% chloroform

and 5% toluene. The obtained results were calibrated to the poly(methyl methacrylate) with molecular weight range of 690 to 1,944,000 g.mol^{-1}.

3.4. Results and discussion

We investigated the living radical polymerization of *N*-isopropylacrylamide (NIPAM), *N*,*N*-dimethylacrylamide (DMA), poly(ethylene glycol) methyl ether acrylate (PEGMA), and sodium styrene sulfonate (NaSS) in water mediated by Cu(0)/Cu(I)/Cu(II). The polymerization behaviour of these monomers under so-called SET-LRP conditions were studies in order to optimize the conditions for the surface initiated polymerization of water soluble polymer brushes (grafting-from approach) from our *tert*-bromine functionalized polymer latex particles (as prepared in Chapter 2).

3.4.1. Aqueous SET-LRP of *N*-Isopropylacrylamide (NIPAM)

N-isopropylacrylamide was selected as one of the monomers to be polymerized by SET-LRP in water as its polymer shows thermoresponsive behaviour (see chemical structure of NIPAM in Scheme 3). The polymer has a characteristic lower critical solution temperature (LCST) in water of approximately 32°C. Above this temperature phase separation is observed as the hydrogen bonding with secondary amine in the NIPAM is weakened in comparison to hydrophobic attractive forces of the two methyl groups which will enhance upon heating, hereby giving the polymer a more hydrophobic nature at elevated temperatures. This temperature trigger can potentially become useful in tuning the behaviour of our targeted Janus particles.

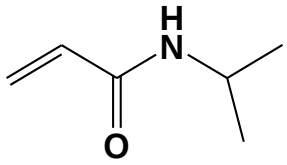

Scheme.3. Chemical structure of NIPAM.

Previous ATRP studies on NIPAM in water carried out at 5°C using methyl-2-chloropropionate as initiator, Me_6TREN:CuCl as catalyst system (molar ratio 1:1), a target number degree of polymerization of 300 and a monomer concentration of 60 wt% lead to fast polymerization, that is near complete conversion in 5 mins, and uncontrolled polymerization as indicated by a poly dispersity index of 8.48 [23]. The use of organic solvents miscible with water as polymerization medium alleviated the issues gaining control of the polymerization [24,25,26]. Note that in addition to poor control in water accompanying concerns regarding the use of NIPAM were raised in that the amide bond may participate in coordination to the transition metal and that halide moiety could be prone to nucleophilic elimination. [24]

An interesting development was reported by Percec and coworkers [27] who used Cu(0) in the form of a wire with Me_6TREN as ligand and was able to successfully polymerize NIPAM and DMA in binary aprotic solvents mixtures such as acetone/water, and binary protic solvent mixtures like methanol/water in controlled manner. Mueller and coworkers polymerized NIPAM in water using 2-bromo-2-methylpropionic acid (**1**) as initiator at 4.0°C. [28] They managed to achieve control of chain growth and thus synthesize polymers with a narrow molar mass distribution by using an additional amount of Cu(II) to control the equilibrium of the reversible activation process. We were interested in living radical polymerizations in water with absence of any co-solvent. We set ourselves the aim not to use organic solvents in the fabrication of our hairy Janus polymer latexes (with the exemption for the

synthesis of our (*tert*-bromine functionalized monomer). The underlying reasons are the ease of preserving colloidal stability of the latex particles in waterborne systems, and the VOC/carbon footprint of industrial scale-up. We used two water soluble *tert*-bromine compounds as initiators, that is 2-bromo-2-methylpropionic acid (**1**), and 2-dihydroxypropane-3-oxy-(2-bromo-2-methylpropionyl) (**2**), their chemical structures are shown in Scheme 4.

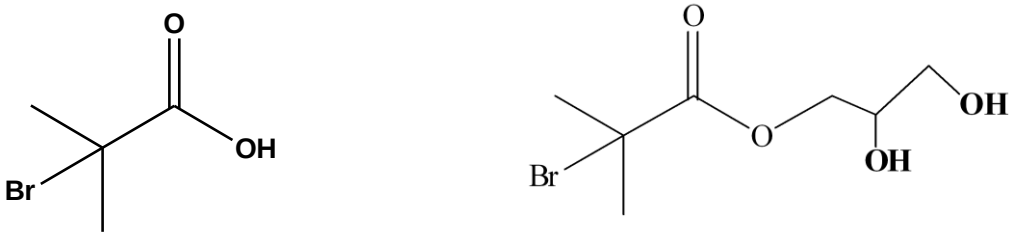

(1) (**2**)

Scheme.4. Chemical structure of the two hydrophilic SET-LRP initiators used, (**1**), 2-bromo-2-methylpropionic acid, and (**2**) 1, 2-dihydroxypropane-3-oxy-(2-bromo-2-methylpropionyl).

We decided to use PMDETA (*N,N,N',N'',N''*- pentamethyl diethylene triamine) (Lig1), and Me_6TREN (tris [2-(dimethyl amino) ethyl] amine) (Lig2) as ligands, the latter associating stronger with the transition metal. [29]

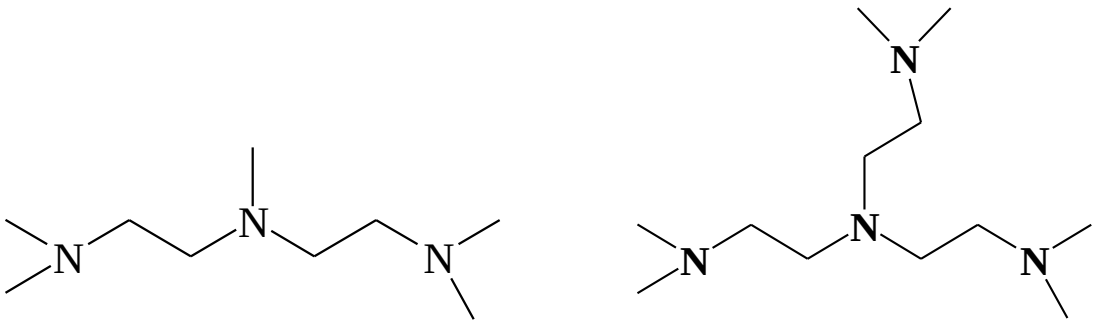

(Lig1) (**Lig2)**

Scheme.5. Chemical structure of the used ligands which in (**Lig1**) is (PMDETA) and (**Lig2**) is (Me_6TREN).

In addition we decided to study the role of the physical state of Cu(0) in the polymerization process. Hence we used Cu(0) in the form of powder and wire as shown in Figure 1. Cu(0) wire with diameter of 0.25 mm and length of 8.0 cm, and Cu(0) powder as platelets shape as seen in SEM image of approximate length and width of 60 and 40 µm respectively. Detailed recipes for the SET-LRP of NIPAM in water are given in Table 1

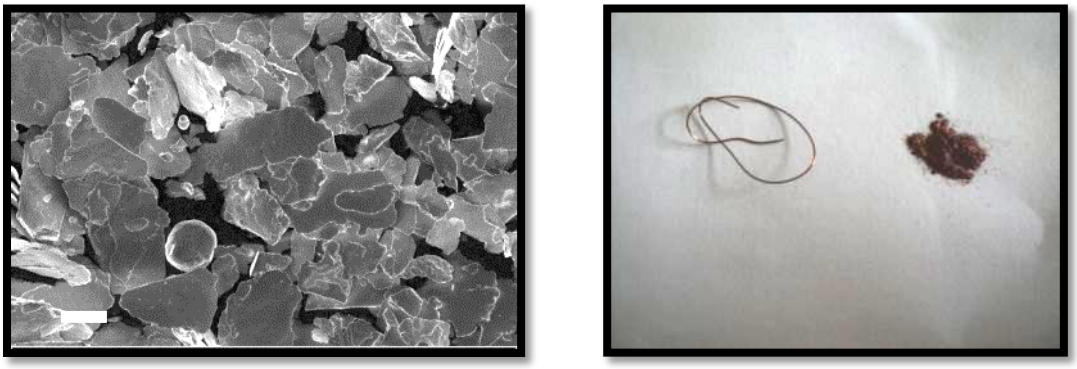

Fig.1. On left is SEM image of the Cu(0) powder (scale bar is 20 µm), and on right is the photograph of Cu(0) wire and powder.

Table.1. Recipes for the SET-LRP of NIPAM in water. $[M_0]$ is the initial monomer concentration, $[I_0]$ initial initiator concentration, [Cu(0)] initial copper (0) concentration, $[CuBr_2]$ initial concentration of copper bromide, [Lig] ligand concentration.

Exp	$[M_0]$/ mol.L^{-1}	Io	[Io]/ mmol.L^{-1}	Lig	[Lig]/ mol.L^{-1}	Cu(0)	[Cu(0)]/ mol.L^{-1}	$[CuBr_2]$/ mmol.L^{-1}
SET-131	0.501	-	0.0	Lig1	0.0136	-	-	-
SET-130	0.519	-	0.0	Lig1	0.0136	wire	0.0342	-
SET-134	0.489	-	0.0	Lig1	0.0136	wire	0.0342	-
SET-129	0.507	2	5.1	Lig1	0.0136	wire	0.0342	-
SET-178	0.286	2	4.9	Lig1	0.0136	wire	0.0342	-
SET- 74	0.296	1	1.76	Lig1	0.0136	wire	0.0342	0.63
SET-75	0.291	1	3.5	Lig1	0.0136	wire	0.0342	0.60
SET-175	0.260	2	5.1	Lig1	0.0136	wire	0.0342	1.81
SET-179	0.282	2	5.2	Lig1	0.0136	Powder	0.0197	1.36
SET- 94	0.247	1	3.0	Lig2	0.0144	wire	0.0342	0.69

The overall rate of polymerization was followed by monitoring the consumption of monomer relative to an internal inert standard, which is ethylene glycol, using ^{1}H NMR spectrometry. A typical ^{1}H NMR spectrum obtained is depicted in Figure 2, which is entry (SET-179) in Table 1. The ^{1}H NMR of (SET-1791) shows the protons that present in NIPAM which are as the following : ^{1}H NMR (300 MHz, D_2O) δ1.2 (d,6H), 3.8 (m,H), 7.9 (d,1H), 6.2 (t,1H), 5.6 (d,2H), and the reference (inert) protons resonances of ethylene glycol in D_2O at 3.5 (s,2H) and 1.8 (t,OH), the protons resonances of the initiator (**2**) is duplicated by the NIPAM and ethylene glycol protons, and the broad proton of H_2O at δ 4.5.

The samples were withdrawn regularly to monitor the decline in the vinyl protons of NIPAM at δ 6.2 (t,1H) and 5.6 (d,2H), the formation of the poly(NIPAM) broad proton resonance at 3.8 (s, 1H). The (SET-1796) ^{1}H NMR resonances shows that the disappearance of vinyl protons of NIPAM at δ 6.2 (t,1H) and 5.6 (d,2H) and the formation of the poly(NIPAM) broad proton resonance at 3.8 (s,1H), this indicate the full monomer conversion of the NIPAM polymerization by SET-LRP polymerization, the protons resonance at δ 2.3 (s,15H) and 2.55 (t, 8H) are belong the ligand PMDETA.

The monomer conversion was calculated by integrating the peak at 5.6 ppm identified as one of the vinyl groups of NIPAM and the peak at 3.5 ppm identified as the combined signal for the methylene groups in ethylene glycol. Overall monomer conversion, X_M, is calculated taking the ratio of the ^{1}H NMR intensity at of vinyl proton ($I_{\text{-}CH=}$) to the intensity of the ethylene glycol ($I_{\text{-}CH_2CH_2\text{-}}$) at zero hour from the polymerization and at time (t) from the beginning of the polymerization as shown in equation (7) .

$$X_M = \frac{\left(\frac{I_{HC=}}{I_{-CH_2CH_2-}} \right)_t}{\left(\frac{I_{HC=}}{I_{-CH_2CH_2-}} \right)_0} \quad (7)$$

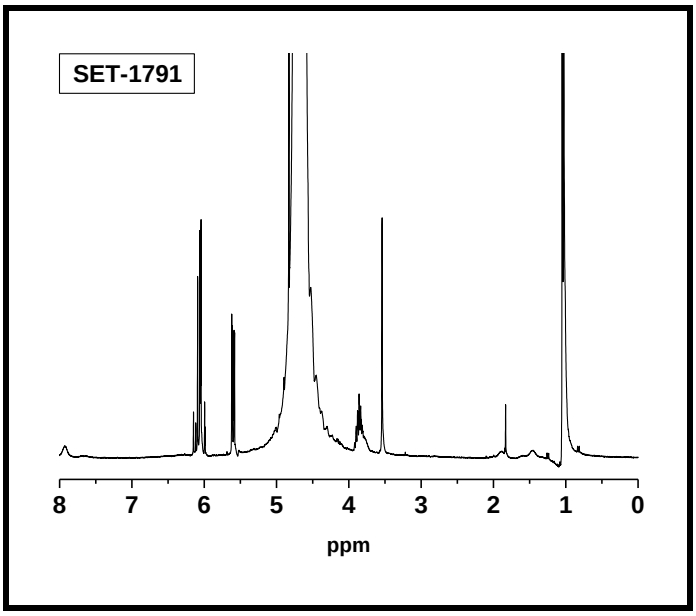

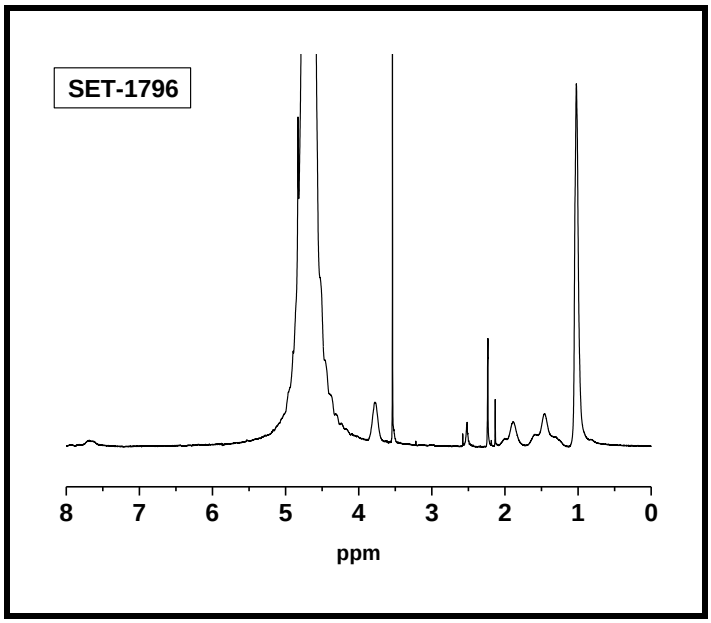

Fig.2. ^{1}H NMR spectrums of polymerization mixture in D_2O before the addition of the ligand (SET-1791), and after 180 mins from the addition of ligand (SET-1796).

Since SET-LRP reactions of NIPAM in water were sparingly reported in literature, often with conflicting results, we decided to carry out several reference polymerizations, this to investigate the role of each of the reagents in the system. In experiment SET-131 no halogen initiator nor Cu(0) were used, thus just the monomer (NIPAM), water, and ligand were present in the polymerization flask. Surprisingly NMR analysis found that approximately 8% of monomer was consumed within 30 mins, after which no further consumption was observed (see Figure 3 for X_M versus time data.

It is important to note that the sample at t = 0 min was taken before the addition of ligand, in the present case PMDETA. No formation of polymer was detected by NMR analyses. The molar ratio of *tert*-amine groups originating from PMDETA and vinyl groups in NIPAM monomer sums up to 8.15%, which is in striking agreement with the determined monomer conversion. An explanation would be that PMDETA catalysis a hydrohydroxylation of NIPAM, in a similar manner as the hydroalkoxylation reactions reported by Connon et al [30] as shown in scheme 6. However, the PMDETA here is used in a catalytic manner, which would not explain why NIPAM is not fully consumed. It could be that the tert-amine group does add in a Michael addition type of way to the vinyl group of the NIPAM and then undergoes methanol elimination instead of hydroxide addition. This would lead to consumption of the *tert*-amine groups and would lead to the observed result. It is important to note that this second reaction preserves the *tert*-amine character of the ligand in that it effectively replaces a methyl group for a NIPAM derived substituent. The modified ligand would still be capable of catalyzing the SET-LRP reactions, which indeed is observed later.

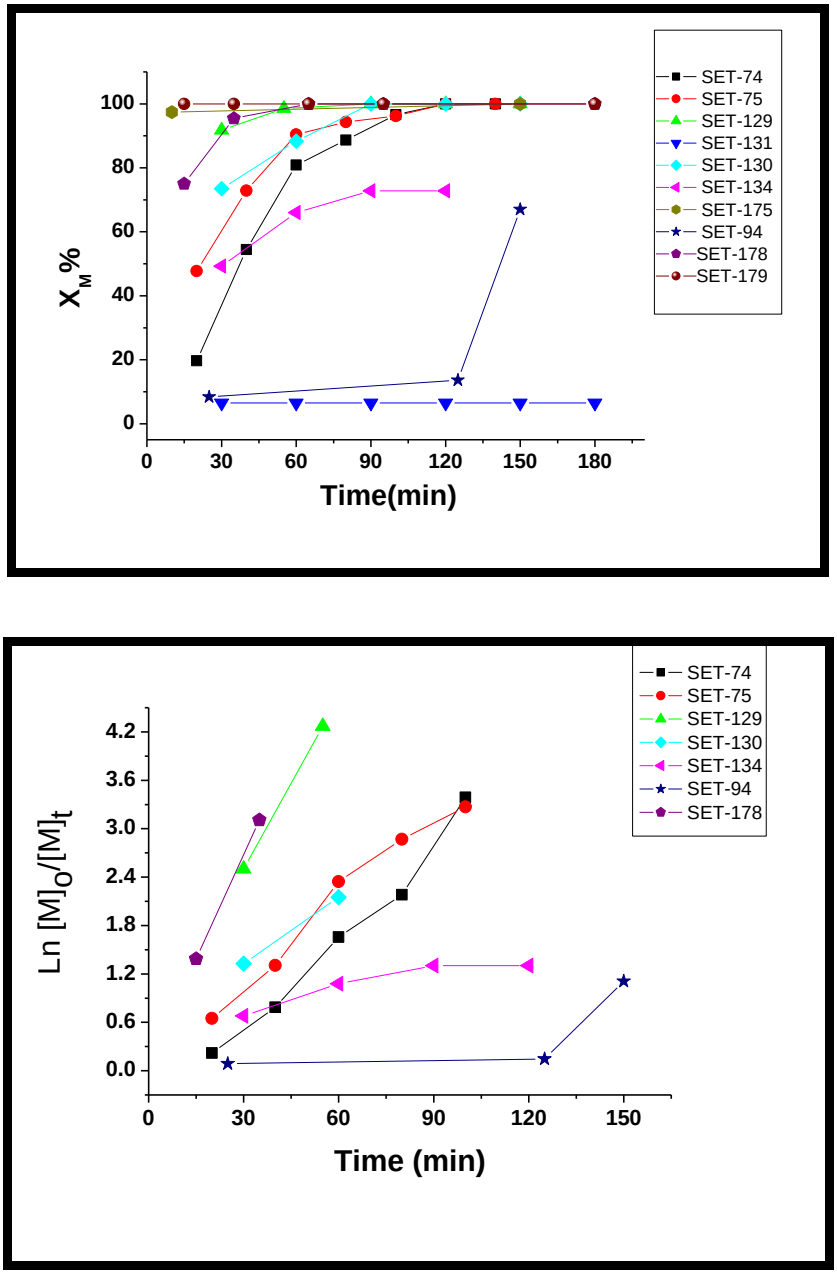

Fig .3. Monomer conversion versus time of the SET-LRP polymerizations of NIPAM in different conditions.

In the next two reference polymerizations, SET-130 and SET-134, we added Cu(0) wire in the initial reaction mixture. No halogen ATRP-type initiator was added. The outcome of these experiments was striking. In both cases high monomer conversions are observed, with values exceeding 50% after just 30 mins.

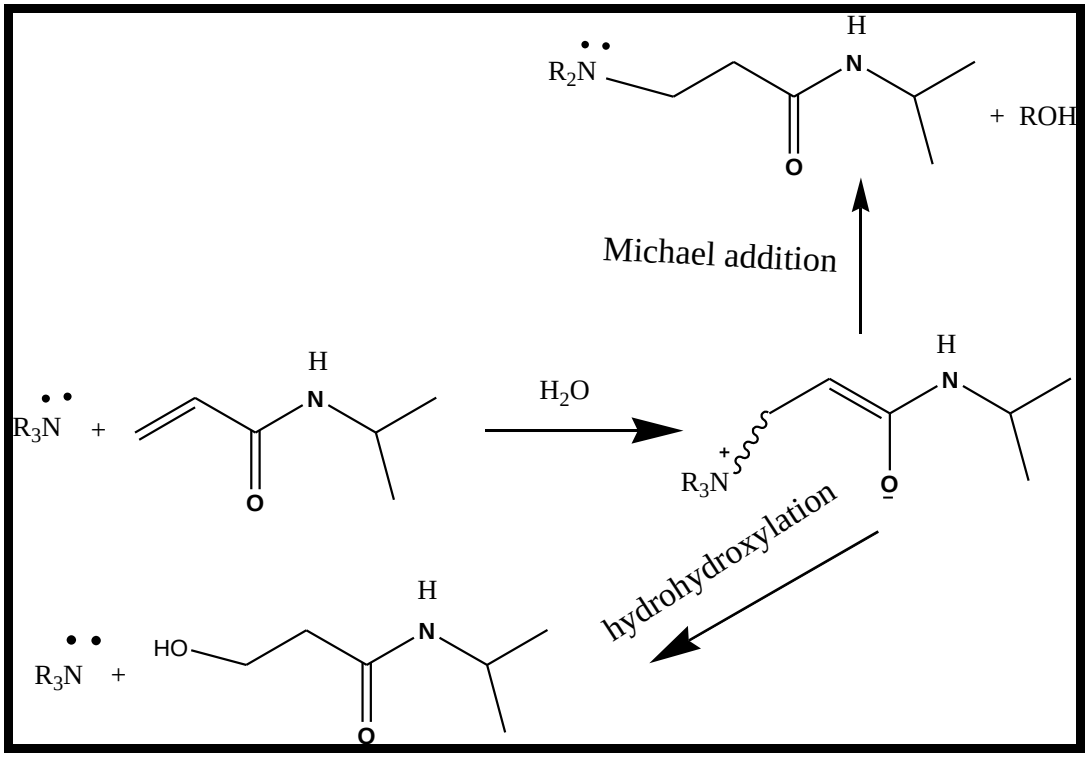

Scheme.6. Mechanisms of the possible side reactions between PMDETA and NIPAM in water.

SET-130 reaches full conversion whereas SET-134 stops at values of around 70%. Analysis of the molar mass distributions by size exclusion chromatography (SEC) using PMMA standards shows uncontrolled chain growth, and thus a polymerization mechanism closer resembling free radical polymerization, with values for M_n of 109 $\times 10^3$ g.mol^{-1} and 38 $\times 10^3$ g.mol^{-1}, and corresponding poly dispersities of 3.19 and 5.39. These results raise the question if the combination of Cu(0) wire and ligand, in the present of PMDETA (or its modified analogue), is able to generate radical species which can initiate a free radical polymerization process.

In the next two reactions, SET-129, and SET-178, we added a *tert*-halogen initiator (2). This initiator has previously been used successfully in water based ATRP systems [21, 31], as it is highly water soluble due to the presence of two hydroxyl groups in its structure. The difference between SET-129, and SET-178 was double

the monomer concentration in SET-129. Very fast overall polymerization rates leading to complete monomer conversion were observed in both cases. SEC analysis showed that these polymerizations did not show pronounced control of chain growth. The experimental M_n's were orders of magnitude larger with dispersities in the range of 2.5-3.3, results not in agreement with ideal control of propagation through living radical polymerization. Noticeable however, was that the molar masses in case of SET-129 were roughly twice those of SET-178, in agreement with the difference in monomer concentration between the two experiments.

Four polymerizations under conventional SET-LRP conditions using additional Cu(II)Br_2 were carried out using either (**1**) as water soluble acidic initiator (experiments SET-74 and SET-75), or (2) (SET-175 and SET-179). Addition of Cu(II) is required to balance the equilibrium between Cu(0), Cu(I), and Cu(II) species. It has been observed in mixed solvent SET-LRP systems that addition of Cu(II) leads to a reduction in inhibition time. The reason is that Cu(I) species, which initiate the activation process of halogen abstraction, area generated in sufficient quantities. For clarification in our experiments carried out in absence of added Cu(II) (SET-129, SET-178) we do not see an inhibition period because of the additional source of radicals being generated. We carried out two experiments, SET-75 and SET-74 in which the initiator concentration of the first was double the value of the second. The overall rate of polymerization was slowed down upon addition of Cu(II) which is logical as it classically traps radical species. Moreover, on the basis of varying the concentration of initiator the expectation is that a reduction in average molecular weight should be observed for SET-75 as the NIPAM monomer units should be distributed over more polymer chains. Indeed SEC analysis confirmed that

in SET-75 the (M_n) is 26 $\times 10^3$ g.mol^{-1}, and in case of SET-74 the (M_n) is 51 $\times 10^3$ g.mol^{-1}.

We replaced the acidic initiator (**1**) for compound (**2**) as reports in literature suggested that (**1**) led to low initiator efficiencies [32]. To our initial surprise using compound (**2**) led to very fast polymerization even in presence of substantially larger concentrations of added Cu(II). Initiator efficiency could be an explanation for this behaviour, but only if it would result in better control of molecular weight. This is indeed the case as the measured number average molar masses of SET-175 and SET-179 are in closer agreement with the theoretical values (see Table 2). There is not much difference between using Cu wire or Cu-powder.

Table.2. Outcome of the polymerizations of NIPAM by SET-LRP process which includes, maximum monomer conversion%, [(M_n,th) (theoretical number average molecular weight)], [(M_n,exp) (Experimental number average molecular weight)]. P1 (peak one), P2 (peak two). M_W (weight average molecular weight), PDI (molecular weight distribution, poly dispersity index).

Exp	Max Conversion%	(M_n, th) g.mol^{-1}	(M_n, exp) g.mol^{-1}	(M_W) g.mol^{-1}	PDI
SET-74	100	19,000	51,000	184,000	3.59
SET-75	100	9,500	26,500	73,500	2.75
SET-129	100	11,000	62,500	205,000	3.27
SET-130	100	No [Io]	109,000	349,500	3.19
SET-134	73	No [Io]	39,000	210,000	5.39
SET-175	100	6,000	(P1, 0.24%) 350,500 (P2, 31%) 7,500	(P1, 0.24%) 369,500 (P2, 31%) 18,500	1.05 2.45
SET-94	67	6,000	(P1, 21.41%) 51,000 (P2, 19.96%) 4,500	(P1, 21.41%) 81,500 (P2, 19.96%) 7,500	1.59 1.72
SET-178	100	7,500	55,500	134,500	2.42
SET-179	100	6,000	5,000	13,000	2.53

As we changed the PMDETA ligand for Me_6TREN (SET-94). In this case a long inhibition period was observed. An explanation could be that Me_6TREN forms a stronger and more stable complex with Cu(II), hereby stabilizing the Cu(II) redox state, and hence not generating substantial amounts of Cu(I) species fast enough.

3.4.2. Aqueous SET-LRP of *N,N*-dimethylacrylamide (DMA)

This monomer is analogous to NIPAM, but this monomer has a tertiary amine compared to secondary amine in case of NIPAM as depicted in Scheme 7.

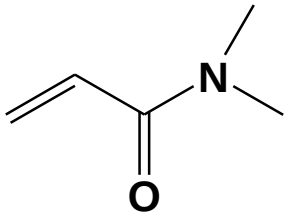

Scheme.7. Chemical structure of DMA.

Poly(DMA) is more hydrophilic than poly(NIPAM) and does not show any LCST behaviour in water between 0-100°C. This give advantage of this water soluble polymer to be solvated in water at elevated temperature in contrast to poly(NIPAM) which becomes insoluble just above 32°C [33]. This monomer is not often used in ATRP reactions as control of propagation is hard to achieve. This might be attributed to complex formation between the amide and the Cu catalyst leading to slower deactivation hereby enhancing the overall concentration of propagating radicals, increasing the kinetic chain length and increasing the probability for chains to terminate permanently thus yielding a wider molecular weight distribution . ATRP reactions in water are very fast, observing 100% monomer conversion in less than 1 min [34]. Nevertheless, DMA was polymerized in a controlled manner under bulk conditions by using a specially designed ligand (*N,N'*-bis(pyridine-2-ylmethyl3-

hexoxo-3-oxopropyl)ethane-1,2-diamine) and using 2-chloropropionate and copper chloride at 80ºC and 100ºC. [35], the degree of polymerization however had to be kept below 100. It should be noted that no additional Cu(II) species were added at the start of the polymerizations. Percec and co-workers attempted polymerization of DMA in mixed aqueous solvent systems. They observed high polymerization rates with limited control of chain growth and suggested the use of an additional amount of Cu(II) to increase the rate of deactivation from the beginning of the polymerization in order to enhance the control . Their catalyst system consisted of Cu(0) wire/Me_6TREN and external amount of $CuCl_2$ in binary solvent of water /DMF or water /methanol [27].

Here in our study DMA was polymerized by SET-LRP mechanism at 25ºC in pure water. Table 3 shows the details of the recipe and conditions of the aqueous SET-LRP of DMA. The conversion of the polymerization was determined by ^{1}H NMR as described for NIPAM previously.

Table.3. Recipes used in several SET-LRP of DMA at room temperature at different conditions.

Exp	[M_0]/ (mol L^{-1})	Io	[Io]/ (mmol L^{-1})	Lig	[Lig]/ (mol L^{-1})	Cu(0)	[Cu(0)]/ (mol L^{-1})	[$CuBr_2$]/ (mmol L^{-1})
SET-176	1.765	(2)	4.8	Lig_1	0.0136	wire	0.0342	1.4
SET-177	1.765	(2)	4.9	Lig_2	0.0255	wire	0.0342	1.6
SET-181	1.765	(2)	5.2	Lig_1	0.0136	Powder	0.0193	1.4

The polymerization was confirmed by a massive reduction of the intensity of vinyl protons of DMA.Three polymerizations were conducted; initiator (**2**) was used in all the polymerizations with external amount of the deactivator. The effect of the type of the ligand was studied in SET-176 and SET-177, when PMDETA was used with

Cu(0)-Wire system as in (SET-176) a very high rate of the polymerization was observed with gel formation and conversion reached to more than 90% monomer conversion in less than 15 minutes (see figure 5). The experimental M_n's are higher than the theoretical ones by a factor 2, with broad values for the poly dispersities, (see table 4).

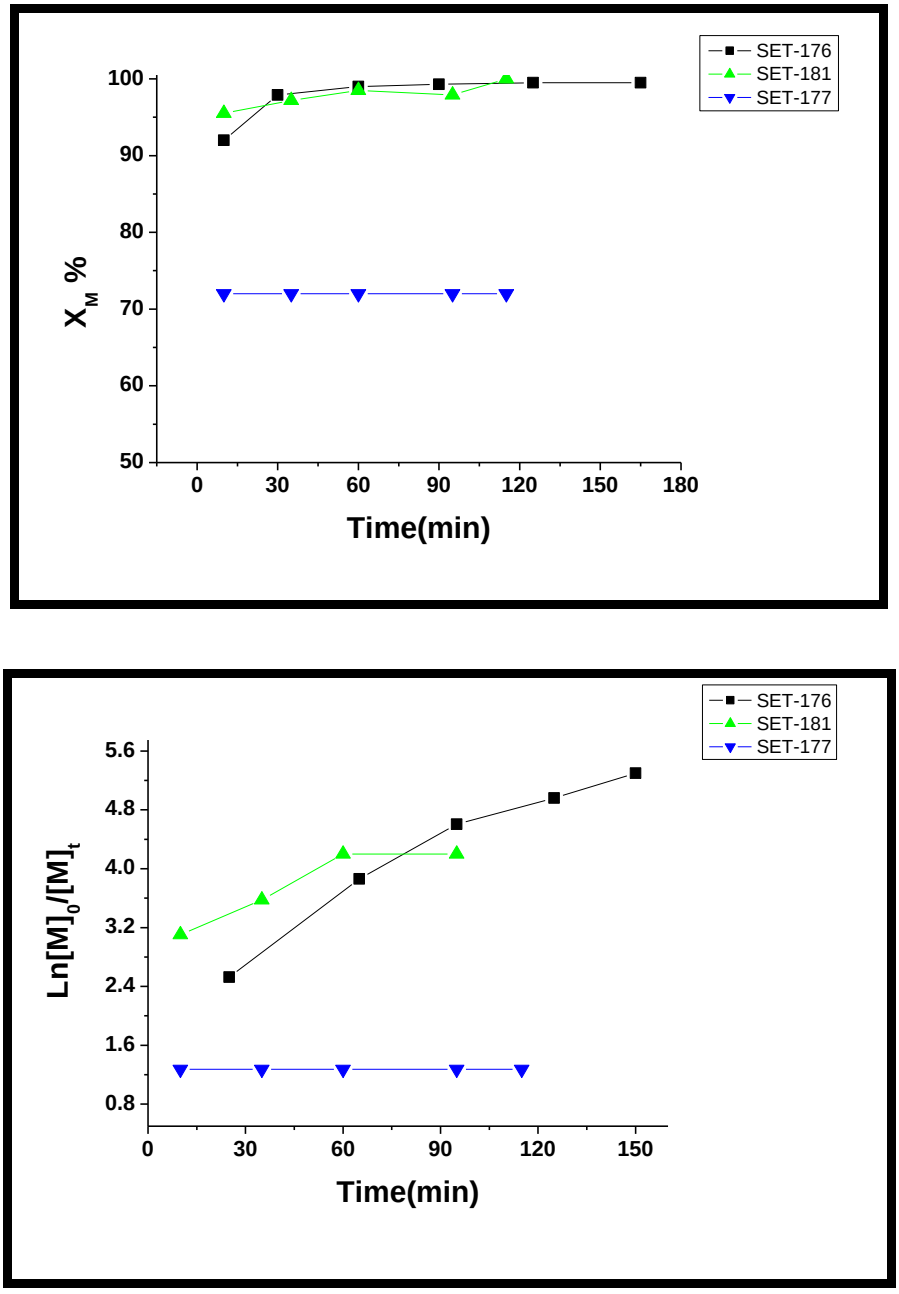

Fig.5. Monomer conversion versus time of the SET-LRP polymerization of DMA in pure water at 25°C.

One interesting observation is that DMA did not show an inhibition period when Me_6TREN was used as ligand (in contrast to our reaction using NIPAM). A fast polymerization was observed, with monomer conversion values of 73% after only 15 mins. However, no further polymerization was observed (Note that this experiment was not repeated therefore it is too speculative to reason further on this.). Molecular weight distribution is relatively improved compared to SET-176 when the Cu(0) powder was used as in case of SET-181.

Table.4. Molecular weight properties of the poly (DMA) after the SET-LRP of DMA at 25°C.

Exp	Time (h)	Max Conversion%	(M_n, th) g.mol^{-1}	(M_n, exp) g.mol^{-1}	(M_w) g.mol^{-1}	PDI
SET-176	**24**	**100**	**36,500**	**51,000**	**170,500**	**3.34**
SET-181	**24**	**100**	**33,500**	**58,000**	**156,000**	**2.68**
SET-177	**24**	**73**	**26,000**	**45,000**	**130,500**	**2.89**

3.4.3. Aqueous SET-LRP of [Poly(ethylene glycol methyl ether) acrylate] (PEGMEA): (Average M_n= 454 g.mol^{-1})

PEGMEA is an interesting acrylate based macromonomer of M_n= 454 g.mol^{-1}, having on average 7-8 ethylene oxide chains. The chemical structure of PEGMEA is depicted in scheme 8. Initial attempts to polymerize a functional acrylate monomer in water were made by using 2- hydroxy ethylacrylate at 50% concentration of monomer in water, using CuBr/2,2'-bipyridine and methyl 2-bromopropinate as initiator at 90ºC.

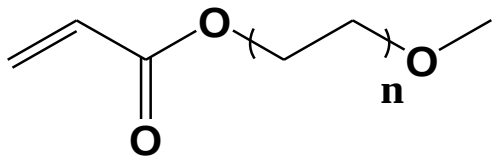

Scheme.8. Chemical structure of PEGMEA.

The dispersity of the molar mass distribution was 1.34 indicating a level of control of chain growth had been established under these aqueous ATRP conditions [36]. PEGMEA has successfully been polymerized by ATRP in a water/THF (10:1) medium. The catalyst systems is CuBr/Me_6TREN and by using methyl-2-bromopropionate at 40ºC. The polymerization reached to 100% conversion after 4 hours, Narrow molecular weight distributions were achieved using these conditions with PDI (1.09) [36-37]. Methyl acrylate monomer can be polymerized by SET-LRP mechanism with Cu(0)-wire/Me_6TREN in DMSO as solvent. Moreover, this acrylate can be polymerized by SET-LRP in the presence of air and without degassing of the ingredient of the polymerization, and under these circumstances a good controlled manner with more than 80% conversion within 60 minutes from the beginning of the polymerization [38]. The analogue monomer of PEGMEA is methoxy-capped oligo(ethylene glycol) methacrylate (OEGMA) which is polymerized in water in controlled manner with low PDI; the polymerization rate was extremely high at 20 ºC [39]. Here in our research PEGMEA was polymerized by SET-LRP under different conditions as described in table 5. The conversion was again monitored by ^{1}H NMR

Table.5. Recipe used in SET-LRP polymerization of (PEGMEA) in pure water at 25 °C.

Exp	$[M_0]$/ (mol L^{-1})	Io	[Io]/ (mmol L^{-1})	Lig	[Lig]/ (molL^{-1})	Cu(0)	[Cu(0)]/ (mol L^{-1})	$[CuBr_2]$/ (mmol L^{-1})
SET-136	0.140	0.0	0.0	Lig_1	0.0136	wire	0.0342	0.0
SET-78	0.082	(1)	1.7	Lig_1	0.0136	wire	0.0342	0.47
SET-138	0.130	(2)	5.3	Lig_1	0.0136	wire	0.0342	0.0
SET-174	0.388	(2)	5.3	Lig_1	0.0136	wire	0.0342	1.97
SET-180	0.391	(2)	5.2	Lig_1	0.0136	powder	0.0200	1.76

Using a similar approach as in the case of NIPAM the first reaction we carried out by mixing monomer, water, Cu(0) wire, and ligand as in reaction (SET-136).

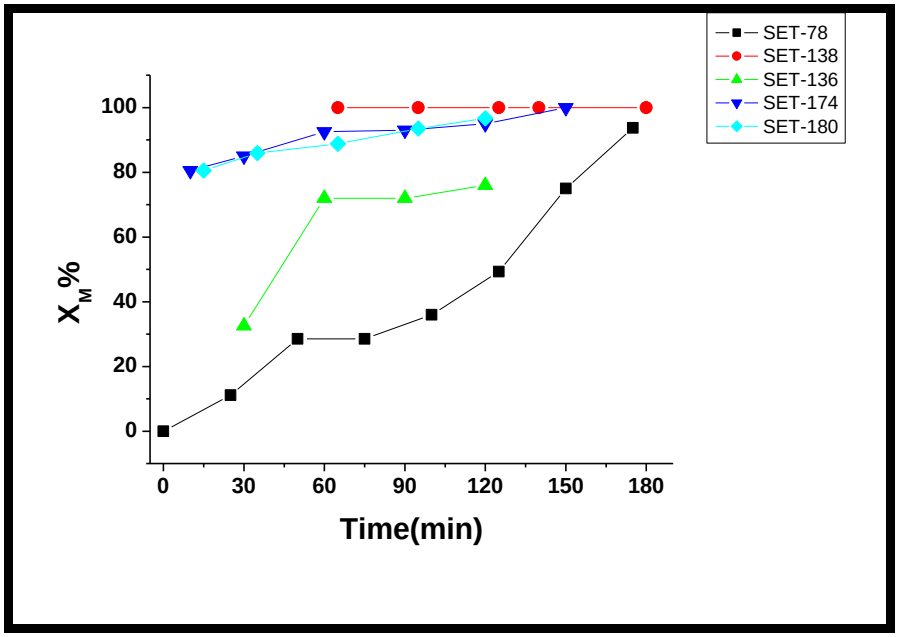

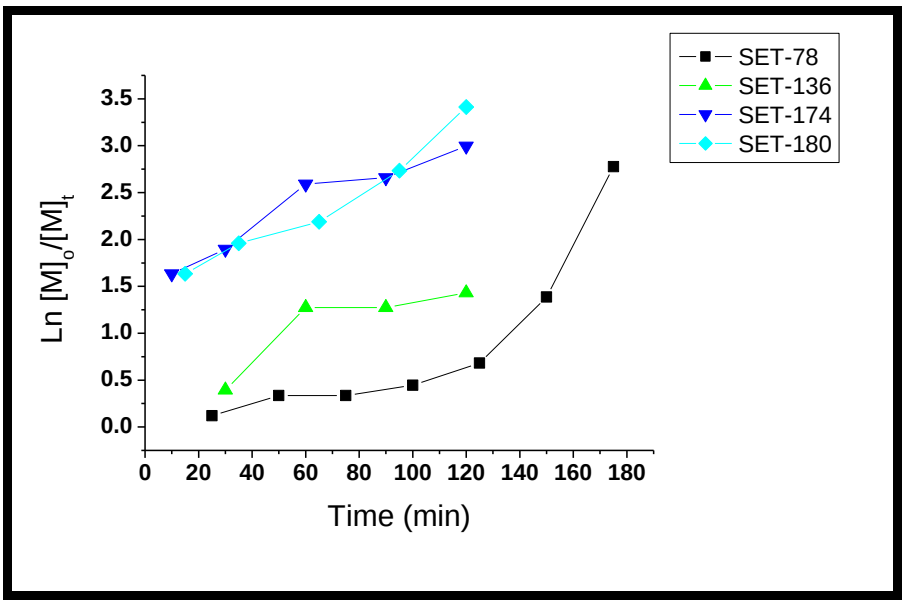

Fig .6. Monomer conversion versus time for the SET-LRP of (PEGMEA) at 25 °C.

Again substantial monomer conversions, exceeding 60 % (see figure 6), and the production of polymer of high molar mass was observed (see table 6). The employment of the acidic *tert*-halogen ATRP initiator (**1**) (SET-78) in combination with added Cu(II) resulted in a reduction of the overall rate of polymerization with relative control, as in reduction, of molar mass.

Overall the results obtained for SET-LRP reactions with NIPAM and PEGMEA were consistent in particular when initiator (**2**) and external amount of Cu(II) was added.

Table.6. Molecular weight properties of PEGMEA after SET-LRP polymerization.

Exp	Time (h)	Max Conversion%	(M_n, th) g/mol	(M_n, exp) g/mol	(M_w) g/mol	PDI
SET-78	**24**	**93**	**20,500**	**45,000**	**125,500**	**2.70**
SET-136	**24**	**75**	**No [Io]**	**74,500**	**140,500**	**1.87**
SET-138	**24**	**100**	**11,000**	**36,500**	**107,000**	**2.93**
SET-174	**24**	**100**	**33,500**	**34,000**	**82,000**	**2.43**
SET-180	**24**	**97**	**33,000**	**33,000**	**73,000**	**2.19**

3.4.4. Aqueous SET-LRP of Sodium Styrene Sulfonate (NaSS)

Poly(sodium styrene sulfonate) is typically used in many applications such as flocculent, antistatic, emulsifier, catalyst, additives used during oil drilling and oil recovery and as ion-exchange resin [40,41]. These many applications will be existed in the fabricated Janus hairy particles with poly(sodium styrene sulfonate) brushes and that will augment the applications of our Janus Particles. Based on that, the motivation to study the aqueous SET-LRP of (NaSS) raised. Beside this motivation, the possibility to visualize the poly(NaSS) brushes by Cryo-TEM which would facilitate the conformation of the anisotropic morphology of our Janus particles [42]. Initial attempts to polymerize (NaSS) (see its chemical structure in Scheme 9) by conventional ATRP condition with catalyst system contains Cu(I)Br/Bipyridine and 2-bromo-2-methylpropionate as initiator in pure water, lead to uncontrolled polymer and with 95% monomer conversion for less than 30 minutes, but the livingness of the polymerization was improved by addition of Cu(II)Br or by mixing the water with co-solvent methanol [40].

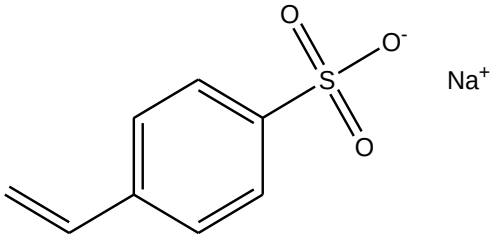

Scheme.9. Chemical structure of (NaSS) .

However, Armes *et al*, study the ATRP of (NaSS) in pure water by using CuCl/ 2,2 bipyridine as catalyst and sodium 4-bromomethylbenzoate as initiator at pH=10, a fast polymerization with 80% monomer conversion and broad molecular weight distribution with PDI of 2.03, and again the livingness of the polymerization was improved by the addition of external amount of $CuBr_2$ and methanol as co-solvent [41]. Here (NaSS) was polymerized by SET-LRP in pure water at different conditions, the detailed recipe for the several SET-LRP of NaSS performed is listed in table 7.

Table.7. Recipe used in the SET-LRP polymerization of (NaSS) in pure water at 25°C.

Exp	$[M_0]$/ (mol.L^{-1})	Io	[Io]/ (mmol.L^{-1})	Lig	[Lig]/ (mol.L^{-1})	Cu(0)	[Cu(0)]/ (mol.L^{-1})	$[CuBr_2]$/ (mmol.L^{-1})
SET-126	**0.106**	**0.0**	**0.0.**	**Lig_1**	**0.0105**	**0.0**	**0.0**	**0.0**
SET-135	**0.298**	**(2)**	**5.7**	**Lig_1**	**0.0136**	**0.0**	**0.0**	**0.0**
SET-132	**0.291**	**0.0**	**0.0**	**Lig_1**	**0.0136**	**wire**	**0.0342**	**0.0**
SET-133	**0.286**	**(2)**	**4.9**	**Lig_1**	**0.0136**	**wire**	**0.0342**	**0.0**
SET-80	**0.147**	**(1)**	**1.76**	**Lig_1**	**0.0136**	**wire**	**0.0342**	**0.5**

The monomer conversion of the polymerizations was determined by ^{1}H NMR as described earlier. First polymerization was studied as in (SET-126) where no initiator nor Cu(o) were used, the outcome of that is no polymerization was observed at all (see figure 9), and when initiator (**2**) was added in experiment (SET-135) a slight consumption of monomer was recorded to 15% from the total added sodium styrene sulfonate and without formation of polymer, this implies a side reaction has occurred between sodium styrene sulfonate and initiator (**2**).

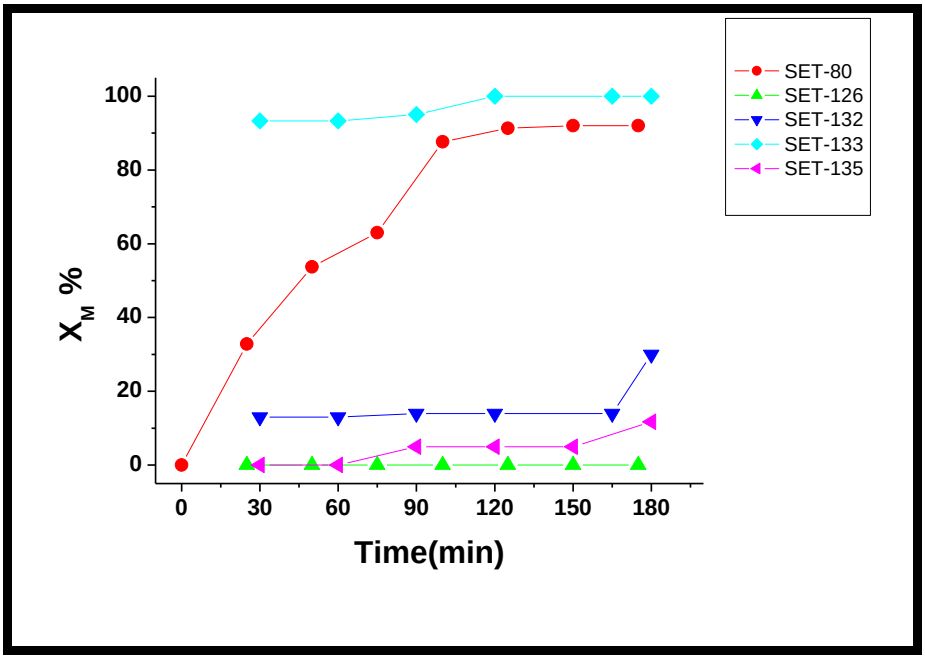

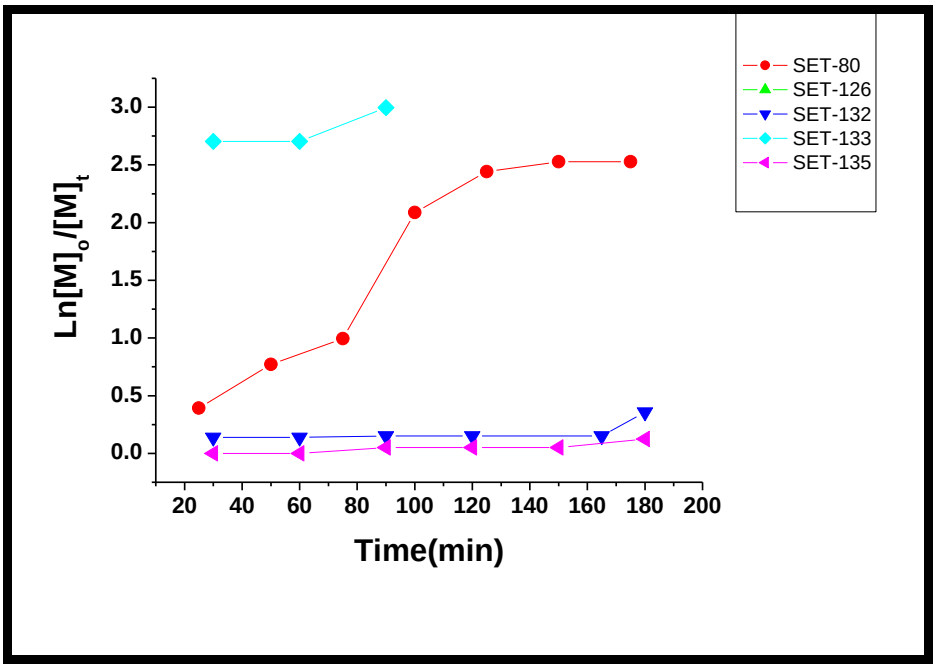

Fig.9. Monomer conversion versus time for the SET-LRP of (NaSS) in water at 25°C.

when just Cu(0) wire was added without initiator as in experiment (SET-132), a fast consumption of sodium styrene sulfonate was observed of approximately 15% ,and then the consumption has stopped and then went up to 20% without any evidence of formation of polymer back bone as that verified by ^{1}H NMR. As a typical SET-LRP condition was used as in (SET-133) with initiator (**2**) and Cu(0) wire, an ultra fast polymerization was observed with monomer conversion above 90% after 30 mins

from the onset of the polymerization, and moderate rate of the polymerization was observed when initiator (**1**) was used in combination of $CuBr_2$ as in (SET-80). The characterization of molecular weight of the obtained poly(NaSS) was difficult, as a result of the polymer just dissolvable in water, and when the measurement was performed in the aqueous GPC, the column was blocked by poly(NaSS) which restrict further measurement.

3.5 Conclusion

SET-LRP (Single Electron Transfer-Living Radical Polymerization) of several water soluble Monomers: *N*-isopropyl acrylamide, *N*,*N*-dimethylacylamide, poly(ethylene glycol methyl ether acrylate) M_n= 454 g/mol, and sodium styrene sulfonate were studied at room temperature in water.

Two types of water soluble ATRP initiators with tertiary bromine functional group which is identical to that one on the surface of latex particles were used which are (**1**) [2-bromo-2-methylpropionic acid], and (**2**) [1, 2-dihdroxypropane-3-oxy-(2-bromo-2-methylpropionyl)] to examine the effect of the chemical nature of the initiator. PMDETA (*N,N,N',N'',N''*-pentamethyldiethylenetriamine) is the main ligand used and at some rare cases Me_6TREN (tris [2-(dimethyl amino) ethyl] amine) was used. Cu(0) was used in both physical state, in powder and wire to explore their effect on the polymerization, and in some experiments an external Cu(II) was added to examine its effect on the polymerization.

In case of aqueous polymerization of NIPAM, the polymerization performed with conditions that neither initiator nor the catalyst were used, no polymerization was observed, but when the catalyst used (Cu(0) wire/PMDETA) alone without an initiator the polymerization occurred which indicates the possible another source of

free radicals to trigger the NIPAM polymerization via side reaction. As (**1**) was used the rate of the polymerization was moderate with full conversion obtained, as the concentration of (**1**) increased the number average molecular weight of Poly(NIPAM) decreased which indicates some degree of controlled although the obtained PDI was high above 2.0. It was observed that when the concentration of an external Cu(II) was high enough this lead to inhabitation of the polymerization. As Me_6TREN was used, the rate of the polymerization was very slow with induction period of 2.0 hour and then the rate of the polymerization increased and the conversion reached to only 70% conversion, this limited conversion when Me_6TREN was used also observed with *N*,*N*-dimethyl acrylamide. It was found out that the best condition to obtain on a good agreement between theoretical M_n and experimental M_n when SET-LRP applied with NIPAM in pure water is to use (**2**) as initiator, PMDETA as ligand, Cu(0) powder and an external amount of Cu(II).

In case of SET-LRP of *N*,*N*-dimethylacrylamide, when the (**2**) initiator used with Cu(0) wire/PMDETA as catalyst and with the presence of external amount of Cu(II) , the rate of the polymerization was ultra-fast and with 90% conversion within 15 minutes from the beginning of the polymerization with gel formation. The PDI of the polymerization was high and this could be improved by utilizing Cu(0) powder instead of Cu(0) wire as the PDI decreased. In case of poly(ethylene glycol methyl ether acrylate), the polymerization was triggered even without the presence of initiator, and with the presence of catalyst as in case of NIPAM, the molecular weight was high, and it was reduced when an initiator and external Cu(II) were used, it was found that the best condition that gives very good agreement between theoretical and experimental M_n is when (**2**) initiator was used with PMDETA ligand

, and whatever the type of Cu(0) powder or wire if the Cu(II) is present. In case of (sodium styrene sulfonate), no polymerization has detected when no initiator nor catalyst were used, but when an initiator (**2**) used alone without catalyst a very low reduction of (NaSS) concentration of about 15% was observed. And when the catalyst used alone as Cu(0) wire, a moderate monomer conversion was achieved around 30%. In a typical condition when both initiator and catalyst present in the system a very high monomer conversion was gained. In general the polymerizations mixtures do not show very high viscosity, and the polymerization can be performed with usage of Cu(0) (wire). Both factors make the colloidal stability of the latex particles less affected and the purification of the hairy latex after SET-LRP much easier. Thereby, SET-LRP in water phase of several water soluble monomers will be polymerized from the surface of latex particles because of those advantages although of the expected poor control of the molecular weight of the obtained polymer brushes.

3.6.References

1- Szwarc, M. *J. Polym. Sci., Part A: Polym. Chem.***1998**, *36*, ix.
2- *Principle of polymerization*, fourth edition, George Odian, ISBN 0-471-27400-
3- Wang, J.-S.; Matyjaszewski, K. *Macromolecules* .**1995**, *28*, 7901-10.
4- Kato, M.; Kamigaito, M.; Sawamoto, M.; Higashimura, T. *Macromolecules.***1995**, *28*, 1721-3.
5- Percec, V.; Guliashvili, T.; Ladislaw, J. S.; Wistrand, A.; Stjerndahl, A.; Sienkowska, M. J.; Monteiro, M. J.; Sahoo, S. *J. Am. Chem. Soc.***2006**, *128*, 14156-14165.
6- Percec, V.; Barboiu, B.; van der Sluis, M. *Macromolecules* .**1998**, *31*, 4053-4056.
7- Matyjaszewski, K.; Coca, S.; Gaynor, S. G.; Wei, M.; Woodworth, B. E. *Macromolecules* .**1997**, *30*, 7348-7350.
8- Beers, K. L.; Woodworth, B.; Matyjaszewski, K. *J. Chem. Educ.* **2001**, *78*, 544-547.
9- Otsu, T.; Yamaguchi, M. *J. Polym. Sci., Part A-1: Polym. Chem.***1968**, *6*, 3075-85.

10- Matyjaszewski, K.; Tsarevsky, N. V.; Braunecker, W. A.; Dong, H.; Huang, J.; Jakubowski, W.; Kwak, Y.; Nicolay, R.; Tang, W.; Yoon, J. A. *Macromolecules*.**2007**, *40*, 7795-7806.

11- Rosen, B. M.; Percec, V. *Chem. Rev.* **2009**, *109*, 5069-5119.

12- Lligadas, G.; Rosen, B. M.; Bell, C. A.; Monteiro, M. J.; Percec, V. *Macromolecules* .**2008**, *41*, 8365-8371.

13- Nguyen, N. H.; Rosen, B. M.; Lligadas, G.; Percec, V. *Macromolecules*.**2009**, *42*, 2379-2386.

14- Qiu, J.; Charleux, B.; Matyjaszewski, K. *Prog. Polym. Sci.* **2001**, *26*, 2083-2134.

15- Gromov, VF.;Bune, EV.; Teleshov, E N. *Russian Chemical Reviews*.**1994**,*63*(6) 507-517.

16- Coca, S.; Jasieczek, C. B.; Beers, K. L.; Matyjaszewski, K. *J. Polym. Sci., Part A: Polym. Chem.* **1998**, *36*, 1417-1424.

17- Wang, X. S.; Lascelles, S. F.; Jackson, R. A.; Armes, S. P. *Chem. Commun.* **1999**, 1817-1818.

18- Wang, X. S.; Jackson, R. A.; Armes, S. P. *Macromolecules*.**2000**, *33*, 255-257.

19- Wang, X. S.; Malet, F. L. G.; Armes, S. P.; Haddleton, D. M.; Perrier, S. *Macromolecules* .**2001**, *34*, 162-164.

20- Coullerez, G.; Carlmark, A.; Malmstroem, E.; Jonsson, M. *J. Phys. Chem. A* .**2004**, *108*, 7129-7131.

21- Haddleton, D. M.; Perrier, S.; Bon, S. A. F. *Macromolecules* .**2000**, *33*, 8246-8251.

22- Bon, S. A. F.; Ohno, K.; Haddleton, D. M. *ACS Symp. Ser.* **2001**, *780*, 148-161.

23- Jewrajka, S. K.; Mandal, B. M. *Macromolecules* .**2003**, *36*, 311-317.

24- Ye, J.; Narain, R. *J. Phys. Chem. B* .**2009**, *113*, 676-681.

25- Masci, G.; Giacomelli, L.; Crescenzi, V. *Macromol. Rapid Commun.***2004**, *25*, 559-564.

26- Feng, C.; Li, Y.; Yang, D.; Li, Y.; Hu, J.; Zhai, S.; Lu, G.; Huang, X. *J. Polym. Sci., Part A: Polym. Chem.* **2009**, *48*, 15-23.

27- Nguyen, N. H.; Rosen, B. M.; Percec, V. *J. Polym. Sci., Part A: Polym. Chem.* **2010**, *48*, 1752-1763.

28- Millard, P.-E.; Mougin, N. C.; Boeker, A.; Mueller, A. H. E. *ACS Symp. Ser.* **2009**, *1023*, 127-137.

29- Queffelec, J.; Gaynor, S. G.; Matyjaszewski, K. *Macromolecules.***2000**, *33*, 8629-8639.

30- Faltin, C.; Fleming Eimear, M.; Connon Stephen, J. *J Org Chem* .**2004**, *69*, 6496-9.

31- Perrier, S.; Haddleton, D. M. *Macromol. Symp.* **2002**, *182*, 261-272.

32- Haddleton, D. M.; Heming, A. M.; Kukulj, D.; Duncalf, D. J.; Shooter, A. J. *Macromolecules* .**1998**, *31*, 2016-2018.

33- Pagonis, K.; Bokias, G. *Polymer* .**2004**, *45*, 2149-2153.

34- Rademacher, J. T.; Baum, M.; Pallack, M. E.; Brittain, W. J.; Simonsick, W. J. *J. Macromolecules* .**2000**, *33*, 284-288.

35- Ding, S.; Radosz, M.; Shen, Y. *Macromol. Rapid Commun.* **2004**, *25*, 632-636.

36- Gu, L.; Shen, Z.; Feng, C.; Li, Y.; Lu, G.; Huang, X. *J. Polym. Sci., Part A: Polym. Chem.* **2008**, *46*, 4056-4069.

37- Zhai, S.; Wang, B.; Feng, C.; Li, Y.; Yang, D.; Hu, J.; Lu, G.; Huang, X. *J. Polym. Sci., Part A: Polym. Chem.***2010**, *48*, 647-655.

38- Fleischmann, S.; Rosen, B. M.; Percec, V. *J. Polym. Sci., Part A: Polym. Chem.***2010**, *48*, 1190-1196.

39- Wang, X. S.; Armes, S. P. *Macromolecules* .**2000**, *33*, 6640-6647.

40- Choi, C.-K.; Kim, Y.-B. *Polym. Bull.* **2003**, *49*, 433-439.

41- Iddon, P. D.; Robinson, K. L.; Armes, S. P. *Polymer*. **2004**, *45*, 759-768.

42- Guo, X.; Weiss, A.; Ballauff, M. **1999**, *32*, 6043-6046.

43- Cohen, N. A.; Tillman, E. S.; Thakur, S.; Smith, J. R.; Eckenhoff, W. T.; Pintauer, T. *Macromol. Chem. Phys.* **2009**, *210*, 263-268.

Chapter 4: Surface Initiated Polymerization from latex particles by SET-LRP in aqueous medium.

4.1. Summary

Cross-linked monodispersed latex particles that contain active sites (tertiary bromine functional group) were used as a macro-initiator for surface initiated polymerization by SET-LRP for several water soluble monomers at room temperature. Two types of latex particles were investigated, one of which was prepared by using the functional comonomer, that is 2-methacryloxyethyl-2'-bromoisobutryrate, in an *ab initio* fashion (batch addition), and one of which was prepared employing shot addition of the monomer after approximately 70 wt% monomer conversion to warrant enrichment of *tert*-bromine groups in the outer regions of the polymer colloids. Rate of the surface initiated polymerizations was fast with monomer conversions exceeding 50% within 30 minutes, irrespectively of the type of the water soluble monomer used and the latex used whether that has made by batch addition or shot addition. The rate of the surface initiated polymerization can be controlled by addition of Cu(II).

Cryo-TEM of the hairy latex made by batch addition shows that the brushes are barely visible, in contrast to that made by shot addition method which are clearly visible as extended arms from the surface of the latex particles toward the water phase. This difference could be explained as a result of differences in brush densities. Shorter polymer brushes can be made by utilizing an external water soluble sacrificial initiator. The method developed to functionalize latex particles with hydrophilic brushes is easy and scalable.

4.2. Introduction

Polymer brushes are a polymer coating consisting of polymer chains that are tethered with one chain end to the interface of an underlying substrate, which for example in our case is a latex particle. At high grafting densities when the distance between the neighbouring points of the polymer chains are small, enhancement of osmotic pressure leads to chain stretching and a brush-type conformation of the surface tethered chains, whereas at lower grafting densities the polymer chains adopt a more entropically less stringent conformation, such as a mushroom or pancake [1]. This coating on the surface of the latex particles obviously will change the physical and chemical properties of the latex particles. For instance the latex particles become "intelligent" as polymer brushes can be responsive to particular external stimuli such as the nature of the solvent, temperature, pH and ionic strength, and that depends on the type of the polymer brushes on the surface of the latex particles

The polymer brushes in a good solvent extend and swell to maximize the contact with the solvent; the opposite situation occurred when a poor solvent is used in which the polymer brushes collapse. In case of thermo-responsive polymer brushes, at temperatures below the lower critical solution temperature (LCST), the polymer brushes are hydrophilic, and by increasing the temperature above the LCST the polymer brushes collapse that due to they become hydrophobic. Poly(NIPAM) brushes show such a thermo-responsive behaviour, but behave differently in comparison to normal free poly(NIPAM) dissolved in water. Varying the pH has negligible impact on the swelling properties of poly(NIPAM) brushes [1]. In case of poly(electrolyte) brushes, it categorizes as pH and ion-sensitive polymer brushes. The coating of the latex particles with a specific type of a polymer brushes would enhance and improve the colloidal stability of the latex and change the particle's

adhesion to particular object and as well as the rheological properties of the latex dispersion[2].

We were interested in tailoring latex particles with a variety of hydrophilic brushes in order to use them as precursors for the preparation of amphiphilic Janus particles made through a phase separating after second stage polymerization process (Seeded emulsion polymerization). The flexibility to functionalize the Janus particles with several polymer brush types allows us to analyse differences in their behaviour. For instance the usage of responsive polymer brushes to external stimuli, such as thermo-responsive polymer brushes as Poly(NIPAM) and ionic responsive brushes (polyelectrolyte) as poly(sodium styrene sulfonate) brushes make these Janus particles smart to interact with specific object selectively.

One of the main reasons to have Janus Particles with a hydrophilic domain consisting of polymer brushes is the possibility to control colloidal stability in an enhanced way. With this we mean that the hydrophilic brushes can cover and thus stealth the hydrophobic lobe under certain conditions, warranting colloidal stability. This is not possible with a smooth hydrophilic surface. Key is the abilities to control grafting density, chain length of the brushes, and chemical nature of the brushes. The presence of polymer brushes with different grafting density would change the interaction among the Janus particles in order to study their physical interaction such as the self assembly as they own amphiphilic character as ordinary surfactant, whereby low grafting density lead to bridging flocculation and high grafting density lead to Van der Waals interaction (depletion effect) , and the middle situation when a moderate grafting density which gives the good stability via steric repulsion mechanism [3].

Another essential difference between modifications of Latex Janus particles by formation of polymer brushes and another type of chemical modification is that the brushes height is determined by the degree of polymerization as the synthesis of the polymer brushes is made by ATRP, and therefore the height can be controlled by the degree of the polymerization. Hence, a simple change in the degree of the polymerization will change of the properties of the modified Janus latex particles [4].

A surface can be modified with polymer brushes using either one of two major approaches. The first is named the "grafting to" method in which polymer brushes are pre-made initially and then attached to the targeted surface via either physi- or chemisorption. This approach suffers from low polymer brushes density and in case of physisorption the process is reversible which can lead to detachment of brushes under harsh conditions. The second approach named the "grafting from" method, polymer brushes are grown from the surface through surface initiated polymerization. Control of brush densities and chain length is achieved and can be markedly further enhanced through employment of a living radical polymerization technique. We chose ATRP and with special interest to the new proposed mechanism by Percec as SET-LRP as explained in more details in chapter 3.

ATRP is the most used process to form polymer brushes by controlled radical polymerization in the literature due to the good tolerance of that process in different conditions. Many parameters should be considered in order to enhance the living nature and the rate of the surface initiated polymerization ATRP, such as the type of the ligand, ligand to transition metal ratio, Cu(II) to Cu(I) ratio, solvent of the polymerization medium, initiator and its stability.

One of the first successful attempts of surface initiated polymerization by ATRP reported the fabrication of poly(acrylamide) brushes through grafting from nonporous silica particles modified with benzyl chloride moieties [5].Gold substrate functionalized with 2-bromoisobutyrate was used also as inorganic substrate to form (PHEMA) brushes in water as a medium using CuCl/$CuBr_2$/bpy as a catalyst system [6]. However in the previous case extremely fast polymerization rates were reported which could harm control of chain growth. Guarani *et al*, functionalized cross-linked latex particles with 2-(2-bromopropionyloxy) ethyl methacrylate (BPEM), and used two types of hydrophilic monomers, that is the nonionic (2-Hydroxyethylacrylate) (HEA) and the cationic (2-(methacryloyl-oxy)ethyl trimethyl ammonium chloride) (MAETACL), in the fabrication of polymer brushes which were grafted from the surface of cross-linked poly(styrene) latex particles, the catalyst system being CuBr/bpy, and polymerizations were conducted in water as medium. The polymerization was very fast at the beginning with 15% conversion reached within 45 minutes and after that the rate decreases with 55% monomer conversion after 24 hours. They assumed this trend could be ascribed to irreversible termination which increased the concentration of $CuBr_2$, hereby shifting the equilibrium between activation-deactivation processes toward the formation of dormant chains [7]. Zhang and coworkers prepared poly(styrene) latex particles cross-linked with 5% DVB by emulsion polymerization which were functionalized with, 2-(2-bromoisobutyryloxy) ethyl methacrylate and DVB through a second seeded polymerization step in order to have ATRP initiator moiety in the surface of the latex particles. Next these particles were used as ATRP's initiator for DMAEMA in acetone/water dispersion medium using ethyl 2-bromoisobutyrate as a sacrificial ATRP's initiator with a catalyst regime of CuCl/bpy at 35°C. Addition of $CuCl_2$

improved control of chain growth (reduction in PDI from 2.14 to 1.12). However, a limited conversion of monomer of 47% conversion after 28 hours was reported when $CuCl_2$ was used. [8]

An example of surface initiated polymerization in water medium through modification of hydroxyl functional poly(styrene) microspheres (diameters of 10 µm to 200 µm) with 2-bromoisobutyryl bromide and subsequent ATRP was reported by Hubbell *et al*, Hydroxyethyl methacrylate (HEMA), *N*,*N*-dimethylacrylamide (DMA), NIPAM and PEG monomethacrylate were each grafted from these beads using ATRP for 90 mins at 20°C, employing CuBr/bpy. [9] Beside to that study cross-linked poly(styrene) beads with sizes of 210-240 µm were functionalized with *N*-chlorosulfonamide by a four steps chemical modification as ATRP initiator sites to grow a poly(acrylamide) shell. The catalyst system used was CuBr/tetramethyl ethylene diamine (TMED), and the polymerization performed at room temperature in water [10]. They suggested in that particular system that the initiation triggered by a redox reaction between *N*-chlorosulfonamide group in the surface of the beads and CuBr which results in the formation of radicals that reacts with acrylamide, this mechanism deviates from the typical ATRP process and they assume that the reverse halogen transfer step to be very slow which means the deactivation is not so sufficient. No free polymer in the water phase was formed in that particular system.

The advantage of the presence of the residual vinyl groups on non-swollen poly(divinyl benzene); whereby Poly(DVB) microspheres were converted into ATRP initiator moieties sites by hydroboration/oxidation and followed by etherification to utilize them as sites for surface initiated polymerization [11-12]. Several hydrophilic monomers were grafted from those poly(DVB) microspheres such as poly(HEMA) and poly(DMAEMA) to obtain on core-shell morphology. The

polymerization was conducted in THF at room temperature and with catalyst system of CuBr/Me_4cyclam.

Wang resin which is cross-linked polystyrene was condensed with 2-bromoisobutyryl bromide to obtain ATRP initiator moieties on the surface of the resin and served as a macro initiator for ATRP of methyl methacrylate in anhydrous toluene with a catalyst system of CuBr/ *N*-(n-propyl)-2-pyridylmethanimine [13]. Another type of microspheres particles based on poly(4-vinylbenzyl chloride) (PVBC) with beads size of 500-600 µm which is cross-linked with ethylene glycol dimethacrylate were used as ATRP initiator by using the chlorine atom as the transfer halogen for ATRP [14]. Poly[2-(dimethylamino) ethyl methacrylate (PDMAEMA) brushes were grown from the surface of the cross-linked (PVBC) beads using CuCl/$CuBr_2$/bpy and DMF as dispersion medium at 100°C for 36 hours. The same type of polymer (PVBC) but with smaller particles size, with size a round of 100 nm , which are synthesized by emulsion polymerization were used as ATRP initiator for the surface initiated polymerization of 3-(trimethoxysilyl) propyl methacrylate using CuCl/PMDETA and ethanol as dispersion medium at room temperature [15]. Furthermore from cross-linked poly(4-vinylbenzyl chloride) synthesized by emulsion polymerization with particle size of 160 nm, 24-27 nm thick poly(4-vinyl pyridine) brushes were grown by surface initiated polymerization using CuBr/$CuBr_2$/Me_6TREN and 2-propanol as dispersion medium at 40°C [16].

As the main water soluble monomers used in our research are NIPAM and NaSS , more details from the literature that deal with grafting of latex particles by Poly(NIPAM) or Poly(sodium styrene sulfonate) will be reviewed in the rest of the introductory part of this chapter.

Latex particles grafted with thermo-responsive shell has transition from swelling state to non swelling state (shrink) upon changing of the temperature and this swelling and shrinking transition can be repeated without degradation and coagulation of latex particles [17], this gives the targeted Janus particles extraordinary properties which will be made later in chapters 5 and 6.

Poly(styrene)-PNIPAM core-shell particles were synthesised by photo-emulsion polymerization. Via this method the attachment of the poly(NIPAM) shell on the latex particles is stronger in contrast to the conventional seeded emulsion polymerization to form core-shell latex particles whereby the attachment mainly occurs in the former case via the chain transfer side reaction of the free polymer in the aqueous phase to the polymer in the surface of the latex particles with weak attachment and inhomogeneous shell structure [18]. In photo-emulsion polymerization the core of latex particles were covered initially by a thin layer of photo-initiator which has two functional groups (Inimer), the first one is the vinyl group which copolymerized by starved condition emulsion polymerization in the surface of the latex particles and the second one is a photo-active functional group which undergoes decomposition via UV radiation to generate free radicals that are able to grow a polymer brushes from the surface of the latex particles in the second stage seeded emulsion polymerization.

In case of formation of outer shell of Poly(NIPAM) around core of poly(styrene) latex particles synthesized by soap-free emulsion polymerization via (grafting from) method and ATRP as tool that has been investigated by initial formation of thin layer of ATRP initiator alone or copolymerized with styrene and DVB [19]. The ATRP polymerization was conducted in water at room temperature with catalyst system consist of ($CuBr/CuBr_2$/Cu(0) powder/HMTETA), the polymerization lasted for 24

hours. The counterpart monomer of NIPAM which is *N*,*N*-dimethylacrylamide (DMA) was used also to form polymer brushes from the surface of negatively charge poly(styrene) latex particle which are synthesised by soap-free emulsion polymerization. Poly(DMA) brushes were grown from the surface of latex particles which are coated with thin layer of (inimer) poly [2-(methyl-2′-chloropropionato) ethyl acrylate] by aqueous ATRP with brush thickness up to around 800 nm. CuBr or CuCl/ ligand was used as the catalyst system and they observed the addition of external Cu(II) and sacrificial initiator improves the control of the polymerization by enhancing the deactivation reactions of the free radicals [20].

It is worth to mention that in the previous example that during the aqueous ATRP surface initiated polymerization a non-ionic surfactant (Brij-35) was used to improve the colloidal stability of the latexes, in addition to that some amount of Cu(0) powder was used as well. By using the same anionic latex particles as macro-initiator, a poly (NIPAM) brushes were grown by aqueous surface initiated ATRP using two different catalyst systems which are PMDETA/CuCl and HMTETA/CuCl, The (M_n) of the grown brushes increases with increasing the monomer concentration and decreases with the addition of external Cu(II) . The usage of sacrificial initiator lead to a reduction in the grafting density of the polymer brushes. The chain extension with (*N*,*N*-dimethyl acrylamide) confirms the presence of survivor halogen atom at the end of the chain of the poly(NIPAM) brushes. The obtained hairy latex with poly(NIPAM) brushes becomes sensitive to temperature and ionic strength [21, 22]. In general, the authors of the previous work observed that the aqueous ATRP from latex surface was completely different from solution counterpart; the main difference is the catalyst used has a positively charged and the surface of latex particles is negatively charged, therefore the surface of latex particles is enriched with catalyst

due to electrostatic interaction which has strong effect in the polymerization mechanism. This method is versatile because not just latex particles were used as substrate to grow Poly(NIPAM) brushes, silica particles coated with ATRP initiator were used as macro-initiator to grow Poly(NIPAM) brushes in controlled manner in 2-propanol as solvent and employing catalyst regime composed of $CuCl/CuCl_2/Me_6TREN$ at ambient temperature, but with lower conversion below 30% after 6 hours from the beginning of the polymerization [23].

In regard of grafting of latex particles with Poly(sodium styrene sulfonate), Ballauf and co-workers performed and investigated the formation of different type of poly(electrolyte) brushes on the surface of latex particles by the second stage seeded photo-emulsion polymerization. Whereby Poly(acrylic acid) brushes were grafted from the surface of the latex particles which were prepared by conventional emulsion polymerization with latex particles contain thin layer of the photo-initiator 2-[*p*-(2-Hydroxy-2-methylpropiophenone)]-ethylene glycol-methacrylate) which covalently attached to the surface of the latex particles [24,25].

By the same synthetic procedure, cationic poly(electrolyte) brushes were grown from the surface of cationic poly(styrene) latex particles, the obtained particles were used to investigate the electrostatic attraction between the cationic brushes on the surface of the particles and the negatively charge surface as mica, the interaction shows very strong attraction and therefore the core-shell morphology of the particles with cationic brushes was verified [26].

Cationic Ludox silica particles were used as macro-initiator after adsorbing anionic ATRP initiator (anionic polymer contains on tertiary bromine functional group) on their surfaces by electrostatic attractions, from the surface of that ludox silica

particles a various hydrophilic monomer were polymerized at room temperature in aqueous environment, 4-styrene sulfonic acid (sodium styrene sulfonate) was also grafted from the surface of these silica particles but with dispersion medium contains 1:1 methanol/water, low conversion only 22% after 24 hours was obtained with catalyst being used is CuBr/bpy. In addition to that electrolyte monomer, another electrolyte monomer which is (3-sulfopropyl methacrylate) was used to grow a poly(electrolyte) brushes from ludox particles with higher monomer conversion around 67% after only 3 hours, but the polymerization was conducted in water as a dispersion medium at ambient temperature [27]. Cationic poly(electrolyte) brushes such as poly(aminoethyl methacrylate hydrochloride) were grown by photo-emulsion polymerization from the surface of cationic poly(styrene) latex particles, these hairy particles were able to be tagged by gold nano-particles by electrostatic attraction interaction [28]. The effect of addition of salt (ionic strength) in the poly(styrene) latex particles that contain cationic or anionic brushes was studied, it was observed that a strong shrinking of poly(electrolyte) upon the addition of sufficient concentration of salt to form quenched brushes [29-30].

Poly(sodium styrene sulfonate) brushes were grafted from dumbbell-shaped latex particles consist of (PS-PMMA) by photo-emulsion polymerization, the structure of the core-shell dumbbell shape latex particles was verified by Cryo-TEM [31]. It is worth to mention in that method to form dumbbell shape particles, small particles (secondary nucleation) were generated during the second stage seeded emulsion polymerization with size of 30 nm and that due to the presence of surfactant during the synthesis of PMMA primary seed particles. Recently, Ballauff *et al*, synthesised poly(acrylic acid) brushes from the surface of poly(styrene) latex particles which were synthesized at lower temperature by redox system, and then during the

formation of latex particles a functional monomer (inimer) which has a thermal decomposing group (bis-(2-propenyl) 2, 2'-azo diisobutyrate) was shot added to copolymerized with the remaining amount of styrene, the time of addition of the functional monomer was either after 100 min or after 150 min from the beginning of the polymerization, after the formation of the outer layer of this thermal initiator on the surface of latex particles and addition of water soluble monomer acrylic acid , the temperature of the emulsion was elevated above 75°C to trigger the surface initiated polymerization [32].

In this chapter after the cross-linked poly(styrene) latex particles were synthesized and dialyzed against water for two weeks, the particles were used as macro-initiator for SET-LRP of several water soluble monomers, to grow a polymer brushes with different characteristic properties from the surface of the latex particles. The conditions of the surface initiated polymerization were varied to obtain a best recipe with each particular monomer that used such as controlled the rate of the polymerization and the colloidal stability. We are motivated to see the difference in how the surface initiated polymerization by SET-LRP will behave from the surface of the latex particles compared to solution polymerization, and the differences between the latex that made by batch and shot-addition in term of the polymerization rate, brushes density and colloidal stability. These hairy latexes will be used in the next step which is swelling and seed emulsion polymerization to form the targeted Janus particles.

4.3. Experimental section

4.3.1. Materials

Copper wire (0.25 mm diameter), 99.9% metals basis, Copper powder for organic synthesis 5-50 µm, flakes, 99% (Aldrich), Copper(I) bromide and Copper(II) bromide, 99% (Aldrich), *N*-isopropylacrylamide, 97% (Aldrich), *N, N, N′,N″,N″*-pentamethyl diethylene triamine (PMDETA), 99% (Aldrich), Ethylene glycol, 99% (Aldrich), 2-Hydroxy ethyl acrylate, 96% (Aldrich) was purified by passing it through a column of basic alumina, 3-Sulfopropyl methacrylate potassium salt, 98% (Aldrich), 4-Styrene sulfonic acid sodium salt (Aldrich), Poly(ethylene glycol methyl ether acrylate), Average M_n= 454 g/mol (Aldrich) was purified by passing it through a column of basic alumina, *N*,*N*-dimethyl acrylamide, 99% (Aldrich) was purified by passing it through a column of basic alumina.

4.3.2. General procedure for surface initiated polymerization by SET-LRP method from the surface of latex particles made by batch addition method

An example will be described here for (SET-62) of the surface initiated polymerization from latex (PS-18) as following: 0.5086 g of NIPAM, 23.5 mg of Cu(0) (powder), 1.6 mg of $CuBr_2$ and then 0.20 g of ethylene glycol were placed in 50 mL round bottom flask. After that 15.0 g of distilled water was added to the mixture, and finally 4.9778 g of PS-18 was added. And then the flask was closed by rubber stopper and placed on a water bath at 25ºC, the mixture was degassed for 30 minutes, and then 2.0 mL of 2 wt% separately degassed aqueous ligand (PMDETA) solution was injected by plastic syringe to the mixture. At that moment the polymerization is considered to be commenced. The degassing of the polymerization mixture was continued all over the course of the polymerization with a low stream of nitrogen gas. Samples were taken after predetermined

intervals to monitor the conversion of the polymerization and the particle size. After the SET-LRP the functionalize latex was purified by ultracentrifuge at speed of 28 Krpm for 24 h, and then the aqueous phase (the supernatant) was separated by removal from the centrifuge tube. The latex was redispersed in water by sonication; finally the redispersed latex in water was dialysis for one week.

4.3.3. General procedure for the surface initiated polymerization by SET-LRP method from the surface of latex particles made by shot addition method

An example will be described here for (SET-63) of the surface initiated polymerization from latex PS-20 as following : 0.5001 g of NIPAM, 23.6 mg of Cu(0) (powder), 2.1 mg of $CuBr_2$ and then 0.2141 g of Ethylene glycol were placed in 50 mL round bottom flask. After that 15.0 g of distilled water was added to the mixture, and finally 4.99 g of PS-20 was added. And then the flask was closed by rubber stopper and placed on a water bath at 25ºC, the mixture was degassed for 30 minutes, and then 2.0 mL of 2 wt% separately degassed aqueous ligand (PMDETA) solution was injected by plastic syringe to the mixture, at that moment the polymerization is considered to be commenced. The degassing of the polymerization mixture was continued all over the course of the polymerization with a low stream of nitrogen gas. Samples were taken after predetermined intervals to monitor the conversion of the polymerization and the particle size. After the SET-LRP the functionalize latex was purified by ultracentrifuge at speed of 28 Krpm for 24 h, and then the aqueous phase (the supernatant) was separated by gently removal from the centrifuge tube, and the remaining sediment hairy latex was redispersed in water by sonication, finally the redispersed latex in water was dialysis for one week.

Cryo-TEM: Two types of TEM were used, The Jeol 2011 is a 200 kV (LaB_6) instrument fitted with a GatanUltraScan™ 1000 camera, The Jeol 2010F is 200 kV Field Emission

Gun instrument, It is fitted with a GatanUltraScan™ 4000 camera. The procedure for sample preparation is as the following: Diluted sample of latex is placed on the 25 lacey grid 400 meshes from agar scientific. The grid is plunged in liquid ethane, which has been cooled into liquid nitrogen. Then the sample is transferred to the cooled Cryo-holder and then to the transmission electron microscope for imaging.

Purification of latex by ultra-centrifuge: 12.0 g of hairy latex was weighed accurately, and then placed on 20 mL of plastic test tube for centrifugation. Then the test tube is placed into the ultra-centrifuge device under vacuum with temperature of 4ºC. The ultra-centrifugation is performed for 24 h at the speed of 28 Krpm. After that the pure light blue aqueous layer (supernatant) is removed and replaced by newly fresh water. The latex is redispersed in water by sonication.

4.4. Results and discussion

As described in chapter 2, two types of lightly cross-linked poly(styrene) latex particles were synthesized by soap-free emulsion polymerization to be used as seed particles for surface initiated polymerization of polymer brushes employing a SET-LRP strategy. The difference between the two types of latexes is the moment at which the *tert*-bromine functional monomer (inimer) added during the emulsion polymerization, that is either *ab initio* (batch addition method) or after intermediate (typically 50-70%, usually after 150 min) monomer conversion (shot addition method). Whereas batch addition is the easiest it may not favour a shell-enriched distribution of the *tert*-bromine groups that will initiate the formation of the brushes. This would lead to a lower density in brushes, which later on will have effects in the swelling and phase separation step in the fabrication process of our anisotropic dumbbell-shaped particles. Firstly, we will discuss the results obtained using

the batch addition method for seed preparation, after which those from the shot addition method will be reported.

4.4.1. Surface Initiated Polymerization (SET-LRP) from particles prepared through batch addition of *tert*-bromine (inimer)

A variety of hydrophilic monomers were studied, NIPAM, sodium styrene sulfonate, poly(ethylene glycol methyl ether) acrylate (PEGMEA), and [2-(methacryloyloxy)ethyl]-trimethyl ammonium chloride](MAETACL). The discussion will be focussed on the first two which NIPAM represent non-ionic monomer and styrene sulfonate an ionic monomer.

The formation of poly(NIPAM) brushes of our latex particles is interesting as these show thermoresponsive LCST behaviour in water. [17] Table 1 shows the recipe and conditions that are used in each individual surface initiated polymerization (SIP) of NIPAM from latexes (macro initiator) that made using the batch addition method.

Table.1. Recipe of the SET-LRP (SIP) of NIPAM from latex particles made by batch addition at 25°C in water. a = the polymerization performed in the presence of cross-linker: *N,N'*-methylene-bis-acrylamide with concentration of 0.019 mol/L.

Exp	Latex	Latex solid weight (g)	[Monomer] $mol.L^{-1}$	Ligand	[Ligand] $mol.L^{-1}$	Cu (0)	[Cu (0)] $mol.L^{-1}$	[$CuBr_2$] $mmol.L^{-1}$
SET-64	PS-10	0.557	0.207	Lig_1	0.0105	Powder	0.0151	0.204
SET-62	PS-18	0.290	0.204	Lig_1	0.0110	Powder	0.0167	0.324
SET-65	PS-18	0.289	0.194	Lig_1	0.0105	Powder	0.0110	0.244
SET-84[a]	PS-18	0.286	0.209	Lig_1	0.0105	Powder	0.0129	0.306
SET-83	PS-18	0.286	0.198	Lig_1	0.0105	Wire	0.0269	0.0
SET-96	PS-18	0.294	0.185	Lig_2	0.0173	Wire	0.0235	0.0
SET-77	PS-18	0.276	0.201	Lig_1	0.0106	Wire	0.0271	0.349
SET-112	PS-24	0.435	0.194	Lig_1	0.0105	Wire	0.0268	1.990
SET-114	PS-24	0.459	0.198	Lig_1	0.0103	Wire	0.0264	0.40
SET-128	PS-24	0.454	0.205	Lig_1	0.0103	0.0	0.0	0.0

As seen in Chapter 3, SET-LRP of NIPAM (and other monomers) in water is very fast, which makes control of chain growth difficult. The best results were obtained

upon addition of Cu(II) species which were able to increase the rates of deactivation and move the equilibrium of the activation process towards the dormant side.

Worth mentioning is that addition of ionic species, especially divalent cations, compress the double layer of electrostatically stabilized colloids, which potentially can lead to colloidal instability and thus coagulation. As was done in Chapter 3, monomer conversion was monitored by ^{1}H-NMR by using ethylene glycol as inert reference. The monomer conversion versus time data for the individual entries in table 1 is given in Figure 1.

In addition to monomer conversion, the average particle size (Fig 2) and its distribution (Fig 3) were measured using dynamic light scattering throughout the polymerization process. It should be clearly noted that the production of water soluble polymer as a side reaction enhances the values obtained for the particle size, due to an increase in viscosity of the medium.

A blank experiment (SET-64) was carried out in which a latex was used that had no *tert*-bromine groups (PS-10). PMDETA was used as a ligand, and Cu(II) was added. No polymerization was observed from both the monomer conversion vs. time data and the particle size data. This is ascribed to the Cu(II) species serving as inhibitors since as we know from chapter 3 that Cu(0) alone with ligand and with no presence of initiator this mixture lead to polymerization of NIPAM to higher conversion of more than 50% conversion.

Next two polymerizations (SET-62 and SET 65) were carried out using latex PS-18 as inimer containing seed and Cu(0) powder and Cu(II). Fast polymerization of NIPAM was observed with limiting monomer conversions of *ca.* 75% from the first point of measurement, with no further increase observed.

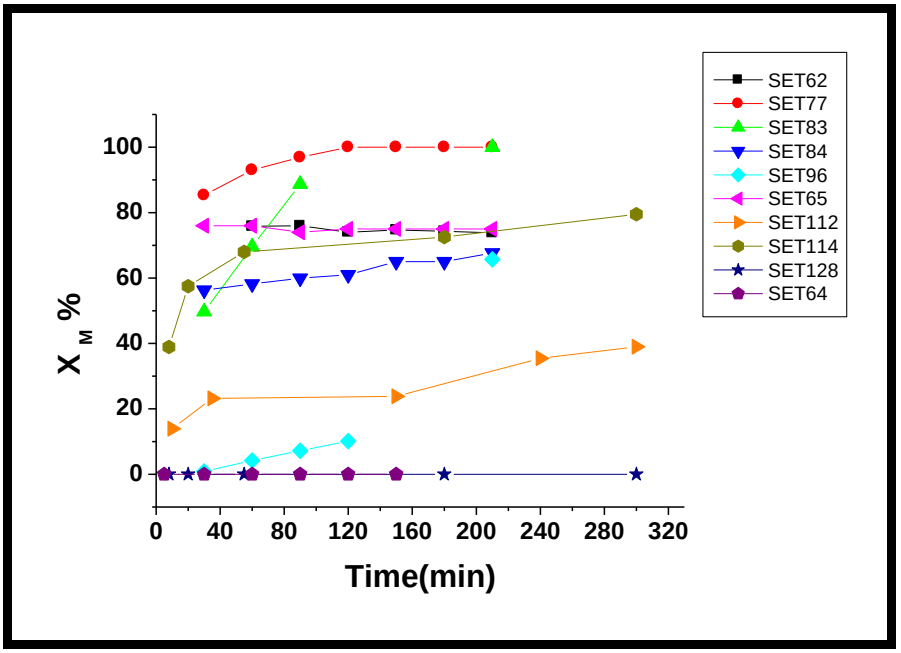

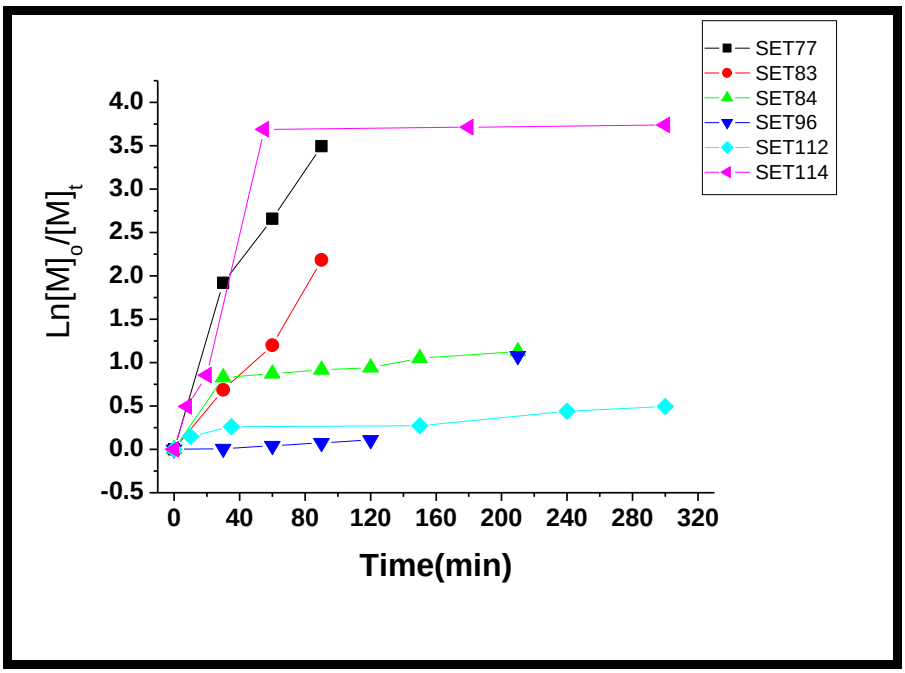

Fig.1. Monomer conversion versus time of the SET-LRP (SIP) polymerizations of NIPAM in different conditions from latex particles made by the batch addition method in water at 25°C.

The analysis of the particle sizes was in agreement, with the average of PS18 of 148 nm, increasing to 540 nm and 490 nm respectively for SET-62 and SET-65. The average particle size in the latter was slightly lower, potentially as in this case a lower concentration of Cu(II) species was added to the system. In a third reaction we tried to fabricate crosslinked poly(NIPAM) brushes (SET-84).

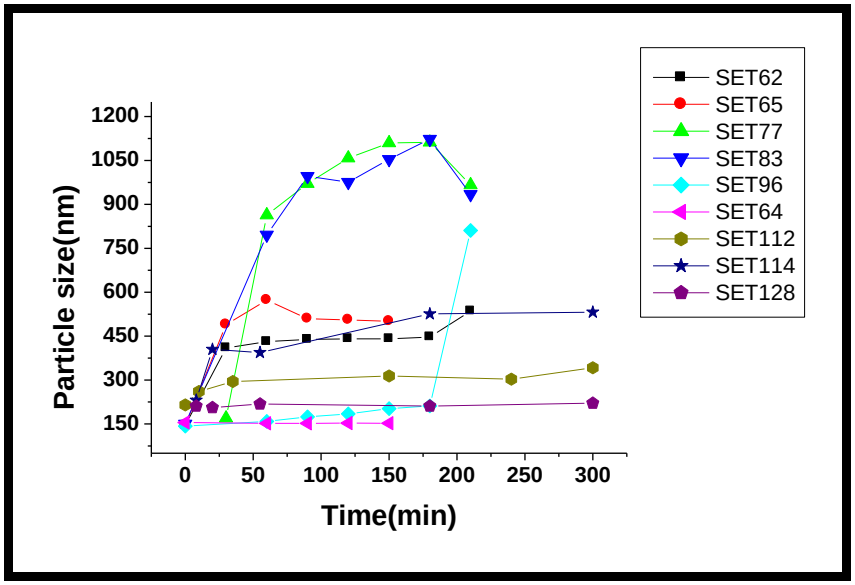

Fig.2. Behavior of the particle size versus time of the SET-LRP (SIP) of NIPAM from the surface of latex particles made by Batch addition method.

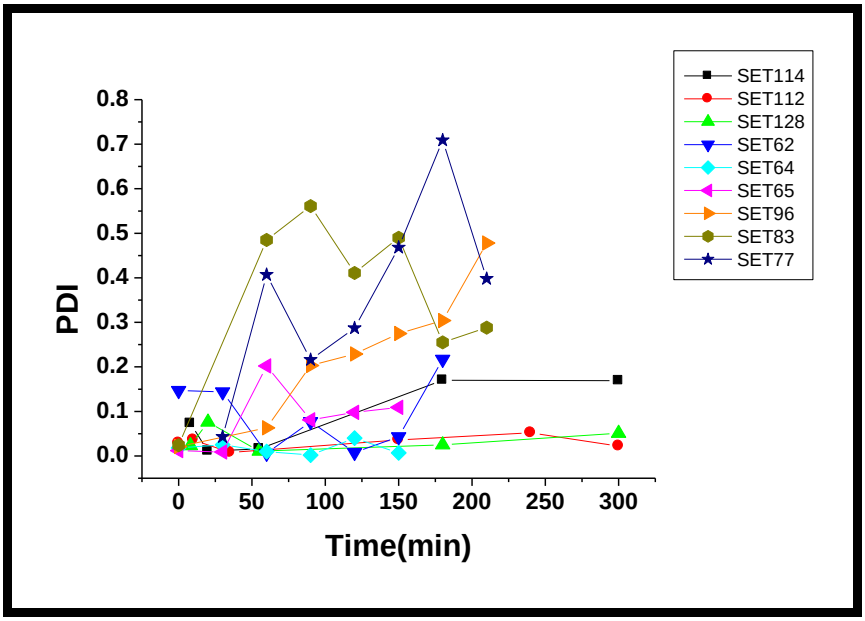

Fig.3. Behavior of the particle size distribution (PDI) versus time of the SET-LRP (SIP) of NIPAM from the surface of latex particles made by Batch addition method.

For this 0.019 mol.L^{-1} of (*N,N'*-methylene-bis-acrylamide) was added as a comonomer. Overall conversion was lower, typically reaching ca. 60%. In the next series of reactions (8.0 cm length, 0.25 mm diameter) Cu(0) wire was used which is wrapped around the magnetic stirrer. Note that the concentration of Cu(0) wire now is at least 1.5 orders of magnitude higher, than in case of powder.

When no Cu(II) species were added, the polymerizations showed some form of retardation, being most pronounced in the system in which we replaced PMDETA for Me_6TREM as ligand as in SET-96, and that was also observed with solution polymerization as reported in chapter 3. In other cases the reactions did reach high monomer conversion, and did show some form of control of brush length as evidenced by increasing values for the diameter of the particles as measured with DLS. Use of excessive amounts of Cu(II) as in the case of SET-112 severely slowed down the polymerization reaction

The Zeta-potential throughout the polymerization process was measured. Addition of ligand and monomer (SET-128) already led to a reduction in values from -35 mV to -20 mV, potentially being caused through (partial) protonation of the tert-amine ligands serving as multivalent counter cations. This emphasizes that not only addition of (Cu) should be taken into account when looking at preservation of colloidal stability. All the latexes obtained from reactions which showed monomer conversion and an increase in particle size, showed a transition from clearly negative values for the zeta-potential, to values which were close to zero mV (see e.g. Fig 4). Effectively the formation of the non-ionic brushes provided steric stabilization, hereby moving the slipping plane to greater distances. Note that the formation of brushes which can provide steric stabilization enhance the colloidal stability of the latexes greatly and make them less prone to coagulation at higher electrolyte concentrations. The fabrication of NIPAM brushes was confirmed by FT-IR after centrifugation and dialysis of the now hairy latexes. A typical spectrum is given in Figure 5 in which a thin polymer film of the latex is analyzed. The FTIR spectrum shows the presence of the significant absorptions of the functional group of Poly(NIPAM) which is the amide bond and the secondary amine bond and these

absorptions were detected by FTIR as the following absorptions: the secondary amine binding vibrations absorption at 755 cm^{-1} and the stretching vibration at 3298 cm^{-1}, the amide binding vibrations absorption at 1639 cm^{-1}.

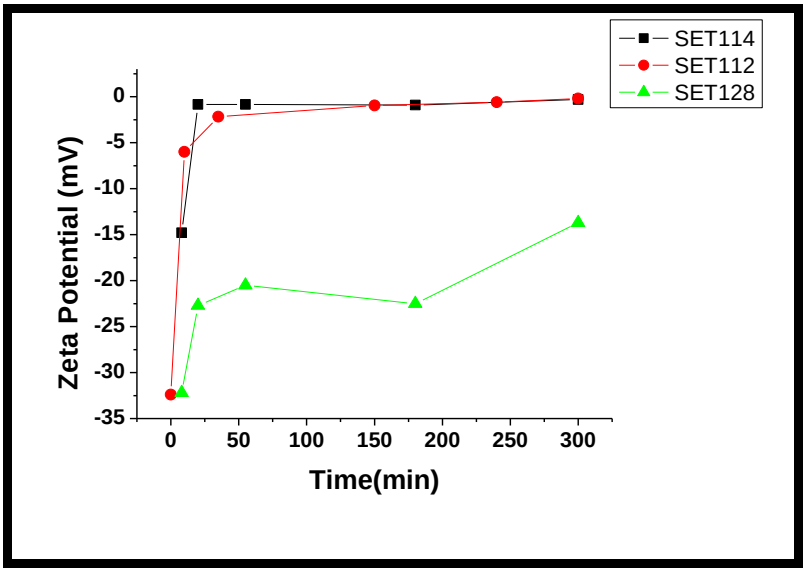

Fig.4. Zeta potential of the latex particles versus time during the SET-LRP (SIP) of NIPAM from latex made by batch addition method.

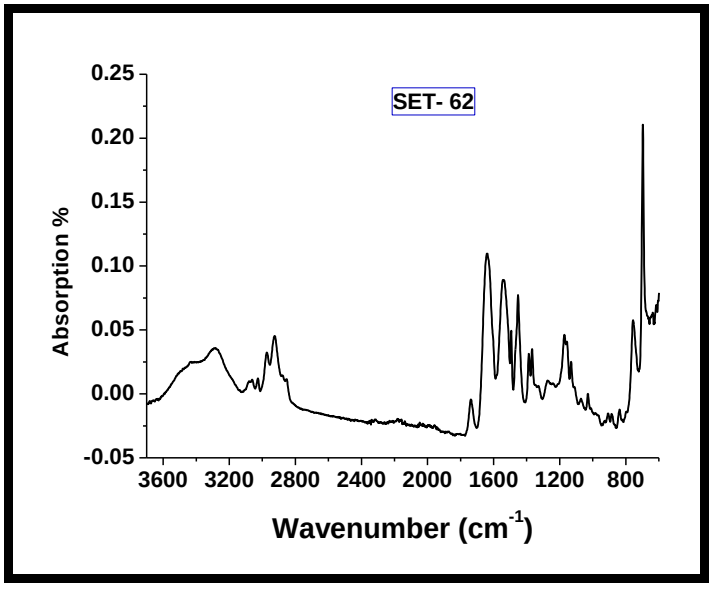

Fig.5. FTIR spectrum of SET-62 latex particles after drying.

The hairy core-shell structure of the colloidal particles was verified in the literature by Cryo-TEM [17-18-19]. The poly(NIPAM) brushes could be observed without the use of staining techniques; however not easily as the brush density was not very high

in case of batch addition method. An example of Cryo-TEM obtained for SET-62 is shown in Figure 6.

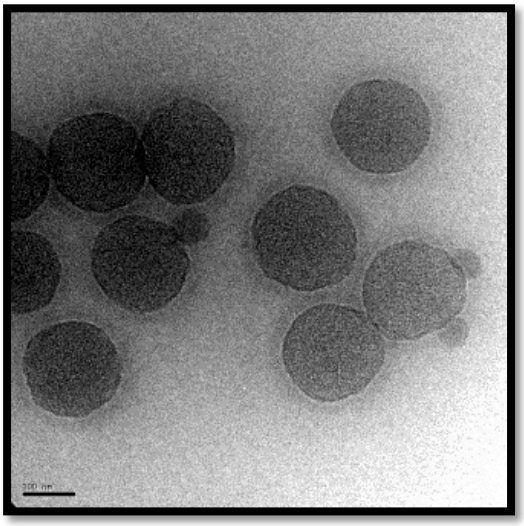

Fig.6. Cryo-TEM image of SET-62 latex particles, Scale bar is 100 nm.

The polymer brushes are barely seen as light dark-grey corona with low electron density around the dark latex particles which has high electron density. In order to verify the degree of control of the polymerization, the free water soluble Poly(NIPAM) which is not grafted from the latex particles was measured by SEC and shows that the experimental M_n's is higher than the theoretical M_n's by at least 4 orders of magnitude and broad molecular weight distribution as shown in the values in table 2. Smaller M_n value when $CuBr_2$ was used compare to Cu(0) used alone which gives higher M_n value.

Table.2. SEC data of the free poly(NIPAM) present in the supernatant after centrifugation.

Exp	[Initiator] $mol.L^{-1}$	Time (h)	Maximum Conversion %	M_n, theoretical $g.mol^{-1}$	M_n , experimental $g.mol^{-1}$	M_W $g.mol^{-1}$	PDI
SET-77	**0.0024**	**24**	**100**	**9,500**	**50,000**	**132,500**	**2.64**
SET-96	**0.0021**	**24**	**66**	**6,000**	**90,000**	**223,500**	**2.48**

The other monomer we studied extensively was sodium styrene sulfonate in order to form polyelectrolyte brushes on the surface of latex particles. Table 3 shows the

experimental conditions for the SET-LRP graft polymerizations. The ATRP and SET-LRP of sodium styrene sulfonate that conducted in aqueous medium and particularly in water was investigated in details in chapter 3. Polyelectrolyte brushes are stiff and extended compared to non-ionic brushes which is attributed to electrostatic repulsion and enhanced osmotic pressures inside the volume that contains the brushes. The first reaction again is a blank in which a seed latex was used that had no *tert*-bromine functionality SET-122. No monomer conversion and increase in particle size was observed (see figures 7& 8), but in solution polymerization a consumption of 20% of sodium styrene sulfonate was observed as in SET-132, the possible reason in case of SET-122 where no consumption of monomer occurred is the presence of the deactivator Cu(II) .

Table.3. Recipe of the SET-LRP (SIP) of Styrene sulfonate (NaSS) from the latex particles made by batch addition method at 25°C in water. a= the polymerization is performed with [2-(methacryloyloxy) ethyl]-trimethyl ammonium chloride 75% solution in water (MAETACL). SET-143* = the polymerization medium is 50:50 methanol /water, and 0.0216 g of external initiator (**2**) was used.

Exp	Latex	Latex solid weight (g)	[Monomer] $mol.L^{-1}$	Ligand	[Ligand] $mol.L^{-1}$	Cu (0)	[Cu (0)] $mol.L^{-1}$	[$CuBr_2$] $mmol.L^{-1}$
SET-97[a]	PS-18	0.290	0.193	Lig_1	0.0105	Wire	0.0268	0.77
SET-109	PS-18	0.284	0.115	Lig_1	0.0105	Wire	0.0277	1.1
SET-110	PS-24	0.502	0.096	Lig_1	0.0100	Wire	0.0263	0.73
SET-116	PS-26	0.354	0.108	Lig_1	0.0105	Wire	0.0275	0.59
SET-117	PS-21	0.210	0.107	Lig_1	0.0105	Wire	0.0275	0.40
SET-122	PS-23	0.346	0.113	Lig_1	0.0105	Wire	0.0275	0.30
SET-124	PS-18	0.297	0.111	Lig_1	0.0105	0.0	0.0	0.0
SET-125	PS-24	0.439	0.111	Lig_1	0.0105	0.0	0.0	0.0
SET-143*	PS-24	0.463	0.107	Lig_1	0.0128	CuBr	0.0092	0.0

Peculiar results are observed in the cases of SET-124 and SET-125 where no copper species are added. Firstly there seems to be an unexplained instantaneous conversion of ca. 10% with further polymerization occurring after prolonged inhibition periods. The only feasible explanation could be if unidentified metal ions were present in the

water phase. Similar results are observed in Chapter 3 for the homogeneous polymerization system, in which polymerization starts after ca. 150 mins in the presence of ATRP initiator as in case of SET-135.

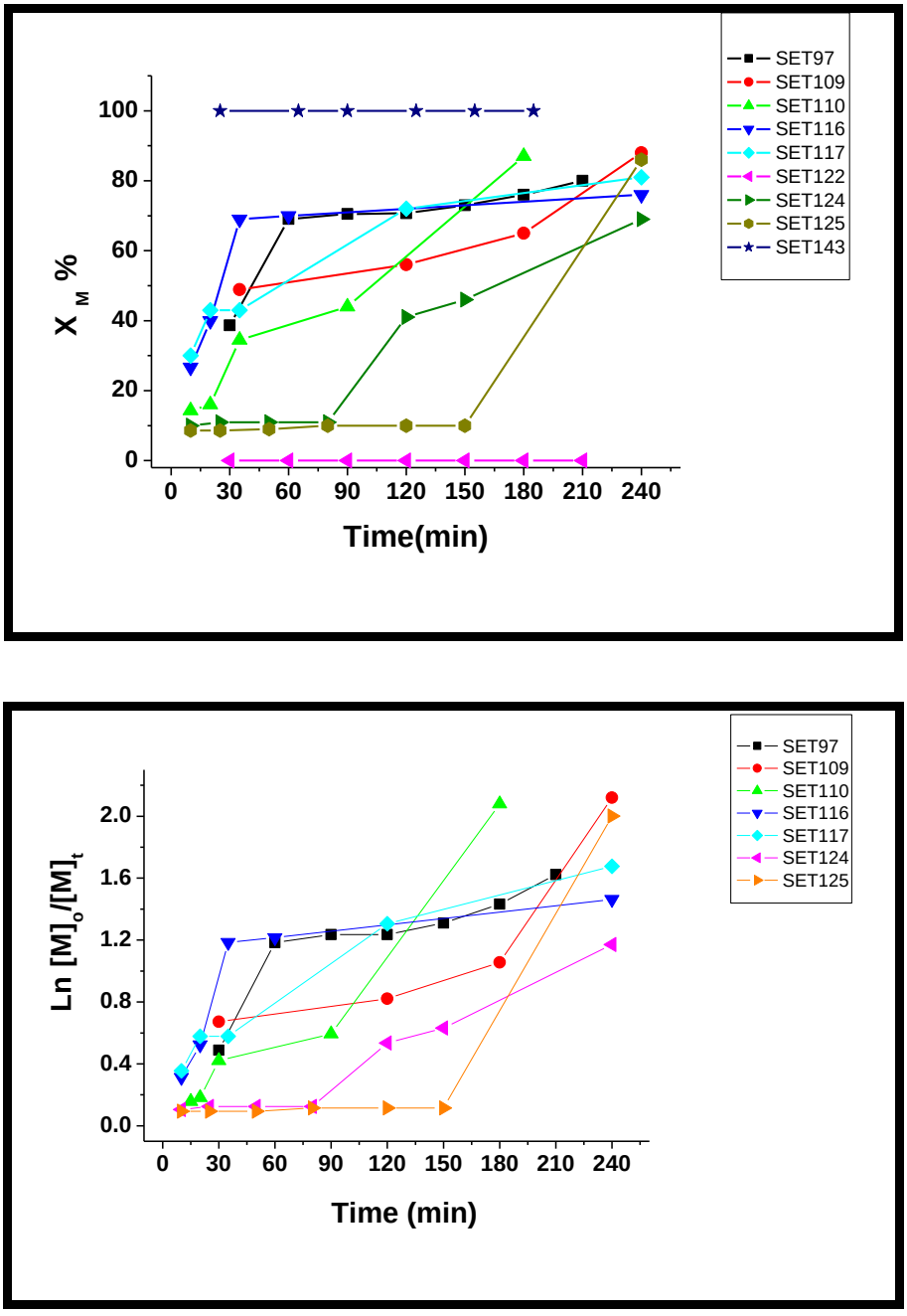

Fig.7. Monomer conversion versus time of the SET-LRP (SIP) of NaSS from latex made by batch addition in water with different conditions at 25°C.

All other reactions showed limited monomer conversions up to 80%, potentially ascribed to a build-up of Cu(II) species, with regardless of SET-143 when an

external initiator used with a combination of methanol as cosolvent and CuBr, 100% monomer conversion was achieved. These reactions showed an increase in particle size and thus formation of polymer brushes of poly(sodium styrene sulfonate). Interestingly is that particle sizes exceeding 1.0 µm are measured (e.g. SET-117). Although no coagulation was observed, the dispersion was very viscous even after precipitation and dialyses of the hairy latexes.

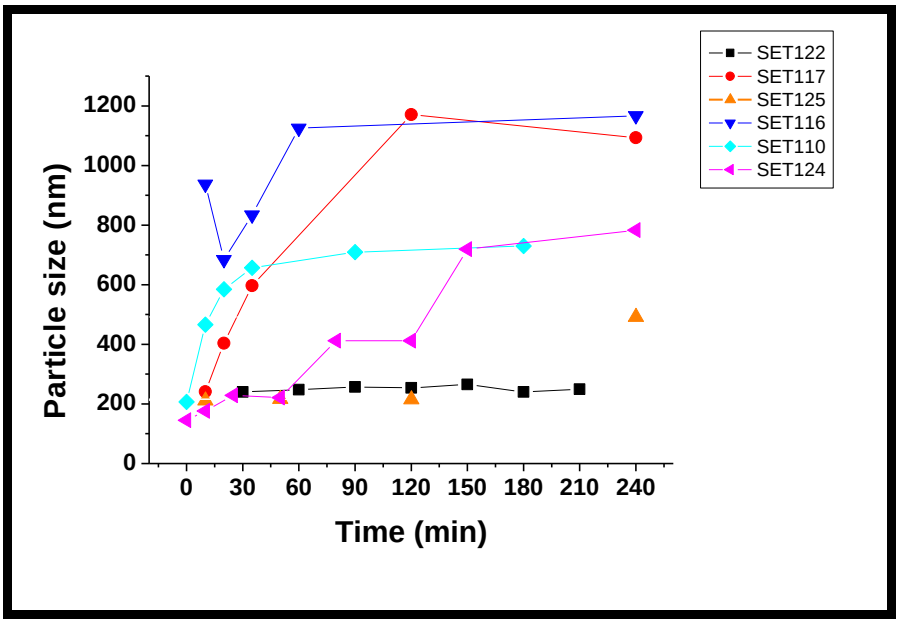

Fig.8. Behavior of the particle size versus time of the SET-LRP (SIP) of NaSS from the surface of latex particles made by Batch addition method.

The zeta potentials now became more negative throughout polymerization, which is logical as charge densities of the latexes increased upon polyelectrolyte brush formation (see Fig 10).

The poly(sodium styrene sulfonate) brushes were confirmed by FT-IR. The FTIR of a film of latex (SET-110) is shown in Fig 11. This FTIR shows significance absorption at 1041 cm^{-1} which comes from the symmetric stretching of sulfonate group (SO_3) and asymmetric stretching at 1184 cm^{-1} of the same group.

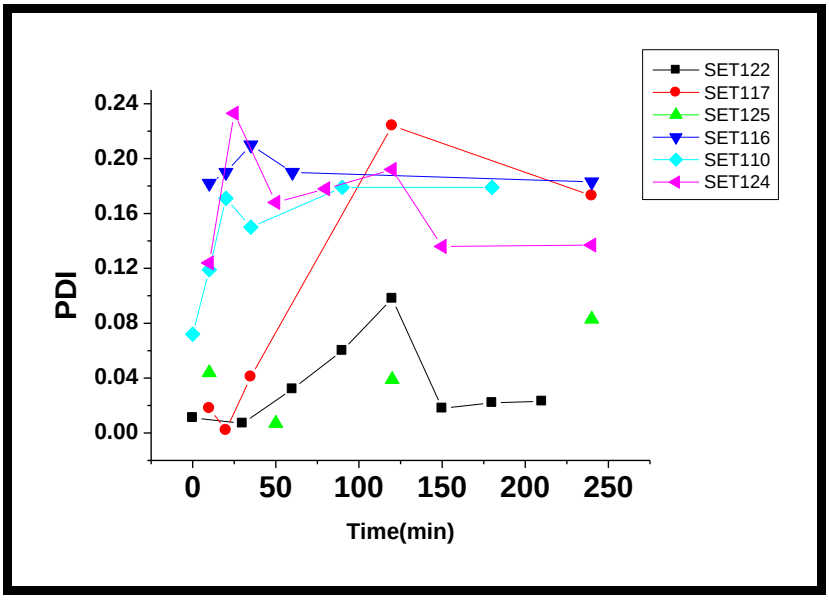

Fig .9. Behavior of the particle size distribution (PDI) versus time of the SET-LRP (SIP) of NaSS from the surface of latex particles made by Batch addition method.

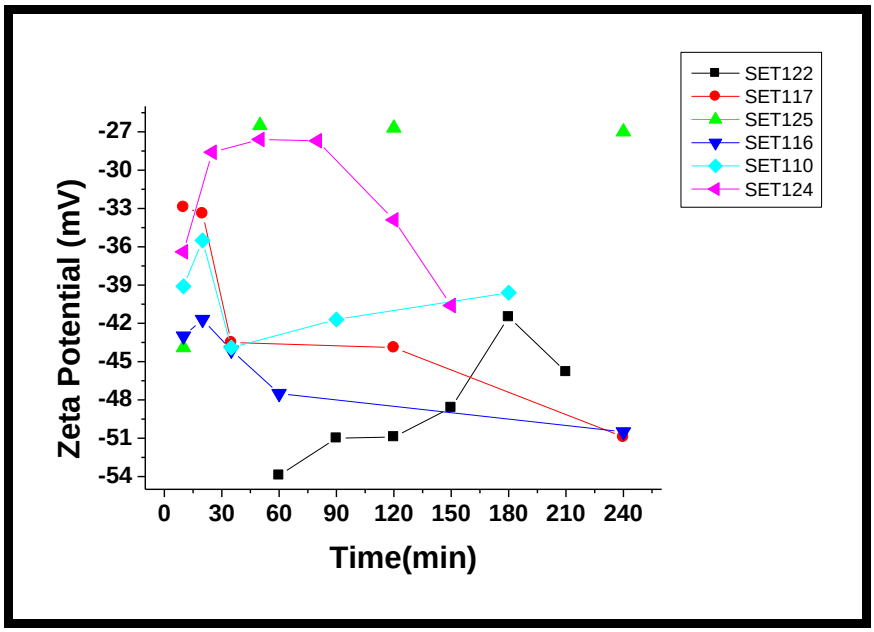

Fig.10. Zeta potential of the latex particles versus the time during the SET-LRP (SIP) of NaSS from latex particle made by batch addition method.

Due to the low density of the poly(sodium styrene sulfonate) brushes that made on the surface of latex particles prepared by batch addition method, the Cryo-TEM would not verify the presence of brushes as that can be concluded from chapter 5.

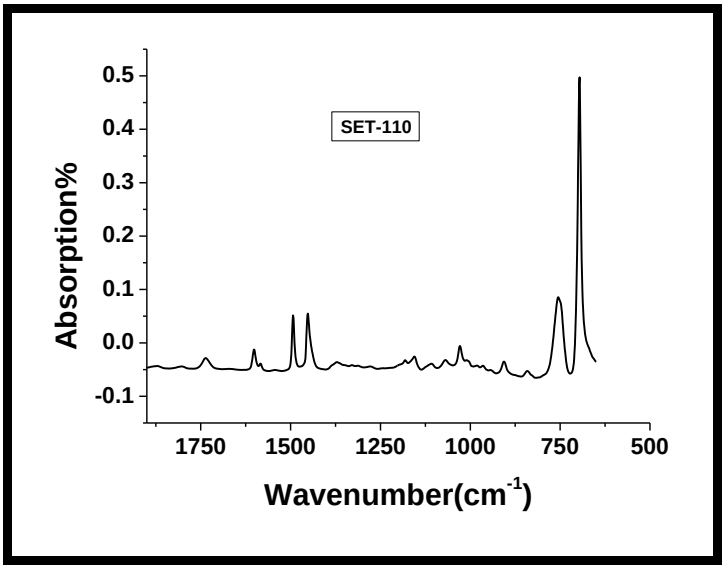

Fig.11. FTIR absorption of SET-110 latex particles.

A cationic monomer was used also which is [2-(methacryloyloxy) ethyl]-trimethyl ammonium chloride 75% solution in water (MAETACL) as in SET-97. The polymerization reached to 70% conversion just after 60 minutes from the beginning of the reaction, and then gradually increases to reach to 80% conversion after 24 hours; this is quite similar behaviour to SET-109 as quite equal conditions were used in both cases. The polymerization at the beginning shows some coagulation and as it continued, the amount of the coagulum decreases and very viscous dispersion is obtained. The latex particles successfully gained a positive charge as the zeta potential has positive value of (16 mV); this means that latex particles with cationic polymer brushes are generated.

4.4.2. Surface Initiated Polymerization (SET-LRP) from latex particles made via the shot Addition method of tert-bromine (inimer)

In this section the latex particles containing *tert*-bromine functional groups made through shot addition of the (inimer) were investigated as macro-initiator substrates for growth of water-soluble polymer brushes from their surfaces. The shot addition method allowed for a higher concentration of tertiary bromine functional group in the surface regions of the latex particles, which should result in denser polymer brushes on the surface of latex particles. This higher density alters the physical properties of these hairy latex particles in comparison to those made from particles using the batch addition method of inimer.

Therefore the SET-LRP (SIP) will behave differently to some extent from that studied by batch addition method. Here we divide the discussion in two parts based on the chemical nature of the water soluble monomers used, whereby the non-ionic monomers like NIPAM, 2-HEA and PEGMEA were studied independently from the ionic monomers (electrolytes) such as NaSS. Table 4 summarizes the ingredients and the conditions which were used in the SET-LRP (SIP) reactions using non-ionic monomers. First the SET-LRP (SIP) of NIPAM from the surface of latex particles will be discussed. The monomer conversion of the polymerization was monitored by ^{1}H-NMR as described before.

Three reactions were carried out with Cu(0) powder, that is SET-63, SET-85 and SET-98. All the three polymerizations show initially very fast polymerization, but the rate of polymerization rapidly decreases to very low values, resulting in limited monomer conversion of approximately 80%, 85-90%, and 60% in realistic reaction times of up to 4 hours (see Fig 12).

Table.4. Recipe of the SET-LRP (SIP) of NIPAM from the latex particles made by shot addition at 25°C in water. a = the polymerization performed with 2-hydroxy ethyl acrylate (2-HEA), b = poly ethylene glycol methyl ether acrylate (PEGMEA), d = the polymerization performed in the presence of cross-linker: *N,N'*-methylene-bis-acrylamide with concentration of 0.0197 mol/L.

Exp	Latex	Latex solid weight (g)	[Monomer] $mol.L^{-1}$	Ligand	[Ligand] $mol.L^{-1}$	Cu (0)	[Cu (0)] $mol.L^{-1}$	[CuBr2] $mmol.L^{-1}$
SET-63	PS-20	0.429	0.199	Lig_1	0.0112	Powder	0.0167	0.42
SET-85[d]	PS-20	0.429	0.201	Lig_1	0.0105	Powder	0.0107	0.42
SET-98	PS-20	0.421	0.176	Lig_2	0.0176	Powder	0.0126	0.68
SET-66	PS-20	0.404	0.209	Lig_1	0.0106	Wire	0.0280	0.33
SET-72	PS-20	0.428	0.190	Lig_1	0.0105	Wire	0.0268	4.3
SET-76	PS-20	0.430	0.199	Lig_1	0.0105	Wire	0.0268	1.28
SET-73	PS-20	0.405	0.217	Lig_1	0.0106	Wire	0.0271	29.4
SET-82	PS-20	0.449	0.197	Lig_1	0.0105	Wire	0.0268	0.0
SET-113	PS-25	0.249	0.202	Lig_1	0.0105	Wire	0.0268	2.8
SET-115	PS-25	0.263	0.201	Lig_1	0.0105	Wire	0.0268	0.32
SET-68[a]	PS-20	0.454	0.204	Lig_1	0.0103	Powder	0.0135	0.46
SET-70[b]	PS-20	0.425	0.052	Lig_1	0.0105	Powder	0.0155	0.40

This can possible be ascribed to the production of Cu(II) species as a result of considerable permanent termination caused by a too high radical concentration. This would slow down the reaction.

The amount of added Cu(II) in SET-98 was approximately 50% higher, and in addition a more active ligand was used, that is Me_6TREN, which resulted in a lower limited monomer conversion. The particle size was monitored throughout polymer brush formation by SET-LRP using dynamic light scattering.

The original particle diameter of the seed latex used (PS-20) was 135 nm. For SET-63 the particle size increases greatly after 5.0 minutes to become around 390 nm, and then constant values obtained for a period of 3 hours. Purification by centrifugation and dialyses of the final latex and analysis of the particle size after cleaning revealed a diameter of 317 nm with narrow particle size distribution of 0.025 and low zeta potential of (-1.85 mV) (see figure 15 and table 6), with very good colloidal stability.

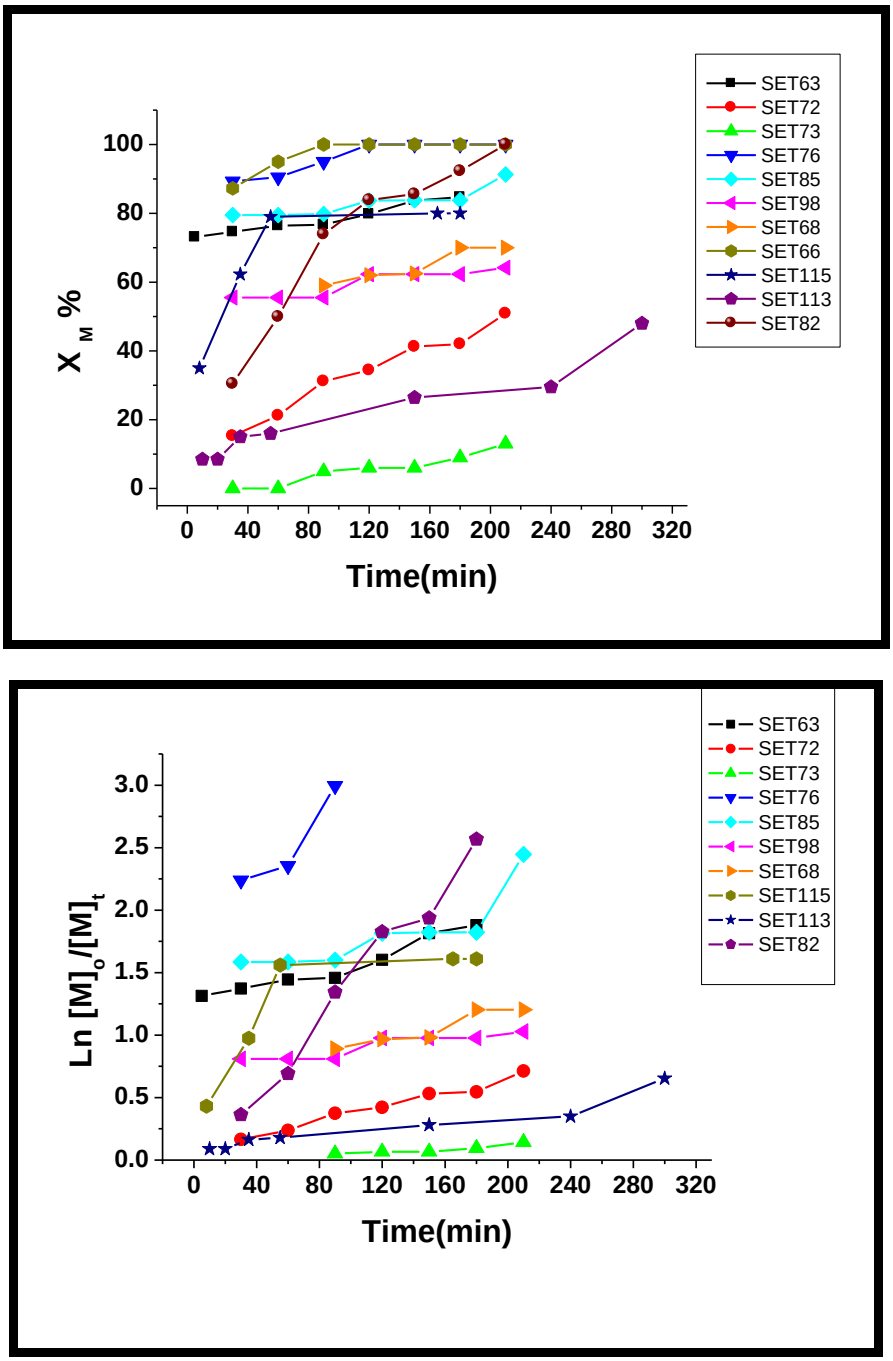

Fig.12. Conversion versus time of the SET-LRP (SIP) polymerizations of NIPAM in different conditions from latex particles made by shot addition method in water at 25°C.

The latter can be attributed to the steric stabilization of the grafted polymer brushes. The difference in particle size before and after cleaning is ascribed to the presence of homopolymer of poly(NIPAM) in the water phase. This is a result of transfer reactions occurring throughout the polymerization process. The presence of

homopolymer enhances the viscosity of the surrounding medium which reflects directly into higher measured values for the particle diameter.

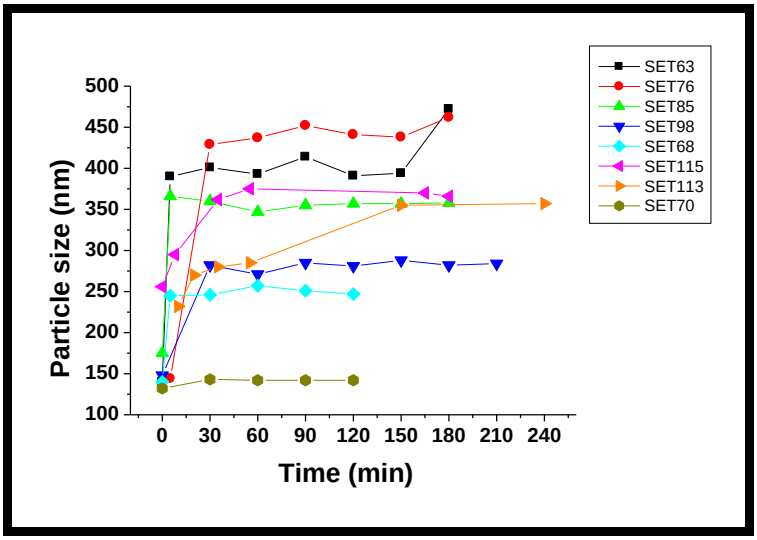

Fig.13. Behavior of the particle size against time of the SET-LRP (SIP) of NIPAM from the surface of latex particles made by shot addition method.

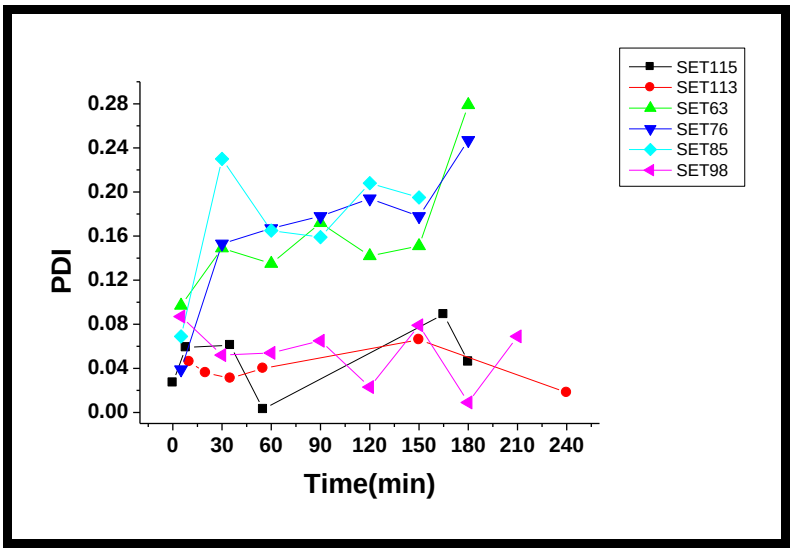

Fig .14. Behavior of the particle size distribution (PDI) against time of the SET-LRP (SIP) of NIPAM from the surface of latex particles made by shot addition method.

This is confirmed by SEC analysis of the supernatant, (see Table 5) which summarized the molecular weight properties of the free water soluble poly(NIPAM) for some polymerizations after removing the water from the supernatant and collecting the free poly(NIPAM).

Table.5. Number average molecular weight (M_n) and the weight average molecular weight (M_w), and molecular weight distribution of the free poly(NIPAM) in the supernatant after purification of the latex.

Exp	[Initiator] mmol.L^{-1}	Time (h)	Maximum Conversion%	M_n (theoretical) g.mol^{-1}	M_n (experimental) g.mol^{-1}	M_W g.mol^{-1}	PDI
SET-63	3.50	24	85	5,500	34,500	87,000	2.51
SET-98	3.00	24	64	4.000	19,000	57,000	2.99
SET-72	3.49	24	51	3,000	8,500	19,000	2.18
SET-76	3.51	24	100	6,500	23,500	57,500	2.43
SET-82	3.67	24	100	6,000	54,000	154,500	2.85

It can be concluded from the table that when a higher concentration of Cu(II) is used a smaller molecular weight will result in regardless of the types of Cu(0) used, for example in case of Cu(0) powder a smaller molecular weight was obtained in SET-98 compared to SET-63 as more Cu(II) was used in SET-98.That was also observed when Cu(0) wire used as smaller molecular weight obtained with high Cu(II) concentration as in SET-72 and the highest molecular weight observed is in SET-82 as no Cu(II) was used.

The use of small amounts of bisacrylamide as crosslinker in SET-85 produced similar results to SET-63. The diameter of the latex particle is in agreement with the conversion versus time data and shows rapid increase in the first 30 mins to reaching values of 360 nm. After cleaning a final particle size of 232 nm with a zeta potential of (-1.15 mV) is measured. This is a considerable lower value than the particle size obtained for SET-63, i.e. 317 nm. A plausible explanation is that the use of crosslinker restricts the hydrodynamic flexibility of the hairs resulting in a more compressed layer of poly(NIPAM). The size of SET-98 increases to 280 nm after 30 minutes and then very slowly increases. After purification the value of the diameter is similar to values measured before the cleaning step, that is 296 nm with low zeta

potential of (-0.160 mV). This suggest that the production of free poly(NIPAM) is restricted due to presence of sufficient amounts of Cu(II) species.

The limited control achieved by using Cu(0) powder let us to perform reactions using Cu(0) wire instead. Typical SET-LRP (SIP) conditions were used with Cu(0) wire / PMDETA / and variable amounts of Cu (II), namely 0%, 1.2%, 4.7%, 16%, 108% relatively to the total weight of Cu(0) wire used. In absence of added Cu(II) species, SET-82, a slower rate of polymerization is observed at the initial stages, suggesting the existence of a retardation period as a result of not sufficient Cu(I) species are present. The latter is formed through Cu(0)/Cu(II) disproportionation. Adding Cu(II) eliminates this retardation period, as seen in SET-66, SET-72 and SET-76. However, fast polymerization results in limited control of chain growth of the brushes. Further increase of Cu(II) slows down the polymerization sufficient in order to have some control over brush length as in SET-73.

The measured particle sizes for the SET-66 hairy latex particle was over 2.0 μm. A very viscous dispersion was obtained which suggest that NIPAM undergoes a side polymerization with Cu(0) wire which produces a large amount of free water soluble poly(NIPAM) which increases the viscosity of the dispersion and this is the possible reason for the complete monomer conversion in this case. The particle size for SET-82 was similarly large before filtration of the latex with particle size above 1.0 μm, but after filtration the particle size decline to be 383 nm and with zeta potential of (-1.22 mV), which reflects the formation of long polymer brushes and the removal of the free water soluble poly(NIPAM). The particle size for SET-76 increases with conversion to be 430 nm after 30 minutes, and then stays constant with slight increase until to be around 460 nm at the end of the polymerization. After

purification of latex, the particle size increases slightly to 490 nm and with low zeta potential of -0.429 mV.

This means longer polymer brushes were produced when Cu(0) wire was used and that was also observed in batch addition method. Reactions carried out with high concentrations of Cu(II), that is SET-72 and SET-73, relative values of 16% and 108% led to partial coagulation of the seed latex due to the presence high concentration of Cu(II) ions in solution and considerable compression of the double layer leading to loss of electrostatic stability of the seed latex PS-20.

In SET-113 and SET-115 the latex used to grow the poly(NIPAM) brushes from its surface is PS-25. This latex is different form PS-20 in some aspects, as it has a low cross-linked density, a bigger particle size, and less amount of surfmer (sodium styrene sulfonate), the presence of buffer in the latex, but has similar concentration of inimer around 5%. Less amount of latex is used in case of PS-25 in the SET-LRP (SIP) because constant weight of latex is usually used of 5.0 g, but the difference it comes from the total latex solid is 5% in case of PS-25, in contrast to PS-20 which has a total solid of 7.5%. The catalyst system used is Cu(0) wire/ PMDETA/Cu(II), the main difference between SET-113 and SET-115 is the concentration of the deactivator $CuBr_2$, which is 10.4% relatively to the total weight of Cu(0) wire used in case of SET-113, and 1.19% in case of SET-115. This is close to the concentration of Cu(II) used in case of SET-72 and SET-66 when PS-20 was used as initiator. In SET-113 the rate of the polymerization was slow with typical behaviour as in case of SET-72, but it is expected to be faster since the concentration of Cu(II) in SET-72 is 16% used compared to 10.4% in SET-113, but it was observed that SET-113 is slower than SET-72, and that might be attributed to the less weight of latex was used in SET-113, and therefore less amount of initiator. The polymerization proceeds

slowly and after 24 hours only 50% monomer conversion achieved with similar total conversion as in case of SET-72. However, in SET-113, latex particles show good colloidal stability in comparison to SET-72 which has poor colloidal stability. The particle size of SET-113 gradually increased with monomer conversion until it reached 350 nm. After purification of the latex, the particle size decreased to be 277 nm with poly(NIPAM) brushes thickness of 55 nm based on dynamic light scattering measurement.

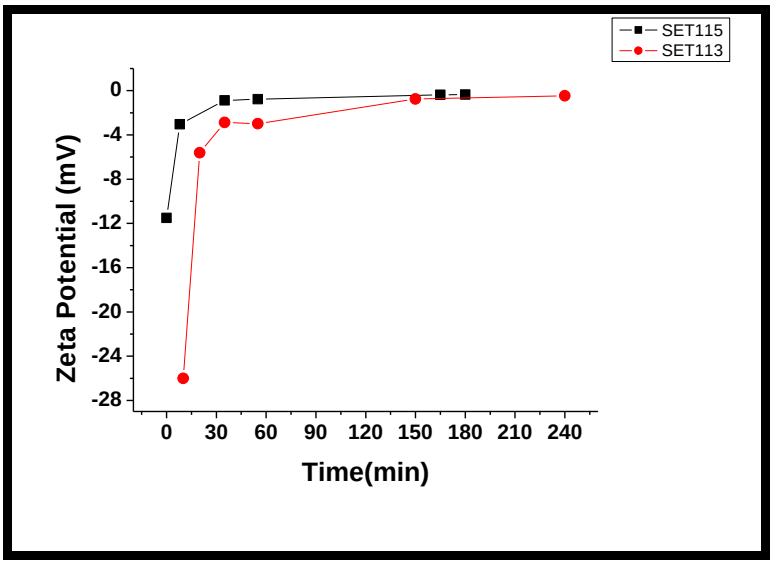

Fig.15. Zeta potential of the latex particles SET-113 and SET-115 versus the time during the SET-LRP (SIP) of NIPAM from latex made by shot addition method.

The latex particles showed a positive zeta potential of 1.72 mV with good colloidal stability which indicates dense and shorter poly(NIPAM) brushes are formed. When the concentration of added Cu(II) is decreased, as in SET-115, the rate of the polymerization is faster and reached to 80% conversion after 60 minutes, with no significance increases in the next few hours of reaction. The conversion was limited to 80% conversion, in contrast to SET-66 when full conversion was achieved; the possible reason behind that is the lower concentration of initiator used in SET-115.

The particle size in SET-115 increase sharply with conversion and goes to around 375 nm after 60 minutes and that concur with monomer conversion of the polymerization. The zeta potential for both polymerizations were monitored with time (see figure 15) and it decreased sharply with time, the drop in the zeta potential in SET-115 was more significant, in contrast to SET-113, and that with good agreement with the conversion since the faster rate of the polymerization and higher conversion in SET-115 facilitates the coverage of the latex with Poly(NIPAM) brushes, more efficiently masking the effect of the negative charges originating from the KPS and Surfmer.

Table.6. Final particle size, PDI and zeta potential of the some hairy latexes after purification made by SET-LRP (SIP) with NIPAM by Shot addition method.

Polymerization	Particle diameter (nm)	PDI	Zeta potential (MV)
SET-63	317	0.025	-1.85
SET-68	202	0.177	-7.71
SET-73	135	0.083	-18.9
SET-76	496	0.248	-0.43
SET-82	383	0.023	-1.22
SET-85	232	0.233	-1.15
SET-98	296	0.167	-0.16
SET-113	277	0.216	1.72

In SET-68 the polymerization was performed with 2-hydroxy ethyl acrylate, as typically the rate of polymerization was high and reached to limited monomer conversion of around 70% as Cu(0) powder used with Cu(II), but the particle size in case of SET-68 grow quickly to 250 nm and decrease after purification to 202 nm .

In case of SET-70, (PEGMEA) was used, a lot of noises in ^{1}H NMR restricted the determination of the monomer conversion, but the particle size stays constant during the whole course of the polymerization as its before the polymerization, this suggests in SET-70 no poly(ethylene glycol methyl ether acrylate) was grafted from the latex.

To confirm the presence of the poly(NIPAM) brushes attached to the surface of the latex particles, Cryo-TEM analysis was carried out. Figures 16 (A, B,C) show the Cryo-TEM images of SET-63 in different areas in Cryo-TEM grid, and Figure 16

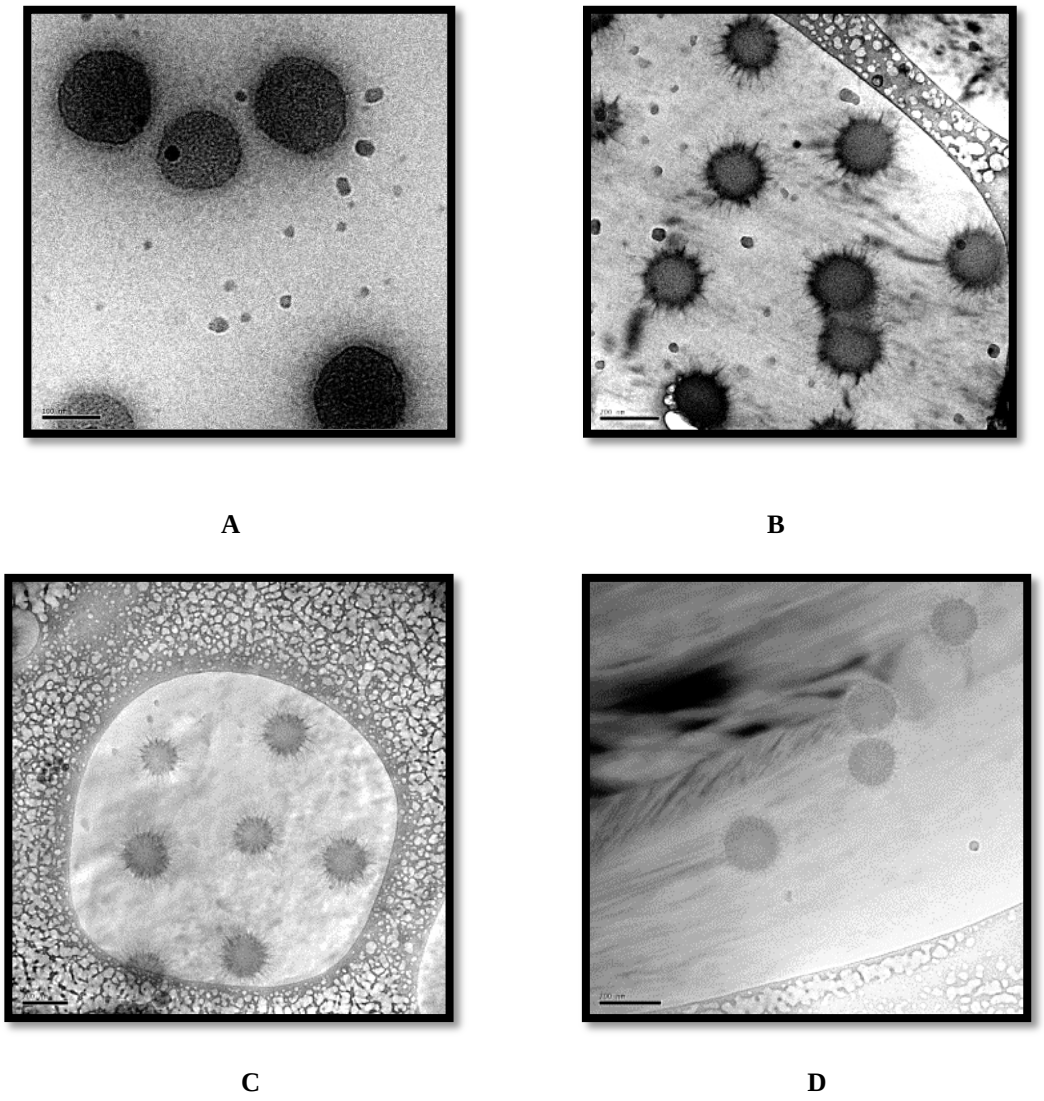

Fig.16. Cryo-TEM images (A, B, C) of SET-63 hairy latex with poly(NIPAM) brushes in different areas in Cryo-TEM grid, and (D) is the Cryo-TEM image of hairy latex SET-68 with poly(2-hydroxy ethyl acrylate), Scale bar in (A) is 100 nm and in (B),(C),(D) is 200 nm.

(D) is Cryo-TEM image of SET-68. In image (A), the poly(NIPAM) brushes appear as gray corona around the dark latex particles and show similarity to the images obtained by the batch addition method. Clearer images can be obtained after searching in another area in the grid, where the ice is thinner, but more importantly where the ice is crystalline. Here the polymer brushes of poly(NIPAM) become more visible as stretchable (hydrated) hair extended in the water phase as in images (B) and (C). Similar observation is also detected with poly(2-hydroxy ethyl acrylate) brushes as revealed in image (D) with hairy latex SET-68.

A plausible reason for the clear appearance of the brushes is that the crystalline domains of the ice have bundled the polymer brushes together, which we refer to as the wet-hair effect, which intensifies their electron scattering. From images (B) and (C) the length of the brushes can be estimated for SET-63 being approximately 80 nm. Conventional SEM analysis of SET-63 (see Figure17) shows that the latex particles are sticking together in clusters indicating that after drying the poly(NIPAM) brushes are interlink.

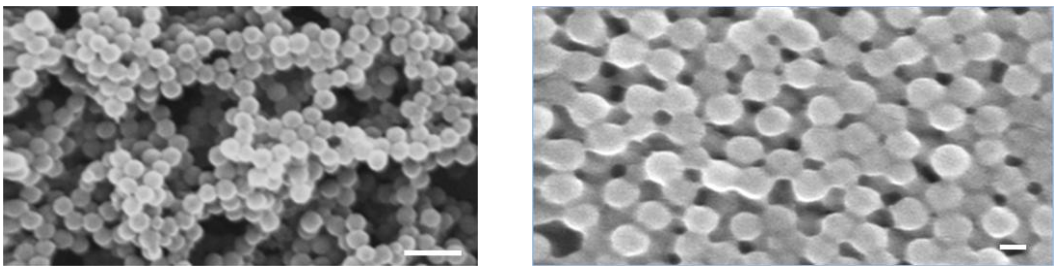

(A) (B)

Fig.17. SEM image of the hairy latex SET-63, Scale bar in image A is 1.0 µm and in image B is 200 nm.

Latexes made by the shot addition method were also used to grow poly(styrene sulfonate) brushes by SET-LRP (SIP) in aqueous media under different conditions, as summarized in Table 7. Cu(0) powder was used in two polymerizations with,

SET-69 and SET-172; the two polymerizations were different in some aspects. For instance, the latex that was used as the initiator in SET-69 was latex PS-20, and in SET-172 latex PS-31 was used as the seed. The catalyst regime was in both cases Cu(0) powder/PMDETA/$CuBr_2$, but the concentration of [$CuBr_2$] was different in each case (3.83% in SET-69 and 7.42% in SET-172) relative to the Cu(0) powder. Both polymerizations showed good monomer conversion (see figure 18). In the case of SET-69, 61% conversion was achieved after 90 minutes, and in case of SET-172, 74% conversion was achieved after 85 minutes. This initial contradictory result on the basis of $CuBr_2$ concentration, which was highest for SET-172, can be explained in that PS-31 was used as the seed, which has a three-fold higher concentration of the (inimer) functional group moiety.

Table.7. Recipe for SET-LRP (SIP) polymerization of (NaSS) from the latex particles made by the shot addition method at 25°C in water, b = Cu (0) wire was placed in the dialysis tube, d = presence of the sacrificial initiator (**2**) in SET-145 with concentration of [0.0051M)] and [0.0040M] in SET-146.

Exp	Latex	Latex solid weight (g)	[Monomer] $mol.L^{-1}$	Ligand	[Ligand] $mol.L^{-1}$	Cu (0)	[Cu (0)] $mol.L^{-1}$	[$CuBr_2$] $mmol.L^{-1}$
SET-69	PS-20	0.420	0.105	Lig_1	0.0106	Powder	0.0133	0.51
SET-172	PS-31	0.416	0.118	Lig_1	0.0105	Powder	0.0136	1.01
SET-123	PS-27	0.097	0.106	Lig_1	0.0101	0.0	0.0	0.0
SET-120[b]	PS-27	0.090	0.114	Lig_1	0.0105	Wire	0.0268	0.0
SET-121	PS-27	0.100	0.108	Lig_1	0.0100	Wire	0.0268	0.0
SET-118	PS-27	0.126	0.135	Lig_1	0.0105	Wire	0.0268	0.30
SET-111	PS-25	0.263	0.110	Lig_1	0.0105	Wire	0.0268	0.61
SET-171	PS-29	0.282	0.113	Lig_1	0.0105	Wire	0.0268	1.13
SET-145[d]	PS-29	0.289	0.110	Lig_1	0.0105	Wire	0.0268	1.1
SET-146[d]	PS-31	0.407	0.111	Lig_1	0.0105	Wire	0.0268	0.99
SET-108	PS-20	0.452	0.105	Lig_1	0.0105	Wire	0.0268	1.36

The particle size obtained in SET-172 was higher than that in SET-69 by two orders of magnitude, which can be seen in Table 8. This is odd as one would expect shorter brushes as the initiator density is higher in the case of SET-172. One possible explanation is that the brushes of two different particles undergo permanent

termination through combination, hereby linking the particles together covalently, Forming dimers or larger clusters.

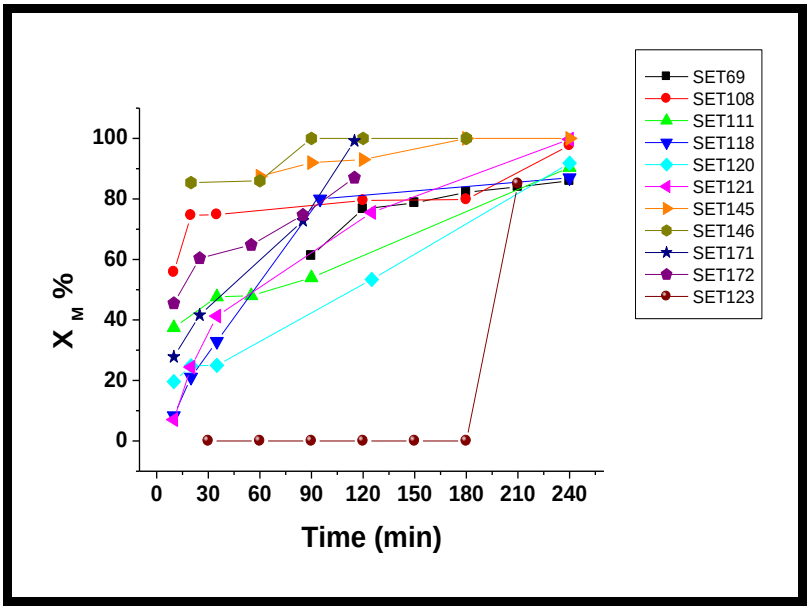

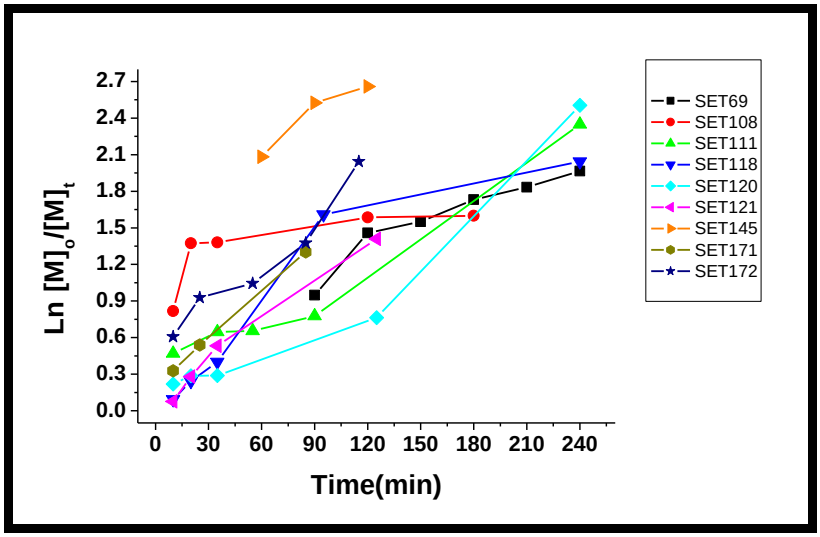

Fig.18. Monomer conversion versus time of the SET-LRP (SIP) polymerization of (NaSS) under different conditions from latex particles made by the shot addition method in water at 25°C.

This was observed in several of the polymerizations carried out, stressing that polymerization conditions are critical in order to avoid this. A cryo-TEM image of SET-172 is shown in Figure 19 to verify the presence of poly(sodium styrene sulfonate) brushes on the surface of the PS-31latex particles.

Table.8. Final particle size, PDI and zeta potential of some hairy latexes (after purification) made by SET-LRP (SIP) polymerization with (NaSS) by the shot addition method.

Polymerization	Particle size (nm)	PDI	Zeta potential (MV)
SET-69	617	0.121	-44.3
SET-108	1027	0.279	-16.3
SET-111	3428	0.299	-11.5
SET-118	1180	0.224	-35.3
SET-120	2233	0.276	-25.9
SET-121	3657	0.263	-28.0
SET-145	260	0.024	-49.7
SET-146	329	0.098	-39.6
SET-171	837	0.204	-7.65
SET-172	1171	0.255	-25.5

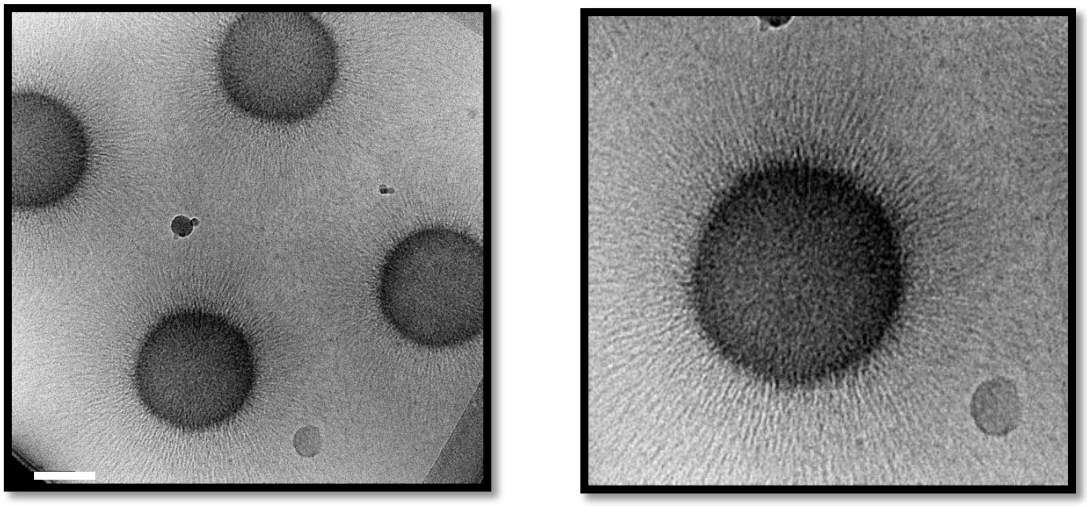

Fig.19. Cryo-TEM image of hairy latex SET-172 with poly(sodium styrene sulfonate) brushes, Scale bar in the image is 100 nm. On the right is close up image of one hairy latex particle.

The cryo-TEM image shows the presence of extended and dense poly(sodium styrene sulfonate) on the surface of the latex particle. The length of the brushes is approximately 100 nm which indicates that the polymer brushes are fully extended to their maximum length, therefore the polymer chain of the brushes is in the state of its contour length. The reason for the poly(sodium styrene sulfonate) brushes in our case to adopt fully stretching chain conformation is attributed to the osmotic pressure of the confined counterions inside the brushes which act to extend the polymer brushes to become osmotic brushes. This was also reported by Ballauff *et al.*, whereby the reasonably similar core-shell structure was observed [25]. The

assumption of theoretical calculation of the contour length (L_c) of the obtained poly(sodium styrene sulfonate) brushes was made due to the absence of the real molecular weight value of the synthesised poly(sodium styrene sulfonate), which indicates that if we have, for instance, a molecular weight of 8×10^4 g/mol as that assumed from the average molecular weight obtained in case of the poly(NIPAM) brushes, and with repeating unit of the length of 0.25 nm [33,34,35], and molecular weight of repeating unit of 206 g/mol, the calculated contour length (L_c) is 97 nm, which is in close agreement with the observed length of the poly(sodium styrene sulfonate) in the Cryo-TEM image which is 100 nm.

The main catalyst for growing poly(styrene sulfonate) brushes was a Cu(0) wire with latex PS-27 used as the macro initiator, four polymerizations were performed, SET-123, SET-121, SET-120 and SET-118, with different catalyst systems. In SET-123, this polymerization examined the absence of copper; the polymerization did not show any monomer conversion over a period of three hours, but after 24 hours, the polymerization had reached around 80% conversion that was also observed in batch addition latexes as in experiments SET-124 and SET-125.

The final partial size of SET-123 was around 1.4 μm (see Fig 20), which indicates that the styrene sulfonate was polymerized in the water phase, but the side polymerization reaction of styrene sulfonate took longer to overcome the induction period. The source of this side reaction could be between the ATRP initiator moiety groups and any other ingredients in the system to generate free radicals, since the free-ATRP initiator latex is inert and cannot initiate the polymerization. This behavior was also observed in latex using the batch addition method as in SET-124 and SET-125, where the particle size of the latex increased slowly over time even

with no polymerization. This could be explained by a loss in colloidal stability, since no polymer brushes were formed to improve the stability by steric stabilization

In SET-121, the polymerization was performed in the presence of a Cu(0) wire alone; the rate of polymerization was relatively faster and conversion reached 40% after 30 minutes, then the conversion increased gradually until it reached complete conversion after 24 hours. The particle size of SET-121 increased sharply after 40 minutes to around 600 nm which indicates a faster rate of polymerization in SET-121. The zeta potential before the addition of the ligand was around -30 mV, and after only 30 minutes of polymerization, the zeta potential decreased to -22 mV; as the conversion increased gradually, the zeta potential increased to -40 mV as shown in figure 25. After purification of SET-121, the final particle size was large, around 3.0 μm, and the zeta potential of the latex was -28 mV. This implies the formation of long polymer brushes which lead to the formation of bridges between the latex particles by a bridging flocculation mechanism.

In SET-120, the Cu(0) wire was wrapped around the magnetic stirrer and then placed inside the dialysis tube, then the dialysis tube was closed. The reasoning behind this polymerization setup was to see the effect of indirect contact between the Cu(0) wire and the polymerization mixture, since some of the Cu(0) wire active species will move from the dialysis tube to the polymerization mixture slowly by diffusion. The polymerization rate was slower, in contrast to SET-121, which means that contact with the Cu(0) wire enhances the rate of polymerization; this also implies that there are some small colloidal Cu(0) nano-particles which diffuse from the dialysis tube to the polymerization mixture to initiate the polymerization.

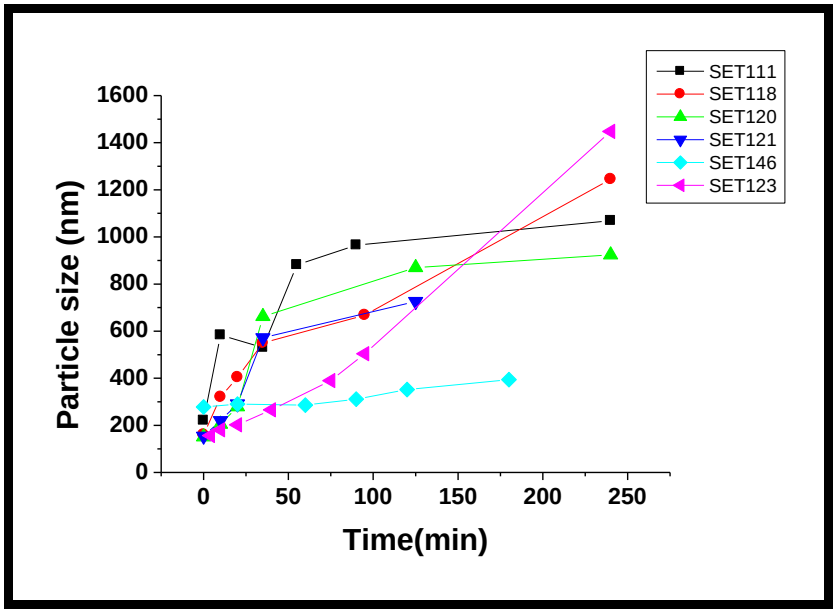

Fig.20. Behavior of the particle size versus time of the SET-LRP (SIP) polymerization of NaSS from the surface of latex particles made by the shot addition method.

The monomer conversion of SET-120 increased gradually to reach 90% conversion. It was noted that the dialysis tube was broken at the end of the polymerization, with latex found inside the tube, but the Cu(0) wire stayed inside the dialysis tube. The particle size increased sharply as in the case of SET-121, and reached 650 nm after 40 minutes. The particle size grew gradually until a size of 900 nm was reached; the zeta potential increased with conversion to -40 mV, which indicates the formation of negatively charged poly(sodium styrene sulfonate) brushes. After purification of the latex SET-120, the final particle size was greater than 2.0 μm with a zeta potential of -25.9 mV, which was close to that for SET-121. In SET-118, polymerization was performed in the presence of Cu(II) at 1.11% relative to the total Cu(0) wire. The rate of the polymerization was similar to that in SET-121 when Cu(0) was used alone. The final monmoer conversion was similar to the other polymerizations performed with PS-27, around 87%. The particle size of SET-118 increased sharply at the beginning of polymerization and then gradually increased until sizes greater than 1.0 μm were reached at the end of polymerization.

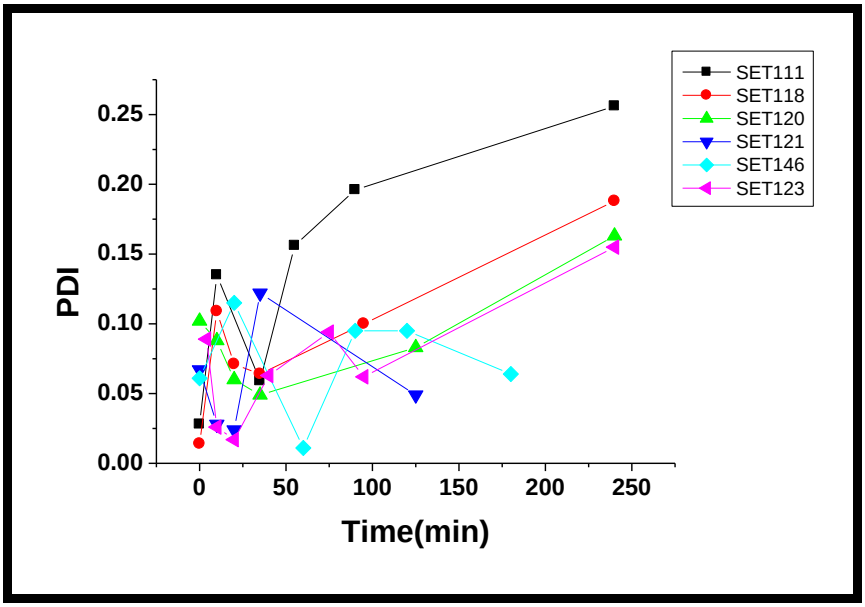

Fig.21. Behavior of the particle size distribution (PDI) versus time of the SET-LRP (SIP) polymerization of NaSS from the surface of latex particles made by the shot addition method.

The zeta potential before polymerization was around -38 mV; when polymerization commenced, the zeta potential decreased to -28 mV and then increased to -40 mV. This behavior was also observed in the other polymerizations when PS-27 was used. After purification of SET-118, the final particle size of the latex was 1180 nm and the zeta potential was -35 mV. To verify the presence of poly(sodium styrene sulfonate) brushes on the surface of the latex particles, cryo-TEM was performed on SET-118, SET-120 and SET-121 latex particles possessing poly(sodium styrene sulfonate) brushes in order to verify the presence of these brushes on the surface of latex particles made by the shot addition method (see figures 22,23 and 24).

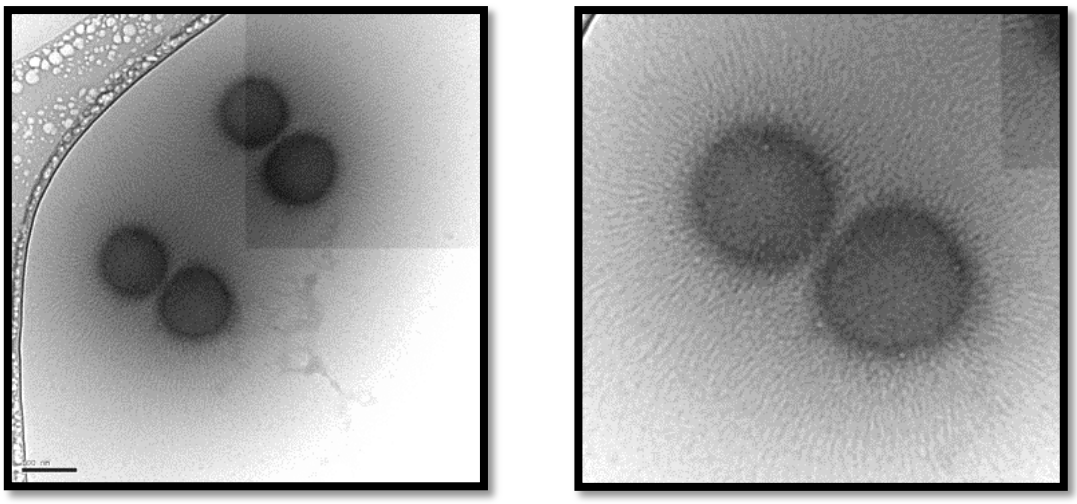

Fig .22. Cryo-TEM image of hairy latex SET-118 with poly(sodium styrene sulfonate) brushes, scale bar is 100 nm. On right is close up image of the hairy latex particles.

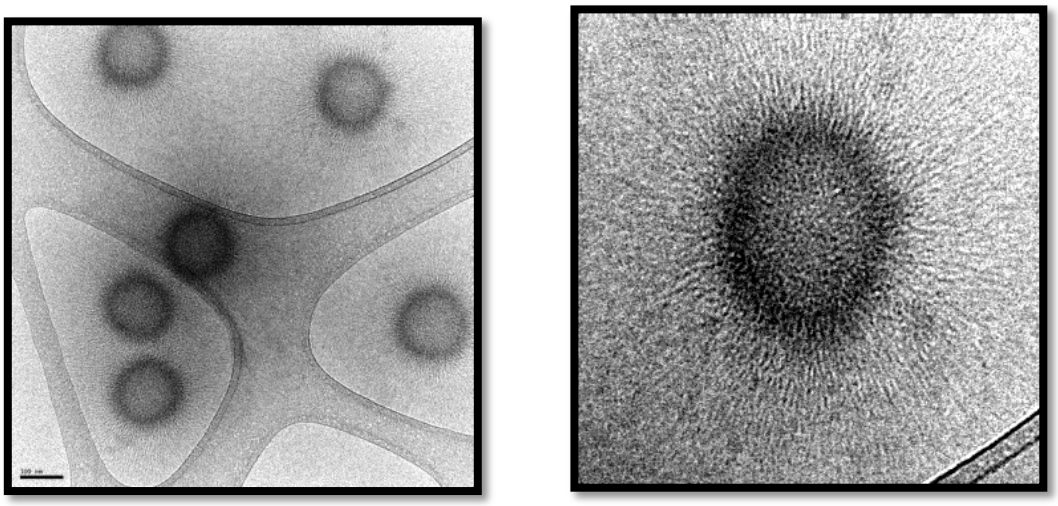

Fig.23. Cryo-TEM image of hairy latex SET-120 with poly(sodium styrene sulfonate) brushes, scale bar is 100 nm. On the right is close up image of one hairy latex particle.

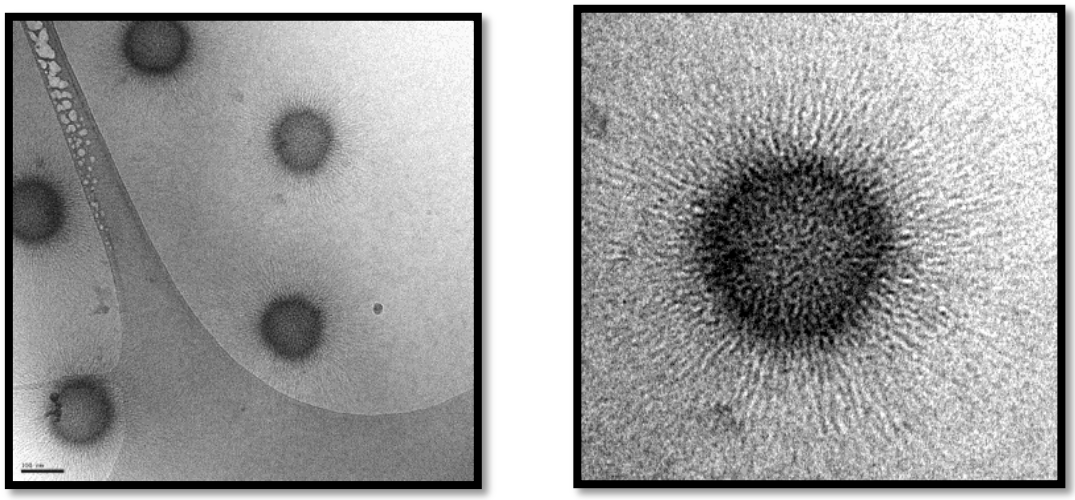

Fig.24. Cryo-TEM image of hairy latex SET-121 with poly(sodium styrene sulfonate) brushes, scale bar is 100 nm. On the right is close up image of one hairy latex particle.

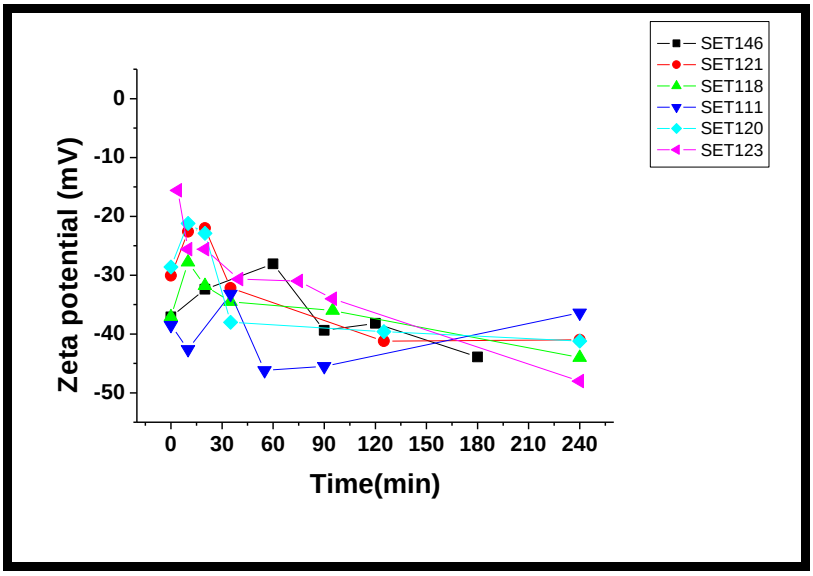

Fig.25. Zeta potential of latex particles of the SET-LRP (SIP) polymerization of NaSS from latex made by the shot addition method.

The cryo-TEM images of SET-118, SET-120 and SET-121 show long and stiff poly (sodium styrene sulfonate) brushes extending (hydrated) from the surface of PS-27 latex particles. It can be seen that long polymer brushes led to bridging flocculation, which made the particle size measured by DLS greater than 1.0 µm. The length of the polymer brushes was around 100 nm as roughly measured from the image. Therefore, the length of the poly(sodium styrene sulfonate) brushes was almost equal to the size of the PS-27 latex (156 nm), which gives the particles a completely hydrophilic shell and a cross-linked hydrophobic core. The Cu(0) wire has also been used with other latexes, not only with PS-27. It has been used with PS-20, as in SET-108; the catalyst used in this case consisted of the typical components including a Cu(0) wire/PMDETA/$CuBr_2$.

The polymerization rate was fast, and the polymerization conversion reached 75% after only 30 minutes, then the conversion slowly increased to reach 97% after 24 hours. This suggests that longer polymer brushes were formed, leading to bridging flocculation. The particle size of the latex was around 1027 nm with a low zeta potential of -16.3 mV.

When PS-25 latex was used, as in SET-111, typical SET-LRP (SIP) components were used, including a Cu(0) wire/PMDETA/Cu (II). The concentration of $CuBr_2$ was 2.27% of the total concentration of the Cu(0) wire. The polymerization was fast and reached 50% conversion after 30 minutes, but was slower in contrast to SET-108, although a higher concentration of Cu(II) was used in the former polymerization. The conversion continued until it reached 90%. Particle size increased sharply to 650 nm after 30 minutes and then slightly increased to 800 nm. The zeta potential at the beginning of the polymerization was - 40 mV, and as the conversion progressed, the zeta potential decreased to -33 mV and then increased to -45 mV, which is a typical trend of the zeta potential of styrene sulfonate SET-LRP (SIP). After purification of the latex, the particle size was greater than 3.0 μm with a low zeta potential of -11.5 mV. The cryo-TEM image of SET-111 is shown in Figure 26.

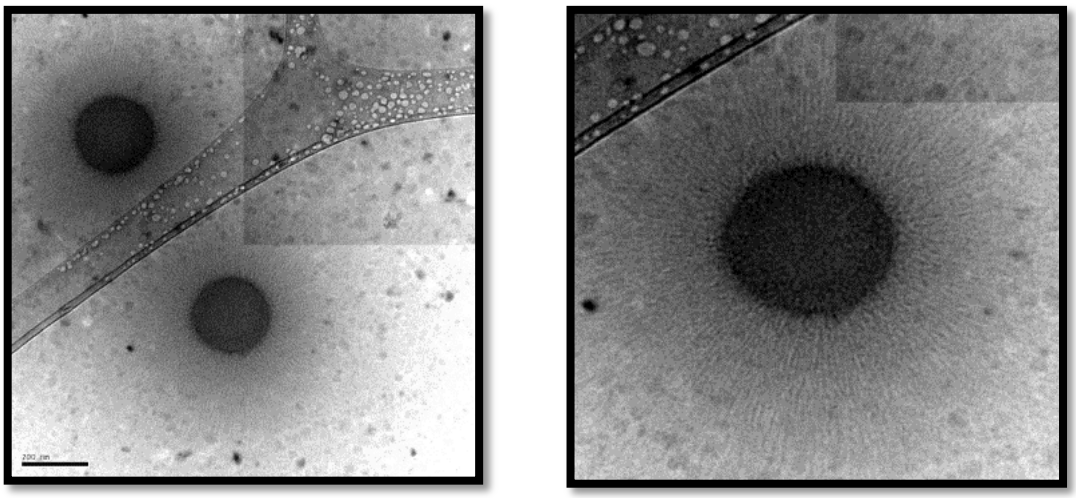

Fig.26. Cryo-TEM image of SET-111, Scale bar is 200 nm. On the right is close up image of one hairy latex particle.

From this image, the poly(sodium styrene sulfonate) brushes are extending toward the water phase. The polymer brushes are quite long, around 200 nm based on a rough measurement applied to the image. In SET-171, PS-29 was used, the recipe

was similar to the one used in SET-108 and SET-111, but the concentration of Cu(II) used was 4.2% of the total concentration of the Cu(0) wire, the rate of polymerization was fast and reached 40% conversion after 30 minutes from the beginning of the polymerization and the polymerization arrived at full conversion after 120 minutes.

The reason for the faster polymerization rate and 100% conversion after 2 hours might be attributed to the concentration of the inimer functional group in PS-29, which is 9.74%, in contrast to 5% in PS-27, PS-20 and PS-25. This may have led to full conversion in a shorter period of time. Cryo-TEM images of SET-171 are shown in Figures 27 and 28 from two different areas of the cryo-TEM grid.

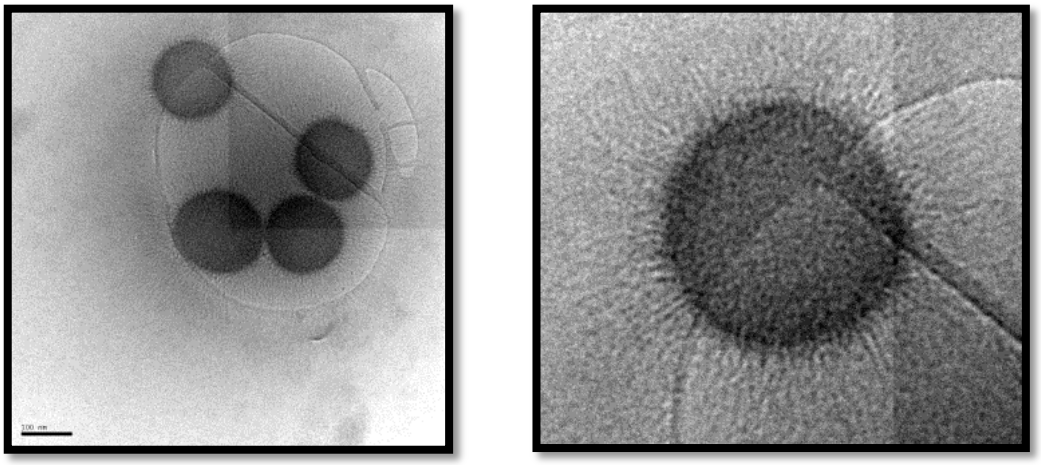

Fig.27. Cryo-TEM image of SET-171, scale bar is 100 nm. On the right is close up image of one hairy latex particle.

The length of the polymer brushes is approximately 100 nm, which is shorter than in the case of SET-111. A possible reason for the shorter poly(styrene sulfonate) brushes in SET-171 is as a consequence of using a higher concentration of inimer which may have led to a smaller number average molecular weight polymer and, therefore, shorter polymer brushes. The particle size of hairy latex SET-171 was

around 830 nm (see table 8), which is smaller than the other hairy latexes; this indeed suggests that shorter polymer brushes were formed in SET-171.

The cryo-TEM image in Figure 28 shows hairy latex SET-171 in different area of the cryo-TEM grid where the ice is thicker than in the previous image, which makes the polymer brushes only visible around the latex particles. This indicates that cryo-TEM gives qualitative details on polymer brushes rather than quantitative information.

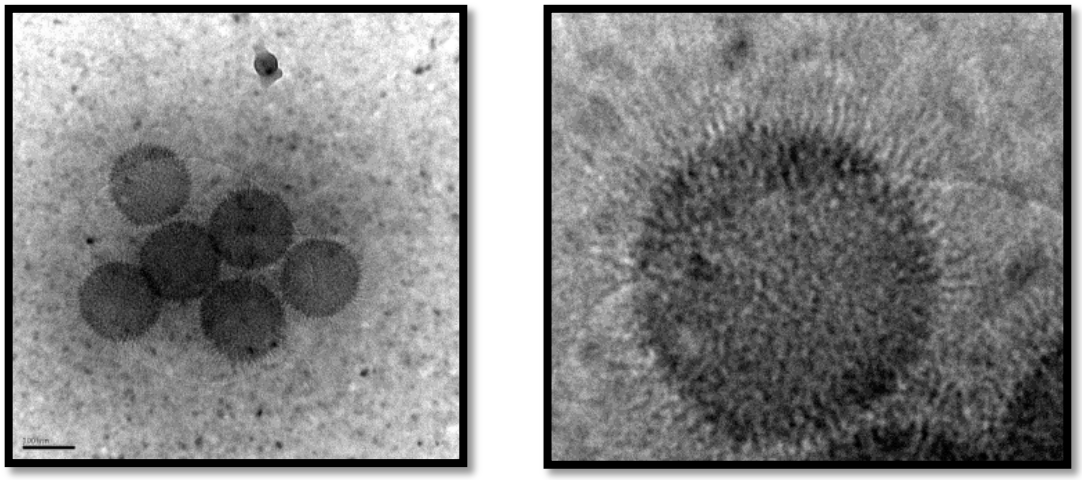

Fig.28. Cryo-TEM image of SET-171, scale bar is 100 nm. On the right is close up image of one hairy latex particle.

We investigated the role of the sacrificial initiator in the polymerization SET-145 with using latex PS-29 particles, and in SET-146 with using latex PS-31 particles. Polymerization was performed using the typical SET-LRP (SIP) protocol, but the concentration of the sacrificial initiator (**2**) was slightly different in both cases (0.0051 mol.L^{-1} in SET-145, and 0.0040 mol.L^{-1} in SET-146). They also differed in the concentration of the deactivator Cu(II) which was 4.1% in SET-145 and 3.69% in SET-146 of the total Cu(0) wire concentration used.

The rate of polymerization for both reactions was ultra-fast, whereby 90% conversion was achieved within the first 20 minutes of beginning polymerization.

The expected reason for ultra-fast polymerization is the usage of the sacrificial initiator which competes in the consumption and polymerization of the monomer with the latex particles. This can be explained by the slight increase in particle size after 90% conversion to 290 nm, increasing from 250 nm latex particles as in SET-146. This is a very small increase in size with conversion, which is usually above 500 nm after 50% conversion when no sacrificial initiator was used. This indicates that most of the styrene sulfonate monomer was polymerized in solution to form free polymers in the water phase rather than as polymer brushes on the surface of the latex particles.

After purification of SET-145 and SET-146, the final particle size in SET-145 was 260 nm, growing from 187 nm with a 70 nm increase in particle size; in SET-146, the particle size was 329 nm, growing from 250 nm with a 80 nm increase in particle size. Both latexes had a narrow particle size distribution as well.

All of these events suggest the presence of shorter polymer brushes as a result of the consumption of most of the styrene sulfonate by the sacrificial initiator to produce water-soluble free poly(sodium styrene sulfonate). Figures 29 and 30 show the cryo-TEM images of SET-145 and SET-146, respectively.

The cryo-TEM images of SET-145 and SET-146 show the presence of shorter poly(sodium styrene sulfonate) brushes which indicates that the length of the polymer brushes can be controlled by the addition of an external water-soluble ATRP initiator.

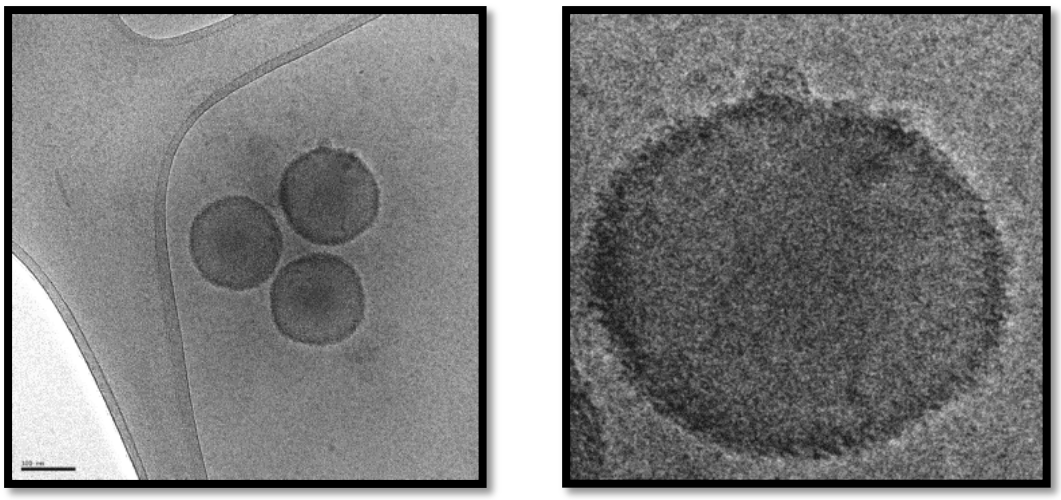

Fig.29. Cryo-TEM image of hairy latex SET-145 with shorter poly(sodium styrene sulfonate) brushes ,scale bar is 100 nm. On the right is close up image of one hairy latex particle.

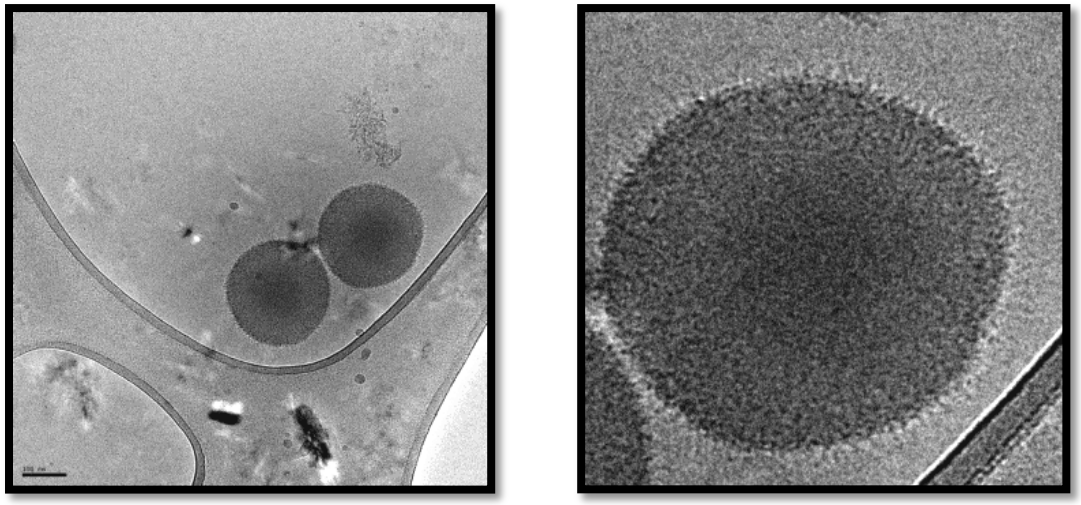

Fig.30. Cryo-TEM image of hairy latex SET-146 with shorter poly(sodium styrene sulfonate) brushes, scale bar is 100 nm. On the right is close up image of one hairy latex particle.

4.5. Conclusion

Cross-linked monodispersed latex particles that contain active sites (tertiary bromine functional group) were used as a macro-initiator for surface initiated polymerization by SET-LRP for several water soluble monomers at room temperature. Two types of latex particles were investigated, one of which was prepared by using the functional comonomer, that is 2-methacryloxyethyl-2'-bromoisobutryrate, in an *ab initio* fashion (batch addition) and one of which was prepared employing shot addition of

the monomer after approximately 70wt% to warrant enrichment of *tert*-bromine groups in the outer regions of the polymer colloids. A multitude of polymerization conditions were investigated in order to control some aspects of the graft polymerization, hereby varying for example the type of catalyst used for instance whether Cu(0) powder or Cu(0) wire was used, the type of ligand, the addition of external deactivator Cu(II) or an external water soluble ATRP initiator. The conversion of the polymerization was monitored by ^{1}H-NMR in D_2O. In a Blank experiment in which non-functionalized latex was used, no evidence of polymerization was detected. The occurrence of polymerization was evident employing both functionalized latex particles. Rate of the polymerizations were fast with monomer conversions exceeding 50% within 30 min, irrespectively of the type of the water soluble monomer that used and the latex used whether that made by batch addition or shot addition. The rate of the polymerization could be controlled by addition of Cu(II). When Cu(0) wire used full conversion was achieved, in contrast to when Cu(0) powder used, monomer conversion was limited to around 80% in all cases, hereby employing PMDETA as ligand. When Cu(0) wire was used with Me_6TREN ligand, lower rates of polymerization were observed with limited monomer conversions of around 60%. The surface of latex particles grafted with Poly(NIPAM) become non-ionic with zeta potential close from the isoelectric point, in contrast to those grafted with poly(sodium styrene sulfonate) and poly([2-(methacryloyloxy) ethyl]-trimethyl ammonium chloride) which make the surface of latex particles an anionic and cationic surface respectively, and that was detected by zeta potential measurement. Cryo-TEM images of the hairy latex that made by batch addition show that the brushes are barely visible, in contrast to that made by shot addition method which are clearly visible as extended arms from the surface of the

latex particles toward the water phase. This difference could be explained as a result of differences in brush densities. Shorter polymer brushes can be made by utilizing an external water soluble sacrificial initiator. The method developed to functionalize latex particles with hydrophilic brushes is easy and scalable. These hairy latexes are ready now to be used in fabrication of hairy Janus particles as that will be described in chapters 5 and 6.

4.5 References

1- Barbey, R.; Lavanant, L.; Paripovic, D.; Schuwer, N.; Sugnaux, C.; Tugulu, S.; Klok, H.-A. *Chem. Rev.***2009**, *109*, 5437-5527.

2- Jain, P.; Dai, J.; Grajales, S.; Saha, S.; Baker, G. L.; Bruening, M. L. *Langmuir* .**2007**, *23*, 11360-11365.

3- Brittain, W. J.; Minko, S. *J. Polym. Sci., Part A: Polym. Chem.* **2007**, *45*, 3505-3512.

4- Yamamoto, S.; Tsujii, Y.; Fukuda, T. *Macromolecules* .**2002**, *35*, 6077-6079.

5- Huang, X.; Wirth, M. *J. Anal. Chem.***1997**, *69*, 4577-4580.

6- Huang, W.; Kim, J.-B.; Bruening, M. L.; Baker, G. L. *Macromolecules* .**2002**, *35*, 1175-1179.

7- Guerrini, M. M.; Charleux, B.; Vairon, J.-P. *Macromol. Rapid Commun.* **2000**, *21*, 669-674.

8- Zhang, M.; Liu, L.; Wu, C.; Fu, G.; Zhao, H.; He, B. *Polymer* .**2007**, *48*, 1989-1997.

9- Bontempo, D.; Tirelli, N.; Masci, G.; Crescenzi, V.; Hubbell, J. A. *Macromol. Rapid Commun.* **2002**, *23*, 417-422.

10- Sonmez, H. B.; Senkal, B. F.; Sherrington, D. C.; Bicak, N. *React. Funct. Polym.* **2003**, *55*, 1-8.

11- Zheng, G.; Stoever, H. D. H. *Macromolecules* .**2003**, *36*, 1808-1814.

12- Lime, F.; Irgum, K. *J. Polym. Sci., Part A: Polym. Chem.* **2009**, *47*, 1259-1265.

13- Angot, S.; Ayres, N.; Bon, S. A. F.; Haddleton, D. M. *Macromolecules*. **2001**, *34*, 768-774.

14- Cheng, Z.; Zhu, X.; Shi, Z. L.; Neoh, K. G.; Kang, E. T. *Ind. Eng. Chem. Res.***2005**, *44*, 7098-7104.

15- Chen, Y.; Kang, E.-T.; Neoh, K.-G.; Greiner, A. *Adv. Funct. Mater.* **2005**, *15*, 113-117.

16- Cheng, Z.; Zhang, L.; Zhu, X.; Kang, E. T.; Neoh, K. G. *J. Polym. Sci., Part A: Polym. Chem.* **2008**, *46*, 2119-2131.

17- Lu, Y.; Mei, Y.; Drechsler, M.; Ballauff, M. *Angew Chem.***2006**, *45*, 813-816.

18- Lu, Y.; Wittemann, A.; Ballauff, M.; Drechsler, M. *Macromol. Rapid Commun.* **2006**, *27*, 1137-1141.

19- Mittal, V.; Matsko, N. B.; Butte, A.; Morbidelli, M. *Eur. Polym. J.* **2007**, *43*, 4868-4881.

20- Jayachandran, K. N.; Takacs-Cox, A.; Brooks, D. E. *Macromolecules* .**2002**, *35*, 6070.

21- Kizhakkedathu, J. N.; Norris-Jones, R.; Brooks, D. E. *Macromolecules* .**2004**, *37*, 734-743.

22- Kizhakkedathu, J. N.; Kumar, K. R.; Goodman, D.; Brooks, D. E. *Polymer* .**2004**, *45*, 7471-7489.

23- Wu, T.; Zhang, Y.; Wang, X.; Liu, S. *Chem. Mater.* **2008**, *20*, 101-109.

24- Guo, X.; Weiss, A.; Ballauff, M. *Macromolecules* .**1999**, *32*, 6043-6046.

25- Wittemann, A.; Drechsler, M.; Talmon, Y.; Ballauff, M. *Journal of the American Chemical Society*. **2005**, *127*, 9688.

26- Mei, Y.; Wittemann, A.; Sharma, G.; Ballauff, M.; Koch, T.; Gliemann, H.; Horbach, J.; Schimmel, T. *Macromolecules* .**2003**, *36*, 3452-3456.

27- Vo, C.-D.; Schmid, A.; Armes, S. P.; Sakai, K.; Biggs, S. *Langmuir* .**2007**, *23*, 408-413.

28- Sharma, G.; Ballauff, M. *Macromol. Rapid Commun.* **2004**, *25*, 547-552.

29- Guo, X.; Ballauff, M. *Phys. Rev. E: Stat., Nonlinear, Soft Matter Phys.* **2001**, *64*, 051406/1-051406/9.

30- Mei, Y.; Ballauff, M. *Eur. Phys. J. E* .**2005**, *16*, 341-349.

31- Hoffmann, M.; Lu, Y.; Schrinner, M.; Ballauff, M.; Harnau, L. *J. Phys. Chem. B* .**2008**, *112*, 14843-14850.

32- Wang, X.; Xu, J.; Li, L.; Wu, S.; Chen, Q.; Lu, Y.; Ballauff, M.; Guo, X. *Macromol. Rapid Commun.**2010**, 31*, 1272-1275.

33- Drifford, M.; Dalbiez, J.-P. *Biopolymers.***1985**, *24*, 1501-1514.

34- Block, S.; Helm, C. A. *The Journal of Physical Chemistry B* .**2008**, *112*, 9318-9327.

35- Adamczyk, Z.; Jachimska, B.; Jasiński, T.; Warszyński, P.; Wasilewska, M. *Colloids and Surfaces A: Physicochemical and Engineering Aspects.* **2009**, *343*, 96-103.

Chapter 5: Synthesis of Poly(styrene) latex Particles with Janus Morphology by Batch Addition Method.

5.1. Summary

Phase separation after seeded emulsion polymerization by using an oil-soluble initiator from swollen non-hairy and hairy latex particles with different crosslinked densities made by the batch addition method was investigated. In the case of non-hairy latex particles, the phase separation depends on several factors such as the crosslinked density in the original seed particles, size of the seed particles, concentration of DVB (crosslinker) in the seeded emulsion polymerization, and monomer to polymer swelling ratio, whereby each latex has its own best system and conditions for obtaining anisotropic particles.

In general the preparation of Janus particles from non-hairy particles made from the batch addition method is not an ideal method, since the visualization of the polymer brushes from the original seed domain is hard due to the low density of the formed brushes, and also the newly formed domain might cover the original seed domain due to the low interfacial tension between the two domains; this was detected as no apparent border between the two domains, and the newly formed domain just covered the original seed domain. The other sign is the low monomer conversion of SET-LEP when the dumbbell particles were used (as seed initiator) which indicates that the tertiary bromine functional group was mostly covered by the newly formed domain after phase separation, although the presence of inimer on the surface of dumbbell particles was confirmed by FTIR.

As hairy latex particles were used in swelling and seeded emulsion polymerization with different types of polymer brushes in their surface, the obtained particles have mainly popcorn and raspberry morphologies, and with special circumstances doublet and triplet Janus particles were made. It was observed that the newly formed hydrophobic domain size increases with decreasing the DVB concentration in the second stage polymerization, as the flow of the swelling monomer will be directed toward the low crosslinked density domain. Based on that, the preparation of Janus particles from hairy latex made by batch addition is possible under particular circumstances, and is not reproducible, as different properties of brushes made after SET-LRP have major influence on the obtained morphology.

5.2. Introduction

The transformation of sub-micrometer latex particles from an isotropic to an anisotropic shape as Janus morphology on a commercial scale is challenging. The proposed method in our current research to make Janus latex particles is based on the formation of a new domain besides the original seed domain to ultimately generate dumbbell shaped particles. The two domains of the obtained Janus particles are different from each other, physically and chemically.

Amphiphilic dumbbell particles can be used in several applications, such as a colloidal surfactant, but the studied particles were limited in micrometer range. [1, 2] These dumbbell particles could selectively adhere to the targeted surface as other Janus particles do. [3] They could self-assemble to clusters as a normal surfactant does; the obtained clusters were predicted by a computer simulation and observed experimentally as with our existing particles (see chapter 7). [4] The dumbbell latex particles are categorized as anisotropic particles if each side of the dumbbell is

different. For instance, one domain contains hard polymer and the other domain soft. An example of the synthesis of this type is the seeded emulsion polymerization by using poly(butyl acrylate) as seed (soft) and poly(styrene) (hard) as the second stage monomer to form a light shell of poly(styrene); the core poly(butyl acrylate) migrated upon aging out from the spherical core-shell particles to generate dumbbell shape particles.[5,6,7]

Another example is when the hard side is poly(methyl methacrylate), whereby 132 nm latex Janus dumbbell particles with one side consist of poly(n-butyl acrylate) which is soft and the other side is hard poly(methyl methacrylate) prepared by emulsion polymerization. This former type of Janus dumbbell particles is selectively oriented on the targeted substrate, which in the hard domain selectively adhere to the hydrophilic surface and the soft domain to the hydrophobic domain. [8]

Dumbbell latex particles with cationic and anionic domains were investigated, whereby dipole-like microsphere latex particles with one pole with a negative charge and another with positive charge were attempted to be made by soap-free seeded emulsion polymerization. The precursor poly(4-vinylpyridine-co-n-butyl acrylate) latex particles were made by soap-free emulsion polymerization in binary solvents of ethyl acetate and water. These latex particles were cross-linked with different concentrations of ethylene glycol dimethacrylate (EGDMA), and then the latex was swollen with styrene or a styrene and n-butylacrylate mixture with different ratios and then polymerized by seeded emulsion polymerization to form a dumbbell/egg-like microsphere particle. The poly(styrene) domain is sulfonated to from a negative pole and the poly(vinyl pyridine) domain was quaternizied to from the positive pole. The synthesized was restricted as a result to many factors affecting the swelling and seeded emulsion polymerization condition. These particles are potentially useful as

charged mosaic membranes which consist of anion-exchange and cation-exchang elements through the membranes. [9, 10]

Dumbbell particles with hydrophilic and hydrophobic domains are amphiphilic Janus particles. An example of synthesising such a type of particle was reported by Karlsson *et al.* They used seed latex containing poly(styrene-co-methacrylic acid) with different concentrations of methacrylic acid; KPS was used as an initiator and sodium dodecyl sulfate as an ionic surfactant. The particle size of the seed latex is in the range of 93 to 55 nm; the size depends strongly on the concentration of methacrylic acid used, whereby a smaller size has a higher concentration of methacrylic acid. These seeds were used in the second stage seeded batch emulsion polymerization or semi-continuous by the addition of different ratio of styrene, isoprene and methacrylic acid in the presence of KPS as an initiator. Via the batch process the latex was mixed with monomer mixtures and KPS for 1 hour and then the temperature increased to 80°C. After the second polymerization, phase separation was induced as a result of the incompatibility of the seed and newly formed domain. Different particle morphologies were obtained from the core-shell, inverse core-shell, dumbbell shape (Janus) and sandwich shape particles; the factors affecting each type of morphology depends on the polymerization condition and the composition in the two stage polymerizations, such as the amount of hydrophilic co-monomer (methacrylic acid) in the seed particles. [11]

The overall idea in our research is to fabricate sub-micrometer amphiphilic dumbbell-shaped latex particles from cross-linked poly(styrene) seed latex particles which have a hydrophilic surface, in some cases in the form of hydrophilic polymer

brushes. And in order to make dumbbell poly(styrene) particles, there are several existing methods used. Four main methods will be described here.

1- Entropic driven phase separation: When cross-linked poly(styrene) latex particles are swollen with styrene, a good solvent for the polymer, the polymer network gets placed under stress. Heating of an elastic cross-linked polymer network results in a volume contraction driven by a gain in entropy. As a direct result of this, some monomer will be expelled from the contracting polymer network, hereby generating a new domain of pure monomer on the outside of the swollen particle. Polymerization of the expelled monomer promotes further phase separation, eventually leading to the desired dumbbell shape. Since the newly formed domain originated from pure styrene (or a mixture of hydrophobic monomers and hydrophobic initiator) it should have a hydrophobic character.

The thermodynamics of the swelling of a cross-linked latex particle can be modelled using a combination of the Morton equation with the Flory-Huggins-Rehner expression. Under equilibrium conditions this is as follows: [12]

$$\Delta G_{m,p} = RT\left[\ln(1 - Vp) + Vp + \chi_{m,p}\, Vp^2\right] + RTNVm\left(Vp^{\frac{1}{3}} - \frac{Vp}{2}\right) + \frac{2\,Vm\,\gamma}{r} = 0 \quad (1)$$

$\Delta G_{m,p}$ = *Chemical potential of monomer in the particle phase during swelling at equilibrium*

R = *Gas constant*, $T = Absolute\ temperature$

$Vp = Volume\ fraction\ of\ polymer\ in\ the\ swollen\ particle$

$\chi_{m,p} = Monomer - polymer\ interaction\ parameter$

$N = Effective\ number\ of\ chains\ in\ the\ network\ per\ unit\ volume$

$\boldsymbol{Vm} = Moler\ volume\ of\ the\ monomer,\ \boldsymbol{\gamma} = Particle - water\ interfacial\ tension$

r = *Radius of the swollen particle*

One can see from Eq. 1 that a higher cross-link density, a higher interfacial tension, and a smaller particle size will restrict swelling. An outstanding question is: what is the influence of hydrophilic polymer brushes on the surface of the seed latex particles? In chapters 5 and 6 we will attempt to shine a light on this.

2- Phase separation induced by incompatibility: When latex particles swollen with incompatible monomer and subsequently polymerized, the latex particles phase separated from the newly formed domain due to the incompatibility that is caused by the low entropy of mixing, as reported by Uglestad *et al.*,[13] whereby 500 nm monodisprsed seed poly(styrene) latex is swollen with a mixture of styrene/hydrophilic acrylate or a mixture of methyl methacrylate/hydrophilic acrylate and subsequently polymerized. During the polymerization the original seed particle is partly expelled from the core-shell shape particle to form anisotropic particles with different morphologies, such as snow man or pear-shaped; the degree of phase separation depends on the extent of the incompatibility in each particle's system.

The morphologies of the two-stage seeded emulsion polymerization with different composition and compatibility were summarized by Lee and Ishikawa.[14] They found the following situations with monomer or monomer mixtures (II) in the presence of polymer seed (I) (homopolymer or copolymer) and the newly formed polymer (II):

1- If polymer (I) is insoluble in monomer (II), polymer (II) will form the surface layer like an ‘onion skin’; for instance, poly(vinylidene chloride)/poly(methyl acrylate).
2- Polymer (II) miscible with polymer (I) and there is no difference in the hydrophilicity between them; polymer (II) rich outside layers will be formed resulting in core-shell latexes; for instance, PS/PS, PMA/PMMA, PEA/PMMA.
3- If monomer (II) swells polymer (I), but polymer (II) is immiscible with polymer (I), phase separation can take place and many different structures are possible; for instance, PEA/PS, PS/P(S-B).
4- If polymer (I) is cross-linked and immiscible with polymer (II), polymer (II) can be trapped to form two interpenetrating continuous phases surrounded by polymer (II) rich shells.
5- Polymer (II) is more hydrophilic than polymer (I); polymer (II) tends to form shell around polymer (I) to generate core-shell morphology.
6- If polymer (I) is more hydrophilic than polymer (II), polymer (II) phase separates into polymer (I) and many different structure morphologies can be formed.

El-Aasser studied a particular system, which is PS/PMMA, to induce phase separation by incompatibility. For example, 0.2 μm poly(styrene) seed particles which have on their surface a non-ionic surfactant were swollen with methyl methacrylate and AIBN or KPS as an initiator in the presence of a non-ionic surfactant for 1 hour at room temperature with a swelling ratio of (latex/monomer) 1:2.3 and then the temperature increased to 70°C. The dumbbell shaped particles of

two distinctive phases were observed after selective staining for each phase with a particular staining agent. [15, 16, 17]

3- Nucleation on the surface and growth: This method depends upon the controlled nucleation and growth of a single particle on the surface of precursor particles. An example of this process is the synthesis of hybrid Janus nanoparticles through the controlled surface nucleation of poly(styrene) latex particles on the surface of inorganic nanoparticles. This method is derived from the growth-seeded emulsion polymerization process, but differs from the phase-separation method in seeded emulsion polymerization, in which the controlled surface nucleation method depends upon using inorganic seed nanoparticles such as silica particles as a precursor. Therefore, an emulsion polymerization of styrene in the presence of silica particles (50-150 nm) which were modified prior to used and make the formation of poly(styrene) nodules is highly favoured on their surfaces to form snow-man shaped hybrid particles.[18] On the other hand, dumbbell-like Janus [Au-Fe_3O_4] nano particles with a size of 20 nm were synthesized by the decomposition of [Fe $(CO)_5$] (iron pentacarbonyl) on the surface of the gold nanoparticles followed by oxidation. These Janus particles show dual properties which are the surface plasmon absorption as a result of the existing gold and the magnetic properties as a result of the presence of iron oxide. [19]

4- Hetro-coagulation: Anisotropic silica dumbbell particles (approximately 400 nm) were formed by slightly destabilizing the dispersion of spherical silica particles to allow the initial stage of aggregation to form dumbbell particles. In order to minimize the massive coagulation, a special method to destabilize the emulsion was applied which is shear-induced aggregation in ammonia/ethanol solution

(orthokinetic aggregation); the increase of ionic strength is the main reason to destabilize the silica particles. [20]

The last two methods to form dumbbell particles show limitations for the formation of pure polymer dumbbell particles; therefore, method 1 or 2 is the possible method to apply in our study, but which one have we chosen?

We prefer the entropic driven phase separation rather than the phase separation by incompatibility; the reasons that reinforced our choice are as follows. In the case of the incompatibility both sides of the dumbbell particles will be physically different which make not only the surface anisotropic but even both cores of the particles are different, but in our selected method only the surface chemistry makes the dumbbell particles anisotropic since both cores are cross-linked poly(styrene).

In the entropic driven approach, the scale-up of the process will be commercially feasible as only one main monomer will be used with a small concentration of the other co-monomers, but in the other approach two main monomers will be used in large quantities which will increase the cost of the synthesis. Besides the previous reasons, the main reason for picking the entropic driven phase separation approach is the limited literature on this method which will make the investigation valuable in terms of polymer science, in comparison to the incompatibility process which is well known.

As the entropic phase separation is the chosen method, the previous works in the literature were reviewed. From the previous studies, there are some parameters that should be considered to induce phase separation by the entropic driven method, as mentioned earlier, such as cross-linked density in the original seed and DVB concentration in the swelling monomer, swelling ratio, particles size, and the

interfacial tension of the particle with water and with expelled monomer (the hydrophilicity of the original seed particles). Here, we present some examples of previous work that investigated those parameters which affect the phase separation.

One of the initial studies to form dumbbell shaped particles by using this approach was reported by Vanderhoff *et al.* for micron-sized seed particles (5.2 μm).[12] They found a minimum amount of 0.03 wt% of DVB was required in order to induce phase separation by entropic contraction. The usage of 2.0 and 6.0 wt% of DVB in the seed latex, and thus relatively high cross-link densities, led to the formation of multiple domains. They showed that initial phase separation occurred upon heating to 70°C. The formation of the new domains was further aided through polymerization, as monomer concentration in the new domain is higher (not the cross-linked density region), causing an internal flux of monomer towards this region throughout the polymerization.

When the swelling was performed not only with styrene but in the presence of small quantities of DVB as a cross-linker, the domain formation still occurred but in a restricted form due to the formation of a full interpenetrating polymer network (Full-IPN). In addition to the effect of the cross-linked network density on the phase separation kinetics, there are other fundamental parameters which should be considered, such as the monomer/latex swelling ratio, polymerization temperature, and seed particle size. [21]

It is worth mentioning that the study by Vanderhoff *et al.*, the presence of non-ionic surfactant in the polymerization should be considered, as in our case a completely soap-free process is studied; the presence of the surfactant will affect the interfacial tension between the particle and water, and the particles with the expelled monomer.

Poehlein *et al.* suggested that one of the key factors to increase the swelling inside the uncross-linked poly(styrene) particles is to use a swelling agent. The swelling agent has to be a chain transfer agent to produce a low molecular weight polymer. The transport of the swelling agent to the particles was enhanced by using an organic co-solvent such as acetone which has some solubility in the water dispersed phase. And they recommend that the way to achieve high swelling without the usage of a swelling agent is to generate a small-droplet-size monomer emulsion which the monomer diffuses quickly from them to the latex particles. [22]

An example of the usage of the co-solvent is described, which in an organic solvent (xylene) was used to enhance the diffusion of the cross-linker (urethane acrylate) inside the poly(styrene) latex particles; consequently, dumbbell shaped cross-linked poly(styrene) particles cross-linked with urethane acrylate were synthesized by the dispersion polymerization method, and it was observed that when the concentration of the cross-linker increased more than 5.0% relative to the styrene, non spherical (dumbbell shaped) particles were formed.[23]

One of the suggested methods to increase the swelling of the latex particles after saturation swelling of styrene inside poly(styrene) latex is by the addition of an electrolyte in the emulsion; a small increase in the monomer concentration inside the latex particles was detected as the electrolyte concentration increased. The proposed explanation for increasing the swelling of monomer inside latex particles was attributed to the increase of the solubility of the monomer by the particles due to the reduction of the charge density of this particle as the ionic strength increased upon the addition of the electrolyte. [24]

Recently, Mock reported the fabrication of poly(styrene) latex particles to form dumbbell shape particles. The seed particles were synthesised by conventional emulsion polymerization by using SDS as an anionic surfactant and KPS as an initiator; the targeted total solid was around 7.0 wt% and the obtained particle diameter was 250 nm. Different types of seed particles based on the concentration of DVB were used in the preparation of the seed with a concentration of 2, 6, 9, 12, 15, 18 and 21% in relatively to the total amount of the used styrene. Their idea was to enhance the phase separation of hydrophobic monomer such as styrene from the latex particles by lowering the interfacial tension between the seed particles and the aqueous phase (maximize the swelling) and increasing the interfacial tension between the seed particle and the expelled monomer. The surface of the latex particles was modified by a thin outer layer of poly(vinyl acetate), or an outer layer of copolymer of acrylic acid and styrene to make the surface of the latex particles more hydrophilic. After that, the modified latex particles were swollen for 22 h at room temperature. Different weight swelling ratios of styrene/latex (M/P) were used as 1:1, 3:1, 7:1 and 9:1. Next, the swollen latex was heated to 80°C for 2 hours, and then a certain amount of SDS was added, accompanied by a water soluble free radicals scavenger. After 1 hour from that step, the AIBN was dissolved in 2.0 ml of styrene and then added to the polymerization mixture, and then the polymerization continued for 24 hours. The obtained particles morphology with an 18% DVB concentration in the unmodified seed particles, and with an M/P ratio of (5:1), resulted in an egg-like and ellipsoidal morphology of the particles being obtained, but with the same DVB concentration and M/P ratio, but with modified seeds with an outer layer of poly(vinyl acetate), the phase separation became more obvious, and it became clearer when the outer layer was a poly(acrylic acid).[25]

Kegel *et al.* studied the changes in diameter of 5% cross-linked poly(styrene) latex particles with a diameter of 1.88 μm over time, which were stabilized with SDS after being swollen with styrene at 20°C with a swelling ratio of 8.14. The particle diameter went up to 2.6 μm after only a short time of swelling, around 30 minutes. And after that the particles begin to de-swell due to the formation of a new protrusion domain which was detected by a further reduction of particle size to around 2.5 μm after 100 minutes (relaxation time). They observed that the increase in the seed particle size (the swelling of the particle), and the cross-linked density led to the formation of a large protrusion domain; this also indicates that the heating is not necessary to induce the phase separation. [26]

In another study with the same range of particle size at 2.7 μm, cross-linked poly(styrene) particles were dispersed in aqueous solution of PVA. These particles were used to synthesize non-spherical particles by swelling with different hydrophobic monomers such as styrene, methyl methacryalte and butyl methacrylate, and subsequently polymerized at elevated temperatures. The effect of the presence of the initiator was investigated. In the case of the presence of an initiator, the phase separation persisted to grow after 100 seconds which points out that the phase separation is also driven by the polymerization of expelled monomer droplets suspended on the surface of the particles, but in the absence of the initiator the phase separation stop after 100 seconds. Consequently, two major factors have driven the phase separations which are the elastic stress and the polymerization. [1]

In order to confirm that the original domain of the dumbbell particles does not migrate to the newly formed region, the poly(styrene) seed particles were swollen with BMA; the poly(styrene) domain was selectively tagged with dye and then

visualized under confocal microscopy, and that confirmed that the formed poly (BMA) domain does not contain any migrated poly(styrene) and this opens the door to selective chemical modification of these dumbbell shaped particles to produce chemically anisotropic particles.[1]

The same research group suggested a method to control the phase separation in seeded emulsion polymerization and subsequently the obtained morphology of latex particles with a micron diameter. The method is based on controlling the direction of the phase separation by manipulating the cross-linked density gradients of the seed particles. From their study, they recommended that the variation in the cross-linked density can be used to overcome the effect of the surface tension of the particles and provide reproducible particles morphology. [27]

In quite a similar study, Park *et al.* synthesized 2.2 µm poly(styrene) particles with the symmetry of water molecules synthesised by four steps of seeded dispersion polymerization with a variation of the concentration of DVB in each step. In step one, the seed particles were cross-linked with 2.0% DVB and then used in three following steps of swelling and seeded polymerization to form the targeted morphology. The swelling monomer mixture consisted of three components (styrene, DVB and benzoyl peroxide as an initiator). The monomer/polymer ratio and the DVB concentration varied in each step as follows: in step one, the original seed particles had 2.0% DVB; in step two, there was a monomer/polymer ratio of 4:1 with 1.0% DVB; in step three, there was a monomer/polymer ratio of 1:1 with 2.0% DVB; in step four, there was a monomer/polymer ratio of 1:1 and a DVB concentration of 1.0%. The control of the final particle morphology was achieved by following these mentioned conditions with a special emphasis on the variation of DVB concentration. [28]

Conversely, a poly(electrolyte) multi-layer (PEM) was deposited on the surface of 1.1 µm non-cross-linked negatively charged poly(styrene) latex particles by electrostatic deposition. These latex particles were swollen with a small amount of THF in aqueous medium at an ambient temperature. After only a few seconds, a new domain was generated that contained a dissolved poly(styrene) chain which was stabilized by the sulfate group which comes from the KPS during the synthesis of the seed particles. The proposed mechanism of the formation of the new domain is the high osmotic pressure inside the latex particle which leads to open holes in the shell of PEM, and in order to open only one hole, the PEM shell should contain 5 to 10 bilayers, so in that case the opening of one hole is kinetically occasionally created. Based on that, different amounts of layers leads to the opening of many holes which are thermodynamically favoured. It is worth mentioning that the newly formed negatively charged domain is completely free from the PEM shell and verified by the selective deposition of 12 nm negative gold nanoparticles to the positively charged PEM layer region. [29]

The formation of sub-micrometer snow-man poly(styrene) latex particles was studied as cross-linked poly(styrene) latex particles with 0.5% DVB which have a particle size of 360 nm, prepared by soap-free emulsion polymerization in the presence of surfmer (acrylic acid) (AA) and KPS as an initiator. These particles were swollen with styrene for 24 hours at room temperature followed by purging the emulsion for 20 minutes, and subsequently gamma irradiation was applied at 20°C. The critical monomer/polymer ratio that gives snow-man morphology was determined to be 5:1, and as that ratio increased to 10:1 as a massive secondary nucleation is generated in parallel to the snow-man particles. Based on that, the degree of phase separation depends on the capability of the cross-linked network

inside the latex particles to accommodate the swelling monomer and also in the surface chemistry of the seed particles. [30]

Once again, Park *et al.* tried to make dumbbell latex particles, but this time on a sub-micrometer scale. They relied on another factor that controlled the phase separation from non-cross-linked poly(styrene) latex particles, which is the formation of an outer cross-linked layer of copolymer of styrene and trimethoxysilylpropyl acrylate (TMSPA) on the surface of the latex particles by seeded emulsion polymerization and using AIBN as an initiator. The obtained core-shell particles were swollen for 30 minutes at room temperature with a mixture of styrene and AIBN and with various ratios of latex/monomer to control the morphology of the obtained non spherical latex particles. After that, the temperature of the mixture was elevated to 70°C to induce the phase separation. [31]

Mock and Zukoski synthesized chemically and shape anisotropic semi interpenetrating poly(styrene) latex particles by seeded emulsion polymerization. Their strategy was based on using low cross-linked density poly(styrene) (0.68%, DVB) particles which has a negatively charge sulfate group which comes from the KPS initiator. Co-monomer 2-(diethylamino ethylmethacrylate) was used which can alter the surface charge of the seed particles by changing the pH. These particles transform form negatively charged at higher pH to positively charge at low pH. These seed particles swell styrene with a monomer/polymer ratio of 1.2:1 at room temperature with a low pH (2.0) for 21h, and then heated up to 80°C for 3 h, followed by the addition of CTAB as a cationic surfactant and hydroquinone to prevent the secondary nucleation in aqueous phase. After the end of the polymerization the pH increased to be around 8.0; the dumbbell particles have a positively charged side in the new domain as a result of adsorbing the CTAB in this

region and negatively charged in the original seed domain by sulfate and the deportation of the co-polymer. But the author did not refer to the fact that the CTAB should cover both domains and not just the newly formed domain, and that is clearly as a result of the electrostatic attraction between the CTAB and the sulfate group in the original domain of the seed particles. [32]

Here in our work in chapters 5 and 6 the phase separation from non-hairy cross-linked poly(styrene) latex particles and hairy cross-linked latex particles that are made from the batch addition of inimer (chapter 5) and shot addition method (chapter 6) was studied to fabricate our targeted amphiphilic Janus latex particles. Several parameters were studied, such as cross-linked density in the original seed latex, DVB concentration in the second stage polymerization, the swelling ratio and the surface chemistry of the seed particles. We expect the direct fabrication of Janus particles after the phase separation from hairy particles, and the obtained non-spherical particles from non-hairy latex particles just need further modification by SET-LRP to form hairy Janus particles.

5.3. Experimental section

5.3.1. Formation of non-spherical latex particles using a non-hairy crosslinked poly(styrene) latexes made by the batch addition method

One representative example presented here is experiment **SW-124:** 1.0 g of (PS18) crosslinked poly(styrene) seed latex which has a total solid content of 6.0% was placed in glass vial; to that 0.206 g of a premade mixture of styrene (6.0 g), divinyl benzene (0.82 g) and (0.060 g) AIBN was added. In addition 8.0 g of demineralized water was added. The vial was degassed by purging with nitrogen gas for 10 min, closed, and placed in an oven (Microarray oven Model 777 SCI Gene) which has a rotating motor to tumble the sample

at a speed of 30 rpm for 24 h at a temperature of 25 ºC. After that the temperature was increased to 70 ºC with the sample being kept inside for another 24 h, in order to induce phase separation and start the polymerization. After this the morphology of the latex particles were screened by SEM analysis. Interesting latexes were further purified by dialysis against water for one week.

5.3.2. General procedure for surface initiated polymerization by the SET-LRP method from the surface of non-spherical poly(styrene) latexes

An example **(SET-93)** is described here for the growth of poly(NIPAM) brushes from the surface of non-spherical latex (**SW-124)** by SET-LRP: 0.440 g of NIPAM, 37.5 mg of Cu (0) (wire, 8.0 cm in length, 0.25 mm in diameter), 5.3 mg of $CuBr_2$, and 0.20 g of ethylene glycol (inert marker to monitor monomer conversion with ^{1}H NMR) were placed in a 50 mL round bottom flask. Next, 16.9 g (0.73% total solid) of SW-124 latex was added. The flask was sealed with a rubber stopper and placed in a water bath at 25 ºC, after which the mixture was degassed for 30 minutes by purging with nitrogen gas after which a small continuous flow of nitrogen gas was maintained at slight overpressure. To start the polymerization, 2.0 mL of a 2 wt% separately degassed aqueous solution of PMDETA was injected. Samples were taken after predetermined intervals to monitor the monomer conversion by (^{1}H-NMR) and the particle size distribution by (DLS). After the SET-LRP reaction, the functionalized latex was purified by ultracentrifugation at a speed of 28 krpm for (24 h). The aqueous phase (the supernatant) was removed gently by syringe from the centrifuge tube, and the remaining sediment of hairy latex particles was redispersed in water by sonication. Finally, the redispersed latex was further purified through dialysis for one week against water.

5.3.3. Formation of non-spherical latex particles by using hairy crosslinked poly(styrene) latexes particles

One representative example is presented here **(SW-114):** 10.3 g of hairy latex particles with poly(NIPAM) brushes (**SET-62**) which has a total solid content of 0.63% was placed in a 20 mL glass vial. Next, 0.20 g from a premade mixture of styrene (6.0 g), divinyl benzene (0.30 g) and (0.060 g) AIBN was added. The glass vial was degassed by purging with nitrogen gas for 10 min, sealed and placed in a rotary oven for 24 h at 30 rpm at 25 ºC. Next the temperature was raised to 70ºC to start the polymerization. The sample was kept in the rotary oven for another 24 h. The final latex was purified using dialysis against water for one week.

5.3.4. TEM (Transmission Electron Microscope).

Joel 2000fx transmission electron microscopy with accelerating voltage of 80 to 200 Kv was used. One drop of the diluted latex was placed on the 400 mesh Copper grid to visualize the sample. After one minute the latex drop was drained by using filter paper to form a dry thin layer of the emulsion.

5.3.5. AFM (Atomic force microscope).

VEECO DI Multimode V (AFM) instrument was used in the tapping mode with a Silicon nitride probe. AFM sample was prepared by placing a thin layer of a diluted latex dispersion onto a glass slide, which then dried for a day.

5.4. Results and Discussion

The aim is to fabricate amphiphilic dumbbell-shaped latex particles. Control of shape is to be accomplished by entropically driven phase separation of swollen and

polymerizing cross-linked seed latex. The chemical nature of the hydrophilic lob is controlled by growth of polymer brushes through SET-LRP.

In order to accomplish our goal we use two routes. In route one we first phase-separate, after which we do the SET-LRP to grow the polymer brushes, whereas in route two we first grow the polymer brushes of the seed latexes, after which we phase-separate. Each route will be described and studied individually as follow.

5.4.1. Phase separation from non-hairy latexes made by batch addition method (Route 1):

We will first discuss the results obtained from route 1. Four different seed latexes were used of variable crosslink density that is 7.48 wt% (PS-21), 6.43 wt% (PS-18), 2.60 wt% (PS-24), and 1.00 wt% (PS-26) respectively, all of which were modified with *ca.* 5 wt% of inimer added under batch conditions. See Table 1 for details on these seed latexes. We will discuss our results in the decreasing order of the crosslink density.

Table.1. key characteristics of the used non-hairy latexes in swelling and seeded emulsion polymerization made by batch addition method.

Latex Key characteristic	PS-21	PS-18	PS-24	PS-26
Inimer (wt %)	5.37	5.20	5.12	5.0
NaSS (wt %)	0.30	0.50	0.257	0.272
Average Particle diameter (nm)	223	148	202	261
Total solid (%)	4.2	5.8	8.7	7.0
Zeta potential (mV)	- 44.5	- 47.6	- 41.4	- 39.7
Crosslinked density (wt %)	7.48	6.43	2.6	1.0

When we use a relatively highly crosslinked seed latex, that is PS-21 of crosslink density 7.48% we expect that swelling is restricted and that phase separation would lead to multiple domains. We performed five different experiments, which are represented in Table 2. Typically the seed latex at 4.2 wt% was mixed with styrene/divinylbenzene/AIBN mixture and diluted with water, swollen, and subsequently polymerized at 70 °C. All resulting latexes were colloidally stable. The resulting particle morphologies were investigated by SEM and are shown in Fig 1.

Table.2. Ingredients used to swell latex PS-21, and the subsequent obtained morphology after polymerization at 70°C, R (M/P) = Ratio of monomer to polymer, S = styrene, D = divinyl benzene (DVB), A= Azobisisobutyronitrile (AIBN), SM = swelling monomers mixture and AIBN.

Experiment	R (M/P)	Latex (t.s) %	Latex Weight(g)
Sw-187	5.20/1.0	4.20	1.03
Sw-211	14.0/1.0	4.20	1.01
Sw-217	7.8/1.0	4.20	1.87
Sw-218	4.2/1.0	4.20	1.17
Sw-240	3.22/1.0	4.20	1.53

Experiment	S+D+A=SM(g)	DVB%	H_20 (mL)	Latex morphology	Colloidal stability
Sw-187	(6.0+0.80+0.064) = **0.224**	13.3	7.5	**Spherical**	Stable
Sw-211	(6.16+0.33+0.068) = **0.60**	5.35	7.0	**Secondary nucleation +Snow man +Spherical**	Stable
Sw-217	(6.08+0.350+0.065) = **0.616**	5.75	7.0	**Non-spherical**	Stable
Sw-218	(6.08+0.350+0.065) = **0.33**	5.75	7.0	**Spherical + Secondary nucleation**	Stable
Sw-240	(6.0+0.010+0.060) = **0.207**	0.16	3.0	**Doublet**	Stable

The first experiment was operated at a swelling ratio 5.20, and with DVB concentration in the monomer feed of 13.3%. The latex obtained (SW-187) retained

its near spherical morphology, with an increase in average particle diameter from 223 nm to around 290 nm. The crosslink density of the original seed latex, 7.48 %, limits the swelling of this latex. At a swelling ratio of 5.20 this basically means that monomer droplets will be present after the swelling stage.

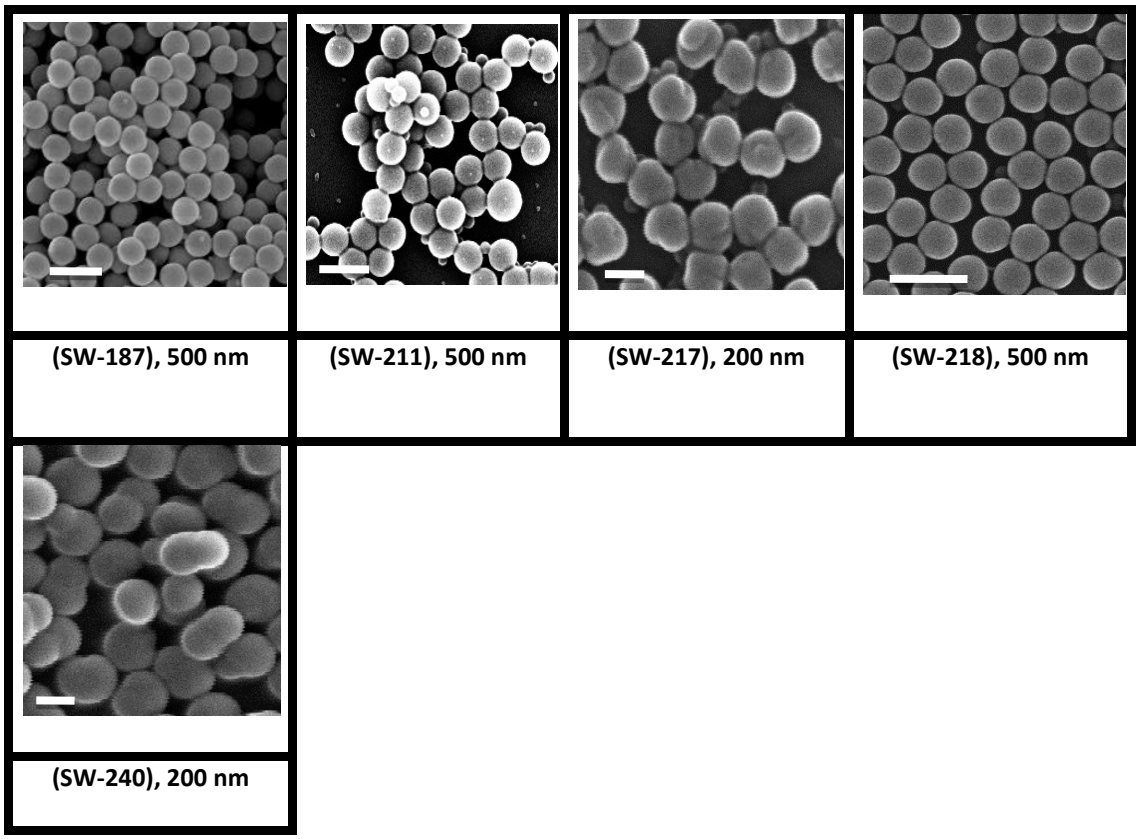

Fig.1. SEM images of PS-21 latex, after swelling and seeded emulsion polymerization. The scale bar in all images is 500 nm with exception of SW-217 and SW-240 which is 200 nm.

If phase separation at all is triggered after heating as a result of entropic phase separation (which seems possible if one looks at the results from experiment SW-240), the effect is diminished upon polymerization. The polymer formed is heavily crosslinked, which limits transport of monomer/polymer and rearrangement. No secondary nucleation was observed; hence the increase in particle diameter with 67 nm should match to the one which can be calculated from the swelling ratio using:

$$d = d_{seed}\left(1+\frac{\rho_M}{\rho_P}\frac{M}{P}\right)^{1/3}$$

d = diameter of latex after swelling and polymerization (nm),

d_{seed} = Seed latex diameter (nm), ρ_M = density of styrene (0.909 g.cm^{-3}), ρ_p= density of polymer (1.05 g.cm^{-3}), M/P = ratio of monomer to polymer.

Calculations using an estimated volume contraction of 0.9 upon polymerization, however, lead to a value for the particle diameter of 415 nm. This means that either we have limited monomer conversion, or a short period of secondary nucleation which had lead to a second set of particles achieving a similar particle size. Both of these can account for the observed 290 nm.

In the next three experiments, SW-211, SW-217 and SW-218 we lowered the DVB concentration to 5.35 %, 5.75%, and 5.75% respectively. By lowering the amount of DVB from the previous 13.3% we envisaged that phase separation upon polymerization could be promoted. More importantly we varied the swelling ratio, being 14.0, 7.80, and 4.20. In all three cases secondary nucleation was observed, though SEM analysis indicated that the amount of the second crop of particles decreased at lower swelling ratios. In all three cases, however, the secondary nucleation happened in the latter stages of the polymerization process as these particles were distinctly smaller, that is typically sub 70 nm, and of broad particle size distribution.

In all three cases, the original seed latexes did not grow to the expected calculated size. This however, could not solely be ascribed to secondary nucleation which meant that limited monomer conversion was the key reason. A plausible explanation for this could be the low monomer concentration in the particles throughout polymerization as of the high amounts of divinyl benzene used and the originally high amount of crosslink density of the seed latex.

In (SW-240), the swelling ratio used was 3.22, and the concentration of DVB was 0.16%; the externally added water was 3.0 mL compared to 7.0 mL in the previous experiments with (PS-21). The obtained morphology shows doublet shape particles with snowman and dumbbell shape morphologies. This latex (SW-240) is a potential candidate to be modified by SET-LRP due to the formation of the distinct doublet shaped particles. The likely reason for the formation of the doublet shape particles is attributed to the usage of a low concentration of DVB in the second stage polymerization, which makes the flow of the swelling monomer much easier and guides the phase separation toward one direction. The doublet shaped latex (SW-240) was used as seed for the surface initiated polymerization SET-LRP (SET-141) to grow poly(styrene sulfonate) brushes from the original seed domains of these doublet particles. The presence of the (inimer) in the doublet particles (SW-240) was verified by FTIR of (SW-240) as shown in (Figure 2).

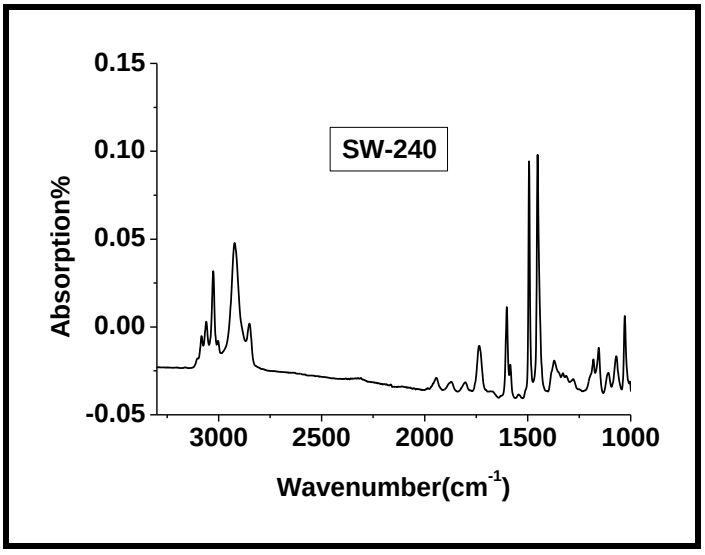

Fig .2. FTIR spectrum of (SW-240) latex particles after dialysis and drying**.**

The spectrum shows the absorption at 1729 cm^{-1} which indicates the present of the (inimer). Table 3 shows the recipe used for surface initiated polymerization (SET-141) from the surface of the dumbbell latex particles SW-240 by SET-LRP

mechanism. The SET-141 polymerization reached to 100% monomer conversion after around 1.0 hour from the beginning of the polymerization since the sacrificial initiator (2) was used.

Table.3. Recipe and ingredients used in SET-LRP (SIP) of sodium styrene sulfonate (NaSS) from the non-spherical latex particle made by batch addition (PS-21) at 25°C in water. An external ATRP initiator (**2**) was used with a concentration of (0.0039 mol.L^{-1}), and 5.33 g of methanol was used in the polymerization as co-solvent.

Exp	Latex	Latex (g)	[Monomer] mol.L^{-1}	Ligand	[Ligand] mol.L^{-1}	Cu (0)	[Cu (0)] mol.L^{-1}	[$CuBr_2$] mmol.L^{-1}
SET-141	SW-240	0.064	0.138	Lig_1	0.013	Powder	0.0147	1.68

The Cryo-TEM image shows that the latex particles are not suspended inside the ice; this means the image appears as a normal TEM image and no evidence from that image can be used to verify the presence of the poly(sodium styrene sulfonate) brushes on one domain of the doublet latex particles SW-240 after SET-LRP.

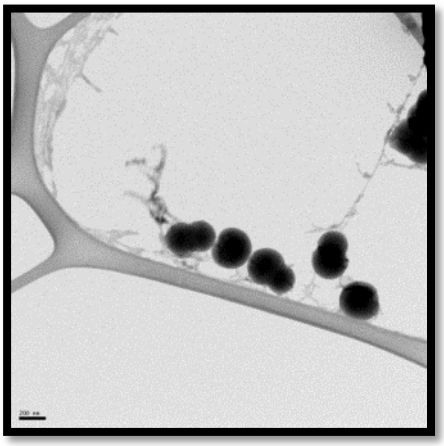

Fig.3. Cryo-TEM image of (SW-240) after surface initiated (SET-141) of sodium styrene sulfonate at 25°C at water and methanol. Scale bar in the image is 200nm.

In case of PS-18 which has a slightly lower crosslink density than PS-21 discussed above, that is 6.43% and 7.48%, respectively. Table 4 shows the ingredients used in the swelling and seeded emulsion polymerization of PS-18 latex. The latex PS-18 has a particle size of 148 nm and crosslinked density of 6.43% (based on the added

amount of DVB), 5.2% of (inimer) was incorporated to the latex by the batch addition method and 0.5% of (sodium styrene Sulfonate) relative to the total amount of styrene used; the latex has a good colloidal stability with high negative charge latex with zeta potential of (-47.6 mV).

Table.4. Ingredients used to swell the latex PS-18, and the subsequent obtained morphology after polymerization at 70°C with speed of mixing of 30 rpm, R (M/P) = Ratio of monomer to polymer , S = styrene, D = divinyl benzene (DVB), A= Azobisisobutyronitrile (AIBN), SM = swelling monomers mixture and AIBN.

Exp	R (M/P)	Latex (t.s) %	Latex Weight (g)
SW-73	3.40/1.0	5.8	1.05
SW-98	3.80/1.0	5.8	1.01
SW-92	3.44/1.0	5.8	1.03
SW-102	3.20/1.0	5.8	1.12
SW-106	3.51/1.0	5.8	1.03
SW-124	3.55/1.0	5.8	1.00
SW-248	3.55/1.0	5.8	1.08
SW-287	3.35/1.0	5.8	1.10

Exp	S+D+A=SM(g)	DVB %	H_20 (mL)	Latex morphology	Colloidal stability
SW-73	(6.00+0+0.06) = **0.206**	0	8.0	**Spherical with some small patches**	Stable
SW-98	(6.0+0+0.06) = **0.222**	0	8.0	**Popcorn**	Stable
SW-92	(6.0+0.3+0.060) = **0.2064**	5	8.0	**Triplet + Doublet + quartet**	Stable + small percentage of coagulation
SW-102	(6.07+0.25+0.0641) = **0.2081**	4.1	8.0	**Non-Spherical + Spherical**	Stable
SW-106	(6.0+0.30+0.0625) = **0.2091**	5.0	8.0	**Triplet + Quartet**	Stable
SW-124	(6.0+0.82+0.06) = **0.206**	13.6	8.0	**Triplet + Quartet**	Stable
SW-248	(6.0+0.010+0.060) = **0.2214**	0.16	3.0	**Doublet, triplet and singlet**	Stable
SW-287	(6.0+0.030+0.060) = **0.214**	0.5	3.0	**Doublet , triplet and singlet**	Stable

The following figure show a summary of SEM images of the obtained morphology after swelling and seeded emulsion polymerization by using PS-18 as a seed in various conditions.

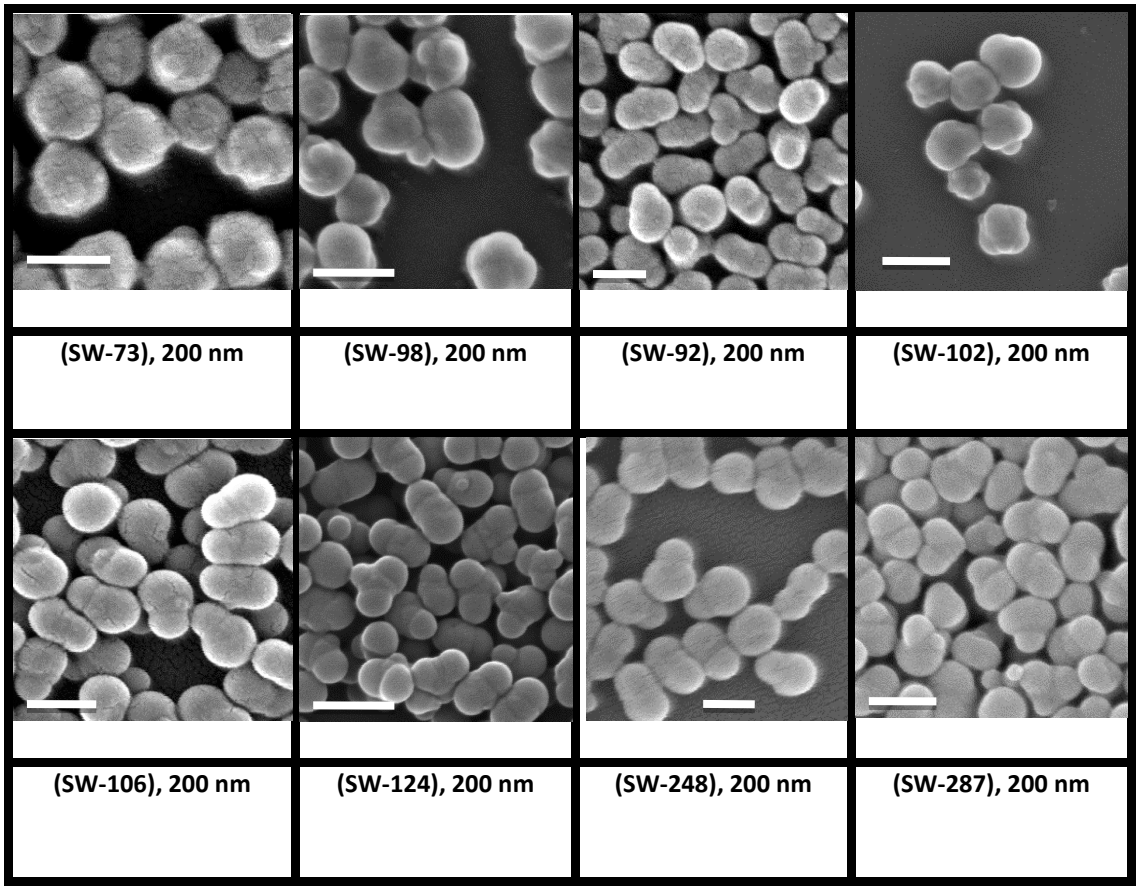

Fig.4. SEM images of PS-18 latex after swelling and seeded emulsion polymerization. The scale bar in all images is 200 nm.

In the first reaction, the monomer to seed ratio (M/P) was 3.40 (SW-73). No divinyl benzene as cross-linker was added to the monomer feed. Typically 1.0 mL of latex was diluted with 8.0 mL of water to reach a total solid content of the seed of ca. 0.52%. After swelling and polymerization (SW-73), small multiple patches on the surface of the latex particles, with size of individual patches of around 30 nm, were observed. Upon increasing the swelling ratio to 3.8 (SW-98), a similar morphology was obtained, but with clearer phase separation and bigger sized protrusions (70 nm); the morphology of the obtained particles resembled a popcorn morphology.

Upon using 5% of crosslinker (DVB) (SW-92), the latex particle showed a lower number of protrusions, mostly two to three but with bigger size, *ca.* 110 nm; this could be attributed to the fact that, when a crosslinker was used, the viscosity inside the latex particles become higher upon polymerization. This most clearly will amplify the Trommsdorff-Norish effect leading to an increase in the overall rate of polymerization locally which means that once a protrusion is formed it will grow more rapidly, which effectively lowers the number of newly formed patches. The average particle size increases to 260 nm from its original value of 148 nm.

In (SW-102) a smaller ratio of monomer to latex of 3.20 and a lower concentration of DVB (4.1%), in comparison with (SW-92) produced two kinds of particle. The first class of particles has small size phase separation and multiple protrusions, as in the case of SW-73 and SW-98; this indicated that a reduction of DVB concentration lead to multiple domain formation, whereas lowering the swelling ration decreased the individual size of the patches. The second type of particle has doublet and triplet phase separation morphologies as a result of using a higher concentration of DVB of 4.1%, as in the case of SW-92. From these initial experiments, it is obvious that there are two main factors influencing the phase separation: the ratio of monomer to latex and the concentration of DVB in the second stage polymerization.

In (SW-106), almost identical conditions to those in SW-92 were used, but with a slightly higher ratio of monomer to latex of 3.51 instead of 3.44. The polymerization provided one domain (doublet) in most of the cases, and triplet shaped particles in a small portion; this indicates that when a higher ratio of monomer to latex and 5.0% DVB concentration was used, the phase separation is more controllable to give doublet and triplet shape morphologies.

When the concentration of DVB was increased dramatically to 13.6% at a swelling ratio of 3.55 (SW-124), the polymerization generated triplet and doublet shape morphology particles as in (SW-92) and (SW-106), consequently the higher increase in the concentration of DVB in the second stage polymerization led to a reduction in the number of newly formed domains.

The question was whether still only 2 or 3 domains would be found if the DVB concentration was lowered severely. Experiments carried out at 0.16% DVB in the monomer feed (SW-248) showed indeed the formation of doublet shaped particles with various morphologies from dumbbell shape to snowman morphology. Note that these experiments were carried out at effectively double the solids content, as only 4 mL of water was added.

Seeded polymerization is very sensitive to very small variations in the concentration of DVB in second stage polymerization and the swelling ratio; this can be concluded from experiment (SW-287) as the concentration of DVB increased by three times to 0.5% instead of 0.16% as in (SW-248), and the swelling ratio was reduced to 3.35 instead of 3.55; this condition gives particles with triplet and doublet shape morphology.

From the above discussion we can summarize the following for the swelling and seeded emulsion polymerization from PS-18:

1- Polymerization without DVB in the second stage polymerization led to the formation of a large number of small protrusions on the surface of latex particles, generating popcorn morphology.
2- If the swelling ratio increased, the size of the newly formed domain increased.

3- Addition of DVB led to a clear reduction in the amount of patches formed, the clearest phase separation being observed close to our targeted dumbbell structure for lower concentration of DVB around 0.16%.

4- Wider particle size distribution of the original seed particles lead to formation of different shape morphologies of doublet shape particles from snowman to dumbbell shape.

As the particle morphology of (SW-106) and (SW-124) both show an anisotropic particle character, these latexes were used as seed in the next step: surface initiated polymerization of hydrophilic monomers by the SET-LRP method, used as an effective and simple method to form polymer brushes from the original seed domain.

Table 5 shows the ingredients used in the surface initiated polymerization (SET-LRP) using seeds SW-106, and SW-124 with NIPAM as monomer, followed by a monomer conversion versus time graph in figure 5.

Table.5. Recipe and ingredients used in SET-LRP (SIP) of NIPAM from the non-spherical latex particle made by batch addition (PS-18) at 25°C in water.

Exp	Latex	Latex (g)	[Monomer] $mol.L^{-1}$	Ligand	[Ligand] $mol.L^{-1}$	Cu (0)	[Cu (0)] $mol.L^{-1}$	[$CuBr_2$] $mmol.L^{-1}$
SET-90	SW-106	0.067	0.224	Lig_1	0.013	Wire	0.0341	0.77
SET-93	SW-124	0.122	0.205	Lig_1	0.012	Wire	0.0312	1.25

The polymerizations were performed with typical conditions to those used when the brushes were grown from normal spherical particles, but the total weight of the used seed was lower than in the case of spherical particles by at least a factor of 2; this will reduce the concentration of the tertiary bromine groups, the consequences of which are lower reaction rate and longer polymer brushes, In the case of SET-90, the rate of the polymerization was high at the beginning, and after 1.0 hour the

conversion stopped growing and then merely increase slightly to around 45% conversion. The Cryo-TEM image of SET-90 is shown in figure 6.

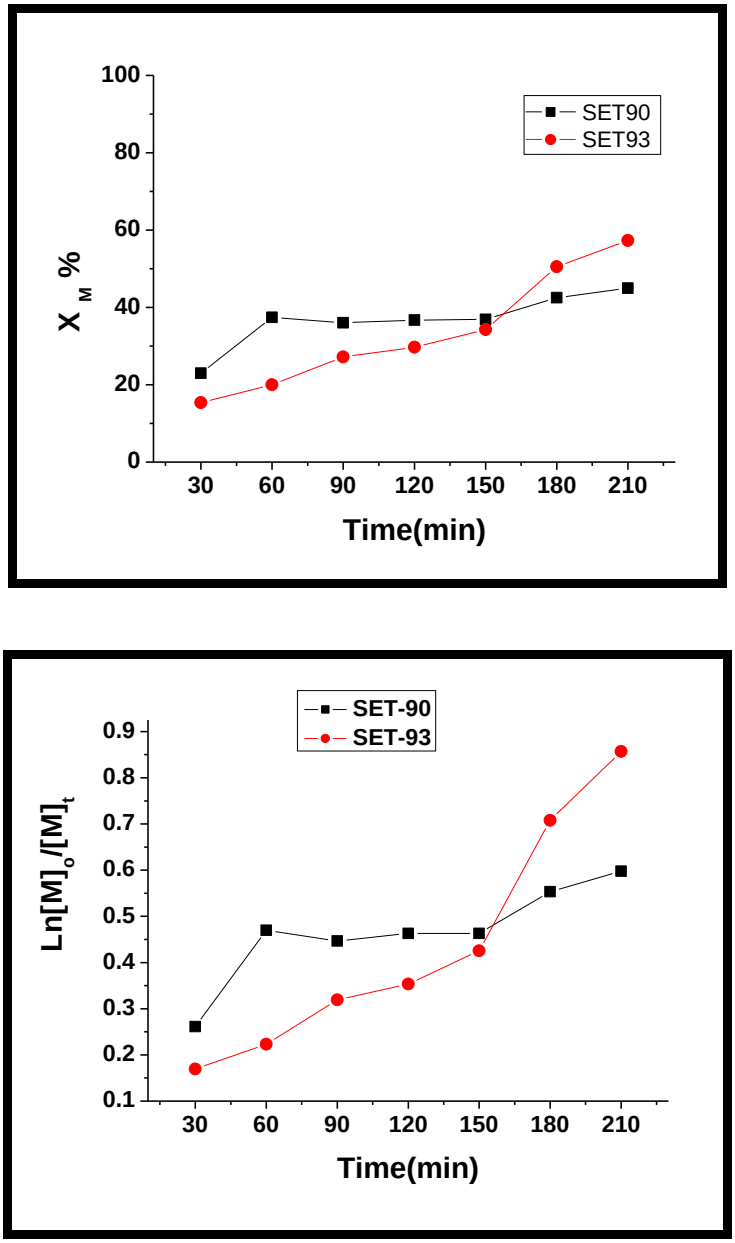

Fig.5. Monomer conversion versus time for the SET-LRP (SIP) polymerizations of NIPAM from non-spherical latex particles (PS-18) made by the batch addition method in water at 25°C.

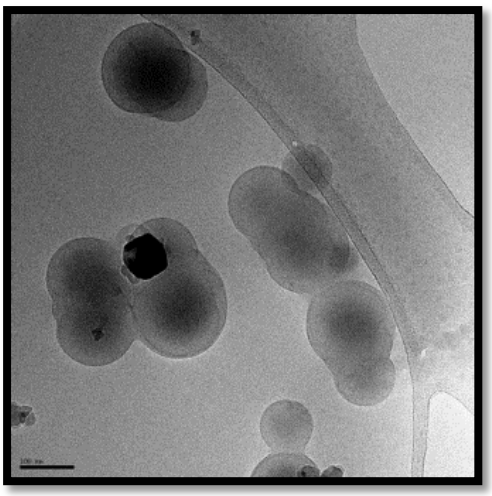

Fig.6. Cryo-TEM image of (SW-106) after surface initiated (SET-90) of NIPAM at 25°C in water. Scale bar in the image is 100 nm.

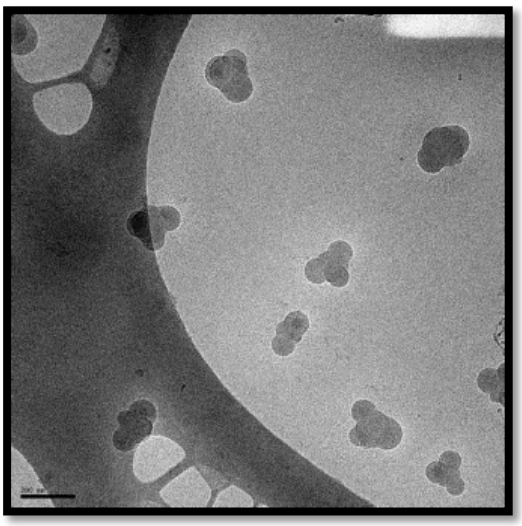

(7 a)

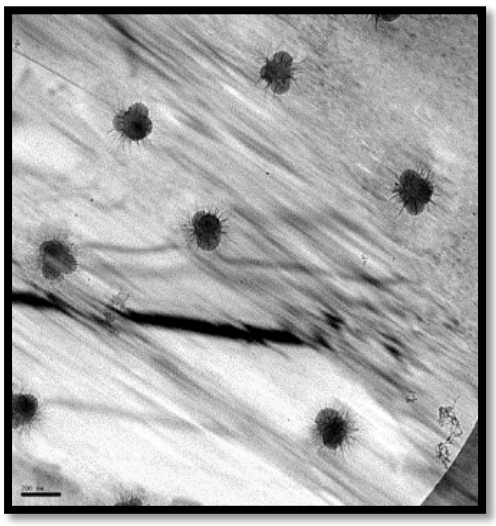

(7 b)

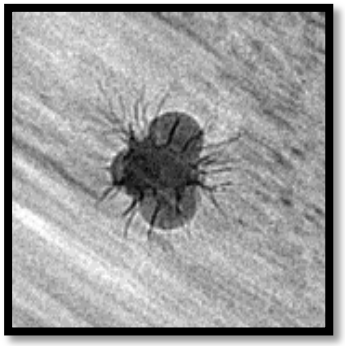

(7 c)

Fig.7. Cryo-TEM images of (SW-124) after surface initiated (SET-93) of NIPAM at 25°C in water, Scale bar in both images is 200 nm, (7c) is close up image of one of the latex particles in latex SET-93 in image (7b).

From the Cryo-TEM image, the polymer brushes are not present although the polymerization reaches 45% conversion. In case of (SET-93), the monomer conversion increased linearly until it reached 57%, the visibility of the poly(NIPAM) brushes by Cryo-TEM for (SET-93) depends on the ice thickness and whether the area type of the ice is amorphous or crystalline.

The poly(NIPAM) brushes are not visible as shown in figure (7 a), but in image (7 b) the poly(NIPAM) brushes are present and extend from the surface of the latex particles toward the water phase with an average length of 100 nm, In (7 c) the close up image of one of the SET-93 particles. Poly(NIPMA) brushes are present in the middle of non-spherical particles which are the original seed domain (PS-18), which contains the tertiary bromine group.

Based on this, a very thin ice layer (crystalline) in the Cryo-TEM grid is required in order to view the poly(NIPAM) brushes made by batch addition method. (SET-93) particles are amphiphilic-hairy particles with hairy hydrophilic domain in the middle, and the other newly formed domains are hydrophobic. The FTIR spectrum of SET-93 dried film is shown in figure 8. The absorption was taken after ultra-centrifugation and dialysis of the latex; the spectrum shows the two absorptions fingerprints of the secondary amine at 3288 cm^{-1} and at 737cm^{-1}, and for the amide bond at 1646 cm^{-1}.

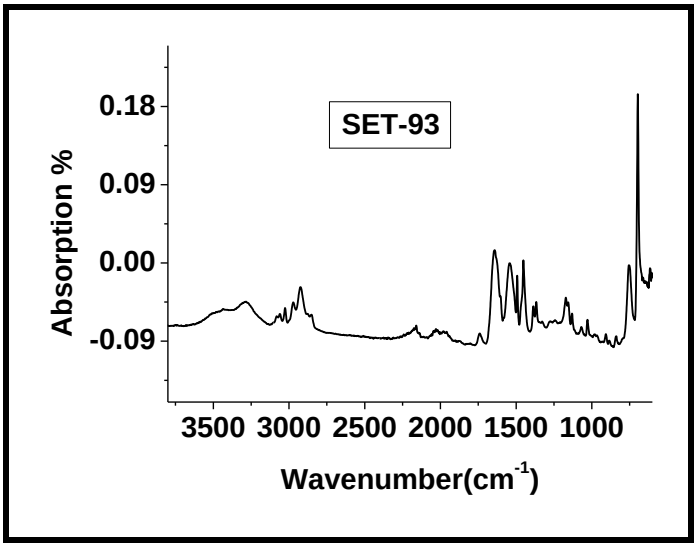

Fig.8. FTIR spectrum of (SET-93) latex particles after purification and drying.

Conversely, Seed latex (PS-24) has a markedly lower crosslinked density compared to the previously discussed latexes, now being only 2.6 %. In addition it has low concentration of co-monomer (styrene sulfonate) with 0.257% in contrast to 0.5% in (PS-18) and 0.30% in (PS-21). PS-24 particle size is 220 nm and the latex has a good colloidal stability with zeta potential of (-41 mV).

This latex is anticipated to be able to take up more monomer, and hence a bigger swelling and obvious phase separation could be achieved, considering that the latex elastic contraction forces will be lower in contrast to the counterpart latexes with higher cross-linked densities. Table 6 shows the recipe and conditions that are used to swell the latex PS-24, followed by figure 9 which shows SEM images of the obtained morphology after swelling and seeded emulsion polymerization.

The first attempt to swell and undertake seeded emulsion polymerization of (PS-24) is experiment (SW-188); the swelling ratio used was 1.5 and the concentration of DVB used was high at 13.3%. The obtained morphology shows oval shaped morphology with a size of 313 nm and this reveals an increase in size of around 100 nm. In (SW-219) the swelling ratio was increased to 7.28, and at lower DVB

concentration of 5.75%, the particles attained dumbbell shaped morphology with particles of size 385 nm, which is the double the size of the original seed particles.

Table.6. Ingredients used to swell the latex PS-24, and the subsequent obtained morphology after polymerization at 70°C with speed of mixing of 30 rpm, R (M/P) = Ratio of monomer to polymer, S = styrene, D = divinyl benzene (DVB), A= Azobisisobutyronitrile (AIBN), SM = swelling monomers mixture and AIBN.

Experiment	R (M/P)	Latex (t.s) %	Latex Weight (g)
Sw-188	1.5/1	8.70	1.66
Sw-219	7.28/1.0	8.70	1.0
Sw-284	2.48/1.0	8.70	1.0
Sw-294	2.88/1.0	8.70	1.0

Exp	S+D+A=SM(g)	DVB %	H_20 (mL)	Latex morphology	Colloidal stability
Sw-188	(6.0+0.80+0.064) = **0.2190**	13.3	7.0	**Oval**	Stable
Sw-219	(6.08+0.35+0.065) = **0.6337**	5.75	7.0	**Oval**	Stable
Sw-284	(6.0+0.030+0.060) = **0.2166**	0.50	3.0	**Dumbbell**	Stable
Sw-294	(6.0+0.030+0.060) = **0.251**	0.20	3.0	**Dumbbell**	Stable

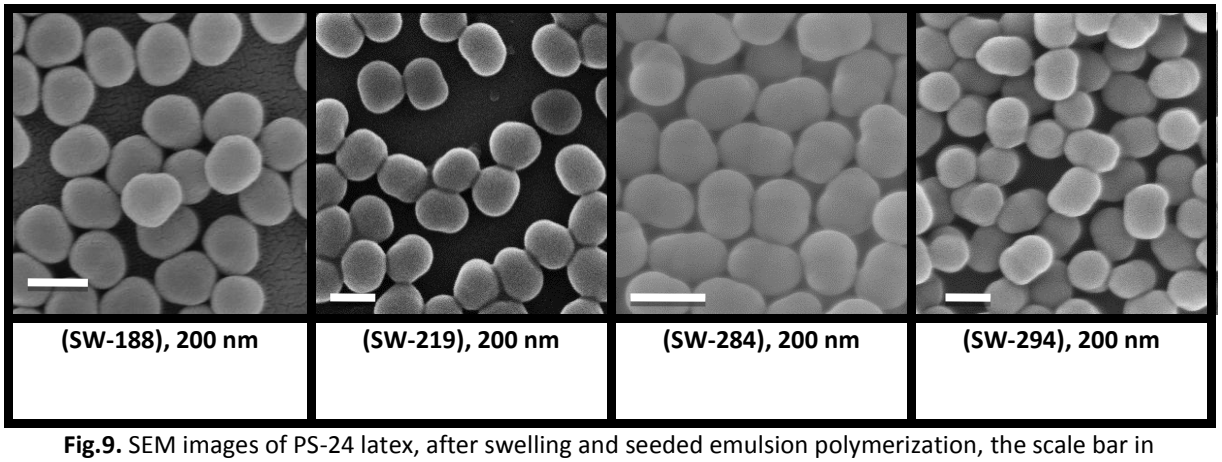

(SW-188), 200 nm | **(SW-219), 200 nm** | **(SW-284), 200 nm** | **(SW-294), 200 nm**

Fig.9. SEM images of PS-24 latex, after swelling and seeded emulsion polymerization, the scale bar in all images is 200 nm.

It is difficult to distinguish the border between the original seed domain and the newly formed domain, but this obtained morphology is excellent latex that can be modified by SET-LRP to make the targeted hairy Janus particles. When the swelling ratio was reduced to 2.48, the concentration of DVB to 0.5%, and externally added water to only 3.0 mL as in (SW-284), the obtained particles are doublet shaped with snowman and dumbbell shape morphologies; the border between the two domains is apparent, and besides that, the width of the newly formed domain is identical to the seed, and that was not the case in the previous examples where the width of the newly formed domain was smaller than the original seed particles. This could be attributed to the higher monomer flux to regions of lower crosslink density, which is the newly formed domain. As the concentration of DVB decreased to 0.20%, and with a slightly higher swelling ratio of 2.88 as in (SW-294), the particles attained doublet shape with snowman and dumbbell morphologies.

To summarize the swelling of the seed PS-24, this latex has a low crosslink density, which helps to prevent the formation of secondary nucleation as a result of the ability of the lower crosslinked latex to absorb all monomer at the experimental swelling ratios. The newly formed domain size can be improved by using a lower concentration of DVB in the second stage polymerization.

The PS-26 latex was synthesized with similar conditions to that used with PS-24, with the exception that the concentration of DVB used with (PS-26) was only 1%. This latex has the lowest crosslinked density among the latexes made by the batch addition method. This latex had a monodisperse particle size distribution, with particle size of 260 nm. This latex shows excellent colloidal stability with zeta potential of (-39.7 mV). This latex is predicted to uptake more swelling monomer owing to the lower crosslinked density inside the latex, and on the contrary, the

elastic contraction force to squeeze the swollen monomer will be lower. Table 7 shows the recipe and conditions that were used to swell this latex, followed by (Figure 10) which shows SEM images of the obtained particles' morphologies.

Table.7. Ingredients used to swell the latex PS-26, and the subsequent obtained morphology after polymerization at 70°C with speed of mixing of 30 rpm, R (M/P) = Ratio of monomer to polymer, S = styrene, D = divinyl benzene (DVB), A = Azobisisobutyronitrile (AIBN), SM = swelling monomers mixture and AIBN.

Experiment	R(M/P)	Latex (t.s) %	Latex Weight(g)
SW-190	2.8/1.0	7.0	1.21
SW-214	8.8/1.0	7.0	1.0
SW-223	8.1/1.0	7.0	1.05
SW-225	8.9/1.0	7.0	1.0

Exp	S+D+A=SM(g)	DVB %	H_20 (mL)	Latex morphology	Colloidal stability
SW-190	(6.0+0.80+0.064) = **0.2365**	13.3	7.0	**Oval**	Stable
SW-214	(6.08+0.350+0.0659) = **0.616**	5.75	7.0	**Dumbbell**	Stable
SW-223	(6.0+0.153+0.064) = **0.60**	2.55	7.0	**Dumbbell**	Stable
SW-225	(6.0+0.0+0.0650) = **0.628**	0.0	7.0	**Dumbbell**	Stable

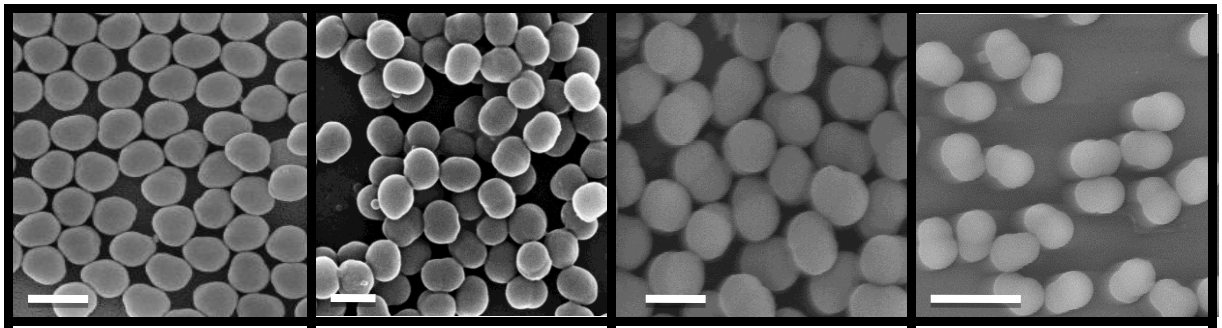

Fig.10. SEM images of PS-26 latex, after swelling and seeded emulsion polymerization. The scale bar in images SW-214 and SW-223 is 200 nm, and the scale bar is 500 nm in SW-190 and SW-225.

The first endeavour to make the doublet shape particles from the seed (PS-26) was when this latex was swelled with a swelling ratio of 2.80 and a DVB concentration of 13.3% as in (SW-190); the particles appeared to have an oval shape morphology

with pushed phase separation toward one direction to form a small new domain. The newly formed domain covered some of the area of the original seed particles, and in particular the area where the phase separation was pushed; the total size of the obtained particle after phase separation was around 380 nm with increase of 120 nm from the original seed (PS-26).

After this experiment, (PS-26) has swelled with higher swelling ratio of 8.8 and with a lower DVB concentration of 5.75% as in (SW-214); the gained morphology revealed doublet shaped particles with dumbbell shaped morphology, with bigger total particle size of around 530 nm; the size of the newly formed domain is identical to the size of the original seed of around 260 nm. No substantial secondary nucleation was observed and that indicates a good absorption of monomer by (PS-26). The very good phase separation in (SW-214) is attributed to the high concentration of the swelling monomer and lower DVB concentration leading to a mild squeeze of the seed to form directed phase separation toward one domain. The other factor is that the size of the latex particles is bigger, which makes the phase separation is easier as a result of the lower pressure in the surface of the latex particles as the surface area of the latex reduces. The DVB concentration was lowered further to 2.55% with a swelling ratio of 8.1 as in (SW-223). The phase separation was very obvious, with dumbbell shaped particles and a small amount of secondary nucleation. The border between the original seed particles and the newly formed domain is highly apparent in this case, the reason is that the lower concentration of DVB in the second stage polymerization means the flow of the swelling monomer migrates faster toward the newly formed domain. This was also observed when the second stage polymerization was completely free from DVB, with a swelling ratio of 8.9 as in (SW-225). The obtained latex has dumbbell shaped

particles with a size of 500 nm; the size of the newly formed region is smaller than in the previous case, at 200 nm. No further modification was applied on the obtained dumbbell particles as the visualization of the polymer brushes made by batch addition is difficult.

5.4.2. Phase separation from hairy latexes made by batch addition method (Route 2):

The hairy latex particles made by batch addition have been synthesized as described in Chapter 4. These hairy latexes were used as seed particles (hydrophilic hairy seed particles) in the second stage seeded emulsion polymerization after swelling with styrene and DVB for 24h. (PS-21) seed latex particles were modified by SET-LRP to form poly(sodium styrene sulfonate) brushes on their surfaces as (SET-117). Two swelling and seeded emulsion polymerizations were performed by using this hairy latex (SET-117); Table 8 shows the recipe and conditions that were used to induce the phase separation, and Figure 11 shows the obtained morphologies.

Table.8. Ingredients used to swell the hairy latex (PS-21) and the subsequent obtained morphology after polymerization at 70°C with speed mixing of 30 rpm, S= styrene, D= divinyl benzene (DVB), A= Azobisisobutyronitrile (AIBN), SM= swelling monomer mixture, CV% = conversion of surface initiated (SET-LRP), R (M/P) = Ratio of Monomer to polymer, t.s% = total solid of latex.

Exp	Latex	Brush type	CV %	Particle size (nm)	R (M/P)	Latex (t.s %)	Latex Weight (g)
SW-196	SET-117	P(NaSS)	80%	1320	5.76/1.0	0.41	7.518
SW-235	SET-117	P(NaSS)	80%	1320	3.50/1.0	0.41	14.07

Exp	S+D+A=SM(g)	DVB %	H_20 (mL)	Latex morphology	Colloidal stability
SW-196	(6.52+0.3622+0.062) =**0.173**	5.55	0.0	**Raspberry**	Stable
SW-235	(6.04+0.018+0.061) =**0.200**	0.30	0.0	**Raspberry**	Stable

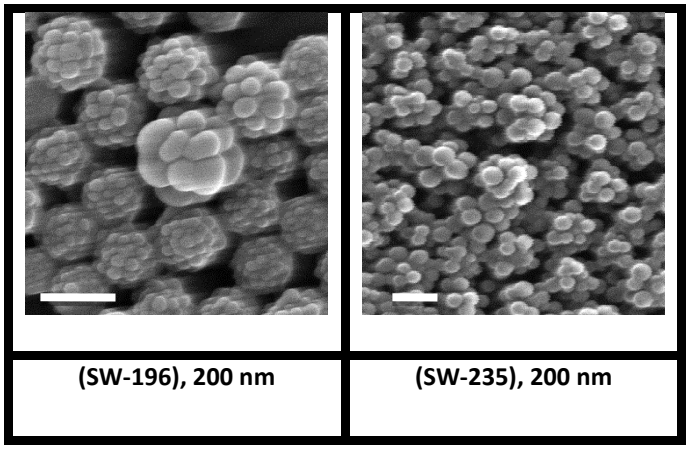

Fig.11. SEM images of PS-21 hairy latex after swelling and seeded emulsion polymerization. The scale bar in both images is 200 nm.

In (SW-196) the swelling ratio used was 5.76, and there was 5.55% of DVB in the monomer feed. These conditions usually make the seed non-hairy particle (PS-21) just grow without observation of phase separation, but when the hairy latex (SET-117) was used as in (SW-196) a raspberry morphology was attained. This indicates that multiple phase separations were promoted when the surface of the seed (PS-21) was grafted with poly(sodium styrene sulfonate) brushes. This could be explained as a result of the high interfacial tension between the hydrophilic surface of (SET-117) seed particles and the expelled monomer leading to the formation of multiple new domains. In experiment (SW-235), we attempted to reduce this massive number of newly formed domains by reducing the swelling ratio to 3.50 and lowering the DVB concentration to allow a directed phase separation. The obtained morphology is a raspberry shaped particle, and the phase separation is much clearer and more significant; this could be attributed to the low concentration of DVB used, which enhances the flow of the swelling monomer to give bigger newly formed domains. This behaviour is completely the opposite of that when non-hairy PS-21was used, this indicates that the poly(styrene sulfonate) brushes play a major role in the morphology of the obtained latex after swelling and seeded emulsion polymerization. Table 9 shows the recipe and the experimental conditions used to

swell and perform seeded emulsion polymerization of hairy latex (PS-18). The hairy latex (SET-62), which has poly(NIPAM) brushes, was used in a swelling and seeded emulsion polymerizations: (SW-114).

Table.9. Ingredients used to swell the hairy latex (PS-18) and the subsequent obtained morphology after polymerization at 70°C with speed mixing of 30 rpm, S= styrene, D= divinyl benzene (DVB), A= Azobisisobutyronitrile (AIBN), SM= swelling monomer mixture, CV%= conversion of surface initiated (SET-LRP), R (M/P) = Ratio of Monomer to polymer, t.s% = total solid of latex.

Exp	Latex	Brush type	Cv %	Particle size (nm)	R (M/P)	Latex (t.s %)	Latex Weight (g)
SW-96	SET-65	PNIPAM	100	500	4.78/1.0	0.40	10.00
SW-114	SET-62	PNIPAM	60	535	3.15/1.0	0.63	10.08
SW-115	SET-65	PNIPAM	100	500	6.0/1.0	0.40	8.47
SW-165	SET-77	PNIPAM	100	966	1.81/1.0	1.2	7.00
SW-166	SET-83	PNIPAM	100	934	3.40/1.0	0.45	10.50
SW-180	SET-96	PNIPAM	65	810	1.80/1.0	1.04	4.51
SW-182	SET-97	2-MAETAC	80	<1000	1.45/1.0	1.18	4.12
SW-184	SET-77	PNIPAM	100	966	1.80/1.0	1.2	7.06
Sw-186	SET-97	2-MAETAC	80	<1000	1.75/1.0	1.18	5.30

Exp	S+D+A=SM(g)	DVB %	H_20 (mL)	Latex morphology	Colloidal stability
SW-96	(6.014+0+0.061) **= 0.1912**	0	0.0	**Raspberry**	Stable
SW-114	(6.0 + 0.30 + 0.0625) **= 0.20**	5.0	0.0	**Triplet**	Stable with sedimentation
SW-115	(6.0 + 0.30 + 0.0625) **= 0.20**	5.0	0.0	**Triplet**	Stable with sedimentation
SW-165	(6.0 + 0.30 + 0.0618) **= 0.1525**	5.0	0.0	**popcorn**	Stable and some big particles
SW-166	(6.0+0.30+0.0618) **= 0.1594**	5.0	0.0	**Popcorn**	Stable and some big particles
SW-180	(6.03+0.341+0.067) **= 0.0681**	5.65	0.0	**Raspberry**	Stable
SW-182	(6.03+0.341+0.067) = **0.0702**	5.65	0.0	**Raspberry**	Stable
SW-184	(6.03+0.341+0.067) = **0.150**	5.65	0.0	**Popcorn**	Stable
Sw-186	(6.0+0.80+00640) = **0.1092**	13.3	4.0	**Raspberry**	Stable

The latex (SET-62) has a bigger particle size after SET-LRP as a result of the extending of the hydrated poly(NIPAM) brushes toward the water phase. The monomer conversion of SET-LRP was not fully completed, with 60% monomer conversion. Since this latex has poly(NIPAM) brushes, the brushes on the surface of the latex extend during the swelling step at room temperature, and collapse when the temperature increases to 70°C in order to start the polymerization, thus the particles are hydrophilic during the swelling stage and convert to being hydrophobic during the polymerization stage, this make the swelling and seeded emulsion polymerization steps different from those for non-hairy latex particles. Figure 12 shows the obtained morphologies after swelling and seeded emulsion polymerization from hairy latex (PS-18).

In the first experiment the hairy latex was swollen with monomer containing 5% of DVB, at a swelling ratio of 3.15 in experiment (SW-114). The obtained morphology is rather intriguing showing linearly arranged triplets with the two outer lobes being larger than the central lobe.

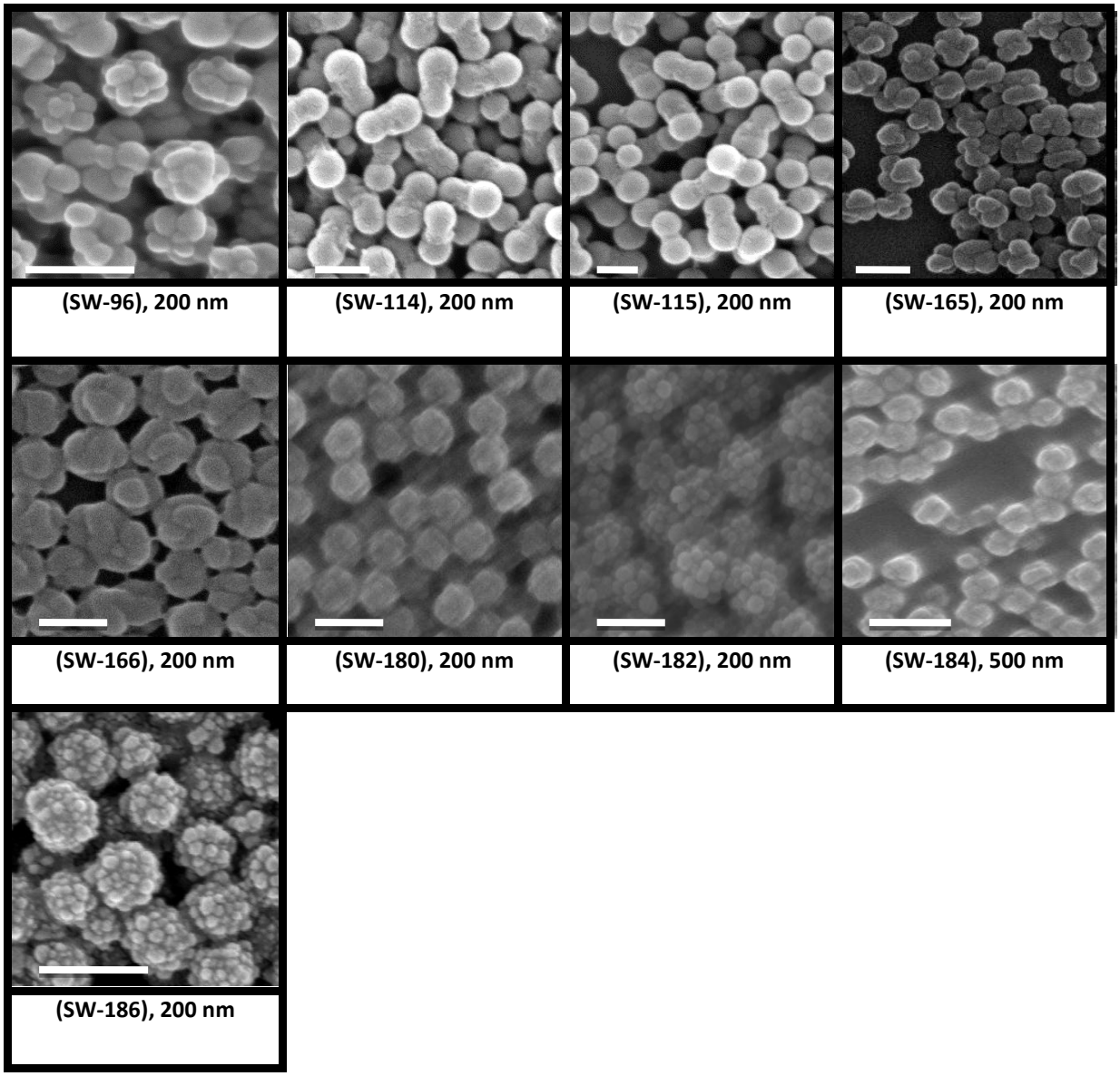

Fig.12. SEM images of PS-18 hairy latex after swelling and seeded emulsion polymerization. The scale bar in all images is 200 nm with exception of SW-184 which is 500 nm.

Cryo-EM investigation (see Figs 13) shows that the central lobes are the one that contain the brushes. The morphology can be formed either through phase separation, but it is interesting that both outer lobes are roughly the same size, or through controlled limited coagulation in which two particles are fused. The same morphology is observed in (SW-115), the only difference being the use of a seed latex with longer hairs, as confirmed by both SET-LRP monomer conversion and DLS measurements on the hairy seed latex (SET-65).

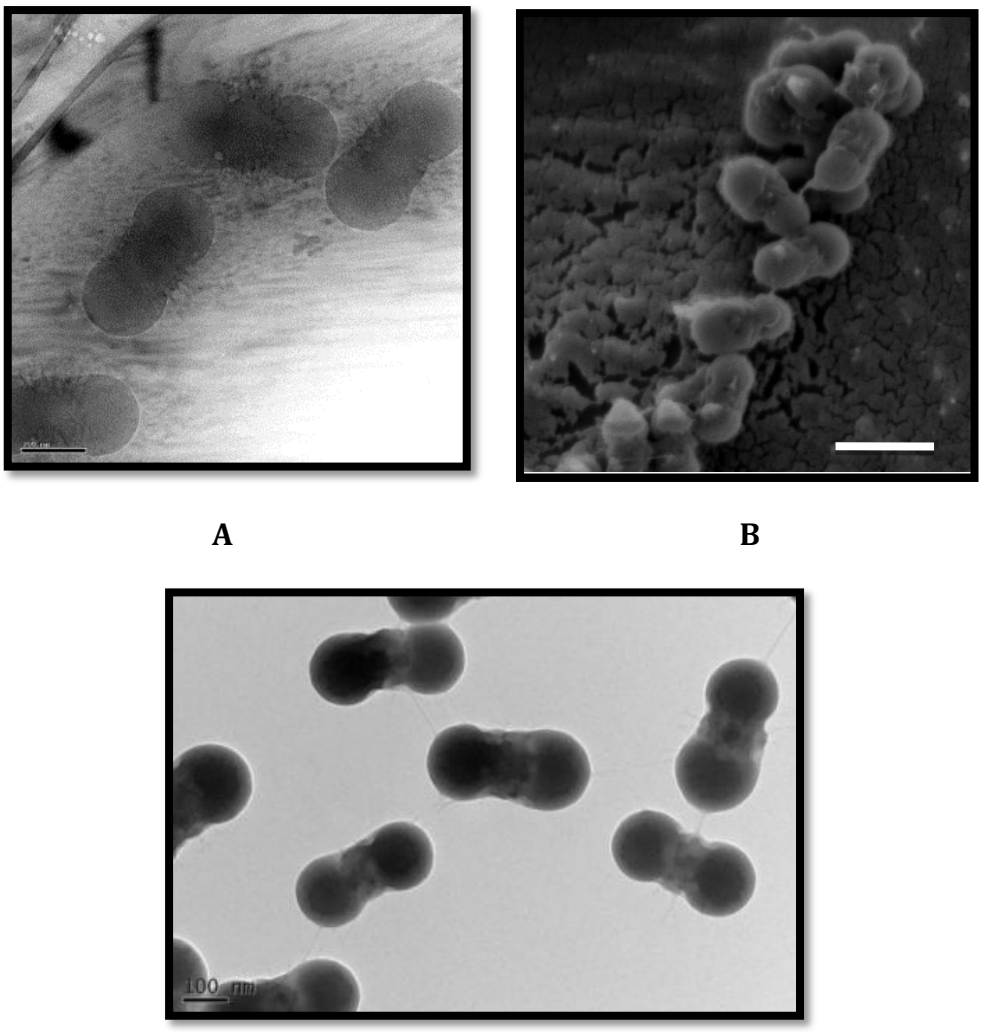

Fig.13. (A) Cryo-TEM image of SW-114, (B) Cryo-SEM image of SW-114, (C) TEM of SW-114, the scale bar is 100 nm in (A) and (C), 200 nm in (B).

Hairy latex (SET-65) was also used in experiment (SW-96) when the polymerization was performed without the use of DVB, with a high swelling ratio of 4.78, and no presence of external water. The particles showed raspberry morphology, which was the expected result because of the absence of the crosslinker in the second stage polymerization

Another latex containing poly(NIPAM) brushes used as seed (SET-77) was used in two experiments (SW-165) and (SW-184). In (SW-165) the swelling ratio is 1.81 and with 5% DVB; the particles after the swelling and seed polymerization gained a

popcorn morphology, which was anticipated as a typical obtained morphology for the non-hairy latex, and can be ascribed to a low swelling ratio. The Cryo-TEM image of the latex (SW-165) is shown in Figure 14, which shows a dark dense region in the middle of these popcorn particles, and a low density region around the centre of the particles.

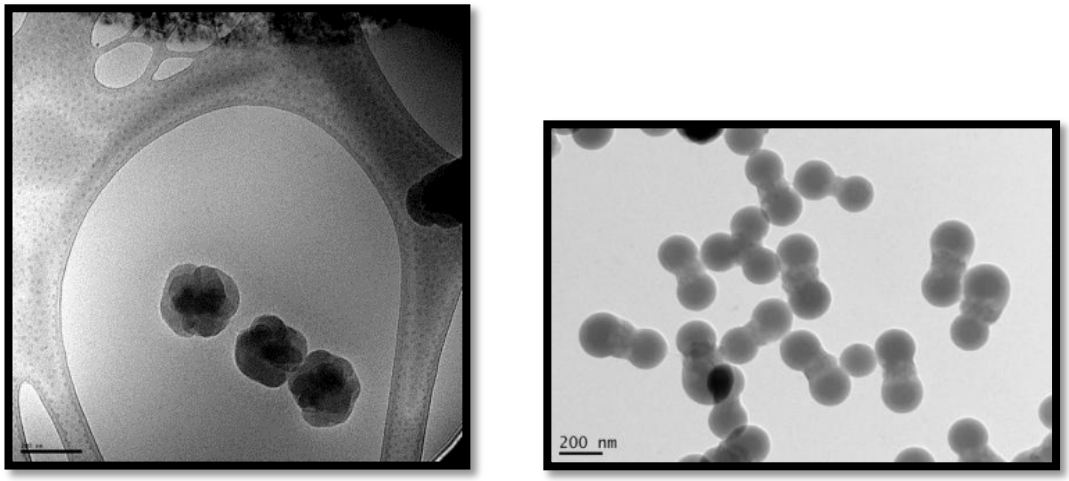

Fig.14. Cryo-TEM image of SW-165 on (left) and TEM image of SW-115 on (right). The scale bar in both images is 200 nm.

(SW-184) has an identical recipe to (SW-165) to check that a reproducible morphology can be obtained, and that was the case: the morphology of the latex (SW-184) had popcorn morphology after swelling and seeded emulsion polymerization.

(SET-83) was used as seed with conditions which could provide triplet shaped particles, as in (SW-114) and (SW-115), in the case of swelling experiment (SW-166). The obtained result shows a popcorn morphology instead of the expected triplet shape morphology; this illustrate that the density and length of the polymer brushes can play a major role in the final obtained morphology, since the seed latex (SET-83) is polymerized by SET-LRP with only Cu(0) alone and that gives longer polymer brushes. This is in contrast to the features when Cu(0) is used along with

$CuBr_2$ which gives shorter polymer brushes, as in (SET-62) , (SET-65) and (SET-77). As (SET-96) used as seed in (SW-180), swelling ratio of 1.80 and 5% DVB concentration, the attained morphology has a raspberry shape as expected, because the swelling ratio is low. In (SW-182) and (SW-186), the seed latex used was (SET-97), this seed latex was grafted with cationic water soluble polymer brushes (poly [2-(methacrylloyloxy) ethyl]-trimethyl ammonium chloride]). (SW-182) swelled with a swelling ratio of 1.46 and 5% DVB concentration; the obtained morphology had a raspberry shape, and in (SW-186), where the swelling ratio was 1.75 and with 13.3% DVB concentration, a raspberry structure was also attained. For both experiments, the lower swelling ratio is the conceivable reason behind the raspberry morphology.

To summarize the swelling of the hairy latex (PS-18), the obtained morphology follows the same trend as in the case of non-hairy latex (PS-18); this indicates that the predominant parameters that control the attained morphology are the swelling ratio and DVB concentration in the second stage, with a small influence by the polymer brushes. This might illustrate that the density of the polymer brushes that are made by batch addition is low; consequently no major effect is governed by the polymer brushes on the obtained morphology. It is essential to mention that experiments with 0.16 and 0.5% DVB concentration in the second stage polymerization of the hairy latex are required to obtain a clearer picture of the swelling of the hairy latex (PS-18) in contrast to the non-hairy latex (PS-18).

(PS-24) seed latex was modified by the grafting of hydrophilic polymer brushes by SET-LRP, and then (PS-24) hairy latex particles were used as seed in the swelling

Table.10. Ingredients used to swell the hairy latex (PS-24) and the subsequent obtained morphology after polymerization at 70°C with speed mixing of 30 rpm, S = styrene, D = divinyl benzene (DVB), A = Azobisisobutyronitrile (AIBN), SM= swelling monomer mixture, CV% = conversion of surface initiated (SET-LRP), R (M/P) = Ratio of monomer to polymer, t.s% = total solid of latex. (NA) = not available.

Exp	Latex	Brush type	CV %	Particle size (nm)	R (M/P)	Latex (t.s %)	Latex Weight (g)
SW-203	SET-110	P(NaSS)	85	1089	2.24/1.0	1.45	4.61
SW-206	SET-110	P(NaSS)	85	1089	3.5/1.0	1.45	4.05
SW-207	SET-110	P(NaSS)	85	1089	5.61/1.0	1.45	4.19
SW-228	SET-110	P(NaSS)	85	1089	4.33/1.0	1.45	4.0
Sw-229	SET-110	P(NaSS)	85	1089	4.19/1.0	1.45	4.0
SW-230	SET-110	P(NaSS)	85	1089	3.73/1.0	1.45	4.0
SW-267	SET-114	P(NIPAM)	80	372	2.02/1.0	1.0	10.0
SW-268	SET-143	P(NaSS)	100	NA	3.17/1.0	1.26	5.0
SW-270	SET-112	P(NIPAM)	40	270	1.63/1.0	1.66	7.80
SW-273	SET-110	P(NaSS)	85	1089	5.62/1.0	0.22	9.70

Exp	S+D+A= SM(g)	DVB %	H_2O (mL)	Latex morphology	Colloidal stability
SW-203	(6.52+0.362+0.062) **= 0.150**	5.5	0.0	**Snow-man Janus particles**	Stable
SW-206	(6.16+0.33+0.06) **= 0.205**	5.35	0.0	**Snow-man Janus particles**	Stable
SW-207	(6.16+0.33+0.06) = **0.340**	5.35	0.0	**Raspberry**	Stable
SW-228	(6.0+0.349+0.064) **= 0.250**	5.0	0.0	**Snow-man Janus particles**	Stable
SW-229	(6.0+0.10+0.064) **= 0.243**	1.66	0.0	**Snow-man Janus particles**	Stable
SW-230	(6.0+0.0613+0.0629) **= 0.2157**	1.02	0.0	**Snow-man Janus particles**	Stable
SW-267	(6.0+0.60+0.060) **= 0.2025**	10.0	0.0	**Secondary nucleation and big triplet particles.**	Stable
SW-268	(6.0+0.06+0.060) **= 0.20**	1.0	0.0	**Doublet and triplet Janus particles**	Stable
SW-270	(6.0+0.60+0.060) **= 0.211**	10	0.0	**Oval**	Stable
SW-273	(6.0+0.06+0.06) **= 0.120**	1.0	0.0	**Doublet Janus**	Stable

and seeded emulsion polymerization in different conditions. Table 10 shows the recipe and conditions that were used to swell (PS-24) hairy latex particles, and Figure 15, which shows SEM images of the obtained morphologies.

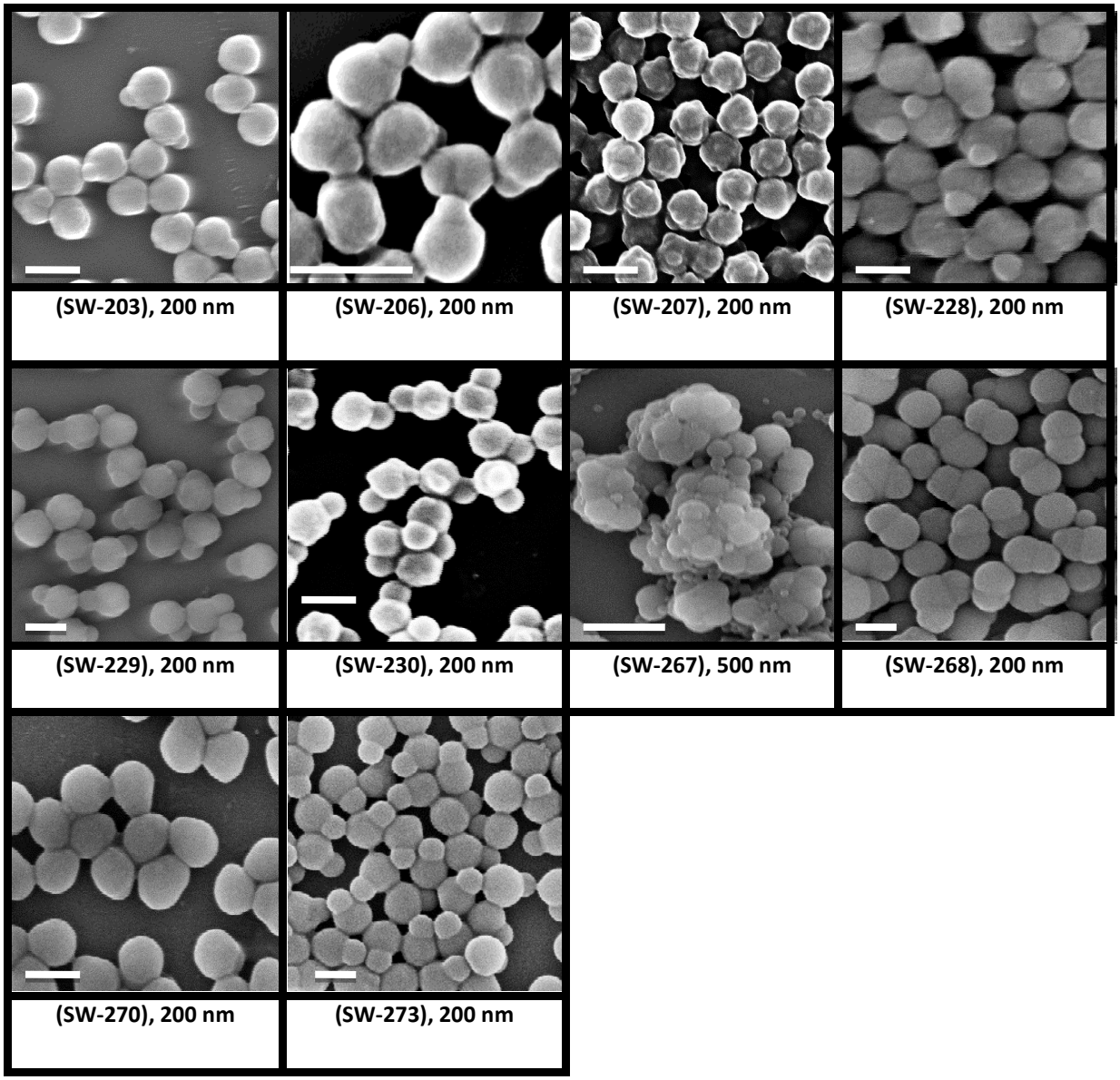

Fig.15. SEM images of PS-24 hairy latex after swelling and seeded emulsion polymerization. The scale bar in all images is 200 nm with exception of SW-267 which is 500 nm.

(SET-110) latex was swollen with a swelling ratio of 2.24 and a DVB concentration of 5.5%, as in (SW-203); the obtained morphology showed doublet shape particles with snowman morphology. The size of the newly formed domain is very small; around 90 nm with a 4:1 ratio relative to the original seed particles. Figure 16 shows the Cryo-TEM image of (SW-203).

In (SW-206) the swelling ratio was increased to 3.5 with the same DVB concentration; the latex formed has similar morphology to (SW-203), with the same

ratio between the newly formed domain and the original seed particles of approximately 4:1. The Cryo-TEM image of (SW-206) shows that the newly formed domain has a smooth surface and the original seed domain has a rough surface (see figure 16). When the swelling ratio was further increased to 5.61, and with the same concentration of DVB as in (SW-207), the particles attained obvious raspberry morphology; this demonstrates the fact that an increase in the swelling ratio does not enhance the size of the newly formed domain. This is because the swelled monomer prefers to stay in the low cross-linked domain which is the original seed domain, which has 2.6% cross linked density in contrast to 5.35% in the newly formed domain.

Based on this, when the swelling ratio was additionally increased, it led to the formation of multiple new domains because most of the monomer favours staying inside the low crosslinked region, and besides that, the increase in the swelling ratio makes the concentration of DVB inside the latex particles enlarged, which causes a high elastic contraction force, which leads to undirected phase separations.

This can be seen when the swelling ratio decreases a little to 4.33, with a lower DVB concentration to 5.0%, as in (SW-228); the particles attained the snowman morphology as in the cases of (SW-203) and (SW-206). Based on this we can see that small changes in the swelling ratio lead to magnificent change in the morphology of the latex particles. The reduction of DVB concentration in the second stage polymerization below the DVB concentration in the original seed latex particles was investigated in (SW-229), where a 4.19 swelling ratio was used with only a 1.6% DVB concentration. All the latex particles attained a snowman morphology, with an enlarged newly formed domain of around 114 nm, which was bigger than that obtained in (SW-203), (SW-206) and (SW-228). The reason behind

the increase in the size of the newly formed domain notwithstanding the small swelling ratio used is the lower concentration of DVB, which makes the swollen monomer flow toward the low crosslinked density region represented by the newly formed domain.

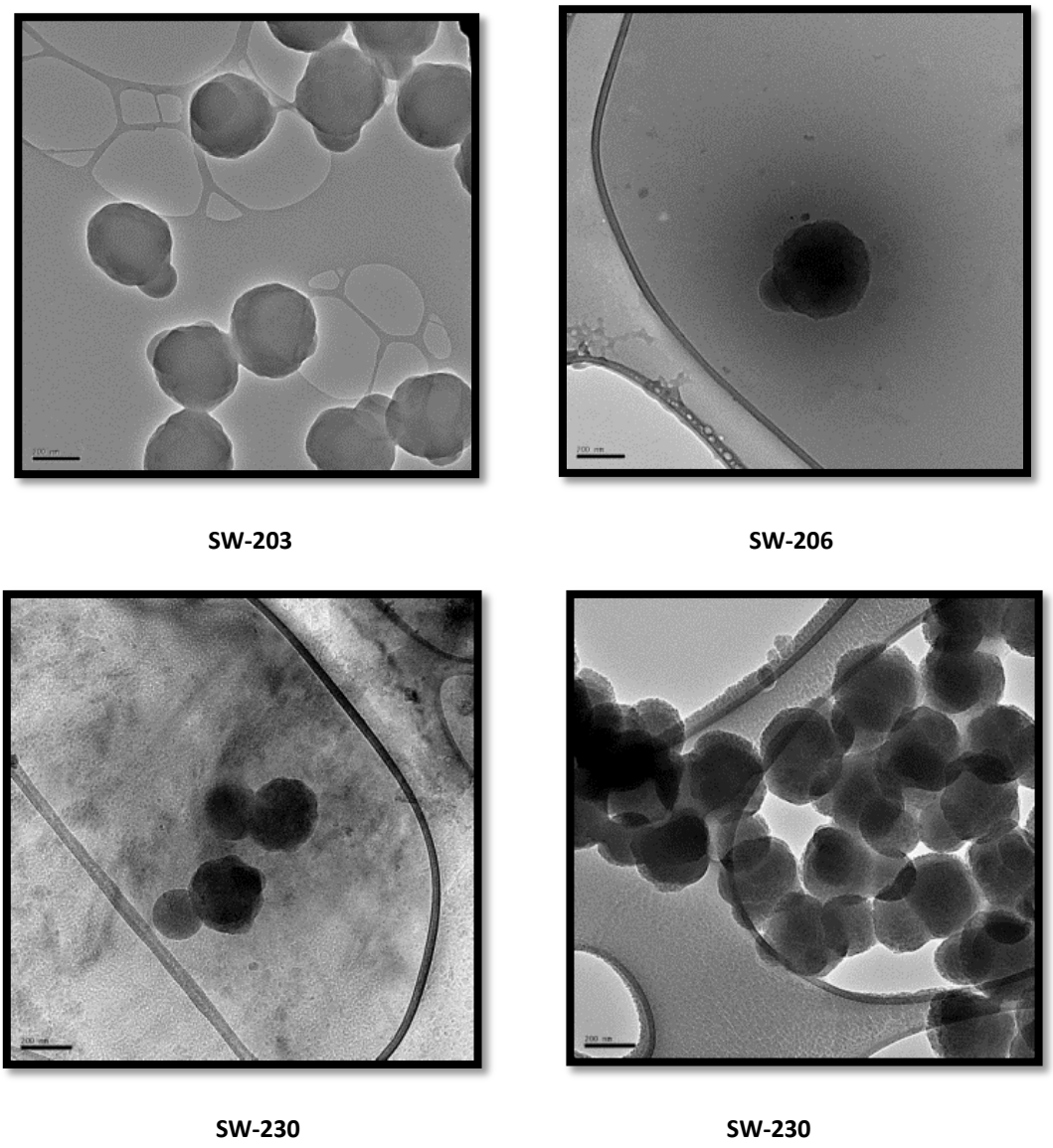

Fig.16. Cryo-TEM image of SW-203, SW-206 and SW-230, the scale bar for all the images is 200 nm

That also can be verified from experiment (SW-230), when a lower swelling ratio was used (3.73), and a lower concentration of DVB (1.02%); most of the latex particles attained the snowman morphology, and the newly formed domain had a bigger size compared to all other previous experiments, at 150 nm . This illustrates

that when the concentration of DVB is lower in the second stage polymerization compared to the original seed domain, it makes the phase separation of the newly formed domain bigger as a result of the enhancement of the flow of the swelling monomer from the high crosslinked region (original seed domain) toward the lower crosslinked domain (the newly formed domain). The Cryo-TEM image of (SW-230) is shown in Figure 16. (SW-230) shows the ideal morphology of Janus amphiphilic particles with snowman morphology, whereby the hydrophilic seed domain is the bigger and rough domain that contains poly(sodium styrene sulfonate) brushes, and the smaller, smooth domain is the hydrophobic domain, which was generated after the swelling and seeded emulsion polymerization. AFM images of (SW-230) particles in dry condition are shown below in figure 17.

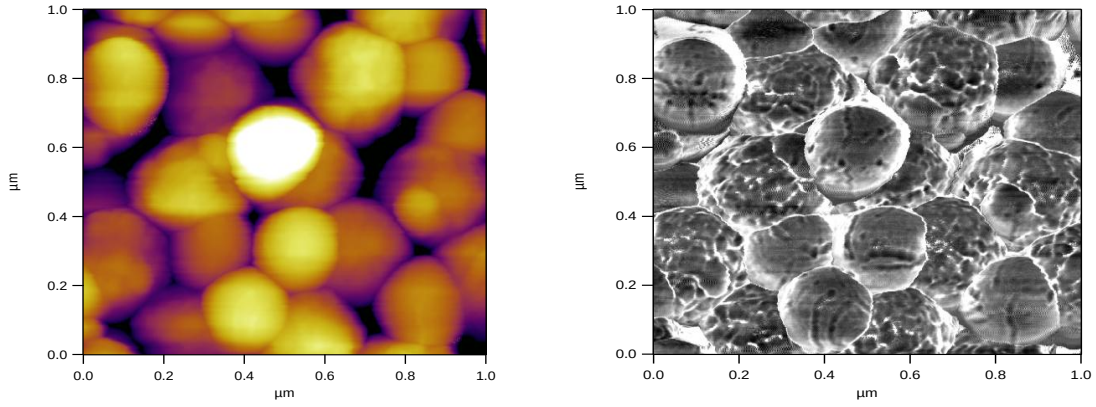

SW-230 (Tapping Mode AFM) SW-230 (Tapping mode-phase contrast AFM image)

Fig.17. Tapping mode and phase contrast AFM images of (SW-230), Scale bar is 0.2 µm.

The phase contrast AFM image shows two distinctive morphologies for each particular domain; the bigger hydrophilic domain that contains poly(sodium styrene sulfonate) brushes appears rough, and the smaller hydrophobic domain appears smooth; consequently the AFM image agrees with that obtained by Cryo-TEM.

With a similar concentration of DVB as that used in (SW-230), but with a higher swelling ratio of 5.62 as in the polymerization (SW-273), the latex attained a snowman morphology with a slightly larger newly formed domain size of 160 nm with a 10 nm incensement in size compared to (SW-230). This indicates that the main factor behind increasing the size of the newly formed domain is a decrease in the concentration of DVB in the second stage polymerization. AFM images of (SW-273) are presented in Figures 18 and 19.

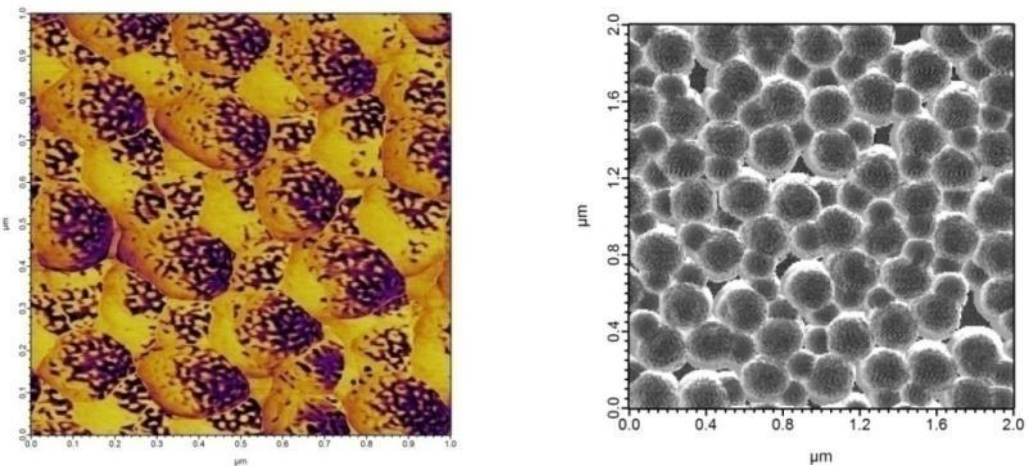

SW-273 (Phase contrast AFM image) SW-273 (Phase contrast AFM image)

Fig.18. Tapping mode-contrast phase AFM images of SW-273.

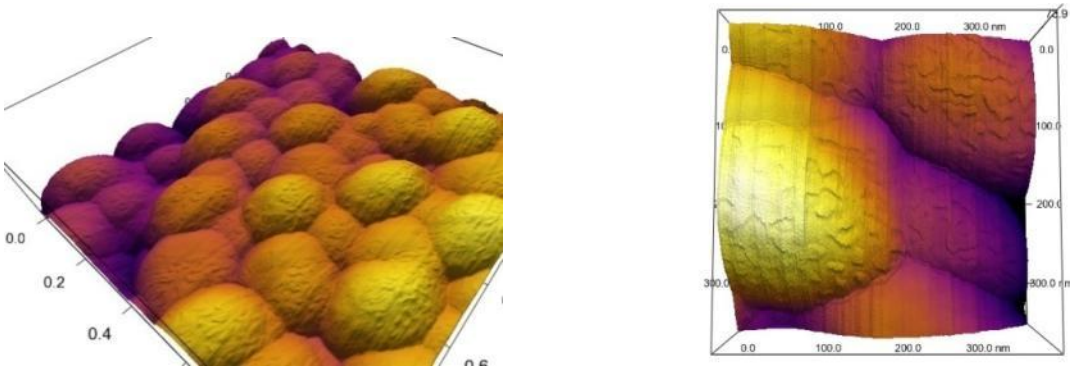

SW-273 (3D- Phase contrast AFM image), scale is in (µm), SW-273 (3D- Phase contrast AFM image) scale in (nm).

Fig.19. 3-D tapping mode phase contrast AFM images of SW-273.

The phase contrast tapping mode AFM images of (SW-273) show two distinctive domains in terms of their surface morphology in each snowman particles: one domain is rough, which includes the original seed particles (hydrophilic side), and one is smooth, which is the newly formed domain (hydrophobic side).

The 3-dimensional (3-D) tapping mode phase contrast image shows the surface morphology of each side with more detail: the larger hydrophilic domain has some roughness in the surface as a result of the presence of the poly(sodium styrene sulfonate) brushes, in contrast to the hydrophobic newly formed domain, which has a very smooth surface.

(SW-273) latex shows fewer defects (the formation of multiple new domains after the seeded polymerization), in contrast to (SW-230) which shows some defects as can be seen in the SEM and AFM images. The reason behind the lower number of defects in (SW-273) is attributed to the high swelling ratio used in (SW-273) 5.6 compared to 3.7 in (SW-230)); consequently the amount of DVB is higher in (SW-273), which guides phase separation toward merely one domain.

When the hairy seed particles (SET-110) are replaced by a new hairy seed which contains the same type of hydrophilic polymer brushes poly(sodium styrene sulfonate) but shorter as in (SET-143), with a swelling ratio of 3.17 and DVB concentration of 1.0%, as in (SW-268), the latex attains doublet and triplet shaped particles. It is interesting that the particles seem to have more than one rough area, which seems to suggest that there are multiple regions of brushed lobes. A feasible explanation is a limited coalescence throughout the polymerization process was occurred. This indeed is evident from the SEM analysis where several larger fused clusters can be observed the Cryo-TEM image of (SW-268) is shown in Figure 20.

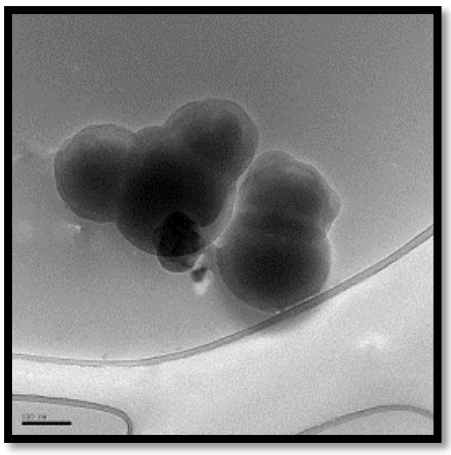

Fig.20. Cryo-TEM image of SW-268, the scale bar is 100 nm

The latex (PS-24) was also grafted with poly(NIPAM) brushes, as in (SET-114) and (SET-112). Total monomer conversion in the case of (SET-114) is 80%; this seed swollen with a swelling ratio of 2.02 and 10% DVB concentration, as in (SW-267). Very high DVB concentration was used in this experiment to reduce the number of separated newly formed domains, as this predominately occurred when the seed latex was grafted with poly(NIPAM) brushes. The obtained morphology shows multiple new domain particles, with a small amount of doublet and secondary nucleation.

(PS-24) was grafted with poly(NIPAM) with only 40% conversion of SET-LRP, as in (SET-112), and swollen with a swelling ratio of 1.63 and DVB concentration of 10%, as in (SW-270); the latex particles attained non-spherical (oval) shape morphology. This indicates that the grafting density and the length of the poly(NIPAM) brushes, in addition to the swelling ratio play a major role in the final morphology, whereas the grafting density and length of the polymer brushes decreases the number of phase separations, and the particles behave like non-hairy latex particles.

Conversely, (PS-26) latex was grafted with poly(sodium styrene sulfonate) brushes by SET-LRP with monomer conversion of 76% as in latex (SET-116). The particle size of the seed increased after the modification to 958 nm, which indicates that longer polymer brushes were grafted from the surface of (PS-26). The reason for carrying out the swelling and seeded emulsion polymerization step with only poly(sodium styrene sulfonate) brushes is twofold.

Table.11. Ingredients used to swell the hairy latex (PS-26) and the subsequent obtained morphology after polymerization at 70°C with speed mixing of 30 rpm, S = styrene, D = divinyl benzene (DVB), A = Azobisisobutyronitrile (AIBN), SM= swelling monomer mixture, CV% = conversion of surface initiated (SET-LRP), R (M/P) = Ratio of monomer to polymer, t.s% = total solid of latex.

Exp	Latex	Brush type	C.V %	Particle size (nm)	R (M/P)	Latex (t.s %)	Latex Weight (g)
SW-199	SET-116	P(NaSS)	76	958	4.50/1.0	0.73	5.03
SW-209	SET-116	P(NaSS)	76	958	8.95/1.0	0.73	5.00
SW-232	SET-116	P(NaSS)	76	958	6.0/1.0	0.70	5.10
SW-234	SET-116	P(NaSS)	76	958	3.46/1.0	0.70	8.5

Exp	S+D+A=SM(g)	DVB%	H_20 (mL)	Latex morphology	Colloidal stability
SW-199	(6.52+0.3622+0.062) **= 0.1617**	5.55	0.0	**Oval**	Stable
Sw-209	(6.16+0.33+0.068) = **0.3270**	5.35	0.0	**Oval**	Stable
Sw-232	(6.0+0.050+0.060) **= 0.2157**	0.80	0.0	**Snowman (Janus) + secondary nucleation**	Stable
Sw-234	(6.0+0.018+0.061) **= 0.2059**	0.3	0.0	**Snowman (Janus) + secondary nucleation + unchanged particles**	Stable

The first reason is the fact that poly(sodium styrene sulfonate) supports phase separation to occur from one direction as that observed with hairy latex (PS-24), and secondly poly(sodium styrene sulfonate) brushes can be visualized easily by Cryo-

TEM. Table 11 shows the recipe and conditions that were used to swell and perform seeded emulsion polymerization by using hairy PS-26 (SET-116) latex as seed, and figure 21, which shows SEM images of the obtained morphologies.

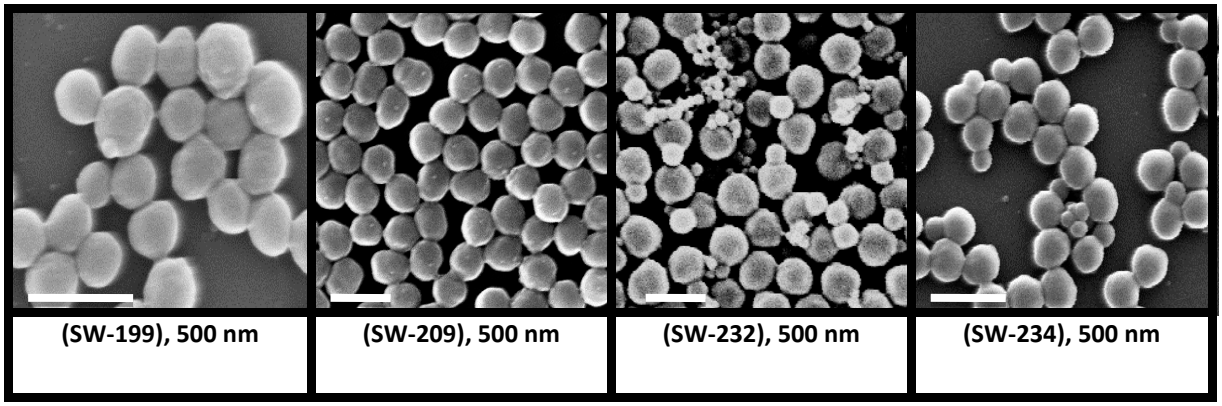

Fig.21. SEM images of (SET-116) hairy latex after swelling and seeded emulsion polymerization. The scale bar in all images is 500 nm

Initially, (SET-116) latex was swollen with a swelling ratio of 4.50 and DVB concentration of 5.55% as in (SW-199); the gained particles shows that most of the hairy particles merely grew from 260 nm to around 400 nm with non-spherical morphology, with some of the particles having a raspberry morphology. It was thought that the absence of phase separation was due to the low swelling ratio. Based on this, in (SW-209) the swelling ratio was increased to 8.95, with a reasonably similar DVB concentration of 5.35%; the obtained particles had a similar morphology to those in (SW-199) with non-spherical morphology and size of around 500 nm; consequently the increase in swelling ratio led to the seed (SET-116) merely growing into bigger particles without clear phase separation.

In (SW-232), the DVB concentration was reduced to 0.80%, with a swelling ratio of 6. The morphology of the particles obtained shows three types of particle were produced. The first was doublet particles with snowman morphology with a size of 500 nm; the size of the newly hydrophobic formed domain is around 200 nm, and the size of the hydrophilic domain is around 300 nm. The second type was particles

without phase separation, with merely growth in size to 300 nm; the number of examples of the second type is lower than the first snowman particles. The third type is small particles (secondary nucleation) with a size of around 90 nm.

These results demonstrate that the reduction in the concentration of DVB in the second stage polymerization induces the phase separation, but the high swelling ratio lead to the formation of secondary nucleation. This was observed based on the result that the phase separation from hairy latex (PS-26) was clearer in contrast to the non-hairy latex, which indicates that the poly(styrene sulfonate) brushes grafted onto the surface of (PS-26) minimize contact between the expelled monomer and the surface of the latex particles, which makes the phase separation much more obvious.

Finally we made an attempt to minimize the secondary nucleation that occurred in (SW-232), by reducing the swelling ratio to 3.46 and DVB concentration to 0.30%, as in (SW-234); the obtained particles have similar three types of particle morphologies, with a smaller total of secondary nucleation compared to that in (SW-232).

5.5. Conclusion

Phase separation after seeded emulsion polymerization by using an oil-soluble initiator from swollen non-hairy and hairy latex particles with different crosslinked densities made by the batch addition method was investigated. In the case of non-hairy latex particles, the phase separation depends on several factors such as the crosslink density in the original seed particles, size of the seed latex, concentration of DVB (crosslinker) in the monomer feed, and the monomer to polymer swelling ratio. It was observed that the newly formed hydrophobic domain size increases with

decreasing the DVB concentration in the second stage polymerization, as the flow of the swelling monomer will be directed toward the low crosslinked density domain.

In general, the preparation of Janus particles from non-hairy particles made by the batch addition method is not an ideal method, since the visualization of the polymer brushes from the original seed domain is difficult due to the low density of the formed brushes, and also the newly formed domain might cover the original seed domain owing to the low interfacial tension between the two domains; this was detected as no apparent border between the two domains, and the newly formed domain which just covered the original seed domain. The other sign is the low monomer conversion of SET-LEP when the dumbbell particles were used (as seed initiator), which indicates that the tertiary bromine functional group was mostly covered by the newly formed domain after phase separation, although the presence of inimer on the surface of the dumbbell particles was confirmed by FTIR.

When hairy latex particles were used in swelling and seeded emulsion polymerization with different types of polymer brushes on their surface, the obtained particles had mainly popcorn and raspberry morphologies, and with special circumstances doublet and triplet Janus particles were made. Based on this, the preparation of Janus particles from hairy latex made by batch addition is possible under particular circumstances, but is not reproducible, as different properties of the brushes made after SET-LRP will have a major influence on the obtained morphology.

5.6. References

1- Kim, J.-W.; Larsen, R. J.; Weitz, D. A., *J. Am. Chem. Soc.* **2006**, *128*, 14374-14377.

2- Kim, J.-W.; Lee, D.; Shum, H. C.; Weitz, D. A., *Adv. Mater.***2008**, *20*, 3239-3243.

3- Pfau, A.; Sander, R.; Kirsch, S., *Langmuir*. **2002**, *18*, 2880-2887.

4- Whitelam, S.; Bon, S. A. F., *J. Chem. Phys*. **2010**, *132*, 074901/1-074901/8.

5- Min, T. I.; Klein, A.; El-Aasser, M. S.; Vanderhoff, J. W., *J. Polym. Sci., Polym. Chem. Ed.* **1983**, *21*, 2845-61.

6- Okubo, M.; Katsuta, Y.; Matsumoto, T., *J. Polym. Sci., Polym. Lett. Ed.* **1980**, *18*, 481-486.

7- Okubo, M.; Katsuta, Y.; Matsumoto, T., *J. Polym. Sci., Polym. Lett. Ed.* **1982**, *20*, 45-51.

8- Okubo, M.; Ando, M.; Yamada, A.; Katsuta, Y.; Matsumoto, T., *J. Polym. Sci., Polym. Lett. Ed.* **1981**, *19*, 143-147.

9- Ni, H.; Ma, G.; Nagai, M.; Omi, S., *J. Appl. Polym. Sci.* **2000**, *76*, 1731-1740.

10- Ni, H.; Ma, G.; Nagai, M.; Omi, S., *J. Appl. Polym. Sci.* **2001**, *80*, 2002-2017.

11- Karlsson, O.; Hassander, H.; Wesslen, B., *J. Appl. Polym. Sci.* **1997**, *63*, 1543-1555.

12- Sheu, H. R.; El-Aasser, M. S.; Vanderhoff, J. W., *J. Polym. Sci., Part A: Polym. Chem.* **1990**, *28*, 629-51.

13- Skjeltorp, A. T.; Ugelstad, J.; Ellingsen, T., *J. Colloid Interface Sci.* **1986**, *113*, 577-582.

14- Lee, D. I.; Ishikawa, T., *J. Polym. Sci., Polym. Chem. Ed.* **1983**, *21*, 147-154.

15- Chen, Y. C.; Dimonie, V.; El-Aasser, M. S., *Pure Appl. Chem.* **1992**, *64*, 1691-1696.

16- Chen, Y. C.; Dimonie, V.; El-Aasser, M. S., *J. Appl. Polym. Sci.* **1992**, *45*, 487-99.

17- Joensson, J. E. L.; Hassander, H.; Jansson, L. H.; Toernell, B., *Macromolecules.* **1991**, *24*, 126-31.

18- Perro, A.; Reculusa, S.; Pereira, F.; Delville, M.-H.; Mingotaud, C.; Duguet, E.; Bourgeat-Lami, E.; Ravaine, S., *Chem. Commun.* **2005**, 5542-5543.

19- Yu, H.; Chen, M.; Rice, P. M.; Wang, S. X.; White, R. L.; Sun, S., *Nano Lett.* **2005**, *5*, 379-382.

20- Johnson, P. M.; Van Kats, C. M.; Van Blaaderen, A., *Langmuir* .**2005**, *21*, 11510-11517.

21- Sheu, H. R.; El-Aasser, M. S.; Vanderhoff, J. W., *J. Polym. Sci., Part A: Polym. Chem.* **1990**, *28*, 653-67.

22- Jansson, L. H.; Wellons, M. C.; Poehlein, G. W., *J. Polym. Sci., Polym. Lett. Ed.* **1983**, *21*, 937-43.

23- Kim, J. W.; Suh, K. D., *Colloid Polym. Sci.* **1999**, *277*, 210-216.

24- Said, Z. F. M.; Fataftah, Z. A., *Polym. Int.* **1996**, *40*, 307-313.

25- Mock Eric, B.; De Bruyn, H.; Hawkett Brian, S.; Gilbert Robert, G.; Zukoski Charles, F., *Langmuir*. **2006**, *22*, 4037-43.

26- Kegel, W. K.; Breed, D.; Elsesser, M.; Pine, D. J., *Langmuir*. **2006**, *22*, 7135-7136.

27- Kim, J.-W.; Larsen, R. J.; Weitz, D. A., *Adv. Mater.* **2007**, *19*, 2005-2009.

28- Park, J.-G.; Forster, J. D.; Dufresne, E. R., *Langmuir*. **2009**, *25*, 8903-8906.

29- Yu, H. K.; Mao, Z.; Wang, D., *J. Am. Chem. Soc.* **2009**, *131*, 6366-6367.

30- Hu, X.; Liu, H.; Ge, X.; Yang, S.; Ge, X., *Chem. Lett.* **2009**, *38*, 854-855.

31- Park, J.-G.; Forster, J. D.; Dufresne, E. R., *J. Am. Chem. Soc.* **2010**, *132*, 5960-5961.

32- Mock, E. B.; Zukoski, C. F., *Langmuir*. **2010**, *26*, 13747-13750.

Chapter 6: Synthesis of poly(styrene) latex particles with Janus morphology by the shot addition method

6.1. Summary

Non-hairy and hairy monodisperse cross-linked poly(styrene) latex particles with various cross-linked densities and average particle sizes synthesized by soap-free (shot addition) emulsion polymerization (see Chapter 2) were used in seeded emulsion polymerization to make anisotropic particles by the formation of a new hydrophobic domain.

In the case of the non-hairy latexes, low cross-linked density (below 2.90%) of the seed latex, a low DVB weight fraction (below 0.5%) in monomer used in the swelling step, and the presence of a hydrophilic surface (as a result of the shot addition method used in contrast to batch addition) were found to be an excellent conditions for inducing phase separation to form new hydrophobic domains in a reproducible manner, thus yielding dumbbell-shaped particles. The lobe originating from the seed latex of the dumbbell particles was modified subsequently by SET-LRP to ultimately form the targeted hairy Janus particles with different types of water-soluble polymer brushes. The obtained hairy Janus particles were characterized by Cryo-TEM.

When hairy latex particles were used as seed, however, the most commonly obtained morphologies were raspberry and popcorn, with the exception of some isolated non-reproducible cases where the aimed dumbbell shaped Janus particles were synthesized. The physical nature of the polymer brushes, especially key properties

such as length and density played a crucial role in the formation of these more complex latex particle morphologies

6.2. Introduction

This chapter is an extension of the routes toward fabrication of Janus particles described in chapter 5. The difference is that now seed latexes are used which had the ATRP initiator functionalized (ethylene glycol)-based methacrylate, referred to as Inimer (see Chapter 2 for synthesis details) incorporated through a shot addition at the later stages of the seed latex emulsion polymerization process. This effectively would lead to a more hydrophilic surface of the latex, in contrast to the latexes used in Chapter 5, which were fabricated by a batch soap-free emulsion polymerization process.

6.3. Experimental

6.3.1. Formation of dumbbell-shaped latex particles using non-hairy cross-linked poly(styrene) latex particles made by shot addition method

One representative example is presented here (experiment SW-241): 4.0 g of (PS-27) latex which had a total solid content of 1.8% was placed in glass vial. To these latex particles, 0.2112 g of a premade mixture of 6.0 g of styrene, 0.010 g of divinyl benzene and 0.060 g of AIBN was added to the latex. The vial was degassed by nitrogen for 10 min and then closed and placed in the tumbling oven which had a rotating motor to tumble the sample at a speed of 30 rpm for 24 h at 25ºC. Subsequently, the oven was heated to 70ºC for another 24 h to commence polymerization after the swelling step. The latex was dialyzed against water for one week with daily replacement of the water.

6.3.2. General procedure for surface-initiated polymerization by SET-LRP from the surface of non-spherical latex made by shot addition method

One example will be described here to graft water soluble brushes from a latex (SW-241) by surface-initiated polymerization (SET-140): 0.4966 g of sodium styrene sulfonate, 37.5 mg of Cu(0) (wire at a length of 8.0 cm, and diameter of 0.025 mm), 4.0 mg of $CuBr_2$, 0.228 g of ethylene glycol (used as inert marker for monomer conversion analysis by ^1H NMR), and 0.022 g of an external sacrificial ATRP initiator **(2),** (used to control the SET-LRP kinetics and moderate length of the brushes) were placed in a 50 mL round bottom flask, then 10.6 g of (SW-241), solids content (0.68 wt%) latex was added with 5.0 g of distilled water. Then, the flask was closed by a rubber stopper and placed in a water bath at 25ºC. Next, the mixture was degassed for 30 minutes, and then 2.0 mL of 2 wt% separately degassed aqueous PMDETA solution was injected using a plastic syringe to the mixture. At that moment, polymerization commenced. The degassing of the polymerization mixture continued over the course of polymerization with a stream of nitrogen gas. Samples were taken at predetermined intervals to monitor the monomer conversion and changes in particle size.

After SET-LRP, the functionalized latex was purified by ultracentrifugation at a speed of 28 Krpm for 24 h, and then the aqueous phase (the supernatant) was separated by gentle removal from the centrifuge tube. The remaining sediment contained hairy non-spherical latex particles were redispersed in water by sonication. Finally, the latex was further purified through dialysis against water for a period of one week.

6.3.3. Formation of non-spherical latex particles using hairy cross-linked poly(styrene) latex particles made by shot addition method

One representative example is presented here (experiment SW-170): 7.14 g of hairy spherical latex particles with poly(sodium styrene sulfonate) brushes (SET-69) with a total solid content of 0.45% was placed in a 20 mL glass vial, then 0.150 g of a homogenous premade mixture of 6.0 g of styrene, 0.30 g of divinyl benzene and 0.060 g of AIBN was added to the latex particles. The glass vial was degassed by nitrogen for 10 min and then closed and placed in the tumbling oven which tumbled the sample at a speed of 30 rpm for 24 h at 25ºC. Next, the oven was heated to 70ºC for another 24 h to start the polymerization after the swelling step. The latex was dialyzed against water for one week with daily replacement of the water.

6.4. Results and discussion

6.4.1. Phase separation from non-hairy latexes made by shot addition method (Route 1).

From the previous Chapter we found that the crosslink density of the seed latex plays an important role to control the morphology of the latex after phase separation. We therefore used several seed latexes which all had a hydrophilic surface as a result of the shot addition of the hydrophilic inimer, but had different crosslink densities as various relative amounts of divinylbenzene were used, that is 7.49 wt%, 5.25 wt%, 3.62 wt%, 3.1 wt%, 2.55 wt%, and 1.95 wt% . The details of these latexes can be found in Table 1. PS-20 latex has an average particle diameter of 135 nm and a monodisperse particle size distribution; this seed latex has a high cross-linked density with a DVB concentration of 7.49 %. The latex was prepared using 0.49 % of sodium styrene sulfonate as comonomer to warrant colloidal stability, and 5.0 % inimer which was added by the shot addition method at elevated conversion.

Table.1. Latex key characteristics of the used latexes in swelling and seeded emulsion polymerization made by shot addition method.

Latex Key characteristic	PS-20	PS-25	PS-27	PS-29	PS-30	PS-31
Inimer (wt %)	5.0	5.15	5.18	9.74	10	17.8
NaSS (wt %)	0.490	0.293	0.284	0.334	0.251	0.295
Average Particle size (nm)	135	220	156	187	230	250+ (100 nm secondary nucleation)
Total solid (%)	8.6	5.0	1.8	5.6	8.0	7.8
Zeta potential (mV)	- 41.0	- 49.8	- 49.7	- 45.5	- 39.5	- 37.0
Crosslinked density (wt %)	7.49	3.1	1.95	2.55	5.25	3.62

It is very important to note that the inimer was added in presence of a small amount of DVB to warrant a crosslinked shell, of vital importance later in the growth of water soluble polymer brushes. The latex shows excellent colloidal stability with a zeta potential of -41 mV. PS-20 latex was swollen with various (styrene, DVB, AIBN) mixtures, polymerized as listed in table 2, and analyzed on morphology by SEM. The results of the SEM analysis are shown in Figure 1.

With a swelling ratio (monomer to polymer by weight) of 2.2, and with a DVB concentration of 5.0% (as in SW-93), the latex particles elongated to a size of 220 nm and contained multiple new domains. When the swelling ratio was increased to 2.61 at a slight reduction in the DVB concentration to 4.1% (as in SW-103), the latex particles merely swelled and grew to 260 nm; this increase of 125 nm was almost equal to the size of the original seed.

Based on these results, any small variation in the swelling ratio and DVB concentration may lead to different morphologies.

Table.2. Ingredients used to swell latex PS-20 and the subsequent obtained morphologies after polymerization at 70°C with a mixing speed of 30 rpm. R (M/P) = ratio of Monomer to Polymer, S = styrene, D = divinyl benzene (DVB), A= azobisisobutyronitrile (AIBN), SM = swelling monomer mixture and AIBN.

Exp	R (M/P)	Latex (t.s)%	Latex weight (g)
SW-93	2.2/1.0	8.6	1.2
SW-103	2.61/1.0	8.6	1.0
SW-108	2.40/1.0	8.6	1.05
SW-125	2.0/1.0	8.6	1.18
SW-249	2.21/1.0	8.6	1.05
SW-288	2.39/1.0	8.6	1.0

Exp	S+D+A=SM(g)	DVB %	H_20 (mL)	Latex morphology	Colloidal stability
SW-93	(6.0+0.30+0.06) **= 0.2218**	5	8.0	**Triplet+ Quartet**	Stable+ some coagulation
SW-103	(6.07+0.25+0.0641) = **0.2073**	4.11	8.0	**Spherical**	Stable+ some coagulation
SW-108	(6.0+0.30+0.0625) **= 0.2148**	5.0	8.0	**Triplet+ Quartet**	Stable+ some coagulation
SW-125	(6.0+0.82+0.06) **= 0.20**	13.6	8.0	**Snowman (multi head)**	Stable
SW-249	(6.0+0.01+0.06) = **0.20**	0.16	2.0	**Spherical and non-spherical**	Stable+ some coagulation
SW-288	(6.0+0.030+0.060) **= 0.206**	0.5	3.0	**Spherical and non-spherical**	Stable+ some coagulation

This could be seen also in experiment SW-108 when the DVB concentration was increased to 5.0% and the swelling ratio was 2.40; the latex particles had popcorn morphology with sizes around 220 nm. These morphological results were similar to those of experiment SW-93, as quite similar conditions were used with an emphasis on the same concentration of DVB that was used in the second stage polymerization. These results concur with the results obtained with PS-18 latex as the seed, which was studied in chapter 5. The effect of a higher concentration of DVB in the second stage polymerization was studied in experiment SW-125, when the concentration of DVB was increased to 13.6%. With a swelling ratio of 2.0, the particles had two types of morphologies, snowman and multiple domain morphologies.

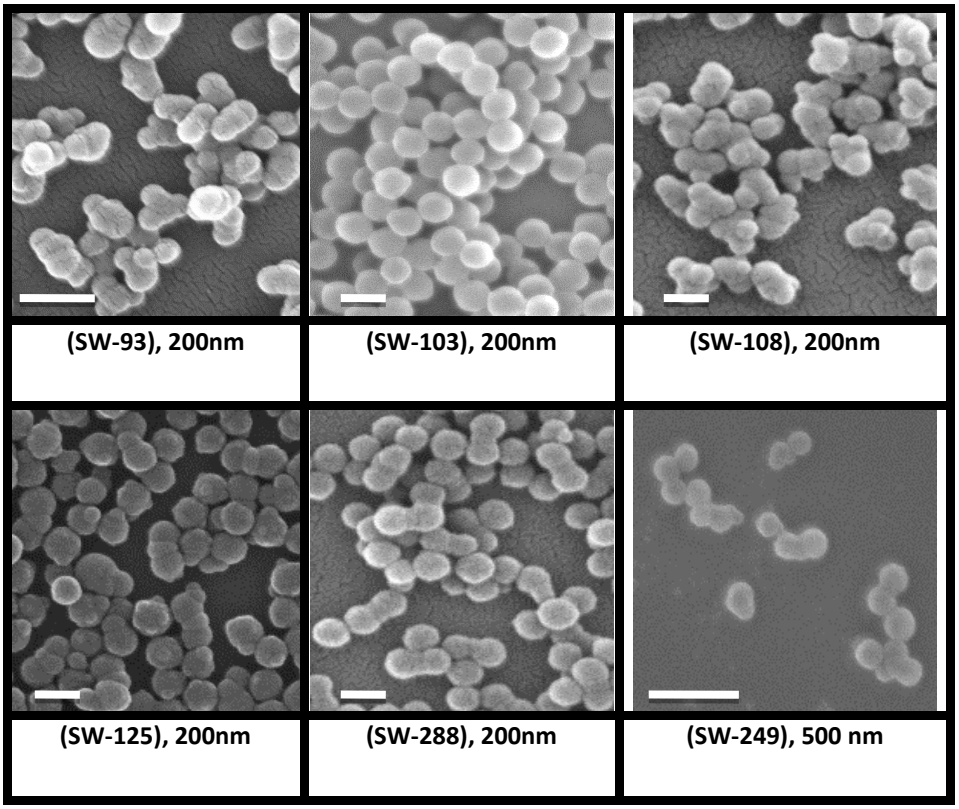

Fig.1. SEM images of PS-20 latex after swelling and seeded emulsion polymerization. The scale bar in all images is 200 nm, with the exception of SW-249 where the scale bar is 500 nm.

These morphologies indicate that higher relative DVB concentrations restricted transport of the monomer inside the latex particles, which led to a reduced phase separation of the newly formed domains, so that snowman and multi-domain morphologies were obtained. In SW-249, a lower DVB concentration was used (0.16%) along with a swelling ratio of 2.21. Two types of particles were formed, larger particles with a size of 400 nm, and a smaller portion with a size of 170 nm. This was also observed in SW-288 when the swelling ratio was 2.39, and with a DVB concentration of 0.5%, but the population of the larger particles was smaller. Both of the aforementioned systems showed some particles with a dumbbell morphology, which indicates that a reduction in the concentration of DVB in the second stage polymerization promotes directed phase separation toward only one domain. The obtained latexes suffered from severe coagulation, which was attributed to the formation of large hydrophobic domains which diminished the colloidal

stability of the latex. The latexes obtained after swelling from PS20 were not further modified to make hairy Janus particles as a result of the presence of defects in the latex such as multiple domains and unchanged particles.

Phase separation from latex PS-25, this seed latex differs from latex PS-20 as it has a lower DVB concentration of (3.1%) in contrast to PS-20 (7.49%). Table 3 shows the protocol and conditions that were used to swell and phase separation from latex PS-25.

Table.3. Ingredients used to swell latex PS-25 and the subsequent obtained morphologies after polymerization at 70°C with a mixing speed of 30 rpm. R (M/P) = ratio of Monomer to Polymer, S = styrene, D = divinyl benzene (DVB), A = azobisisobutyronitrile (AIBN), SM = swelling monomer mixture and AIBN.

Exp	R (M/P)	Latex (t.s %)	Latex weight (g)
SW-189	3.65/1.0	5.0	1.19
SW-212	8.20/1.0	5.0	1.00
SW-216	3.40/1.0	5.0	1.23
SW-239	3.40/1.0	5.0	1.22
SW-227	2.16/1.0	5.0	1.08
SW-285	3.35/1.0	5.0	1.24
SW-286	3.41/1.0	5.0	1.20

Exp	S+D+A=SM (g)	DVB %	H_20 (mL)	Latex morphology	Colloidal stability
SW-189	(6.0+0.80+0.064) **= 0.218**	13.3	7.0	**Spherical**	Stable
SW-212	(6.52+0.362+0.0623) **= 0.4087**	5.55	7.0	**Popcorn**	Stable
SW-216	(6.08+0.35+0.065) **= 0.209**	5.75	7.0	**Raspberry**	Stable
SW-239	(6.0+0.010+0.06) **=0.207**	0.16	3.0	**Triplet+ Quartet+ doublet**	Stable
SW-227	(6.0+0.30+0.060) **= 0.117**	5.0	7.0	**Raspberry**	Stable
SW-285	(6.0+0.030+0.060) **= 0.208**	0.50	3.0	**Triplet + doublet**	Stable+ some coagulation
SW-286	(6.0+0.060+0.060) **= 0.205**	1.0	3.0	**Triplet + doublet**	Stable+ some coagulation

Note that, this latex had a lower concentration of sodium styrene sulfonate (surfmer) compared to PS-20. The latex showed a narrower particle size distribution as a result of the reduction in use of surfmer, with an average particle diameter of 220 nm, excellent colloidal stability with a zeta potential of -49.85 mV. Figure 2 shows the SEM images of the obtained morphologies.

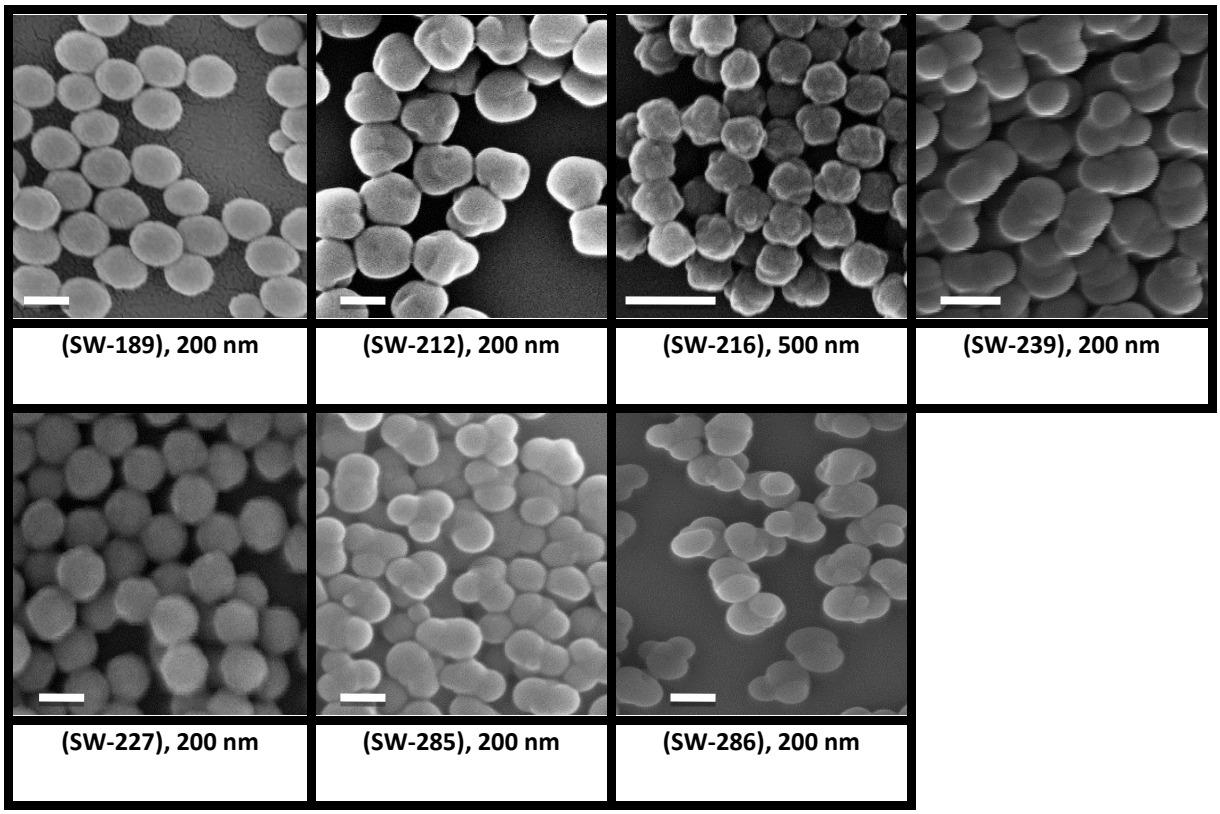

Fig.2. SEM images of PS-25 latex, after swelling and seeded emulsion polymerization. The scale bar in all images is 200 nm, with the exception of SW-216, where the scale bar is 500 nm

Firstly, PS-25 latex swelled with a swelling ratio of 3.65 and with a high DVB concentration of 13.3%, as in SW-189. The latex particles merely swelled and grew to sizes around 325 nm with a 100 nm increase in size. This was attributed to restricted motion of the monomer during the seeded polymerization as a result of the formation of a very dense cross-linked network. When the concentration of DVB was decreased to 5.75%, and with a swelling ratio of 3.40, as in SW-216, the latex particles displayed a raspberry morphology with sizes around 330 nm; this indicates

that the reduction in the DVB concentration lead to a decline in the viscosity inside the latex particles, which enhanced the motion of the swelling monomer in comparison to SW-189. This promotes multiple phase separated domains.

When the swelling ratio was decreased to 2.16, with the same concentration of DVB at 5.0% as in SW-227, the latex particles acquired a raspberry morphology with sizes around 320 nm and with a similar morphology to those obtained in SW-216. When the swelling ratio was increased to 8.20 and with a DVB concentration of 5.5% as in SW-212, the latex particles displayed popcorn morphology with an average size of 370 nm. With the number of phase separated domains limited to one or two, and with a greater size of the phase separated domains, a high swelling ratio consequently caused the phase separated domains to coalescence with each other to form larger phase separated domains.

When the DVB concentration was further decreased to 1.0%, with a swelling ratio of 3.41 as in SW-286, and with a lower amount of external water added (3.0 mL instead of 7.0 mL), the latex particles showed a quartet morphology with three newly formed domains with different sizes of 170, 140 and 90 nm. The sizes of the newly formed domains were larger because the monomer tended to flow from the highly cross-linked region of the original seed to the lower cross-linked regions, which were the newly formed domains.

When the concentration of DVB was furthermore decreased to 0.50% or 0.16% and with a swelling ratio of 3.35 or 3.40 as in SW-285 and SW-239, respectively, the latex particles has similar morphologies to those obtained with SW-286, with latex particles of triplet and quartet morphologies.

Note: It would be interesting to carry out experiments at a low DVB concentration around 1.0%, at higher swelling ratio, say above 6.0. Potentially doublet morphology can be obtained since the high swelling ratio should lead to directed phase separation, and the lower DVB concentration should lead to a phase separated domain of greater size. No further modifications were performed on the obtained latexes after swelling and seeded emulsion polymerization since the obtained particles did not gain the required dumbbell morphology to form hairy Janus particles.

Phase separation from latex PS-27, from the results in Chapter 5 and above it became apparent that lower crosslink densities in the seed latex favored the formation of lesser new domains, putting our targeted dumbbell morphology within reach. Latex PS-27 has a low cross-link density at a DVB concentration of 1.95%; a lower crosslink density means that the latex can swell up to a greater extend. The latex has an average particle size of 156 nm with a narrow particle size distribution and very good colloidal stability with a zeta potential of -49.7 mV. Table 4 shows the recipe and conditions that were used to swell PS-27, followed by Figure 3 which shows the SEM images of the obtained morphologies after swelling and seeded emulsion polymerization.

Following the same pathway as before, PS-27 latex was swollen with a high swelling ratio of 8.46, using a high DVB concentration of 5.75 % as in SW-221. The resulting latex particles had popcorn morphology with an average size of 270 nm; the number of newly formed domains was around 10 with individual sizes of around 60 nm. When the swelling ratio was reduced to 2.77 at the same concentration of DVB (5.0%) as in SW-226, the latex particles did not show a clear phase separation and simply grew to 190 nm with an increase in size of about 30 nm.

In SW-241, when the swelling ratio was 2.90 and with a very low DVB concentration of 0.3%, the latex particles showed a doublet shape with an average size of 270 nm, wherein the hydrophilic original seed domain was the larger domain with an average size of 154 nm, in agreement with the 156 nm of the original seed, and the small, newly formed hydrophobic domain had an average size of 113 nm.

The area percentage of the hydrophilic domains of these Janus particles was 58%, and 42% for the newly formed hydrophobic domains. Since the conditions used for experiment SW-241 were able to produce only one newly formed domain of greater size, other experiments were performed by using reasonably similar conditions as those used in SW-241

Table.4. Ingredients used to swell latex PS-27, and the subsequent obtained morphologies after polymerization at 70°C with a mixing speed of 30 rpm. R (M/P) = ratio of Monomer to polymer, S = styrene, D = divinyl benzene (DVB), A = azobisisobutyronitrile (AIBN), SM = swelling monomer mixture and AIBN.

Exp	R (M/P)	Latex (t.s %)	Latex weight (g)
SW-221	8.46/1.0	1.8	4.06
SW-226	2.77/1.0	1.8	4.00
SW-241	2.90/1.0	1.8	4.00
Sw-247	2.95/1.0	1.8	4.00
SW-250	2.90/1.0	1.8	4.07
SW-251	3.09/1.0	1.8	4.04
SW-252	2.77/1.0	1.8	4.01
SW-253	3.48/1.0	1.8	4.04
SW-254	4.16/1.0	1.8	4.00
SW-258	4.29/1.0	1.8	4.02
SW-259	3.46/1.0	1.8	4.06
SW-260	5.7/1.0	1.8	4.01
SW-261	2.82/1.0	1.8	4.01
SW-274	2.95/1.0	1.8	4.00
SW-275	3.64/1.0	1.8	4.13
SW-289	5.88/1.0	1.8	4.77
SW-298	2.79/1.0	1.8	4.00
SW-299	2.92/1.0	1.8	8.09
SW-300	2.88/1.0	1.8	4.00

Exp	S+D+A=SM(g)	DVB %	H_20 (mL)	Latex morphology	Colloidal stability
SW-221	(6.08+0.350+0.0659**)** **= 0.618**	5.75	3.0	**Popcorn**	Stable
SW-226	(6.0+0.30+0.060) **=0.20**	5.0	0.0	**Spherical**	Stable
SW-241	(6.0+0.018+0.061) **= 0.2112**	0.30	0.0	**Dumbbell**	Stable
SW-247	(6.0+0.030+0.060) **= 0.2130**	0.50	0.0	**Dumbbell**	Stable
SW-250	(6.0+0.060+0.03) **= 0.210**	0.50	0.0	**Dumbbell**	Stable
SW-251	(6.0+0.054+0.0624) **= 0.2248**	0.90	0.0	**Snowman**	Stable
SW-252	(6.0+0.1762+0.0755) **= 0.20**	2.93	0.0	**Raspberry**	Stable
SW-253	(6.0+0.030+0.060) **= 0.253**	0.50	0.0	**Dumbbell**	Stable
SW-254	(6.0+0.010+0.060) **= 0.30**	0.16	0.0	**Dumbbell**	Stable
SW-258	(6.0+0.0634+0.064) **= 0.311**	1.05	0.0	**Spherical**	Stable
SW-259	(6.0+0.0396+0.0607) **= 0.253**	0.66	0.0	**Dumbbell+ triplet**	Stable
SW-260	(6.0+0.030+0.060) **= 0.412**	0.50	0.0	**Dumbbell**	Stable
SW-261	(6.0+0.03+0.060) **= 0.2031**	0.5	0.0	**Dumbbell**	Stable
SW-274	(6.0+0.030+0.060) **= 0.2130**	0.5	0.0	**Dumbbell**	Stable
SW-275	(6.0+0.030+0.060) **= 0.270**	0.50	0.0	**Dumbbell+ triplet**	Stable
SW-289	(6.0+0.030+0.060) **= 0.50**	0.50	0.0	**Non-Spherical**	Coagulation
SW-298	(6.0+0.030+0.060) **= 0.2022**	0.166	0.0	**Dumbbell**	Stable
SW-299	(6.0+0.030+0.060) **= 0.426**	0.50	0.0	**Dumbbell+ triplet**	Stable
SW-300	(6.0+0.030+0.060) **= 0.2080**	0.5	0.0	**Snowman**	Stable

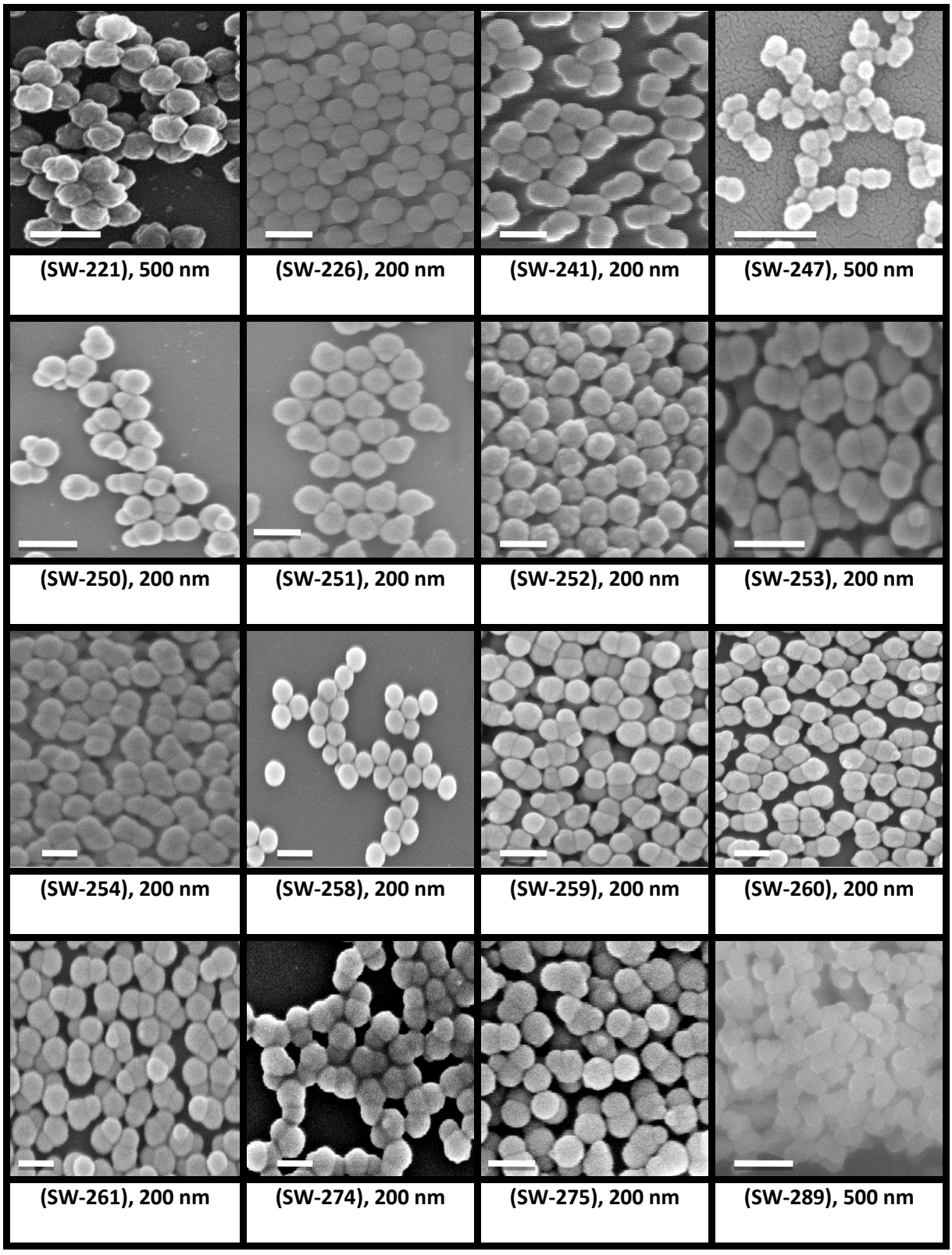
(SW-221), 500 nm
(SW-226), 200 nm
(SW-241), 200 nm
(SW-247), 500 nm
(SW-250), 200 nm
(SW-251), 200 nm
(SW-252), 200 nm
(SW-253), 200 nm
(SW-254), 200 nm
(SW-258), 200 nm
(SW-259), 200 nm
(SW-260), 200 nm
(SW-261), 200 nm
(SW-274), 200 nm
(SW-275), 200 nm
(SW-289), 500 nm

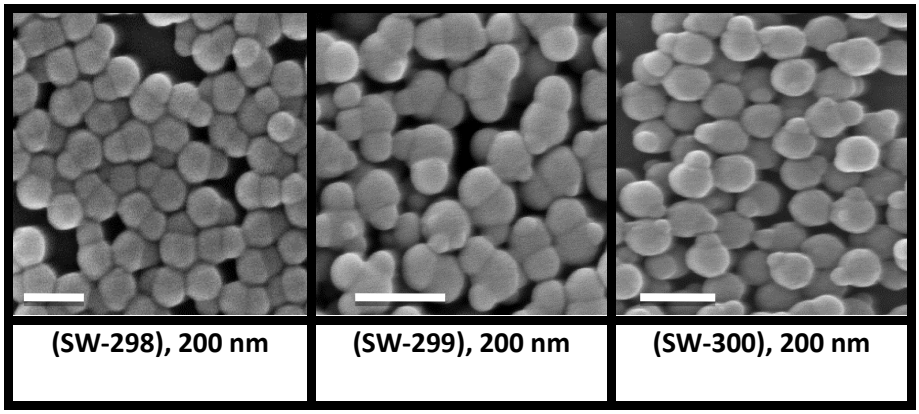

Fig.3. SEM images of PS-27 latex, after swelling and seeded emulsion polymerization. The scale bar in all images is 200 nm, with the exception of SW-221, SW-247 and SW-289 in which the scale bar is 500 nm.

One plausible reason for obtaining the ideal doublet shaped particles in SW-241 by applying these conditions is the low concentration of DVB used in the swelling step and the characteristics of PS-27.Such as the low cross-linked density inside the latex which enhances swelling by the monomer. This latex has a highly hydrophilic surface, as the use of the shot addition method makes the surface of the latex particles more incompatible with the expelled monomer, leading to reduced wetting of the original seed domain by the expelled monomer. All of these factors affect the formation of ideal doublet shaped Janus particles. To ensure that the synthesis was reproducible and to synthesize more doublet particles, various experiments with different swelling ratios and a constant DVB concentration of 0.5% were performed as listed in Table 5.

From the obtained results, shown in Table 5, when a constant concentration of DVB was used in the swelling step, the increase in the swelling ratio caused an increase in the hydrophobic domain, but a high swelling ratio led to the formation of more than one newly formed domain (defects), as occurred in SW-253, SW-260 and SW-275. When a small swelling ratio was used, the newly formed domains were smaller and

without defects, and the particles appeared to have snowman morphology as seen in SW-250, SW-261 and SW-300.

Table.5. Swelling ratios and the percentage ratios of the hydrophilic and hydrophobic domains of the obtained particles after swelling and phase separation from latex PS-27 with 0.5 % DVB in the second stage of polymerization.

Experiment	Swelling ratio	Average diameter (nm)	Hydrophilic domain %	Hydrophobic domain %
SW-261	2.82	250	60 %	40%
SW-300	2.88	223	69 %	31%
SW-250	2.90	248	63 %	37%
SW-299	2.92	246	54 %	46%
SW-247	2.95	264	58 %	42 %
SW-274	2.95	264	58 %	42 %
SW-253	3.48	276	52 %	48 %
SW-275	3.64	268	54 %	46 %
SW-260	5.70	274	57 %	43 %

A moderate swelling ratio of around 2.95 was used in SW-247 and SW-274, which led to moderately sized newly formed domains with dumbbell shaped particles possessing fewer defects. When the DVB concentration was increased to 0.90%, and with a moderate swelling ratio of 3.09 as used in SW-25, the obtained latex particles displayed a snowman morphology, whereby the newly formed hydrophobic domain had a percentage of 30%, while 70% of the original hydrophilic seed domain remained. Based on these results, a doubling of the DVB concentration affected the diffusion of the swelled monomer toward the newly formed domain which resulted in smaller newly formed domains.

With a high swelling ratio of 4.29 and 1.0% DVB as used in SW-258, the latex particles did not undergo phase separation. They merely swelled to an average size

of 190 nm with a size increase of 30 nm compared to the original seed particles. Therefore, the elastic force squeezing the particles could not overcome the high viscosity inside the latex particles. That was attributed to the high swelling ratio used, which means that there was more DVB inside the system. In contrast to SW-252 when a high DVB concentration of 2.93% was used, but a low swelling ratio of 2.77, the latex particles showed poor phase separation with a snowman morphology.

When the DVB concentration was decreased to 0.16% with a low swelling ratio of 2.79 as used in SW-298, the obtained latex particles had a doublet shape with no defects. The particles had an average size of 243 nm, and the hydrophobic domain had high percentage of 44.4%, and with 55.5% for the hydrophilic domain. Based on these results, a reduction in the DVB concentration led the monomer to flow toward the sparsely cross-linked region throughout the seeded polymerization, which made the hydrophobic domain bigger even though a low swelling ratio was used.

When the DVB concentration was slightly increased to 0.66% and with swelling ratio of 3.46, as seen in SW-259, the latex particles attained a dumbbell shape with additional small protrusions observed in some particles (defects). The percentage ratio of the newly formed hydrophobic domain was 47.7%, and the hydrophilic original domain was 52.3%. Based on these results, a slight increase in the DVB concentration at that particular swelling ratio did not have a major influence on particle morphology.

When the DVB concentration was changed to 0.16% and with very high swelling ratio of 4.16, as in SW-254, the obtained latex particles had a dumbbell shape with some defects. The percentage ratio of the newly formed hydrophobic domain is 44.8%, and the hydrophilic domain was 55.2%. This slight increase in the hydrophobic domain was attributed to the lower concentration of DVB which slowed

the diffusion of the swelled monomer from the highly cross-linked region to the sparsely cross-linked region. In general, a moderate swelling ratio between 2.5 to 3.0 and a low DVB concentration of typically less than or equal to 0.5 in the seeded emulsion polymerization results in dumbbell shaped PS-27 latex particles with a lower number of defects.

The obtained dumbbell shaped latex particles were used as the seed in surface-initiated polymerization SET-LRP to grow hydrophilic polymer brushes from the original seed domain as it contains tertiary bromine functional groups. Table 6 shows the recipe and ingredients used for the selective surface modification of the original seed domain by SET-LRP.

Before performing the SET-LRP reaction from the surface of the dumbbell shaped latex particles, FTIR was performed after dialysis of the dumbbell shaped latex particles in order to verify that the tertiary bromine group was immobilized on the original seed domain. The FTIR spectra of some dumbbell shaped particles are shown in Figure 4.

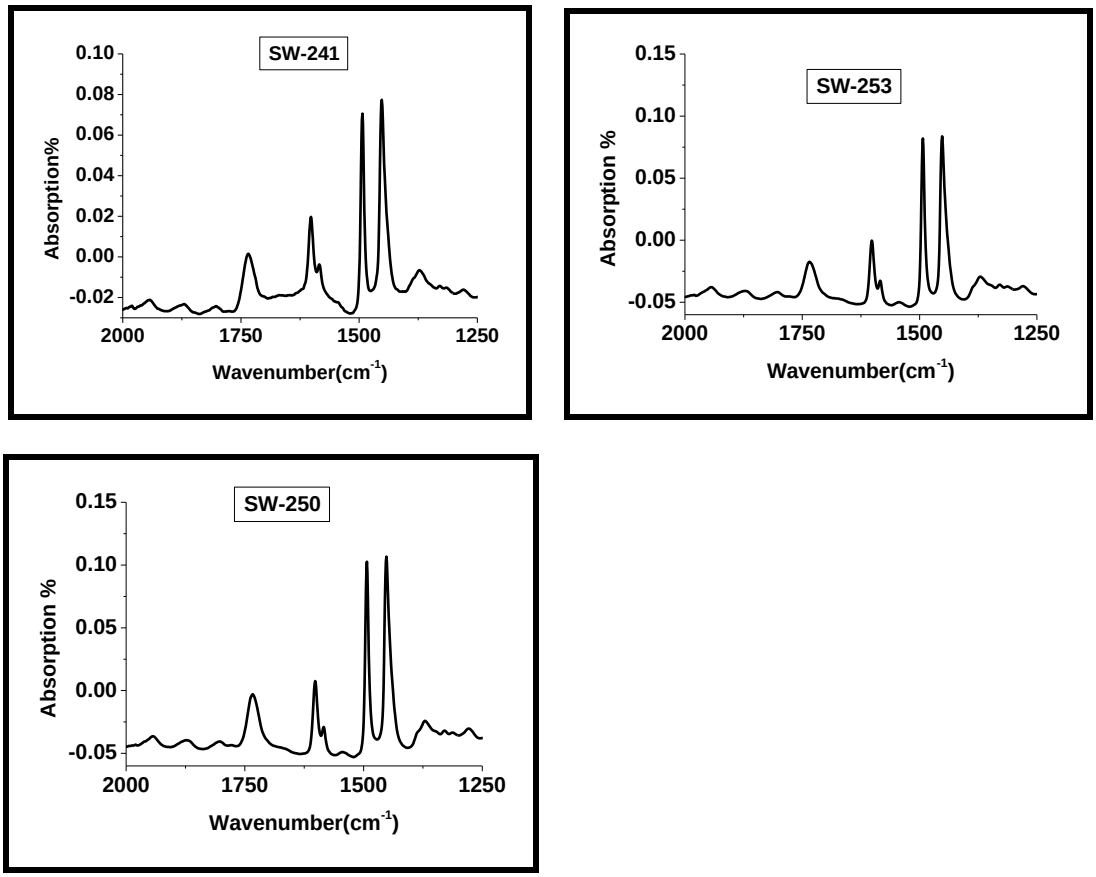

Fig.4. FTIR absorption spectra of the purified dry powder of dumbbell shaped latex particles made from PS-27 before surface-initiated polymerization (SET-LRP).

All the FTIR absorptions showed a specific absorption between 1727 and 1729 cm^{-1}, which is the fingerprint of FTIR absorption of the carbonyl group present in the inimer. This confirms the presence of the tertiary bromine group on the surface of the latex particles which has not been mobilized. In all cases, an external initiator was used to obtain short polymer brushes, because long brushes can "hide" the newly formed domain and made the anisotropic particles isotropic when dispersed in water. In the kinetic analysis, most of the polymerizations reached to full conversion after *ca.* 30 mins from the beginning of polymerization, and the rate of the polymerization was ultra-fast since an external ATRP initiator (**2**) was used. Very high conversion was achieved within 30 minutes of the beginning of polymerization, as shown in Table 7.

Table.6. Recipe and ingredients used in surface-initiated SET-LRP from dumbbell shaped latex seed particles made from latex PS-27 with different conditions and monomers. The ligand used was (Lig1).

Exp	[External initiator (2)] $mol.L^{-1}$	Latex	Latex (g)	[Monomer] $mol.L^{-1}$	Monomer type	[Ligand] $mol.L^{-1}$	Cu (0)	[Cu (0)] $mol.L^{-1}$	[$CuBr_2$] $mmol.L^{-1}$
SET-140	0.0049	SW-241	0.072	0.137	(NaSSA)	0.0131	Wire	0.033	1.0
SET-144	0.0039	SW-247	0.072	0.148	(NaSSA)	0.0125	Wire	0.032	0.90
SET-147	0.0037	SW-250	0.073	0.306	(DMA)	0.0096	Wire	0.024	0.80
SET-148	0.0034	SW-253	0.072	0.121	(NaSSA)	0.0105	Wire	0.026	0.80
SET-153	0.0032	SW-260	0.072	0.115	(PEGMEA)	0.0105	Wire	0.027	1.1
SET-151	0.0032	SW-261	0.072	0.239	(2-MAETAC)	0.0097	Wire	0.025	0.80
SET-156	0.0023	SW-274	0.072	0.174	(NaSSA)	0.0136	Wire	0.035	1.3
SET-157	0.0026	SW-275	0.074	0.182	(NaSSA)	0.0144	Wire	0.037	4.4
SET-163	0.0023	SW-259	0.072	0.134	(3-SPAM)	0.0144	Wire	0.037	1.5

There were three cases when the rate of the polymerization was moderate: SET-151, SET-157 and SET-163, as shown in Figure 5. In the case of SET-151, the moderate rate of the polymerization could be attributed to the type of the monomer used, which was the cationic monomer (2-MAETAC), which also shows a moderate rate of polymerization in normal surface-initiated polymerization from the surface of spherical particles. In the case of SET-157, the high concentration of the deactivator ($CuBr_2$), which was three orders of magnitude greater than the concentration in the other polymerizations with sodium styrene sulfonate, led to a lower the rate of polymerization.

Table.7. High monomer conversion gained after a very short time from the beginning of SET-LRP polymerization from dumbbell shaped particles prepared from latex PS-27.

Experiment	Monomer Conversion %	Time required to reach to that conversion (mins)
SET-140	93	25
SET-144	70	30
SET-147	82	35
SET-148	78	10
SET-153	73	15
SET-156	84	15

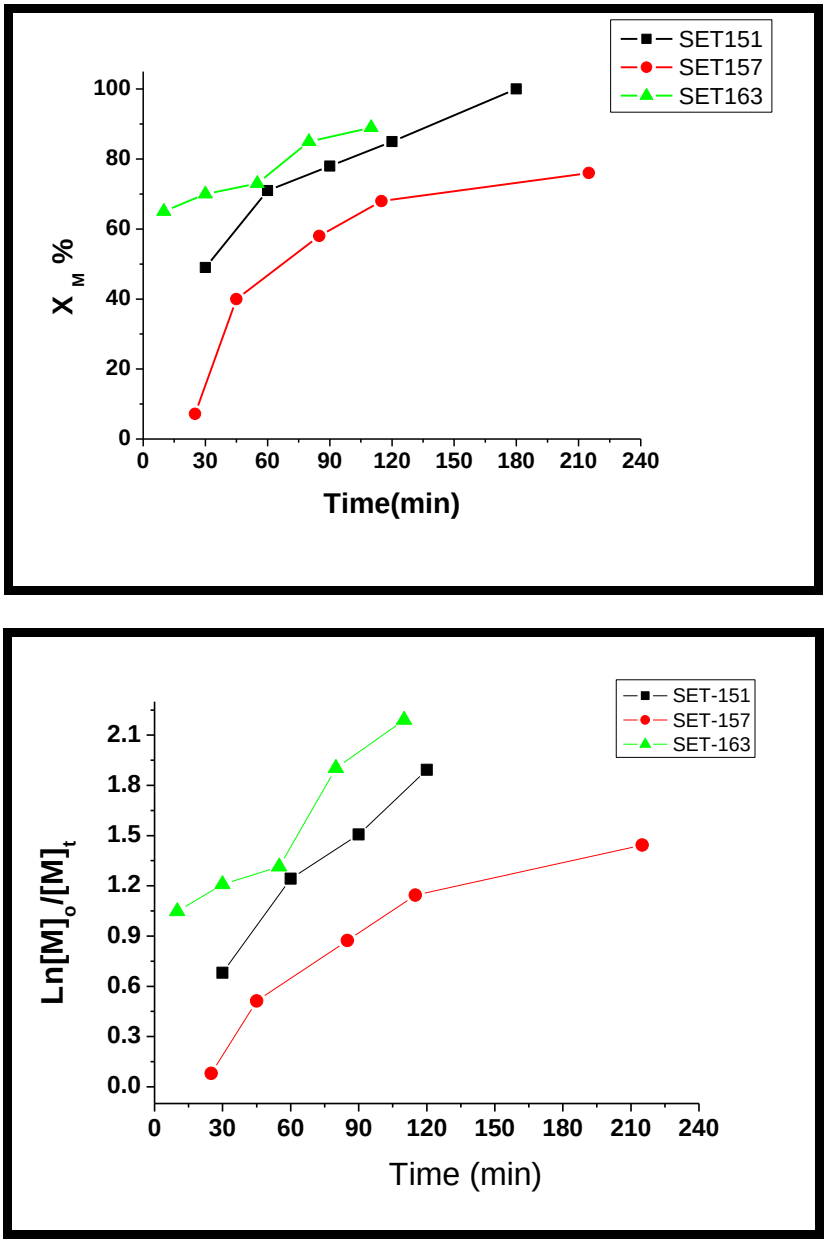

Fig.5. Monomer conversion versus time of the surface-initiated polymerization of SET-151, SET-157 and SET-163.

In SET-163, the relatively low rate of polymerization was the result of the (3-SPAM) monomer, which polymerizes differently than sodium styrene sulfonate with low monomer conversion. In order to verify the formation of hydrophilic polymer brushes from the original seed domain of the dumbbell shaped particles after SET-LRP, Cryo-TEM was used to visualize the extended and hydrated polymer brushes in their native environment (the aqueous phase). The brushes were expected to cover only the original seed domain, and the newly formed domain should be bald

(absence of polymer brushes). Figure 6 shows the cryo-TEM image of the Janus particles obtained after SET-LRP with sodium styrene sulfonate. The cryo-TEM image of SET-140 shows two distinctive domains, a gray domain which is the newly formed domain, and a black domain which is the original seed domain which contains short poly(sodium styrene sulfonate) brushes approximately 10 nm in length covering that domain and extending toward the water phase. This can be also seen in SET-144, which proves the formation of two different domains; one domain is bald, and the other domain is hairy.

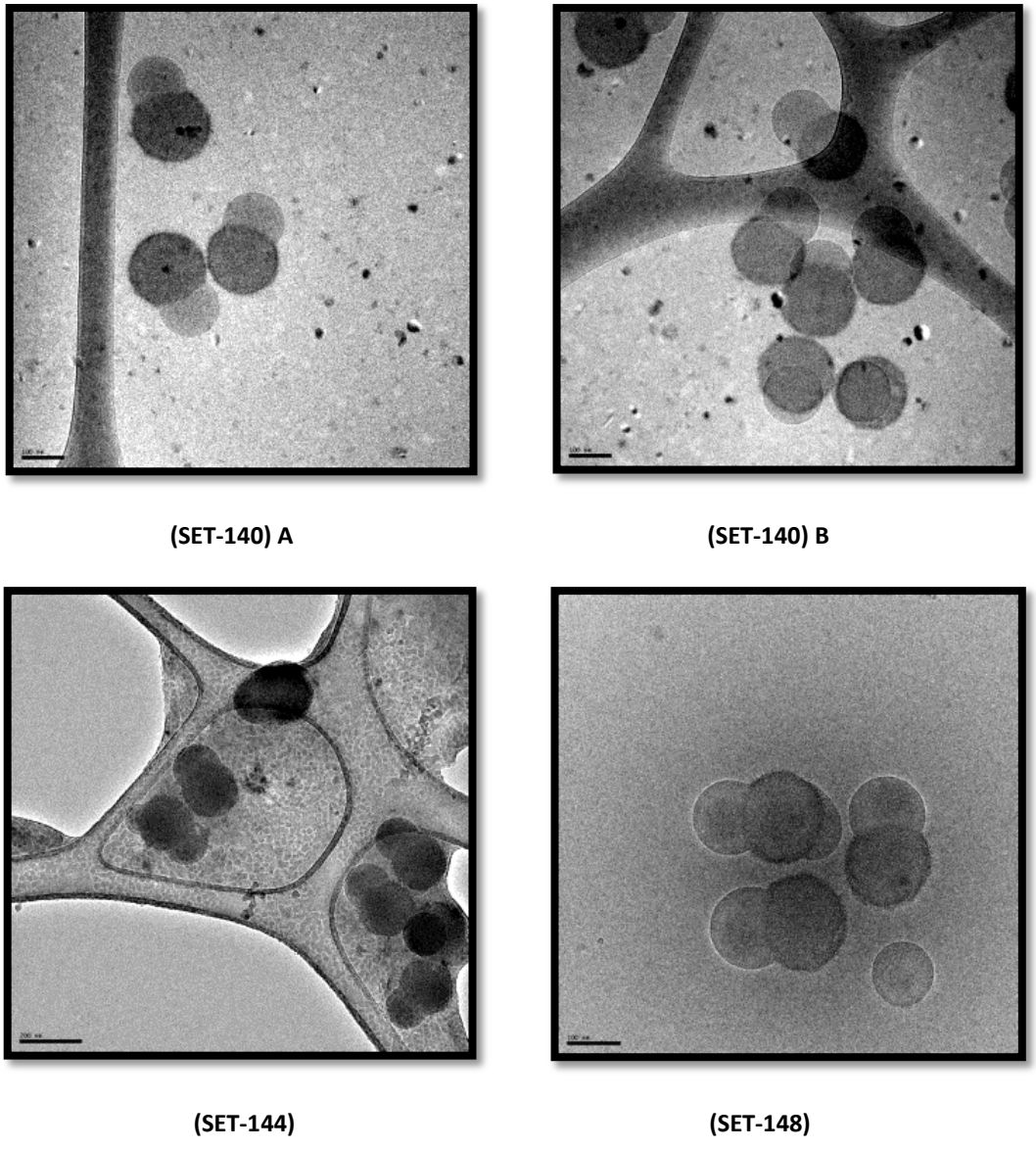

(SET-140) A **(SET-140) B**

(SET-144) **(SET-148)**

Fig.6. Cryo-TEM images of Janus particles (SET-140 A and B, SET-144 and SET-148). The scale bar in all images is 100 nm, with the exception of SET-144 where the scale bar is 200 nm.

The length of the polymer brushes is a little longer with an approximate length of 25 nm, which is 15 nm longer than that in SET-140. One reason behind the longer brushes in SET-144 is the lower concentration of the external initiator used, which resulted in higher molecular weight polymers; a second reason is the relatively higher monomer concentration used.

In the cryo-TEM image of SET-148, the particles show two different domains, the bald newly formed hydrophobic domain, and the hairy hydrophilic domain, ultimately resulting in octopus shaped Janus particles.

The length of the poly(styrene sulfonate) brushes is approximately 17 nm. It is worth mentioning that in the case of SET-148, there were some defects in the shape of the doublet Janus particles as a result of the presence of another hydrophobic domain which formed during swelling and seeded emulsion polymerization, and also some spherical particles as a result of the secondary nucleation. Noteworthy is that this new crop of particles are smooth.

A tapping mode AFM image of SET-140 is shown in Figure 7. The phase contrast AFM image shows that the dumbbell shaped latex particles are divided into two distinctive parts, the coarse domain which is the newly formed domain, and the smooth domain which is the hairy domain. This can also be distinguished in the 3D-contrast tapping mode AFM image.

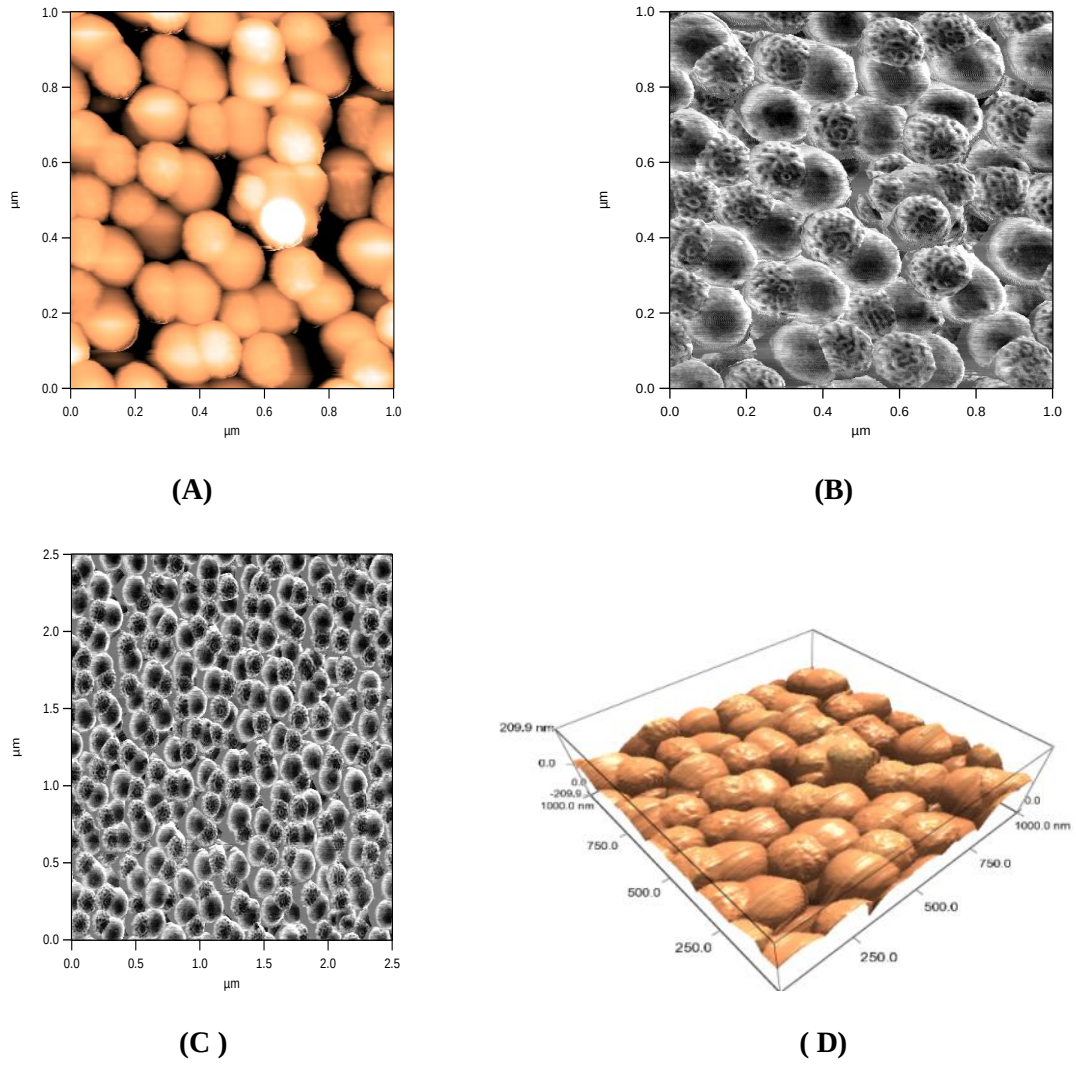

Fig.7. Tapping mode AFM images of SET-140, A (tapping mode image), B and C (phase contrast tapping mode images), D (3-D image of the phase contrast tapping mode).

The cryo-TEM images of other dumbbell shaped particles after SET-LRP to form another type of polymer brush instead of poly(sodium styrene sulfonate) are shown in Figure 8. In the cryo-TEM image of SET-147, the original domain of the seed particles was grafted with poly(*N*, *N*-dimethyl acryl amide) (DMA). The dumbbell latex particles show two distinctive domains, although the poly(DMA) brushes are not visible.

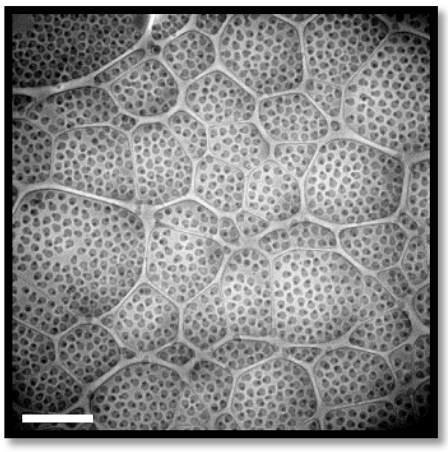

(SET-147) A

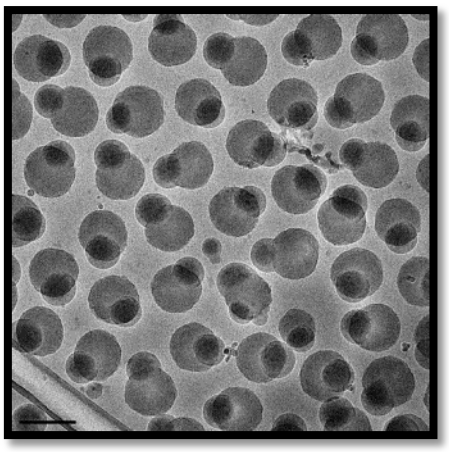

(SET-147) B

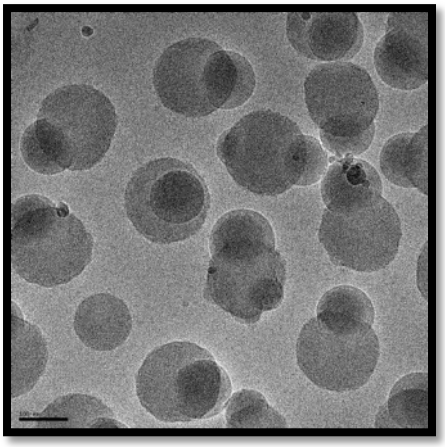

(SET-147) C

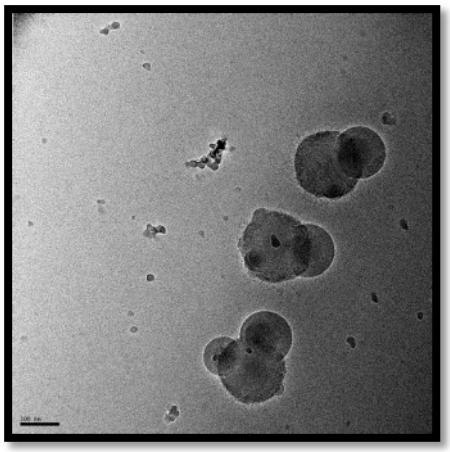

(SET-153) A

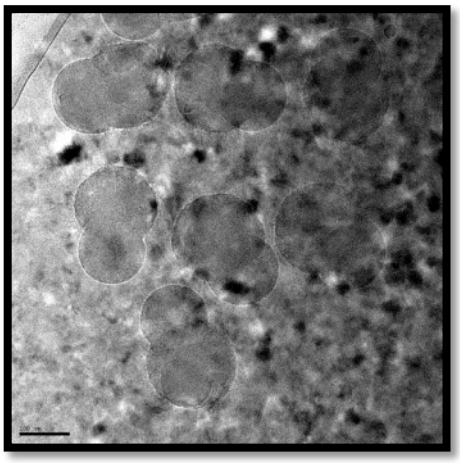

(SET-153) B

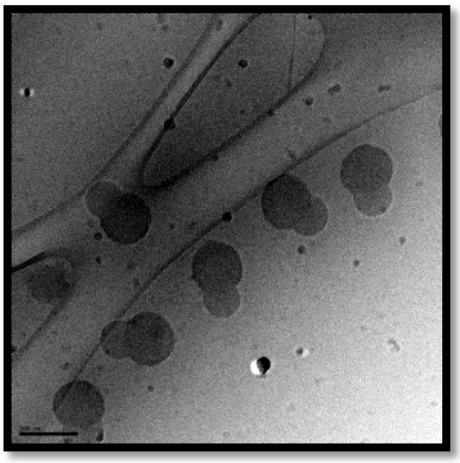

(SET-151)

Fig.8. Cryo-TEM image of SET-147 A, B and C, SET-153 A and B, and SET-151. The scale bar is 1.0 µm in SET-147A, 200 nm in SET-147B, 100 nm in SET-147C, 100 nm in SET153 A and B and 200 nm in SET-151.

The newly formed domain is darker than the original seed domain, which is due to the fact that the original seed domain was covered with less electron dense polymer brushes poly(DMA) layer which makes that domain gray, whereas the newly formed bald domain is darker. An interesting aspect of the latex particles formed in SET-147 was that the hydrophilic domains were not touching each other, due to steric repulsion between the polymer brushes on the surface of the hydrophilic domain, This is in contrast to hydrophobic domains which tend to face each other in many cases, as seen in images (SET-147B) and (SET-147C), to minimize their contact with water. However, the steric repulsion between the hydrophilic domains prevented the formation of clusters. These Janus particles were packed in hexagonal manner, which supports the existence of attractive and repulsive forces on these particles as seen in image (SET-147A), but inn the case of the original seed domain grafted with poly(styrene sulfonate), the hydrophilic domains tended to stick to each other which might be the result of covalent bonds between the brushes in each particles, leading to the formation of a network of particles similar to that also observed with spherical particles grafted with poly(styrene sulfonate).

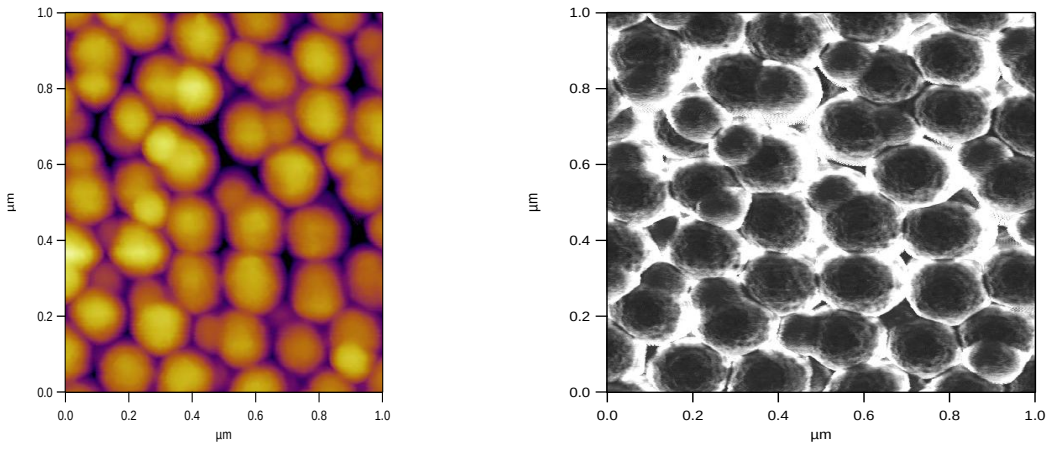

Fig.9. Tapping mode AFM image of SET-147 (A), and (B) phase contrast image.

In addition, the presence of $CuBr_2$ decreased the colloidal stability of the negatively charged particles which made the hairy domains stick to each other. The tapping mode AFM image of SET-147 is shown in Figure 9. The image does not show a significant difference between the two domains, which agrees with the image obtained by cryo-TEM. However, the newly formed domain in this case is less coarse than the original seed, which indicates that there are different types of forces between the tip of the AFM and the surface of the latex particles. The cryo-TEM images of SET-153 A and B are shown in Figure 8. The original seed domain in this case was grafted with poly(ethylene glycol methyl ether acrylate) (PEGMEA). The dumbbell shaped latex particles showed a clear difference in the surface morphology between the two domains, whereby the newly formed hydrophobic domain was perfectly spherical with a smooth surface, in contrast to the hydrophilic domain which had barely visible PEGMEA brushes which gave that domain a coarse appearance. In the SET-153 B image, the image was taken from another area of the cryo-TEM grid. In that area, the ice was more crystalline, this enhanced visualization of the PEGMEA brushes. The cryo-TEM image of SET-151 is shown in Figure 8. The original seed domain was grafted with a cationic monomer to form cationic poly[(2-methacrylloyloxy) ethyl]-trimethyl ammonium chloride) brushes. The image shows dumbbell shaped latex particles with two different domain surface morphologies. The newly formed hydrophobic domain is bright whereas the original cationic seed domain is dark, which is an indication that poly(electrolyte) brushes were grafted, as seen in SET-140. The next polymer latex we investigated was PS-29, which differs from the other latexes in two key aspects: the concentration of hydrophilic inimer is increased from 5 wt% to 9.74 wt%, whereas the DVB concentration is increased from ca 1.95% to 2.55%. This latex has an average

particle diameter of 187 nm, and shows excellent monodispersity. These particles have very good colloidal stability with a zeta potential of -45.5 mV. Table 8 shows the recipe and conditions used for swelling and phase separation of latex PS-29, followed by Figure 10 which shows the SEM images of the obtained latex particles after swelling and seeded emulsion polymerization.

Table.8. Ingredients used to swell latex PS-29, and the obtained morphologies after polymerization at 70°C with a mixing speed of 30 rpm, R (M/P) = ratio of Monomer to polymer, S = styrene, D = divinyl benzene (DVB), A = azobisisobutyronitrile (AIBN), SM = swelling monomer mixture and AIBN.

Exp	R (M/P)	Latex (t.s %)	Latex weight (g)
SW-255	3.65/1.0	5.65	1.00
SW-262	4.25/1.0	5.65	1.05
SW-265	7.1/1.0	5.65	1.02
SW-276	4.40/1.0	5.65	1.03
SW-277	6.50/1.0	5.65	1.09
SW-281	4.43/1.0	5.65	1.00
SW-290	4.23/1.0	5.65	1.15
SW-295	4.70/1.0	5.65	1.00
SW-296	5.09/1.0	5.65	1.00
SW-297	4.53/1.0	5.65	1.00

Exp	S+D+A=SM(g)	DVB %	H_20 (mL)	Latex morphology	Colloidal stability
SW-255	(6.0+0.010+0.060) **= 0.207**	0.16	3.0	**Dumbbell**	Stable
SW-262	(6.0+0.03+0.060) **= 0.250**	0.50	3.0	**Dumbbell**	Stable
SW-265	(6.0+0.03+0.06) **= 0.410**	0.50	3.0	**Dumbbell +Seconday nucleation**	Stable
SW-276	(6.0+0.030+0.06) **= 0.254**	0.5	3.0	**Dumbbell**	Stable
SW-277	(6.0+0.070+0.06) **= 0.40**	1.16	3.0	**Snowman**	Stable
SW-281	(6.0+0.03+0.06) **= 0.250**	0.5	3.0	**Snowman**	Stable
SW-290	(6.0+0.03+0.060) **= 0.275**	0.5	3.0	**Dumbbell**	Stable
SW-295	(6.0+0.03+0.060) **= 0.266**	0.5	3.0	**Dumbbell**	Stable
SW-296	(6.0+0.03+0.06) **= 0.302**	0.5	3.0	**Dumbbell**	Stable
SW-297	(6.1+0.0119+0.061) = **0.256**	0.195	3.0	**Dumbbell**	Stable

At first, a high swelling ratio was used, as in SW-265 and SW-277, with different concentrations of DVB in the monomer feed. In SW-265, the swelling ratio was 7.1, with 0.5% DVB. The obtained latex formed dumbbell shaped particles, with 41% composed of the newly formed hydrophobic domain and 59% of the original hydrophilic seed domain.

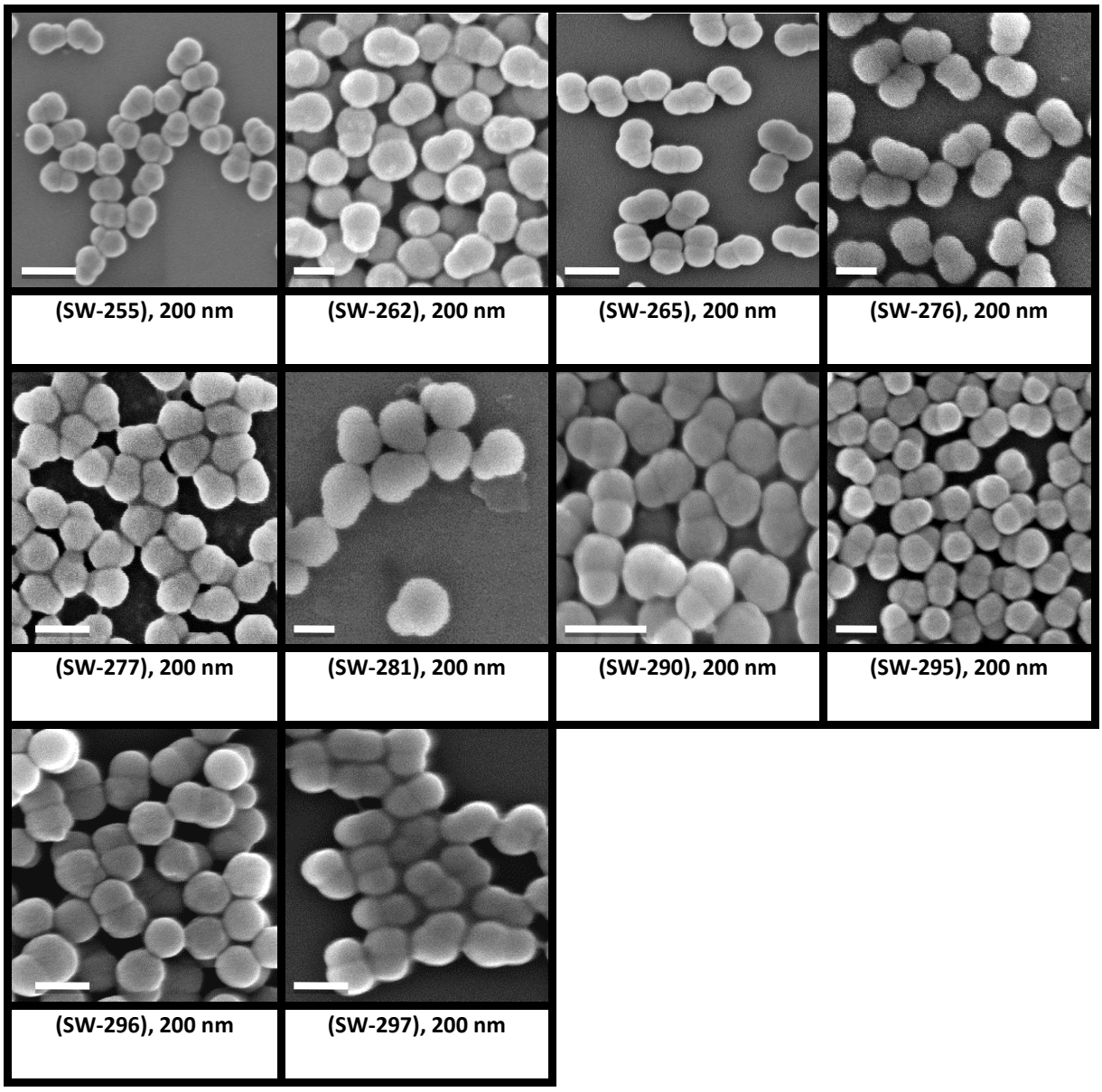

Fig.10. SEM images of PS-29 latex after swelling and seeded emulsion polymerization. The scale bar in all images is 200 nm.

Very few defects were observed in the obtained particle which is against expectations, since high swelling ratios usually lead to many defects. Rather, the formation of a small population of smaller particles (secondary nucleation) with an average size of 128 nm was observed. This indicates that the high concentration of inimer used and a DVB concentration of 2.55% in PS-29 caused the phase separation to grow toward one direction. Although a high swelling ratio was used, the latex was able to take up most of the monomer and grow to average size of 217 nm with a 20 nm increase from the original seed. Due to the excess concentration of the monomer and a slightly higher cross-linked density compared to PS-27, secondary nucleation took place to form small particles rather than defects in the dumbbell particles.

When the DVB concentration was increased to 1.16%, and with swelling ratio of 6.5 as in SW-277, the latex particles had snowman morphology. The ratio of the newly formed hydrophilic domain was 29% with a reduction of around 10% in comparison to SW-265. This was due to the increase in the DVB concentration used in the second stage polymerization which restricted the diffusion of the monomer toward the newly formed domain throughout the polymerization process; this was due to the high viscosity inside the latex particles as a high concentration of DVB was used.

When both the swelling ratio and the DVB concentration decreased to 3.65 and 0.16%, respectively, as in SW-255, the acquired latex particles had a dumbbell shape. The ratio of the newly formed hydrophobic domain was 43%, which was bigger than that observed in the case of SW-265. The combination of a lower swelling ratio (hereby eliminating the possibility of secondary nucleation) with a lower concentration in DVB in the monomer feed led to a dumbbell rather than snowman morphology as the latter promoted monomer transport throughout the polymerization process hereby enhancing the phase separation.

Several experiments were performed at a constant DVB concentration of 0.5%, at various swelling ratios, in order to produce more dumbbell particles from latex PS-29. The ratios of the hydrophobic and hydrophilic domains of the produced dumbbell particles are listed in Table 9. It can be summarized that all spherical PS-29 latex particles transform into doublet morphologies after swelling and phase separation. No secondary nucleation was observed, nor were small protrusions on the surface of the hydrophilic domain (defects). The ratio of the hydrophobic domain increases by increasing the swelling ratio and decreasing the DVB concentration.

Table.9. Swelling ratio and the percentage of the obtained morphology after swelling and phase separation from latex PS-29 with a DVB concentration of 0.5% in the second stage polymerization.

Experiments	Swelling ratio	Average size (nm)	Hydrophilic domain %	Hydrophobic domain %
SW-296	5.09	352	54 % (191 nm)	46 % (161 nm)
SW-295	4.70	335	52 % (173 nm)	48 % (162 nm)
SW-281	4.43	312	62.5 % (195 nm)	37.5 % (117 nm)
SW-276	4.40	355	56 % (199 nm)	44 % (156 nm)
SW-262	4.25	322	57 % (184 nm)	43 % (138 nm)
SW-290	4.23	308	57 % (177 nm)	43 % (131 nm)

Some of the dumbbell shaped particles were used as seeds in surface-initiated polymerization (SET-LRP) to grow different types of hydrophilic polymer brushes from the original seed domain. Table 10 shows the recipe and the conditions used for grafting polymer brushes on the original seed hemisphere.

Before performing the SET-LEP reaction, the FTIR spectrum was taken for the dumbbell shaped particles (SW-255) to ensure that the tertiary bromine functional group was immobilized on the surface of the original seed hemisphere, as shown in Figure 11.

Table.10. Ingredients and conditions used to grow different types of hydrophilic polymer brushes from the original seed hemisphere of dumbbell shaped PS-29 particles by SET-LRP. The ligand used is (Lig1).

Exp	[External initiator (2)] mol.L^{-1}	Latex	Latex (g)	[Monomer] mol.L^{-1}	Monomer type	[Ligand] mol.L^{-1}	Cu (0)	[Cu (0)] mol.L^{-1}	[$CuBr_2$] mmol.L^{-1}
SET-149	0.0032	SW-255	0.056	0.116	(PNaSS)	0.0105	Wire	0.027	1.1
SET-152	0.0031	SW-262	0.059	0.176	(PNIPAM)	0.0101	Wire	0.026	0.8
SET-158	0.0025	SW-276	0.058	0.331	(P2-HEA)	0.0130	Wire	0.033	1.6
SET-162	0.0025	SW-265	0.057	0.184	(PPEGMEA)	0.0127	Wire	0.032	1.3

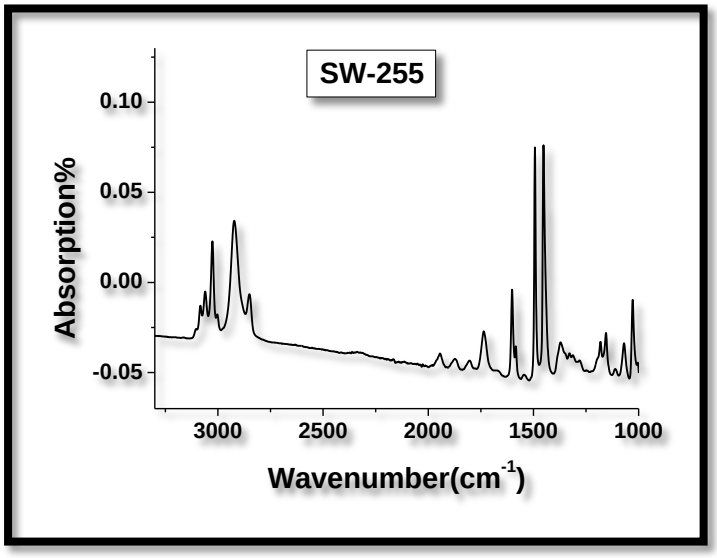

Fig.11. FTIR absorption spectrum of a purified dry powder of SW-255.

The graph shows a specific absorption at 1729 cm^{-1}, which indicates the presence of the carbonyl group and the existence of the inimer on the surface of one hemisphere of the dumbbell shaped particles. All four polymerizations were performed in the presence of an external initiator in order to obtain shorter polymer brushes. All polymerizations reached full conversion and arrived at a high conversion in a short period of time, as listed in Table 11. This high conversion concurs with the high conversion that was also obtained with dumbbell shaped particles that were produced from PS-27; this indicates that the overall rate of polymerization was very high.

Table.11. Time required reaching high conversion for surface-initiated polymerization (SET-LRP) from dumbbell shaped particles made from latex PS-29.

Experiment	Conversion %	Time required to reach to that conversion (min)
SET-149	72	10
SET-152	90	30
SET-158	79	15
SET-162	75	15

In order to visualize the polymer brushes created from the original seed hemisphere, cryo-TEM was performed for SET-149 and SET-152, as shown in Figure 12.

The cryo-TEM image of SW-255 after SET-149 shows that the original seed hemisphere is covered with poly(sodium styrene sulfonate) brushes, seen as short black strips, and the newly formed hydrophobic domain is bald, as seen in the images SET-149 A and B. The length of the formed poly(sodium styrene sulfonate) brushes is approximately 15 nm. This obtained morphology is similar to those made from dumbbell shaped PS-27 latex, which indicates that the black strips are indeed poly(styrene sulfonate) brushes. This also reveals that the process used to make this type of Janus particle is reproducible.

As the type of grafted brushes was replaced by poly(NIPAM), as in the case of SET-152, the original seed hemisphere (SW-262) was grafted with poly(NIPAM). It is known from this research that poly(NIPMA) brushes are barely visible by cryo-TEM unless the image is taken in an icy crystalline area of the cryo-TEM grid (as observed in chapter 4). This was the case where SET-152 was imaged in amorphous ice; the poly(NIPAM) brushes were not visible, the original seed hemisphere merely appeared coarse and the newly formed domain had a smooth surface.

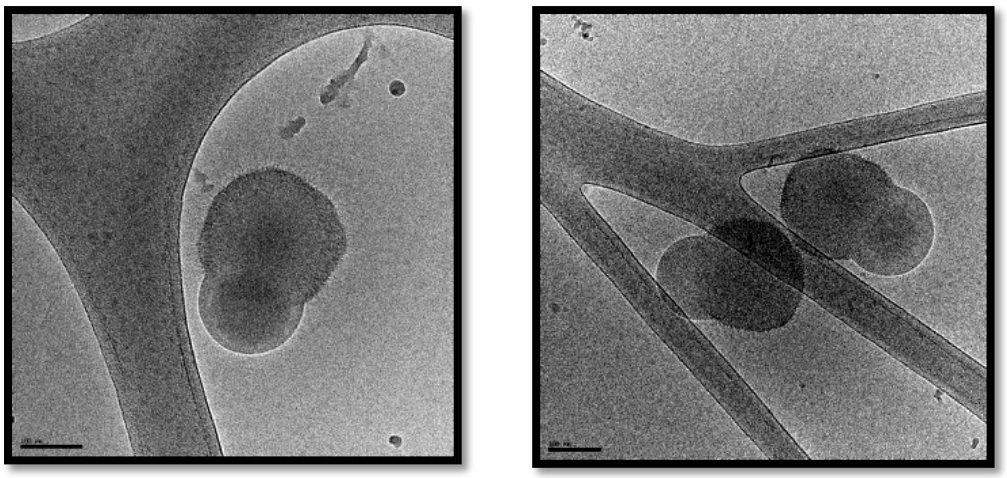

(SET-149) A **(SET-149) B**

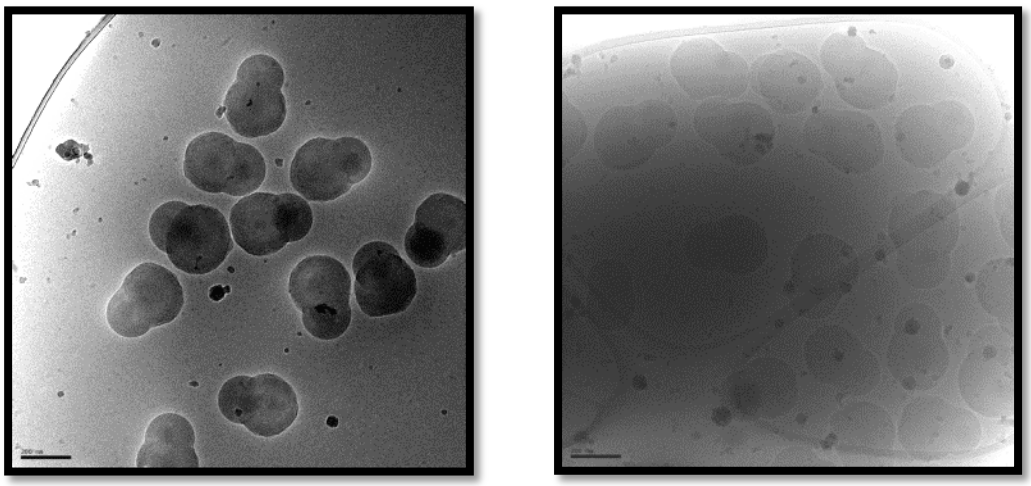

(SET-152) A **(SET-152) B**

Fig.12. Cryo-TEM images of Janus particles made from latex PS-29. The scale bar in SET-149 is 100 nm and 200 nm in SET-152.

It is interesting that SET-152 Janus particles behave like SET-147 Janus particles, as they self-assemble to form hexagonal packing as seen in the image of SET-152 B. This indicates that acryl amide brushes induce the formation of hexagonal packing as a result of the competitive forces between the attraction forces of the hydrophobic domains and the repulsive forces of the hydrophilic domains of the acryl amide brushes.

Phase separation from latexes PS-30 and PS-31, PS-30 has a high cross-linked density with a DVB concentration of 5.25%, but also has a high inimer concentration

of 10%. This latex has an average particle diameter of 240 nm with very good colloidal stability, and with a zeta potential of - 39.55 mV. Conversely, latex PS-31 contains 17.8% inimer. PS-31 was synthesized via seeded emulsion polymerization by using dialyzed latex PS-23 as the seed; the inimer copolymerized with styrene and DVB on the surface of PS-23 as described in chapter 2. This latex has a moderate cross-linked density with a DVB concentration of 2.87%. Latex PS-31 has an average particle size of 250, and small particles are generated via secondary nucleation with an average size of 125 nm. The population of secondary nucleation particles is almost equal to the number of original seed particles. Table 12 shows the recipe and conditions used to swell latexes PS-30 and PS-31, followed by Figure 13 which shows the SEM images of the obtained particle morphologies.

The highly cross-linked density latex PS-30 was treated under identical conditions as those used with PS-27 and PS-29. The swelling ratio used was 2.60 with low DVB concentration of 0.16% (SW-256). The obtained particles were of two types; the first type was dumbbell shaped particles with a separation region of around 50 nm between the two domains as typically observed during swelling of high cross-linked density latex as in the case of PS-20. The second type had a snowman morphology with 37% comprised of the newly formed hydrophobic domain. This mixture of two particles indicates that highly cross-linked density latex tends to generate particles with no uniform shape.

Based on these results, the investigation into swelling and phase separation of these latex particles ceased, and more focus given to the low cross-linked density latex PS-31. When latex PS-31 was swollen and polymerized under similar conditions as described for PS-30 (SW-264), the latex transformed into dumbbell shaped particle

without a separation region between the two domains, similar to those obtained from PS-27 and PS-29.

Table.12. Ingredients used to swell latex PS-30 as in the case of SW-256, and PS-31. The obtained morphology is shown after polymerization at 70°C with a mixing speed of 30 rpm. R (M/P) = ratio of Monomer to Polymer, S = styrene, D = divinyl benzene (DVB), A = azobisisobutyronitrile (AIBN), SM = swelling monomer mixture and AIBN.

Exp	R (M/P)	Latex (t.s %)	Latex weight (g)
SW-256	2.60/1.0	8.0	1.0
SW-257	2.57/1.0	7.8	1.0
SW-263	2.0/1.0	7.8	1.38
SW-264	2.62/1.0	7.8	1.37
SW-278	3.15/1.0	7.8	1.23
SW-279	2.83/1.0	7.8	1.20
SW-280	2.14/1.0	7.8	1.50
SW-291	2.89/1.0	7.8	1.25
SW-293	3.02/1.0	7.8	1.28

Exp	S+D+A=SM(g)	DVB %	H_20 (mL)	Latex morphology	Colloidal stability
SW-256	(6.0+0.010+0.060) = **0.206**	0.16	3.0	**Dumbbell**	Stable
SW-257	(6.0+0.010+0.06) = **0.20**	0.16	3.0	**Dumbbell**	Stable
SW-263	(6.0+0.030+0.06) = **0.2153**	0.50	3.24	**Dumbbell**	Stable
SW-264	(6.0+0.06+0.06) = **0.280**	0.50	3.05	**Dumbbell**	Stable
SW-278	(6.0+0.07+0.06) = **0.30**	1.16	3.0	**Snowman**	Stable
SW-279	(6.0+0.03+0.06) = **0.265**	0.50	3.0	**Dumbbell**	Stable
SW-280	(6.0+0.03+0.06) = **0.250**	0.50	3.0	**Snowman**	Stable
SW-291	(6.0+0.03+0.06) = **0.282**	0.50	3.0	**Dumbbell**	Stable
SW-293	(6.0+0.03+0.06) = **0.3011**	0.50	3.0	**Dumbbell**	Stable

In addition, no small protrusions (defects) were observed on the surface of the hydrophilic domain. The low cross-linked density and more hydrophilic surface of

PS-31 in contrast to PS-30 was the main reason for obtaining doublet particles without defects.

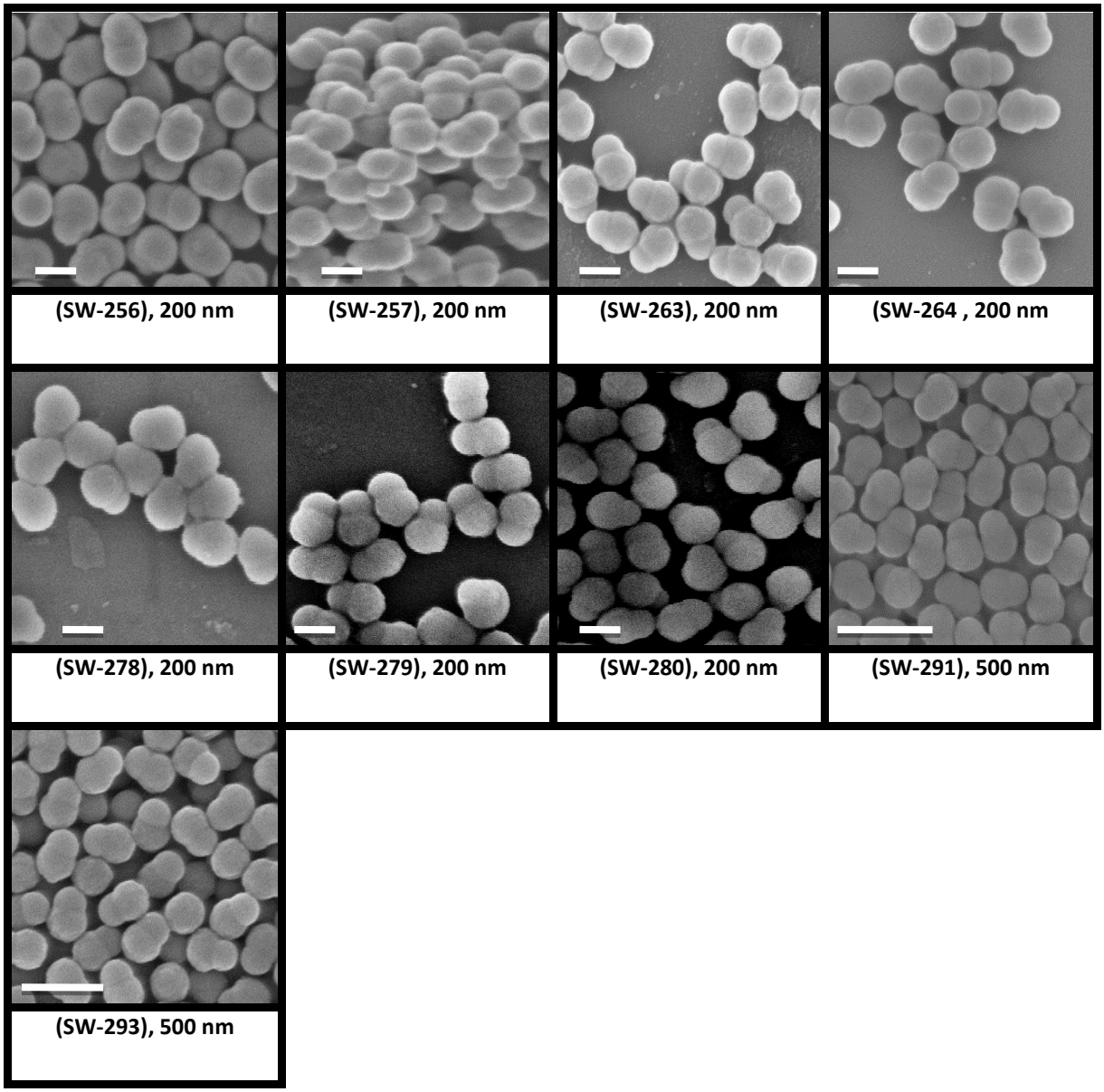

Fig.13. SEM images of PS-30 as seen in SW-256, and PS-31 in the rest of the images after swelling and seeded emulsion polymerization. The scale bar in all images is 200 nm with exception of SW-291 and SW-293, where the scale bar is 500 nm.

Based on these results, a series of polymerizations with a constant DVB concentration of 0.5% were performed to obtain more dumbbell shaped latex particles to be modified in the next step via surface initiated polymerization. The percentage of the obtained domains is listed in Table 13; it was observed that when the swelling ratio increased the hydrophobic domain ratio slightly increased.

Table.13. Swelling and the percentage ratio of the obtained morphology after swelling and phase separation from latex PS-31 with a DVB concentration of 0.5 % in the second stage polymerization.

Experiment	Swelling ratio	Average size (nm)	Hydrophilic domain%	Hydrophobic domain%
SW-293	3.02	397	56 % (222 nm)	44 % (175 nm)
SW-291	2.89	383	57.5 % (220 nm)	42.5% (163 nm)
SW-279	2.83	435	61 % (265 nm)	39 % (170 nm)
SW-264	2.62	440	65 % (285 nm)	35 % (155 nm)
SW-280	2.14	383	62 % (237 nm)	38 % (146 nm)
SW-263	2.0	410	62 % (255 nm)	38 % (155 nm)

Table 14 shows the ingredients and conditions used for the SET-LRP polymerizations using some of the obtained dumbbell particles.

Table.14. Ingredients and protocol used for surface-initiated polymerization (SET-LRP) from dumbbell shaped latex particles made from PS-31. The ligand used was (Lig1) with Cu(0) wire as catalyst.

Exp	[External initiator (2)] ($mol.L^{-1}$)	Latex	Latex solid weight (g)	[Monomer] $mol.L^{-1}$ and type	[Ligand] $mol.L^{-1}$	[Cu(0)] $mol.L^{-1}$	[$CuBr_2$] $mmol.L^{-1}$
SET-150	0.0034	SW-257	0.078	0.240 (2-HEA)	0.0105	0.027	0.7
SET-154	0.0043	SW-263	0.107	0.109 (3-SPAM)	0.013	0.034	1.1
SET-155	0.0	SW-264	0.106	0.099 (NaSSA)	0.0092	0.023	0.9
SET-160	0.0024	SW-279	0.093	0.385 (DMA)	0.012	0.032	1.5
SET-161	0.0024	SW-280	0.117	0.350 (DMA)	0.012	0.032	0.0

The FTIR absorption spectrum of SW-257 shows the fingerprint absorption of a carbonyl functional group at 1734 cm^{-1} which indicates the presence of the tertiary bromine on the surface of the original seed domain of the dumbbell shaped latex that made from PS-31 latex.

This also indicates the surface modification of PS-23 by seeded polymerization to form an outer layer of a copolymer of (styrene-DVB-inimer) was successfully accomplished as shown in Figure 14.

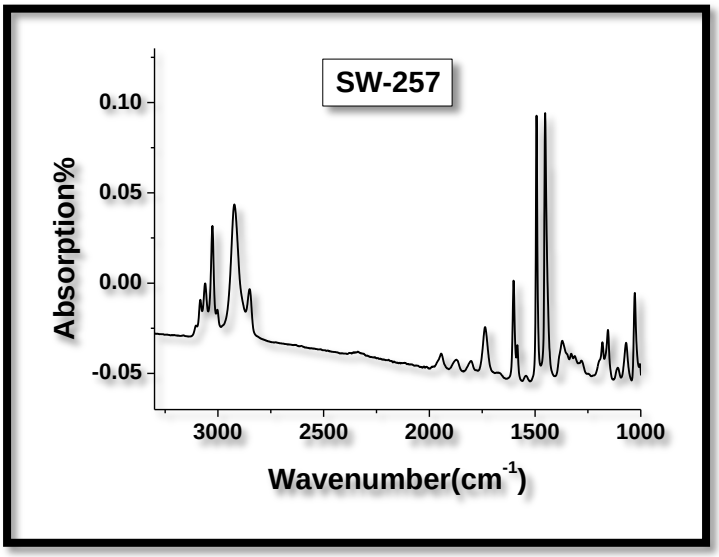

Fig.14.FTIR absorption spectrum of a purified dry powder of SW-257.

The rate of polymerizations was high for all the polymerizations performed in the presence of an external initiator, and reached high conversion above 70%.

However, in the absence of an external initiator, the rate of the polymerization was very fast but after 10 mins no increase in monomer conversion could be detected as in experiment SET-155 as shown in Figure 15.

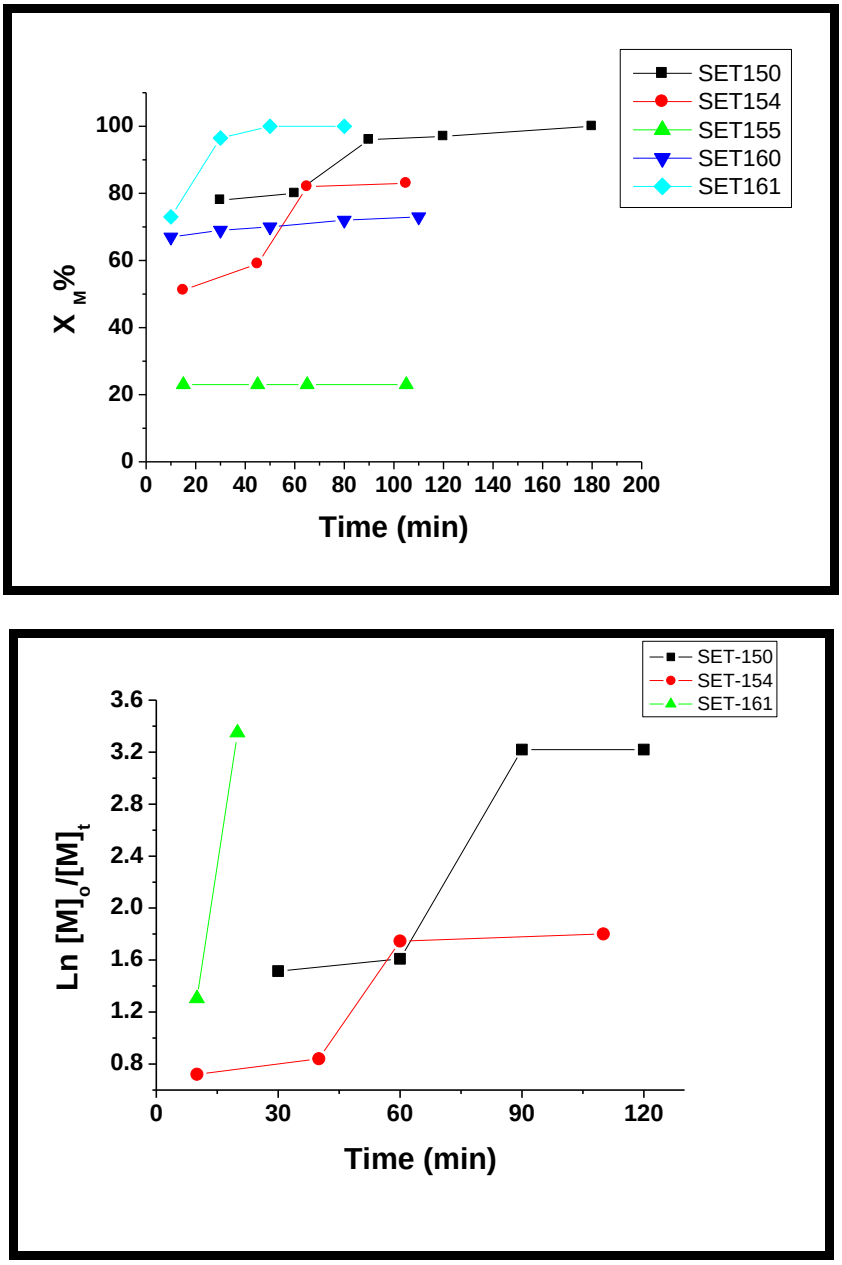

Fig.15. Monomer conversion versus time for surface-initiated polymerization from dumbbell shaped particles made from PS-31 latex particles.

The cryo-TEM images of some of the obtained latexes after SET-LRP are shown in Figure 16. As expected, the polymer brushes were barely visualized, unless the type of polymer brushes was poly(sodium styrene sulfonate), as in the case of SET-155 which shows very long polymer brushes formed due to the absence of an external water soluble ATRP initiator, despite the low monomer conversion.

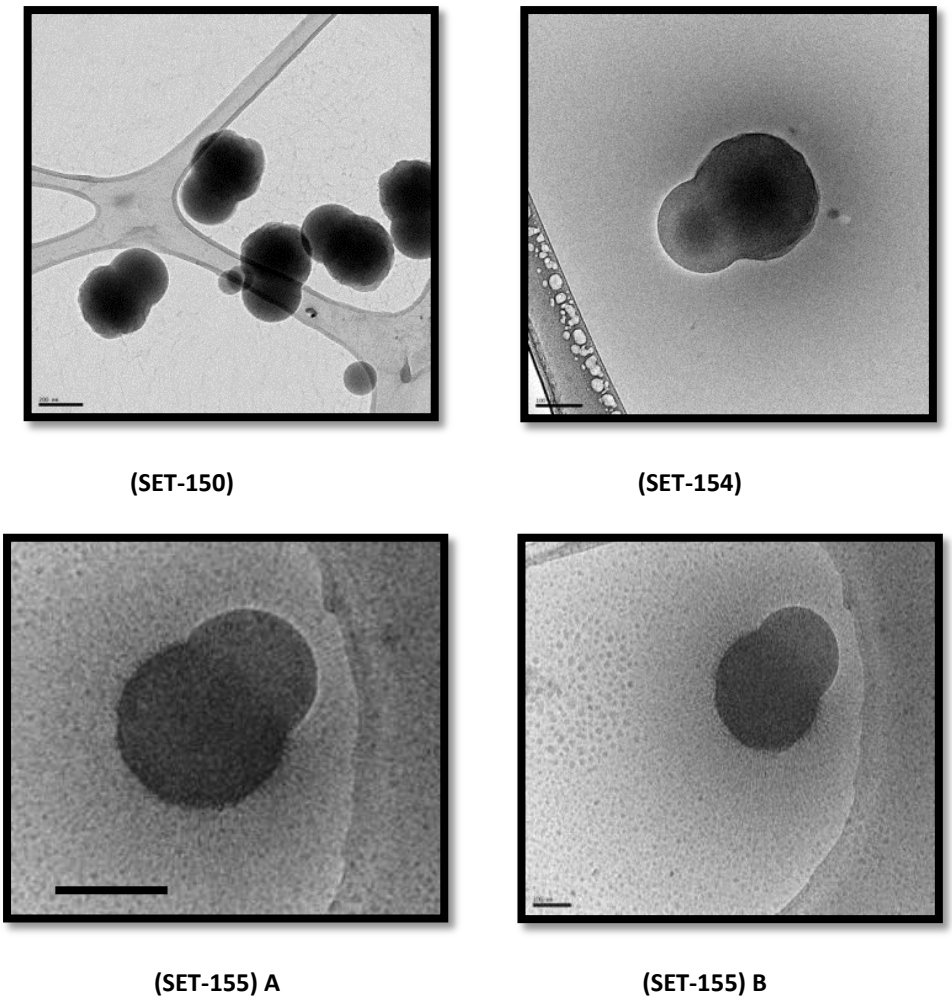

Fig.16. Cryo-TEM images of Janus particles made from latex PS-31. The scale bar in SET-150 and SET-155 A is 200 nm, and 100 nm in SET-154 and SET-155 B.

In the case of SET-150, when the original seed domain was grafted with poly(2-hydoxy ethyl acrylate), it appeared coarse and rough compared to the newly formed hydrophobic domain which appeared smooth. This was also observed in the case of SET-154, as the original seed domain grafted with poly(3-sulfopropyl methacrylate) became dark and rough, and the newly formed hydrophobic domain was bright.

6.4.2. Phase separation from hairy latexes made by the shot addition method (Route 2).

In the previous parts of this chapter we focused on the swelling and phase separation of crosslinked seed latexes which had a hydrophilic surface due to the presence of the inimer (shot-addition method). This surface effectively was smooth, which we referred to as "non"-hairy. One interesting question is what would happen to the swelling and phase separation if we used "hairy" seed latexes? That is, the ones which had polymer brushes grafted onto their surface via SET-LRP.

Firstly we used the hairy latex derived from PS-20, which had a high cross-linked density at a DVB concentration of 7.49%. These hairy latexes from PS-20 were used as hairy seeds in the second stage swelling and seeded emulsion polymerization. Most of the obtained morphology gained a raspberry and popcorn morphology, therefore we will summarize the results by comparison of the obtained morphology after swelling and seeded polymerization of non-hairy PS-20 with hairy PS-20 at identical conditions. In addition to the popcorn and raspberry morphology some isolated cases can give Janus shape morphologies but with not reproducible fashion, these will be described also.

Table 15 shows the recipe and conditions used for swelling and seeded polymerization, followed by Figure 17 which shows the SEM images of the obtained particle morphologies of both non-hairy and hairy PS-20 latex particles after swelling and seeded polymerization at almost identical conditions.

The hairy latex SET-82 with poly(NIPAM) brushes was swollen with a swelling ratio of 2.15 and a DVB concentration of 5.0% in experiment (SW-169). The particles grew to 340 nm and without a clear phase separation. The particles became

merely non-spherical with little heterogeneity on the surface of the latex particle, in contrast to the similar experiment (SW-93) when non-hairy PS-20 latex was used as seed, which is swollen with swelling ratio of 2.20 and with 5.0% DVB concentration, the obtained latex have a triplet and popcorn morphology. This indicates that the presence of the poly(NIPMA) brushes has an influence in the phase separation process.

Table.15. Ingredients used to swell the hairy latex PS-20 and the obtained morphologies after polymerization at 70°C with a mixing speed of 30 rpm. S = styrene, D = divinyl benzene (DVB), A = azobisisobutyronitrile (AIBN), SM = swelling monomer mixture, CV% = conversion of surface-initiated (SET-LRP), R (M/P) = monomer to polymer ratio, t.s. % = total solid of latex.

Exp	Latex	Brush type	CV %	Particle size (nm)	R (M/P)	Latex (t.s.) %	Latex (g)
SW-169	SET-82	P(NIPAM)	100	383	2.15/1.0	0.75	9.82
SW-116	SET-63	P(NIPAM)	100	317	4.04/1.0	0.50	10.01
SW-170	SET-69	P(NaSSA)	85	617	4.70/1.0	0.45	7.14
SW-195	SET-69	P(NaSSA)	85	617	2.0/1.0	0.45	11.90

Exp	S+D+A=SM(g)	DVB %	H_20 (mL)	Latex morphology	Colloidal stability
SW-169	(6.0+0.30+0.0618) **= 0.158**	5.0	0.0	**Non-spherical**	Stable + some coagulation
SW-116	(6.0+0.30+0.060) **= 0.202**	5.0	8.0	**Quartet**	Stable + some sedimentation
SW-170	(6.0+0.30+0.0618) **= 0.150**	5.0	0.0	**Snowman (Janus particles)**	Stable
SW-195	(6.52+0.3622+0.062) **= 0.150**	5.55	0.0	**Snowman (Janus Particle)**	Stable

One of the isolated cases that gave anisotropic particles is when the hairy latex SET-63 which has a poly(NIPAM) brushes was swollen with higher swelling ratio of 4.0 and with the presence of 5.0% DVB in experiment (SW-116), the latex particles attained a quartet morphology, wherein three new hydrophobic domains with sizes around 120 nm were generated from the hairy latex which had a size of 180 nm.

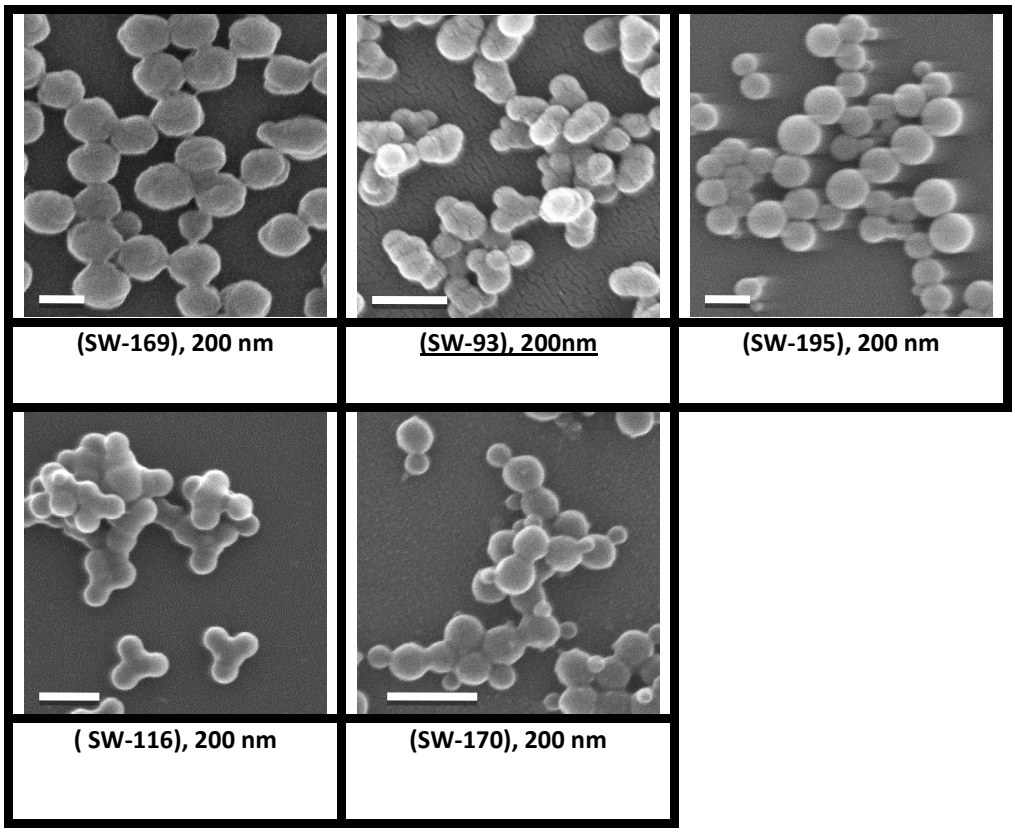

Fig.17.SEM images of PS-20 hairy latex after swelling and seeded emulsion polymerization. The scale bar in all images is 200 nm.

This morphology was visualized by cryo-TEM as shown in Figure 18. The obtained morphology indicates that, the increase in the swelling ratio promotes the size of the newly formed domain at a constant DVB concentration.

When the type of the polymer brushes was replaced by poly(sodium styrene sulfonate) as in SET-69, this latex had a poly(electrolyte) hairy outer layer which extended and elongated toward the water phase as a result of the osometic pressure exerts from the counter ions inside the polymer brushes. This elongated conformation of the polymer chains acted oppositely against the elastic squeeze force to contract the latex particle which minimized the number of phase separations or directed phase separation toward one direction with only one formed domain.

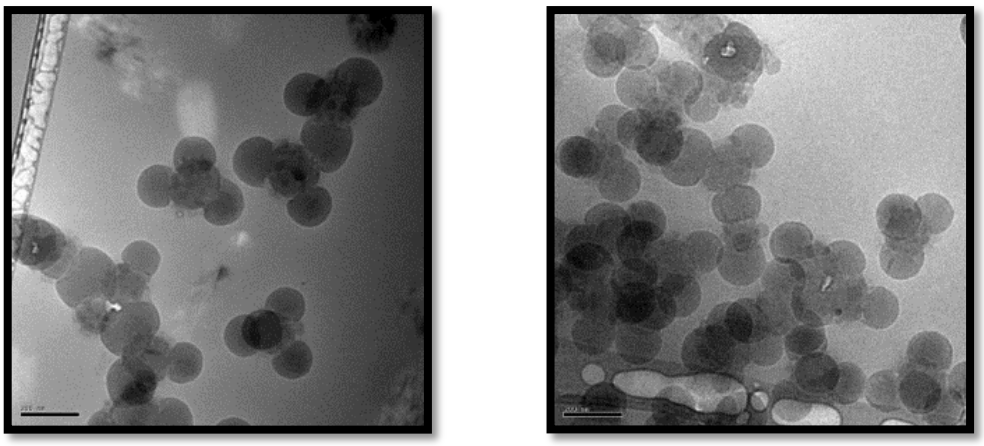

SW-116 **SW-116**

Fig.18. Cryo-TEM images of SW-116. The scale bar is 200 nm.

Besides this effect, the high interfacial tension between the expelled hydrophobic monomer and the hydrophilic surface of the latex induce the separated domain to adjust its shape to be more uniform and spherical in order to minimize its contact with water and the surface of the latex particle. SET-69 latex was swollen with a swelling ratio of 4.70 and a DVB concentration of 5.0% in experiment SW-170. The latex obtained after swelling experiment appeared as doublet shaped particles with a snowman morphology (Janus particles); some hairy latex particles remained without phase separation, as shown by cryo-TEM in Figure 19. This case also represents one of the isolated cases that can provide hairy Janus particles with non-reproducible manner.

As can be seen from the cryo-TEM image, some of the obtained latex particles had two different domains: the original hairy seed domain is the hydrophilic side containing poly(sodium styrene sulfonate) brushes with a brush length of around 60 nm and with an average particle size around 200 nm including the brushes, and the newly formed hydrophobic domain with an average size of 90 nm to ultimately resulted in snowman shaped amphiphilic latex particles.

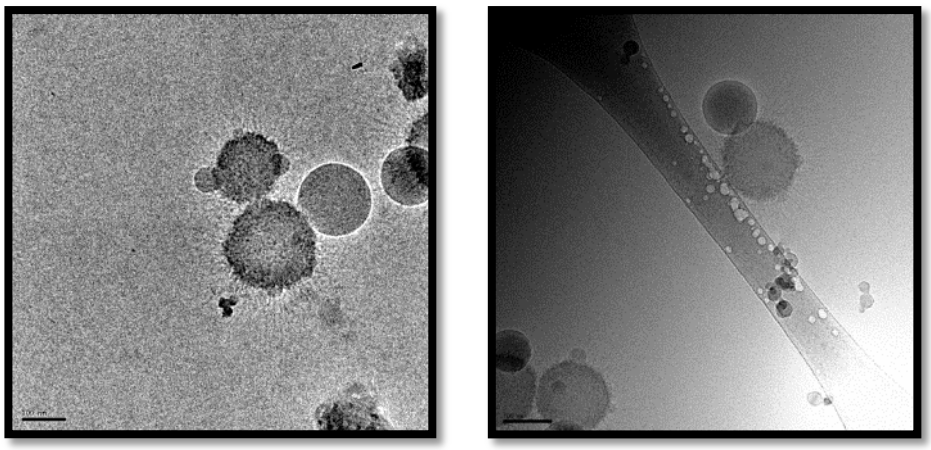

SW-170 (a)

SW-170 (b)

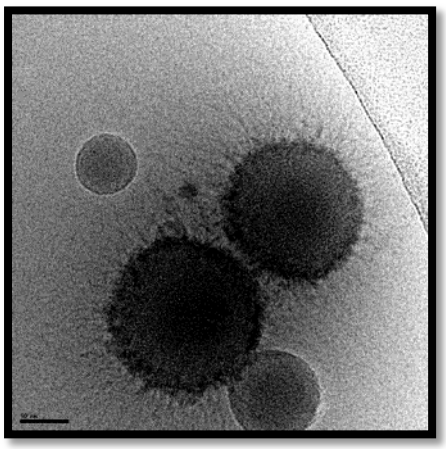

SW-170 (c)

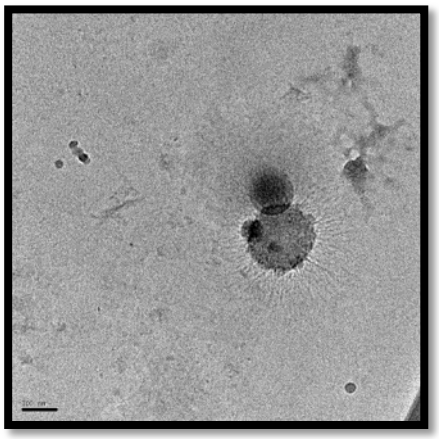

SW-170 (d)

Fig.19. Cryo-TEM images of latex SW-170. The scale bar is 100 nm in (a), (b) and (d) and 50 nm in (c).

Similar particle morphologies were also observed when the hairy seed SET-69 was swelled with a swelling ratio of 2.0 and a DVB concentration of 5.55% as in SW-195. On the other hand when the non-hairy PS-20 latex swollen with quite similar conditions as in SW-170 in experiment (SW-93), but with a little higher DVB concentration of 5.5% and swelling ratio of 2.2 , different morphology was obtained, this indicate the obvious effect of the poly(sodium styrene sulfonate) brushes on the obtaining morphology.

Based on these results, the length, density and the type of polymer brushes affect the types of phase separation from latex particles. Since the hairy latexes were made under different SET-LRP conditions which resulted in different length and density of the formed polymer brushes, consequently, different particle morphologies will be gained after swelling and seeded emulsion polymerization. It is worth examining the effect of reducing the concentration of DVB in the second stage polymerization during the swelling and seeded emulsion polymerization of hairy latex with poly(sodium styrene sulfonate). This might enhance the formation of larger hydrophobic domains and also minimize the population of unchanged hairy latex particles.

Phase separation from hairy latex PS-25, this latex has lower crosslinked density of 3.1wt% DVB and grafted with two types of hydrophilic polymer brushes, poly(NIPAM) and poly(sodium styrene sulfonate). Table 16 shows the conditions and the recipe used to swell these hairy latexes, followed by Figure 20 which shows SEM images of the obtained particle morphologies. In the case of poly(NIPAM) brushes, two hairy latex particles were used, SET-113 and SET-115. The obvious difference between SET-113 and SET-115 is the total monomer conversion of SET-LRP during the grafting of poly(NIPAM) brushes.

In the case of SET-113, the total monomer conversion was 48% whereas in SET-115 this was 80%. When the hairy latex SET-113 was swollen with a swelling ratio of 2.5 and a DVB concentration of 5.55% as in SW-198, the latex particles showed a raspberry morphology. This was expected as the non-hairy latex PS-25 gave the same morphology as in (SW-227), when the non-hairy latex PS-25 was swollen with 2.16 swelling ratio and 5.0% DVB concentration

Table.16. Ingredients used to swell the hairy latex PS-25 and the obtained morphologies after polymerization at 70°C with a mixing speed of 30 rpm. S = styrene, D = divinyl benzene (DVB), A = azobisisobutyronitrile (AIBN), SM = swelling monomer mixture, CV % = conversion of surface-initiated (SET-LRP), R (M/P) = monomer to polymer ratio, t.s. % = total solid of latex.

Exp	Latex	Brush type	CV %	Particle size (nm)	R (M/P)	Latex (t.s.) %	Latex (g)
SW-197	SET-111	P(NaSSA)	90	3000	4.20/1.0	0.695	5.16
SW-198	SET-113	P(NIPAM)	48	277	2.50/1.0	0.713	9.01
SW-201	SET-115	P(NIPAM)	80	375	4.7/1.0	0.339	10.0
SW-236	SET-111	P(NaSSA)	90	3000	2.97/1.0	0.695	10.14

Exp	S+D+A=SM(g)	DVB %	H_2O (mL)	Latex morphology	Colloidal staiblity
SW-197	(6.52+0.362+0.0623) **= 0.150**	5.5	0.0	**Raspberry**	Stable
SW-198	(6.52+0.362+0.0623) **= 0.1595**	5.5	0.0	**Raspberry**	Stable
SW-201	(6.52+0.362+0.0623) **= 0.1595**	5.5	0.0	**Popcorn**	Stable
SW-236	(6.0+0.018+0.061) **= 0.2081**	0.3	0.0	**Raspberry**	Stable

When SET-115 was swollon with a swelling ratio of 4.7 and a DVB concentration of 5.55% as in SW-201, the latex particles attained popcorn morphology. This was also expected as the non-hairy latex PS-25 showed popcorn morphology as a result of an increase in the swelling ratio which resulted in larger separated domains because of the coalescence of separated domains as in experiment SW-212.

Based on these results, the presence of poly(NIPAM) brushes on the surface of PS-25 did not show a major effect in terms of swelling and phase separation as similar morphologies were obtained with the non-hairy latex particles.

In the case of swelling and phase separation from PS-25 latex grafted with poly(sodium styrene sulfonate) brushes as in SET-111, the polymerization reached to 90% conversion and resulted in long polymer brushes with a length of 140 nm.

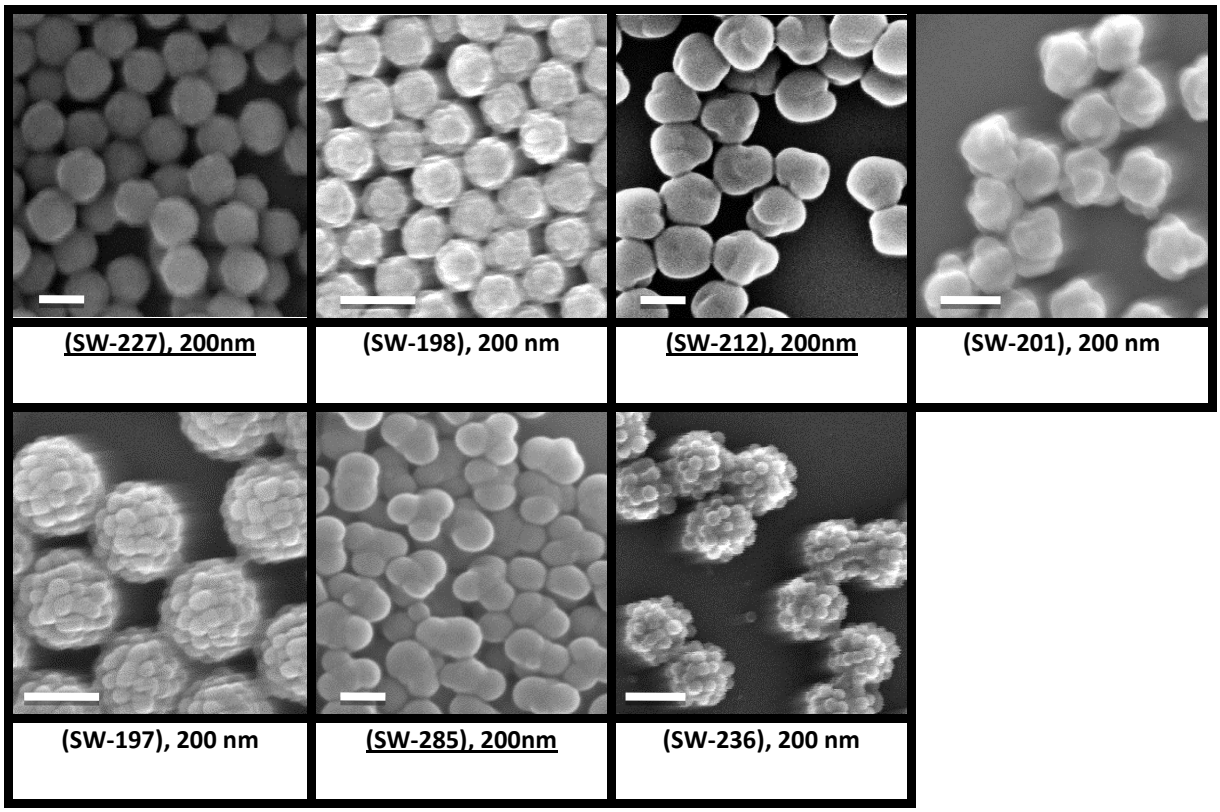

Fig.20. SEM images of the hairy latex PS-25 after swelling and seeded emulsion polymerization. The scale bar in all images is 200 nm.

The measured particle size by DLS appeared to be greater than 1.0 μm due to the flocculation that occurs among latex particles as the polymer brushes entangle with each other. Two swelling experiments were performed; the first when the hairy latex SET-111 swollen with a swelling ratio of 4.2 and a DVB concentration 5.5% as in SW-197. Popcorn morphology was expected under these conditions with non-hairy PS-25, but a raspberry morphology was obtained which indicates that the poly(sodium styrene sulfonate) brushes lead the hydrophobic phase separated domains to become more spherical and independent to minimize their contact with the hydrophilic surface of SET-111.

The raspberry shapes particles showed uniform and identical shapes among the latex particles with an average size of 420 nm which was double the size of the original

seed latex without poly(sodium styrene sulfonate) brushes. The number of newly formed domains was above 40 with an average size of 70 nm.

When the swelling ratio was decreased to 2.97, and with a lower DVB concentration of 0.3% as in SW-236, the obtained latex particles showed a raspberry morphology as showed in figure 21. The number of newly formed domains was lower as a lower swelling ratio was used. The average size of the newly formed domains was around 70 nm. With conditions nearly similar to that used in SW-236, the non-hairy latex PS-25 was swollen with swelling ratio of 3.35 and with lower DVB concentration of 0.5% as in experiment (SW-285), triplet and quartet particles was obtained. This clearly indicates that, the presence of the poly(sodium styrene sulfonate) brushes has an influence in the phase separation.

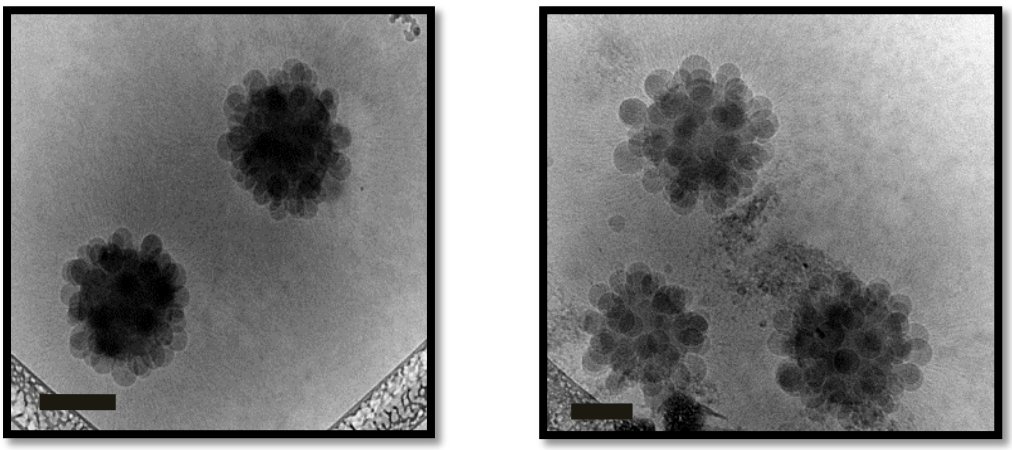

Fig.21. Cryo-TEM images of SW-236, scale bar is 200 nm in both images.

Cryo-TEM image of SW-236 shows the raspberry morphology; in addition to that the surface of the particle has an anisotropic morphology with two different characteristics, which are hydrophilic poly(styrene sulfonate) brushes and small patches of hydrophobic poly(styrene).

Based on these results, the swelling of hairy latex PS-25 with different types of polymer brushes predominately results in a raspberry morphology, regardless of the swelling ratio or DVB concentration used in the second stage polymerization.

Phase separation from hairy latexes PS-27, PS-29 and PS-31. Three hairy latexes particles were made using PS-27 which was grafted with poly(sodium styrene sulfonate) brushes. These hairy latexes were used as the seed in the second stage seeded emulsion polymerization as shown in table 17.

Table.17. Ingredients used to swell the hairy latex PS-27 in (SW-243, SW-266, and SW-269), PS-29 in SW-271 and PS31 in SW-272, and the subsequent morphologies obtained after polymerization at 70°C with a mixing speed of 30 rpm. S = styrene, D = divinyl benzene (DVB), A = azobisisobutyronitrile (AIBN), SM = swelling monomer mixture, CV% = conversion of surface-initiated (SET-LRP), R (M/P) = monomer to polymer ratio, t.s. % = total solid of latex.

Exp	Latex	Brush type	CV%	Particle size (nm)	R (M/P)	Latex (t.s.) %	Latex (g)
SW-243	SET-118	P(NaSSA)	87	1180	3.15/1.0	0.67	10.05
SW-266	SET-120	P(NaSSA)	91	2233	2.01/1.0	1.0	9.89
SW-269	SET-121	P(NaSSA)	99	3657	2.21/1.0	0.90	10.12
SW-271	SET-145	P(NaSSA)	100	260	3.15/1.0	0.90	7.07
SW-272	SET-146	P(NaSSA)	100	329	2.4/1.0	1.20	7.04

Exp	S+D+A=SM (g)	DVB %	H_2O (mL)	Latex morphology	Colloidal stability
SW-243	(6.0+0.010+0.060) = **0.211**	0.16	0.0	**Raspberry**	stable
SW-266	(6.0+0.060+0.060) = **0.20**	1.0	0.0	**Raspberry**	stable
SW-269	(6.0+0.6+0.060) = **0.2022**	10	0.0	**Raspberry**	stable
SW-271	(6.0+0.3+0.06) = **0.20**	5	0.0	**Spherical**	stable
SW-272	(6.0+0.6+0.060) = **0.20**	10	0.0	**Oval**	stable

All the three hairy latexes produced particles with a raspberry morphology after swelling and seeded emulsion polymerization, although different swelling and DVB concentrations were examined. This indicates that the hydrophilic character of the

hairy latex PS-27 led to multiple phase separations as shown in SEM image in Figure 22 and cryo-TEM Figure 23. It was observed that the size of the newly formed domains decreased as the DVB concentration increased as in SW-266 and SW-269, in contrast to the greater size seen in SW-243. Conversely, when the non-hairy counterpart swollen with nearly similar conditions as in SW-251 and SW-274, a dumbbell shape particles were produced. This explains the major influence of the poly(sodium styrene sulfonate) brushes on the obtaining morphology after swelling and seeded emulsion polymerization.

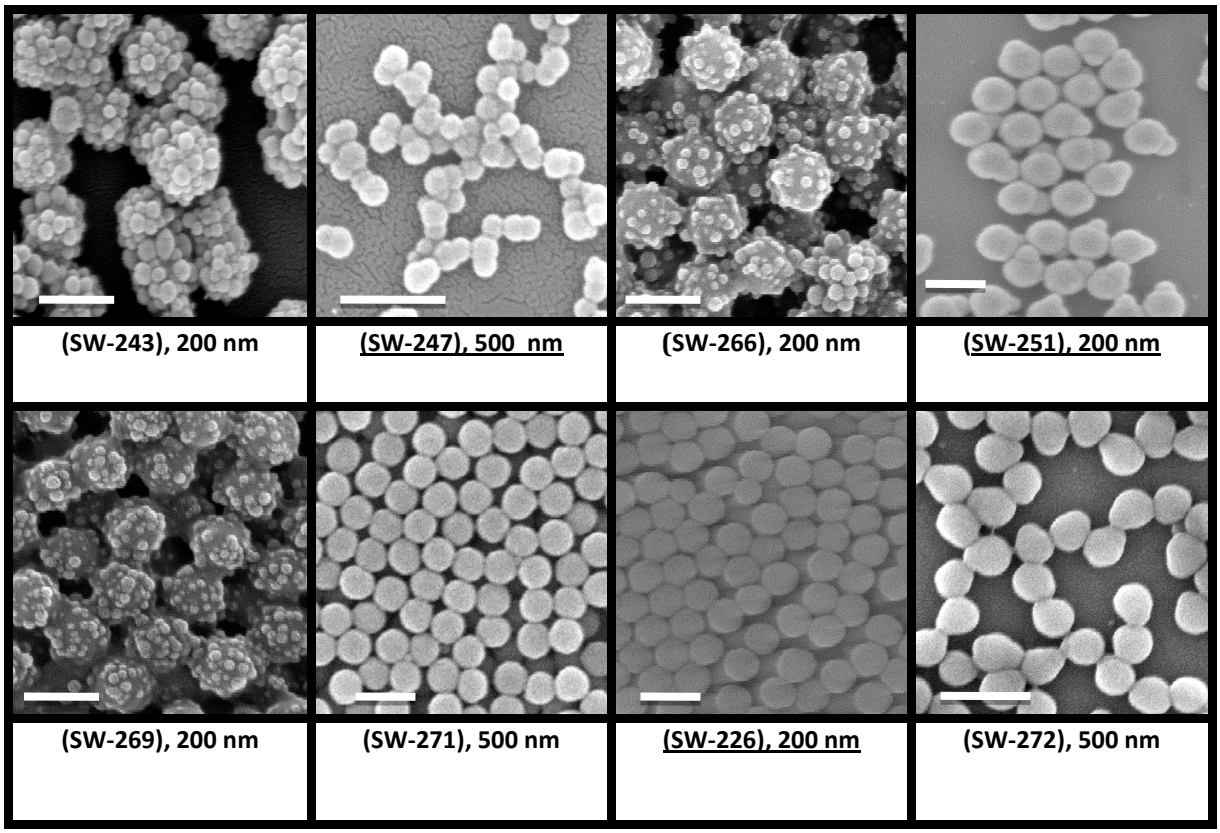

Fig.22. SEM images of PS-27 (SW-243, SW-266, SW-269), PS-29 in SW-271 and PS-31 in SW-272 hairy latexes after swelling and seeded emulsion polymerization. The scale bar in images SW-243, SW-266 and SW-269 is 200 nm, and 500 nm in images SW-271 and SW-272.

Cryo-TEM images of SW-266 and SW-269 showed raspberry morphology with two different characteristics, which are hydrophilic poly(sodium styrene sulfonate) brushes and small patches of hydrophobic poly(styrene). Latexes PS-29 and PS-31 were grafted with poly(sodium styrene sulfonate) brushes using SET-LRP in the

presence of an external water soluble initiator (**2**). Consequently, shorter poly(sodium styrene sulfonate) brushes were formed on the surface of latexes PS-29 and PS-31.

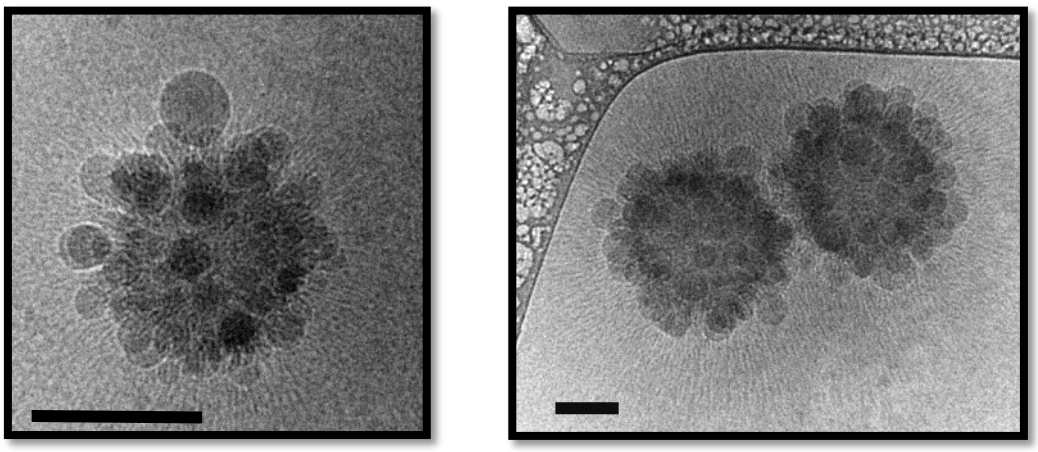

SW-266 **SW-269**

Fig.23. Cryo -TEM of SW-266, Scale bar is 200 nm. And SW-269, Scale bar is 100 nm**.**

In the case of PS-29, the hairy latex SET-145 was swelled with a swelling ratio of 3.15 and a DVB concentration of 5% as in SW-271. The reason for the high concentration of DVB used is to minimize the number of phase separations, which is what indeed occurred; spherical particles were formed without any change in the SET-145 hairy seed particles. This result concurs with that obtained when a non-hairy latex particles PS-27 was used with nearly similar conditions as in SW-226. This indicates the increase in the concentration of DVB in the monomer feed suppressed the phase separation.

In the case of hairy latex SET-146 which was made from PS-31, it was swelled with a swelling ratio of 2.4 and with a DVB concentration of 10%. This latex resulted in oval shape morphology. This again confirmed the significant influence of DVB concentration to stop the phase separation.

6.5. Conclusion

Non-hairy and hairy monodisperse cross-linked latex particles with different cross-linked densities and particle sizes synthesized by soap-free (shot addition) emulsion polymerization were used in second stage seeded emulsion polymerization after swelling to make anisotropic particles through formation of a new hydrophobic domain.

In the case of the non-hairy latexes, it was found that a low cross-linked density below 2.90% in the seed, a low DVB concentration in the swelling step below 0.5%, in addition to the presence of a highly hydrophilic surface as a result of the shot addition method in contrast to batch addition, resulted in phase separation with the formation of only one new hydrophobic domain in a reproducible pattern to form dumbbell shaped particles. The original seed domain of the formed dumbbell particles was modified by SET-LRP to ultimately form the targeted hairy Janus particles with different types of polymer brushes. The obtained hairy Janus particles were characterized by cryo-TEM.

In the case of hairy latex particles, it was found that the most commonly obtained morphologies were raspberry and popcorn. However, in some rare cases, hairy Janus particles were produced after swelling and seeded emulsion polymerization, but the synthesis was not reproducible. The differences in brush properties such as length and density as a result of diverse SET-LRP conditions used produce the observed morphologies after swelling and seeded emulsion polymerization were not reproducible. Based on these observations and findings, the best conditions to reproducibly make dumbbell shaped hairy Janus particles are:

1- Precursor particles should be synthesized by the shot addition method of soap-free emulsion polymerization to make the surface of the particles more hydrophilic.

2- Cross-linked density in the precursor particles should be between 2.9% and 1.9%.

3- The size of the precursor particles should be between 150 and 250 nm.

4- The swelling ratio should be between 4.0 and 2.0

5- A low DVB concentration between 1.0 to 0.15% should be used in the swelling step.

Chapter 7: Fields of potential application of the synthesized Janus particles.

7.1. Summary

The usages of the already synthesised complex particles in three different applications were studied. First application is their usage as an active stabilizer agent for carbon nanotubes (CNTs) in aqueous medium. It was observed that hairy Janus particles with short or long poly(sodium styrene sulfonate) brushes are good aqueous phase stabilizers for multi-walled carbon nanotubes (MWCNTs) for short term stability (1 month); after that the MWCNTs begin to flocculate and sediment. The Cryo-TEM images suggest that the strong interaction of poly(sodium styrene sulfonate) brushes with the MWCNTs is a possible reason for the stabilization. However, the hairy core-shell particles with poly(sodium styrene sulfonate) brushes are very good stabilizers for MWCNTs for even long term stability (1 year) and this is a result of the absence of the hydrophobic domains in those types of hairy particle in which the attractive forces between hydrophobic domains lead to the flocculation and sedimentation of MWCNTs.

Second application is their use as Pickering stabilizers. This was investigated using two immiscible liquids. Dodecane, hexadecane and paraffin wax were used as the oil phases and water as the polar phase. It was observed that ionic particles, whatever their morphology (spherical, hairy, patchy-hairy, hairy-Janus and non-hairy Janus particles) were strongly hydrophilic and tended to remain in the water phase; however; non-ionic particles, whatever their morphology, tended to form stable Pickering emulsions. We propose that there are two main factors for forming stable Pickering emulsions: the presence of non-ionic polymer brushes on the surface of the

latex particles, as in the case of hairy latex, e.g. poly(*N*,*N*-dimethyl acrylamide) and poly(PEGMEA) brushes, and the amphiphilic nature of hairy Janus particles.

The study of the directed self-assembly of dumbbell Janus latex particles was induced by changing the ionic strength of the latex aqueous medium by the addition of an electrolyte. In the case of non-hairy dumbbell Janus latex particles, the electrolyte concentration required to decrease the zeta potential of the latex to below -25 mV is 0.1M, with a slight increase in the particle size; above this concentration a massive increase in the particle size was observed which indicates that a typical coagulation of the latex particles was occurring. However, the spherical and snowman non-hairy Janus latex particles require a higher concentration of the electrolyte, above 0.2 M, to decrease the zeta potential to below -25 mV with a slight increase in the particle size and this indicates that the larger hydrophilic domain is the more stable latex. This also highlights that in the case of the dumbbell non-hairy Janus particles the responsible factor for the destabilization of the latex and self-assembly is the bigger hydrophobic domain in those particles. The Cryo-TEM images of the dumbbell non-hairy Janus particles suggest that more than 70% of the interactions among the particles are head to head (hydrophobic–hydrophobic domain interactions) and the remaining interactions are either head to tail or tail to tail (hydrophobic-hydrophilic) (hydrophilic-hydrophilic). In this chapter each application will be separately described and studied in details as follow

7.2. Dispersion of carbon nanotubes (CNTs)

7.2.1. Summary

The use of different types of complex latex particles, including spherical particles, hairy core-shell particles, hairy Janus particles and non-hairy Janus particles, as stabilizers for carbon nanotubes (CNTs) dispersions in water was investigated. It was observed that hairy Janus particles with short or long poly(sodium styrene sulfonate) or poly(sulfo propyl methacrylate) brushes are good aqueous phase stabilizers for multi-walled carbon nanotubes (MWCNTs) for short term stability (1 month); after that the MWCNTs begin to flocculate and sediment. The Cryo-TEM images suggest that the strong interaction of poly(sodium styrene sulfonate) brushes with the MWCNTs is a possible reason for the stabilization. However, the hairy core-shell particles with poly(sodium styrene sulfonate) brushes are very good stabilizers for MWCNTs for even long term stability (1 year), and this is a result of the absence of the hydrophobic domains in those types of hairy particle in which the attractive forces between the hydrophobic domains lead to the flocculation and sedimentation of MWCNTs. As hairy Janus particles with cationic or non-ionic brushes were used, short term stability was observed, but only the hairy Janus particles with poly(NIPAM) non-ionic brushes provide long term stability. On the other hand, when non-hairy Janus and spherical particles were used, a direct phase separation was observed. This indicates that the presence of polymer brushes is essential to provide stability for MWCNTs. The stable aqueous dispersions of MWCNTs that were stabilized by complex latex particles were used as filler with less than a 3% ratio of MWCNTs to the latex matrix to form nanocomposite dispersion. The nanocomposites showed a very good distribution of MWCNTs through the latex matrix.

7.2.2. Introduction

Carbon nanotubes (CNTs) are cylinders composed of rolled graphite planes with a diameter of nano scale dimensions. Based on their geometry, there are two types of CNTs: Single-walled carbon nano-tubes (SWCNTs) and multi-walled carbon nano tubes (MWCNTs) [1]. SWCNTs consist of a single graphene layer rolled up into a seamless cylinder, whereas the MWCNTs consist of two or more concentric cylindrical shells of graphene sheets coaxially arranged around a central hollow core with Van der Waals forces between adjacent layers. CNTs have high mechanical properties (tensile strength in range of 10 to 63 GPa) [2], and exceptionally high electrical and thermal conductivity, 1000 $\Omega^{-1}m^{-1}$ and (200 W/mK) respectively [3]. These unique physical and mechanical properties make CNTs potential candidates for reinforcing the properties of other materials such as polymers to make conducting plastic, thermal conductors and conductive adhesive [4]. In order to form a uniform nanocomposite material, the CNTs need to be dispersed evenly distributed throughout the polymer matrix, ideally as individual CNTs. Therefore the method used to separate and stabilize the individual CNTs against agglomeration inside the polymer matrix is essential. We are interested in fabrication of advanced materials from colloidal components which are dispersed in water. Based on this, in order to make a CNTs/latex nanocomposite through film formation of a waterborne blended dispersion three requirements should be met: Firstly, the CNTs need to be exfoliated , as in the van der Waals attractive forces between bundles of nanotubes need the be overcome, when brought in contact with water to generate a colloidal stable dispersion. Secondly, when the polymer latex is added to this dispersion the system should not phase separate. Thirdly, upon film formation both of these requirements need to prevail.

Two major methods are used to disperse carbon nanotubes in water: Chemical modification of the surface of the nanotubes (fluorination, cycloaddition, carbene and nitrene addition, chlorination, bromination, hydrogenation and silanization), and physical methods by using surfactant such as sodium dodecylsulfate. The first method is a questionable approach as it may deteriorate the physical and mechanical properties of the tubes. An example is the work of Mao Peng and co-workers who oxidized MWCNTs with a concentrated mixture of nitric and sulphuric acid. The modified MWCNTs were easily dispersed in water. A nanocomposite using a cationic PMMA latex was made upon slow addition of the anionic tubes, making use of heterocoagulation. The coagulum was filtered, dried, and pressed into a nanocomposite material [5].

The second method such as wrapping a polymer around the CNTs, and the use of surfactant to disperse CNTs; the physical method is more attractive for dispersing the CNTs since this method will not create any major damage to CNTs. Nadia Grossiord reviewed the methods used to disperse CNTs into polymer to obtain conductive nanocomposite [6]. Several examples of dispersing of CNTs by utilizing the physical method are described as follow: Stable dispersion of oxidized MWCNTs in methanol mixed with stable anionic poly(styrene) stabilized by SDS in methanol by ultra-sonication led to the formation of a stable nano-composite [7]. A (PTFE) poly(tetrafluoroethylene)/MWCNTs nano-composite was prepared by the method described previously whereby an electrostatic attraction was utilized to form coagulation between the positively charged MWCNTs, which are stabilized by the cationic surfactant (CTAB), and the negatively charged PTFE latex particles [8]. 25-30 nm PMMA latex particles were prepared by micro-emulsion polymerization in

the presence of reactive surfactant 1-(2-acryloyloxyundecyl)-3-methylinidazolium and used to stabilize oxidized SWCNTs in an aqueous medium [9].

An aqueous solution of Poly(sodium styrene sulfonate) was able to stabilize graphene nanoplatelets and SWCNTs, it is claimed that the stabilization is attributed to the interaction between the graphitic surface and the aromatic ring of the poly (sodium styrene sulfonate) [10, 11, 12]. This stable dispersion of graphene was mixed with matrix latex particles to make a nanocomposite after freeze drying [13]. Uniform distribution of MWCNTs and poly(styrene) latex particles with size of 40 nm was achieved in situ during the microemulsion polymerization; these small poly(styrene) latex particles are deposited along the MWCNTs. It is speculated that the possible reason for the attachment of the small poly(styrene) latex particles with the MWCNTs is the Brownian motion of emulsified monomer droplets and MWCNTs, which causes collisions between them, and the interaction between the aromatic ring of poly(styrene) with MWCNTs via π- π stacking providing anchoring sites for the small poly(styrene) latex particles on the surface of the MWCNTs [14]. Larger poly(styrene) latex particles made by soap-free emulsion polymerization in the presence of ethanol were used to make a nanocomposite with purified MWCNTs with acid treatment by freeze drying [15]. Organic nanoparticles ZrO_2 with a size of 5-10 nm were used to stabilize SWCNTs via non-covalent interaction and electrostatic attraction mechanisms between the charged nanoparticles and SWCNTs [16]. Here in our research we are interested in using complex latex particles that fabricated in chapters 4, 5 and 6 as stabilizer to disperse CNTs in water.

7.2.3. Experimental

7.2.3.1. Materials

Multi-walled carbon nanotubes (MWCNTs2) with OD = 60-100 nm, ID = 5-10 nm, length = 0.5-500 µm, 95+% purity (Aldrich), multi-walled carbon nanotubes (MWCNTs1) had OD = 20-50 nm, wall thickness =1-2 nm, length =0.5-2.0 µm, > 95% (Aldrich). Single-walled carbon nanotubes (SWCNTs) were of 70+%C purity, Nanocyl 1100.

7.2.3.2 General procedure for Stabilization of CNTs with complex latex particles

The procedure for preparing the (MJ13) CNTs dispersion will be described as a representative example for the stabilization process of CNTs as follows: 2.0 mL of latex (SET-111, 0.695 t.s%) was mixed with 0.01 g of (MWCNTs2) inside a 100 mL glass jar, and then 13.0 mL of distilled water was added. The glass jar containing the mixture was placed in an ice bath, the head of the digital sonifier (BRANSON) was immersed in the mixture and the sonification started with amplitude of 70% for a certain time period, usually 15 or 30 minutes (with interval of 1 minute sonication and then 30 seconds hold) . After this the mixture was poured into a 20 ml glass vial for SEM and Cryo-TEM characterization.

7.2.3.3.General procedure for Formation of the Carbon nanotubes-Latex nanocomposite

The procedure for making the (NC8) (nanocomposite) will be described as a general example as follows: 15.0 mL of (2.9% solid content) soap-free poly(methyl methacrylate)-*co*-poly(butyl acrylate) latex particles were mixed with 10.0 mL of

(MJ13) CNTs dispersion by simple mixing using a magnetic stirrer at high speed for 30 minutes at room temperature.

7.2.4. Results and discussion

7.2.4.1. Formation of stable waterborne dispersion of carbon nanotubes using "hairy" latex particles.

An issue with stabilizing carbon nanotubes with molecular surfactants in water is that they may cover the majority of the surface of the CNTs, hereby potentially altering their efficacy as thermal and electrical conductors and potentially also having a detrimental effect on mechanical reinforcement properties. We therefore wanted to investigate if the complex latex particles made in Chapters 4, 5 and 6 were suitable as particle-based stabilizers.

Two types of MWCNTs with different dimensions were used. The first type is (MWCNTs1) which has dimensions: length 0.5-2.0 μm, OD = 5-20 nm, wall thickness 1-2 nm and 95% purity; the second is (MWCNTs2) which is mainly used in this study with length of 0.5 to 500 μm, diameter of OD: 60-100 nm and ID: 5-10 nm with 95% purity. However, in some experiments the SWCNTs (70% purity, Nanocyl 1100) were used as well. Table 1 summarizes the experiments that investigated the stabilization of CNTs with different types of spherical particles and hairy latex particles. Control experiments were conducted by mixing the MWCNTs2 with water only as in (MJ7), and experiment (S7), whereby the (MWCNTs2) was dispersed in water via the use of the ordinary conventional surfactant SDS (sodium dodecyl sulphate); (15.0 mL of 0.15% SDS solution) was mixed with (MWCNTs2) for 30 minutes with ratio of SDS to MWCNTs of 2.4 which is near from the typical value of 1.5 which is usually used to stabilize the CNTs in the literature. As the

MWCNTs2 was just mixed with water a direct phase separation was observed as in (MJ7), and as ordinary surfactant was used as in (S7) stable foamy dispersion even after 4.0 months from the mixing (long term stability) as that indicated in Table 2 and in the photographic image in figure1. This indicates the necessity of stabilizer to disperse the CNTs in water.

Table.1. Recipe and conditions used to disperse the CNTs with spherical and hairy latex particles: (a) type number one (MWCNTs1), (b) type number two (MWCNTs2) and (C) is SWCNTs, (J/M) ratio of Janus latex particles to CNTs. The mixing was performed with using digital sonifier. (PNaSS) Poly(sodium styrene sulfonate).

Exp	Latex	Brush types	Brush density	Brush length	Latex (mL)	Latex (g)	MWCNTS (g)	H_20 (mL)	Ratio (J/M)	Time of mixing
MJ7	0.0	------	------	------	-----	-----	(b) 0.01	15.0	-----	30
S7	0.0	------	------	------	-----	-----	(b) 0.01	15.0 (0.15% SDS)	2.4	30
MJ 8	PS-24	------	------	------	5.0	0.435	(b) 0.01	10.0	43.5	30
MJ 11	PS-26	------	------	------	0.2	0.014	(b) 0.01	15.0	1.4	15
MJ 12	PS-26	------	------	------	0.60	0.042	(C) 0.01	15.0	4.2	15
MJ 1	SET-110	PNaSS	Low	Long	5.0	0.011	(b) 0.01	10.0	1.1	30
MJ 2	SET-171	PNaSS	high	Long	5.0	0.040	(b) 0.01	10.0	4.0	30
MJ 13	SET-111	PNaSS	high	Long	2.0	0.014	(b) 0.01	13.0	1.4	15
MJ 14	SET-111	PNaSS	high	Long	2.0	0.014	(C) 0.01	13.0	1.4	15
MJ 19	SET-118	PNaSS	high	Long	2.0	0.013	(C) 0.01	13.0	1.3	15

Fig.1. On the left, Photograph of MWCNTs2 dispersions (S7) in water stabilized by using 0.15% of SDS aqueous solution, on the right phase separation of MWCNTs2 in water (MJ7).

Besides these two experiments another three control experiments were conducted by mixing the MWCNTs2 with normal soap-free spherical anionic poly(styrene) latex particles as in experiments (MJ8), (MJ11) and with SWCNTs in experiment (MJ12).

Table.2. Short and long term stability of the CNTs dispersion stabilized by spherical and hairy latex particles.

MWCNTS dispersion	Short term stability (one week)	Long term stability (1 month)
S7	Stable	Stable
MJ1	Stable	Stable
MJ2	Stable	Stable
MJ7	Unstable	Unstable
MJ8	Stable	Unstable
MJ11	Unstable	Unstable
MJ12	Unstable	Unstable
MJ13	Stable	Stable
MJ14	Stable	Unstable
MJ19	Stable	Unstable

Fig.2. Photograph of phase separation of MWCNTs2 in experiments (MJ8, MJ11) after mixing with anionic spherical latex particles, and phase separation of SWCNTs in experiment MJ12.

As spherical normal soap-free emulsion latex (PS-24) was used in mixing experiment MJ8, a clear phase separation was observed one week after the mixing; the same feature was observed in the cases of MJ11 and MJ12 when the soap-free

latex PS-26 was used in a lower ratio with CNTs, but the phase separation occurred within few hours after mixing. Both soap-free latexes were formed by soap-free emulsion polymerization in the presence of a co-monomer (sodium styrene sulfonate), therefore one can expected that the poly(sodium styrene sulfonate) in nature of brushes may play role in the stability of MWCNTs2 dispersion. It was also observed that in MJ11 and MJ12 as lower ratio was used, the spherical latex particles were coagulated with CNTs and that indicates that these particles can not tolerate the high vigour mixing by the sonifier.

After these previous initial experiments and the observations gleaned from them, five mixing experiments were undertaken (MJ1, MJ2, MJ13, MJ14 and MJ19) using four different hairy latex particles with poly(sodium styrene sulfonate brushes). The photographic image of MWCNTs2 dispersions with these different hairy latex particles is shown in Figure 3. All the MWCNTs2 dispersions show a very good long term colloidal stability with the exception of dispersions (MJ14) and (MJ19) which showed only short term stability as SWCNTs was used.

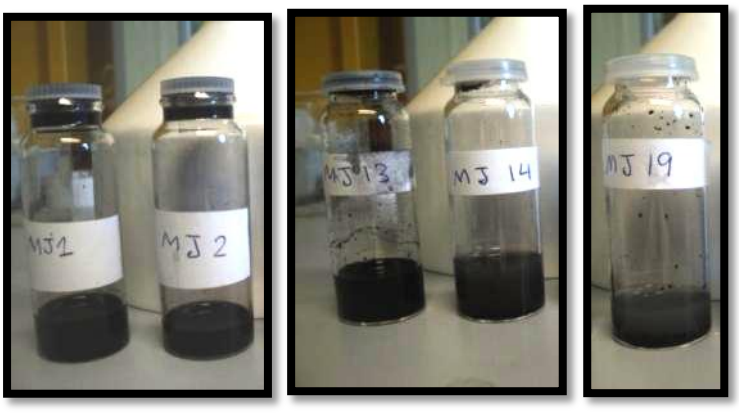

Fig.3. Photograph of CNTs dispersions after mixing with different hairy spherical latex particles containing poly(sodium styrene sulfonate) brushes.

The hairy latex particles (SET-110) that contain poly(styrene sulfonate) brushes with low density as they made by the batch addition method was mixed with MWCNTs2

in mixing experiment (MJ1);The SEM and Cryo-TEM images of the (MJ1) dispersion are shown in figure 4.

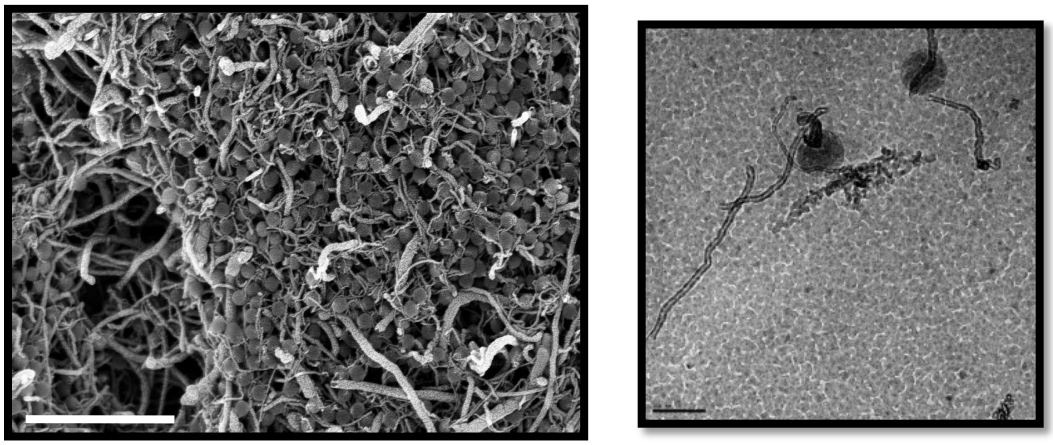

SEM of **MJ1** Cryo-TEM of **MJ1**

Fig.4. SEM and Cryo-TEM images of MJ1**.** The scale bar in SEM image is 1.0 µm and 200 nm in Cryo-TEM image.

The SEM image shows a very good distribution of the hairy latex SET-110 around the MWCNTs2 and the Cryo-TEM image shows the adhesion of the MWCNTs2 to the surface of the hairy latex SET-110. It is worth mentioning that the hairy latex SET-110 has low brush densities (made by the batch addition method) which is the reason of that the poly(styrene sulfonate brushes) are not visible. Hairy latex SET-171 has high density and long poly(sodium styrene sulfonate) brushes as they made by the shot addition method and was mixed with MWCNTs2 in mixing experiment (MJ2).The SEM and Cryo-TEM images of MWCNTs2 dispersion with SET-171 (MJ2) are shown in Figure 5.

The SEM image shows the SET-171 distributed and adhered to the MWCNTs2. From the Cryo-TEM images it is obvious that the poly(sodium styrene sulfonate) brushes of the latex SET-171 adhere to the MWCNTs and disperse them in the aqueous phase, without allowing them to entangle again to form an aggregate.

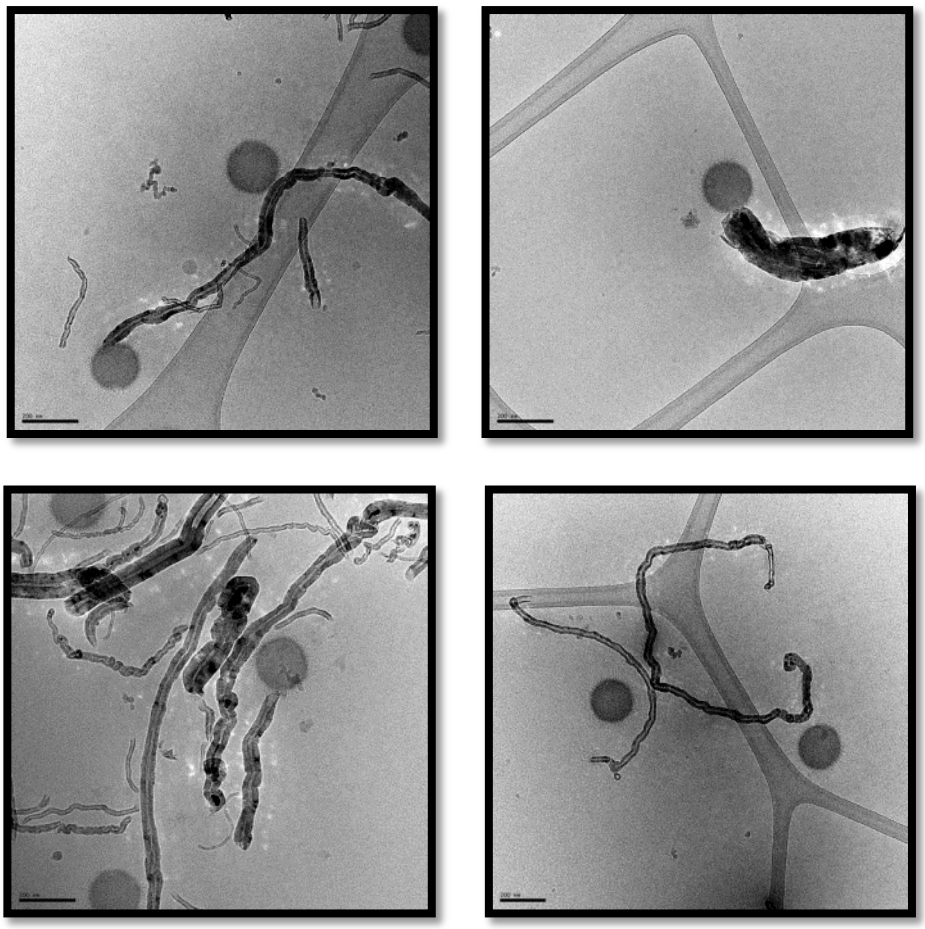

Cryo-TEM images of (**MJ2**)

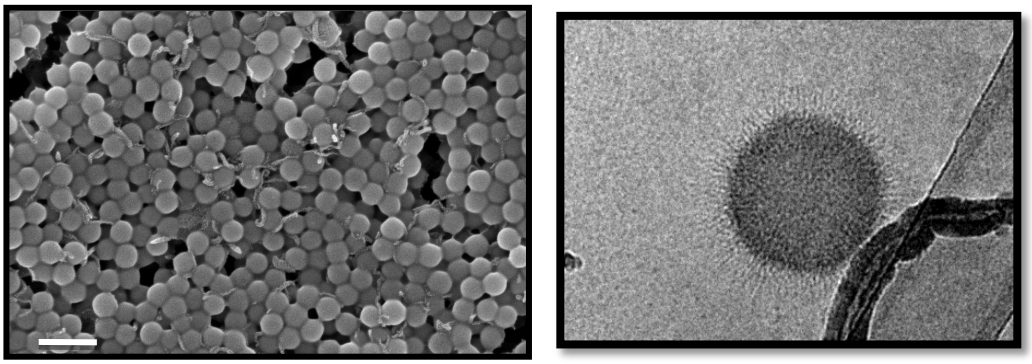

SEM of **MJ2**

Close up of cryo-TEM image of **MJ2**

Fig.5. Cryo-TEM image of (MJ2), scale bar in all images are 200 nm, and SEM image with scale bar of 500 nm.

In a further set of experiments, another completely hairy latex SET-111with high density and long poly(sodium styrene sulfonate) brushes was used to disperse both the MWCNTs2 in mixing experiment (MJ13), and the SWCNTs in experiment MJ14. The dispersion (MJ13) shows very good short and long term stability as

expected from the similar behaviour was observed in the case of experiment (MJ2) when hairy latex SET-171 was used. The SEM and cryo-TEM images of (MJ13) show very good distribution of hairy latex SET-111 through the MWCNTs2 as shown in figure 6 below.

Moreover, the Cryo-TEM image of MJ13 shows the strong adhesion of the hairy latex SET-111 to the MWCNTs2 which is the reason behind the very good stability of that dispersion, as each MWCNTs2 is stabilized through electrostatic and steric repulsion among the MWCNTs2 via the poly(sodium styrene sulfonate) brushes.

When the same hairy latex (SET-111) was used to stabilize the SWCNTs in mixing experiment (MJ14), the dispersion had only short term colloidal stability, but after one month the SWCNTs flocculated as large aggregates. The reason behind the difference in stability between MWCNTs2 and SWCNTs is that the former appears as a sticking sheet and needs to exfoliated for a longer time rather than the 15 minutes performed in our experiment. In contrast, the MWCNTs2 just need high speed mixing for a short time period to disentangle the MWCNTs2.

Similar behaviour was also observed when hairy latex particles (SET-118) with high density and long poly(sodium styrene sulfonate) brushes were used to disperse the SWCNTs as short term stability was only detected as in mixing experiment (MJ19); the SEM image of the dispersion (MJ19) is shown in Figure 7. The SEM image shows strong interaction between the SWCNTs and SET-118 latex particles, but still some of the SWCNTs need to be exfoliated.

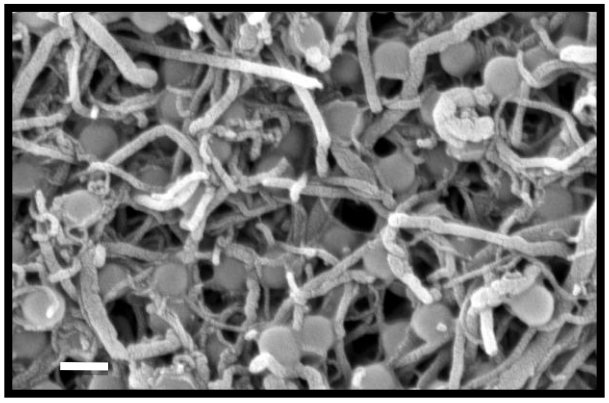

SEM of MJ13

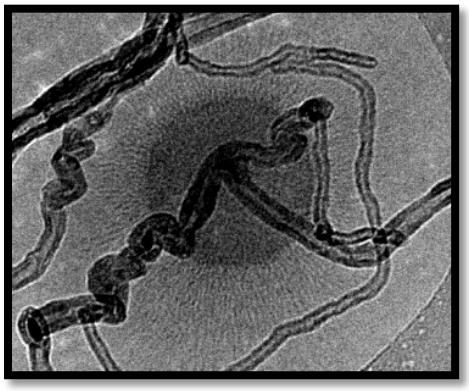

close up image of Cryo-TEM image of MJ13

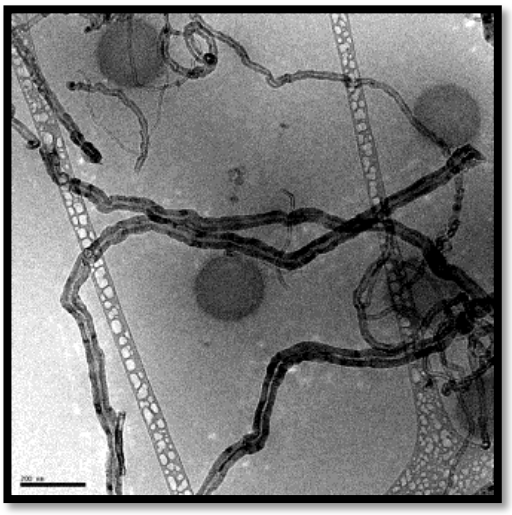

a

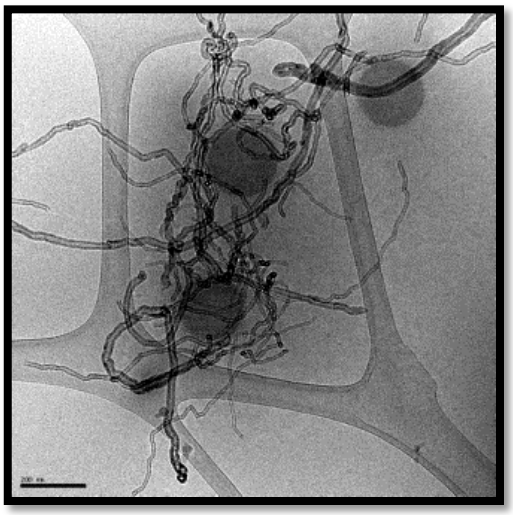

b

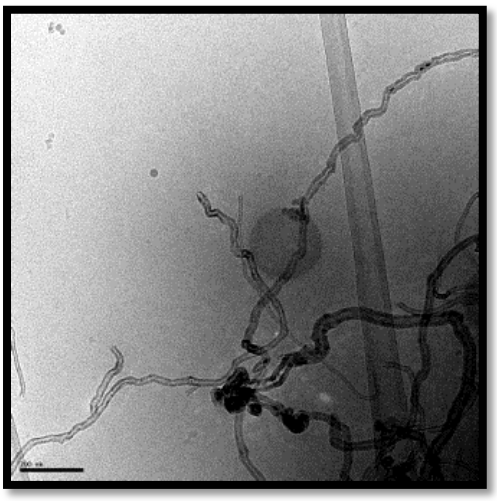

C

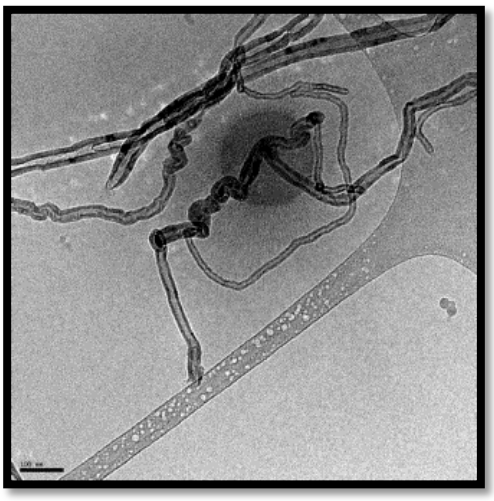

d

Fig.6. SEM image of MJ13. Scale bar is 200 nm, and Cryo-TEM image of MJ13. Scale bars in (a), (b) and (c) are 200 nm, and 100 nm in (d).

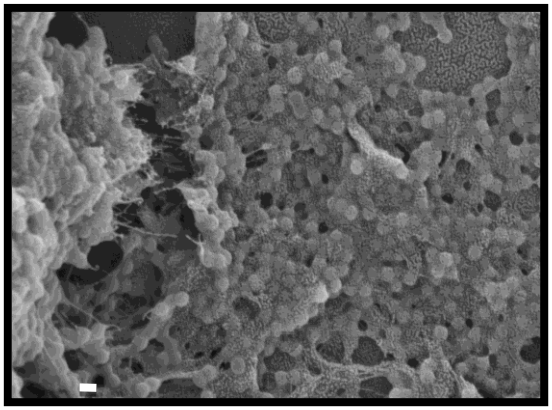

Fig.7. SEM image of MJ19. Scale bar in the image is 200 nm.

7.2.4.2. Formation of stable waterborne dispersion of carbon nanotubes using "hairy Janus" latex particles.

As observed in the previous part that the hairy latex particles with Poly(sodium styrene sulfonate) brushes are able to form waterborne dispersion of MWCNTs2. Here we will investigate the usage of the hairy Janus particles with different types of polymer brushes to stabilize CNTs dispersion as ordinary surfactants do. Table 3 showed the recipe and the conditions used to stabilize CNTs by using different types of Janus Particles.

In a control experiment when dumbbell shaped non-hairy Janus particles (SW-298) were used to disperse the MWCNTs2 in experiment (MJ21); the MWCNTs2 dispersion just sediment directly after the mixing .This also proves that the brushes in the hairy particles play a significant role in the dispersion of the MWCNTs2. The photograph of MJ21 is shown in the figure 8. At the same time another experiment was performed using of hairy-Janus particles SET-140 and SET-155. Both Janus particles have a hydrophobic surface domain crosslinked poly(styrene) and a hydrophilic domain which contains short poly(styrene sulfonate) brushes, and long poly(styrene sulfonate) brushes in the case of SET-155. In the case of SET-140,

Table.3. Recipe and conditions used to disperse the CNTs with using hairy Janus latex particles : (a) type number one (MWCNTs1), (b) type number two (MWCNTs2) and (C) is SWCNTs, (J/M) ratio of Janus latex particles to CNTs. The mixing was performed with using digital sonifier.(PNIPAM) poly(*N*-isopropyl acrylamide), (PNaSS) Poly(sodium styrene sulfonate), (PPEGMEA) poly[poly(ethylene glycol methyl ether) acrylate],P(MAETACL) Poly[2-(methacryloyloxy)ethyl]-trimethyl ammonium chloride], (PHEA) Poly(2-hydroxy ethyl acrylate), (PSPMA) poly(sulfo propyl methacrylate).

EXP	Latex	Brush type	Bruhs density	Brush length	Latex (mL)	Latex (g)	CNT_s (g)	H_2O (mL)	Ratio (J/M)	Time of mixing (min)
MJ21	Sw-298	-----	-------	-------	1.0	0.015	(b) 0.01	15	1.5	15
S9	SET-140	P(NaSS)	high	Short	5.2	0.0029	(b) 0.014	10.0	0.20	30
S1	SET-155	P(NaSS)	High	Long	6.0	0.012	(a) 0.01	4.0	1.2	30
MJ24	SET-155	P(NaSS)	High	Long	4.0	0.008	(c) 0.01	11.0	0.80	15
MJ10	SET-149	P(NaSS)	High	Short	5.0	0.015	(b) 0.01	10.0	1.5	30
MJ3	Sw-273	P(NaSS)	Low	Long	5.0	0.0049	(b) 0.01	10.0	0.49	30
MJ25	SET-163	P(SPMA)	High	Short	4.0	0.0205	(b)0.01	11.0	2.05	15
MJ5	SET-151	P(MAETACL)	High	Short	5.0	0.0215	(b) 0.01	10.0	2.15	30
MJ6	SET-153	P(PEGMEA)	High	Short	5.0	0.005	(b) 0.01	10.0	0.50	30
MJ18	SET-158	P(HEA)	High	Short	4.0	0.01	(b) 0.01	10	1.0	15
MJ22	SET-158	P(HEA)	High	Short	4.0	0.01	(c) 0.01	11.0	1.0	15
MJ9	SET-152	P(NIPAM)	High	Short	5.0	0.0048	(b) 0.01	10.0	0.48	30

SET-140 was mixed with MWCNTs2 in mixing experiment (S9) and SET-155 was mixed with MWCNTs1 in mixing experiment (S1) for 30 minutes at room temperature. Both Janus particles were able to form stable dispersion of the two types of MWCNTs for short term stability (one month); after that the MWCNTs starts to form flocculants on the top of the dispersion or sediment on the bottom of the dispersion. The photographic images of both dispersions are shown in Figure 8 and the status of the dispersion stability is indicated in Table 4.

S9 S1

Fig.8. Photograph of different dispersions of CNTs after mixing with non-hairy Janus particle in experiment (MJ21) and with hairy Janus Particles with Poly(sodium styrene sulfonate) brushes in experiments (S1, S9,MJ24,MJ10 and MJ3).

SEM images for both dispersions were taken directly after the formation of the dispersion. The SEM image indicates a strong interaction between MWCNTs2 and SET-140, and between MWCNTs1 and SET-155, as can be seen in Figure 9. The SEM image of S9 and S1 shows very good distribution of hairy Janus particles around the MWCNTs.

Table.4. Short and long term stability of the CNTs dispersion stabilized by hairy Janus latex particles.

MWCNTs dispersion	Short term stability (one week)	Long term stability (1 month)
S1	Stable	Unstable
S9	Stable	Unstable
MJ3	Stable	Stable
MJ5	Stable	Unstable
MJ6	Stable (with foams)	Unstable
MJ9	Stable (with foams)	Stable
MJ10	Stable	Unstable
MJ18	Stable	Unstable
MJ21	Unstable	Unstable
MJ22	Stable	Unstable
MJ24	Stable	Unstable
MJ25	Stable	Stable

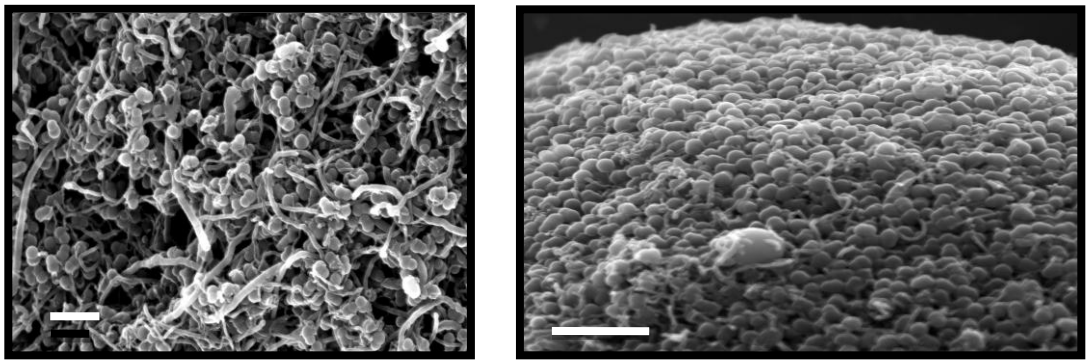

S9 **S1**

Fig.9.SEM images of the dry dispersion of S9 and S1 MWCNTs dispersions. Scale bar in S9 is 200 nm and 1.0 µm in S1.

In order to expand our visualization to see how these particles interact with the MWCNTs in the wet state inside the aqueous dispersion instead of just seeing the interaction after drying as can be concluded from the SEM image, Cryo-TEM images for both dispersions were taken, and can be seen in figure 10 in the case of S9 and in 11 in the case of S1.

As can be seen in the Cryo-TEM images of S9, the MWCNTS2 adheres to the hydrophilic domain (hairy side) that contains poly(sodium styrene sulfonate) brushes selectively, contrary to our expectations, since the MWCNTS has a hydrophobic character that should lead them to adhere selectively to the hydrophobic domain of Janus particles to minimize their contact with water; but the MWCNTS2 interacts with the hairy hydrophilic side of the Janus particles, and the hydrophobic domain faces the water phase; perhaps this is a potential reason for the short term colloidal stability of the MWCNTs2 dispersion using Janus particles SET-140. In the case of SET-155 the same behaviour was observed: the MWCNTs1 adheres selectively to the hairy domain of the Janus particles. It is worth mentioning that the SET-155 Janus particles have long poly(styrene sulfonate brushes) which almost cover the

hydrophobic domain (see Chapter 6) and this is the possible reason why in some cases the MWCNTs stick to the hydrophobic domain.

To examine the reproducibility of the obtained results, another hairy Janus latex particles with short poly(sodium styrene sulfonate) SET-149 was used in experiment (MJ10), the MWCNTs2 dispersion shows very good short term stability, but the dispersion starts to form flocks after one month, which indicates poor long term

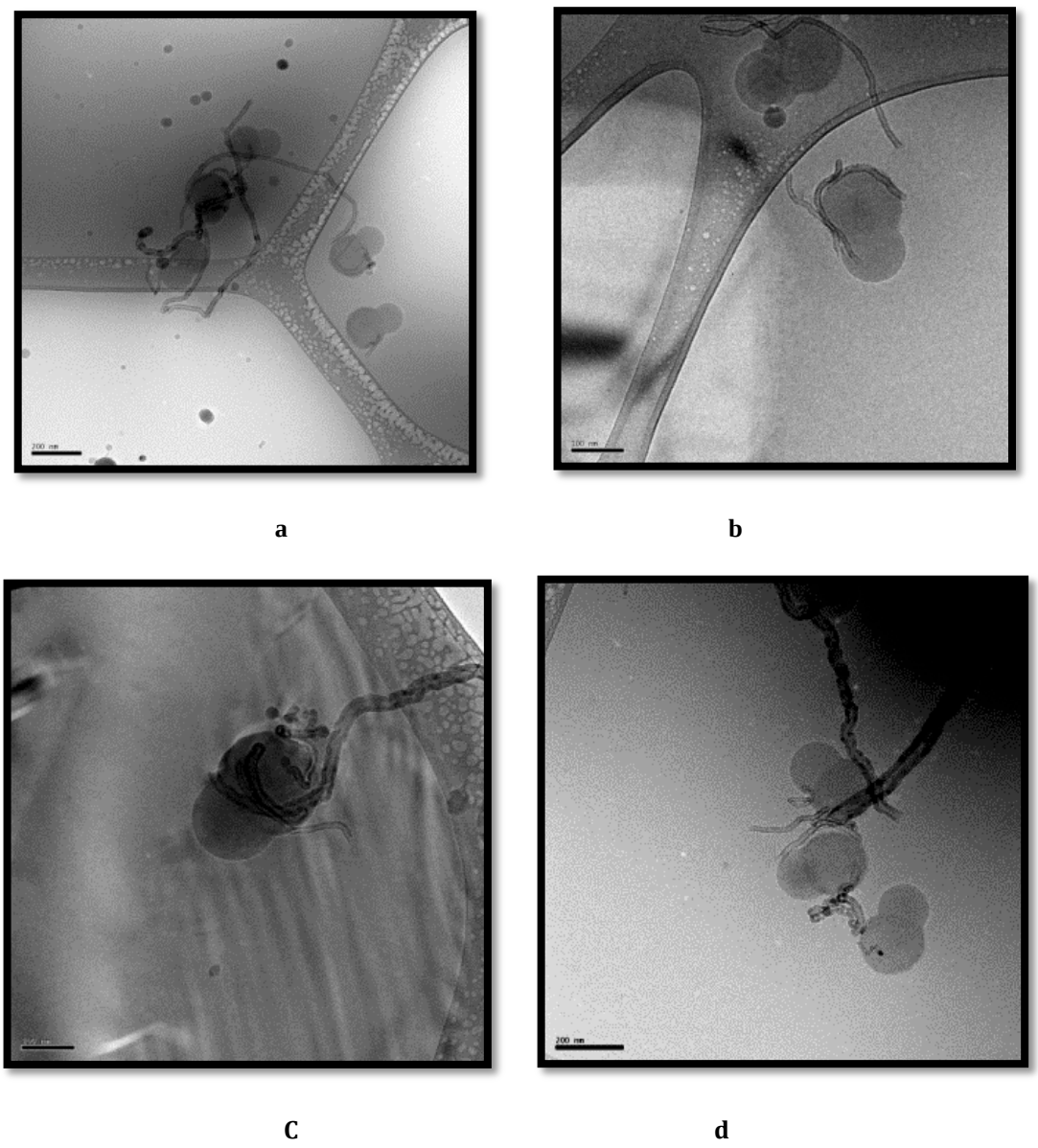

Fig.10. Cryo-TEM images of S9. Scale bar in (a) and (d) is 200 nm, and 100 nm in (b) and (c)

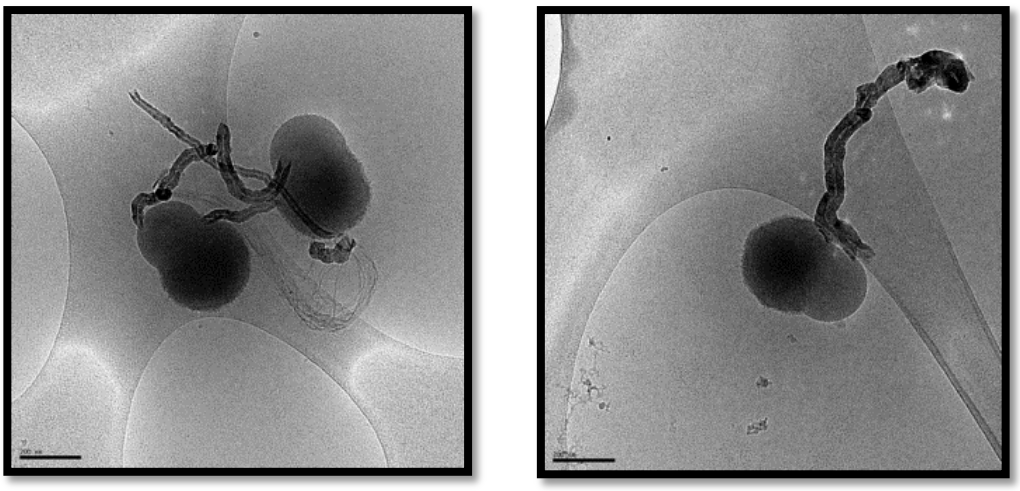

Fig.11. Cryo-TEM image of S1. Scale bar in the image is 200 nm.

stability; this behaviour was observed precisely in the case of (S9) and even in the case of (MJ10), which used even a 7 times higher concentration of Janus hairy particles. Like hairy latex, hair-Janus latex (SET-155), which is a Janus particle with long poly(sodium styrene sulfonate) brushes was only able to stabilize the SWCNTs dispersion in short term period, as observed in mixing experiment (MJ24). The SEM image of (MJ24) shows that the latex SET-155 has a strong interaction with the SWCNTs, but still the majority of the SWCNTs need to be exfoliated.

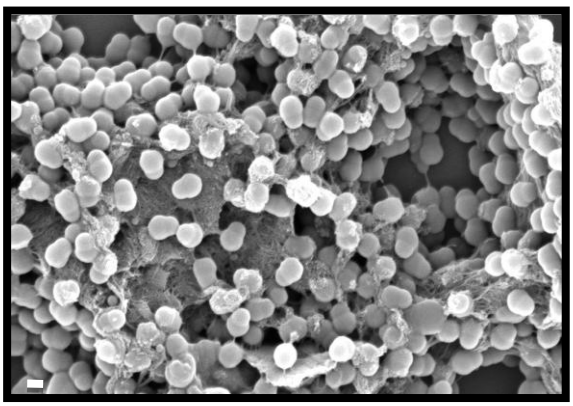

Fig.12. SEM of MJ24 mixture. Scale bar in the image is 200 nm

Conversely, hairy Janus particles with low brushes density as were made by the batch addition method, as in the case of SW-273 was mixed with MWCNTs2 in experiment (MJ3); the SEM and Cryo-TEM images of (MJ3) are shown in figure 13.

The SEM image shows a very good distribution of Janus particles SW-273 through the MWCNTs2, and the Cryo-TEM images show a selective adhesion of MWCNTs2 to the hydrophilic hairy domain that contains poly(styrene sulfonate) brushes. The poly(styrene sulfonate) brushes are not visible because the brushes were formed by the batch addition method which led to low density brushes

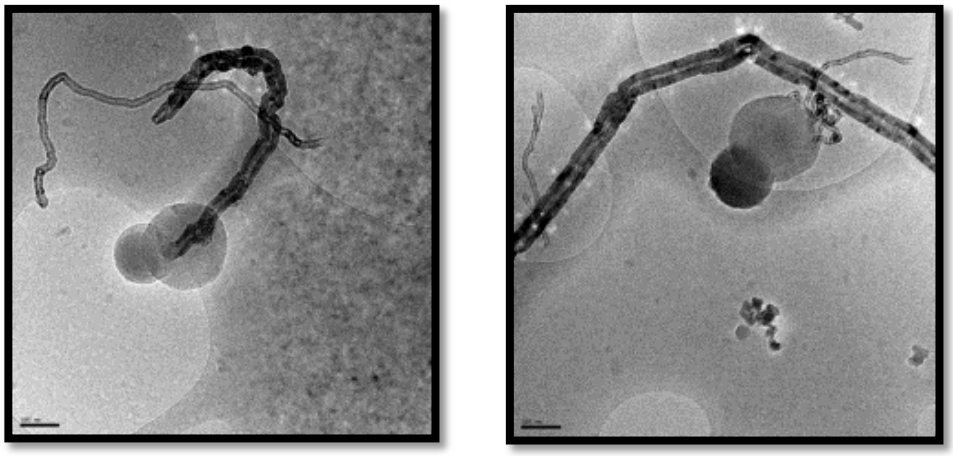

Cryo-TEM of **MJ3**

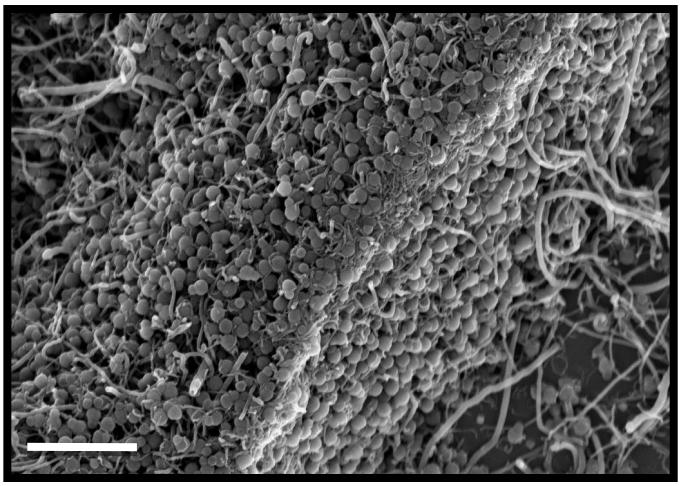

SEM of **MJ3**

Fig.13. SEM and Cryo-TEM images of MJ3. Scale bar in Cryo-TEM is 100 nm and 1.0 µm in SEM

The (MJ3) dispersion shows very good dispersion for even long term stability, in contrast to its counterpart (S9) which shows only short term stability, and this could be attributed to the low ratio of (J/M) used in (S9) which is only 0.20 indicating that

a sufficient amount of hairy and hairy-Janus particles are required to form long term stable MWCNTs2 dispersion.

Latex SET-163, which is a hairy Janus particle with poly(3-sulfopropyl methacrylate) brushes, was used to disperse the MWCNTs2 in mixing experiment (MJ25); the dispersion shows very good short and long term stability. This indicates that the negatively charged brushes of (3-sulfopropyl methacrylate) play a role in stabilizing the MWCNTs2 as in the case of poly(sodium styrene sulfonate). The SEM image of (MJ25) shows a very good distribution of SET-163 through the MWCNTs2 as showed in figure 14.

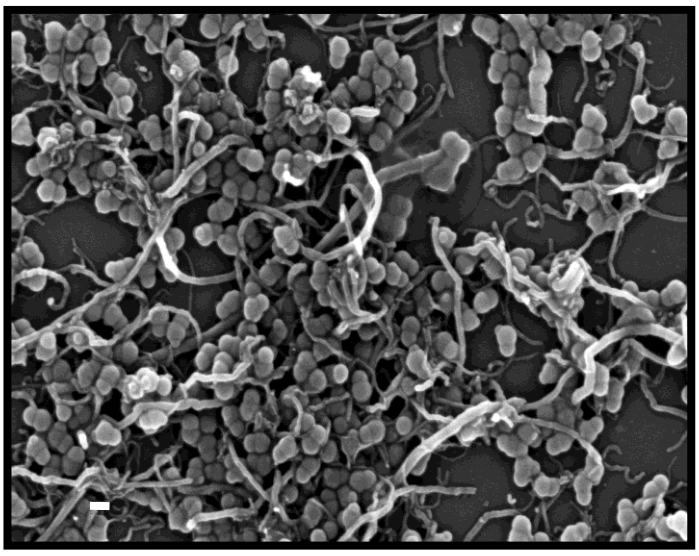

Fig.14. SEM of MJ25. Scale bar in the images is 200 nm.

Another type of Janus particles which consists of another kind of brushes, such as SET-151 which has cationic poly[2(methacryloyloxy) ethyl]-tri methyl ammonium chloride] brushes was mixed with MWCNTs2 in experiment (MJ5), Dispersions MJ5 have only short term colloidal stability of less than one month. Figure 15 shows the photograph of MJ5 and MJ25 dispersions.

Fig.15. Photograph of MWCNTs2 after mixing with hairy Janus particle SET-151 in experiment (MJ5), and with hairy Janus Particles SET-163 brushes in experiments (MJ25).

The Cryo-SEM images for MJ5 are shown in Figure 16. The Cryo-SEM image shows a clear strong interaction between the MWCNTs2 and the cationic Janus particles SET-151. This indicates that not only the poly(sodium styrene sulfonate) brushes on Janus particles are able to stabilize the MWCNTs2 but that also cationic Janus particles could play the same role; but only for short term colloidal stable dispersion occurred when hairy cationic Janus particles were used.

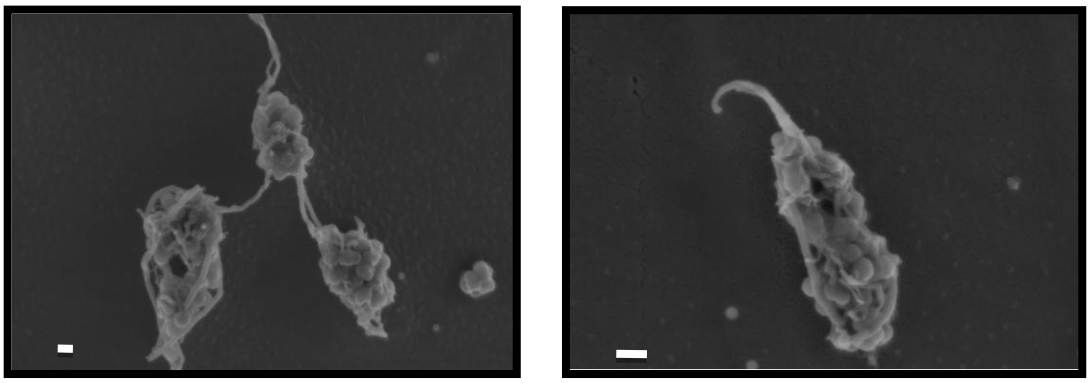

Fig.16. Cryo-SEM images of MJ5. Scale bar in both images is 200 nm.

Hairy-Janus particles with non-ionic brushes were used as in mixing experiments (MJ6, MJ18, MJ22 and MJ9). Only hairy Janus particles with Poly(NIPAM) brushes show long and short term stability of MWCNTs2 as in mixing experiment MJ9. The SEM and Cryo-TEM images for MJ9 are shown in Figure 17.

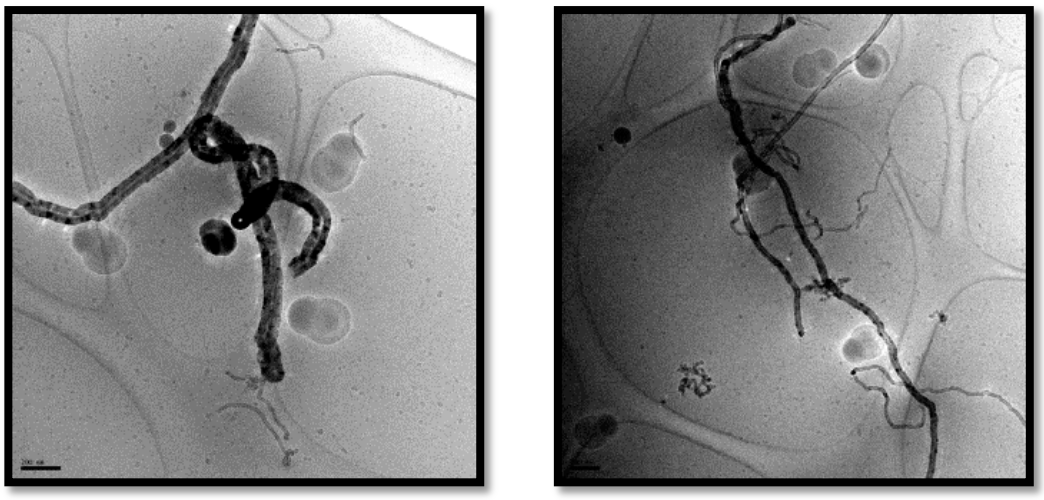

Cryo-TEM of **MJ9**

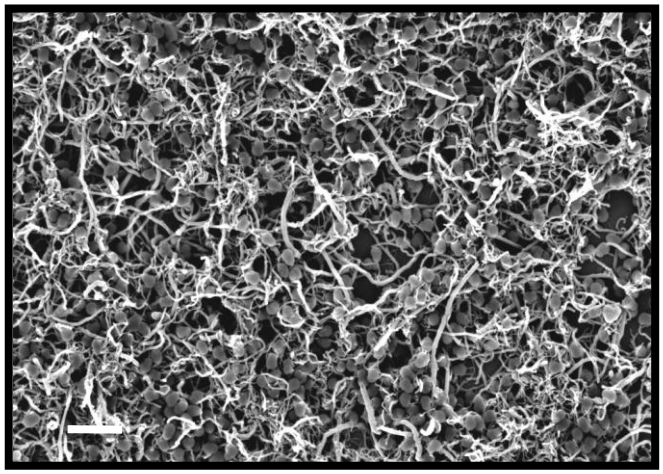

SEM of **MJ9**

Fig.17. SEM and Cryo-TEM images of MJ9. Scale bar in the SEM image is 1.0 μm and 200 nm in the Cryo-TEM image.

The SEM image of (MJ9) shows a very good distribution of non-ionic Janus particles which contain short poly(NIPAM) brushes through the MWCNTs2, and the Cryo-TEM image shows the non-selective adhesion of Janus particles in the wall of MWCNTs2; this indicates that in the case of the Janus particles with poly(NIPAM) brushes, both domains are effective in stabilizing the MWCNTs and this is the possible reason for the strong activity of these types of Janus particle in stabilizing the MWCNTs. Janus-hairy particles with non-ionic brushes consisting of poly(ethylene glycol methyl ether acrylate) (PEGMEA) as in SET-153 latex, which

is mixed with MWCNTs2 in mixing experiment (MJ6). Dispersions MJ6 have only short term colloidal stability of less than one month stability with a lot of foam generated.

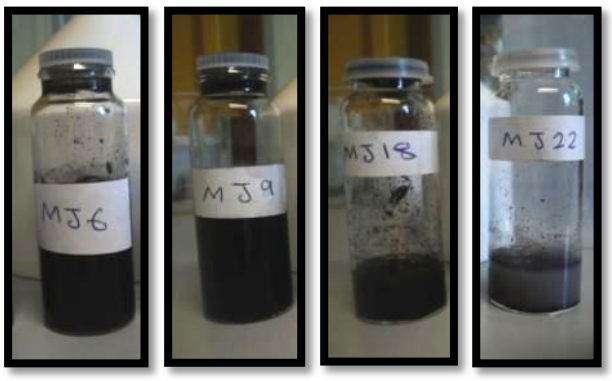

Fig.18. Photograph of MWCNTs2 after mixing with non-ionic hairy Janus particle.

Non-ionic hairy Janus particle with poly(2-hydroxy ethyl acrylate) brushes SET-158 was used to stabilize both the MWCNTs2 and the SWCNTs in mixing experiments (MJ18) and (MJ22) respectively, both CNTs dispersions showed only short term stability and flocculation occurred one month after the mixing; this indicates that the poly(2-hydroxy ethyl acrylate) brushes are not effective in binding with the CNTs. The SEM image of (MJ22) is shown in Figure 19; shows that the SWCNTs are not very well distributed and there is no clear adhesion of Janus particles SET-158 with the SWCNTs.

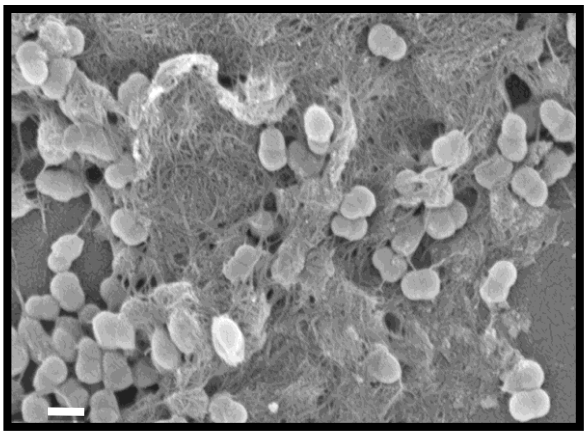

Fig.19. SEM images of MJ22. Scale bar in the image is 200 nm.

7.2.4.3. Formation of the Carbon nanotubes-Latex nanocomposite

After the observations that indicate that some hairy latex (core-shell) and hairy Janus particles are very good for forming stable aqueous dispersion of MWCNTs2, these MWCNTs2 dispersions were used as filler with a low ratio below 3% to mix with different types of waterborne spherical latexes such as normal spherical cross-linked poly(styrene) as PS-26 latex, and soap-free copolymer of (methyl methacrylate 40% and 60% butyl acrylate)- (Latex A), and the commercial latex of copolymer(styrene-butyl acrylate-acrylic acid) (Latex B) that contains surfactant. This concentration of MWCNTs2 filler is commonly used in commercial products to improve the mechanical and electrical properties of the final product. Table 5 shows the formulations that were used to form the latex-MWCNTs nanocomposites.

Table.5. Formulations used to make the CNTs-Latex nanocomposite. PS26 is cross-linked poly(styrene) latex made by soap-free emulsion polymerization. Latex A is (copolymer latex of PMMA 40% - PBA 60%) made by soap-free emulsion polymerization. Latex B is commercial latex consist of (copolymer latex of styrene – BA – AA). The nanocomposites were formed after mixing the filler (stabilized aqueous dispersion of CNTs by complex latex) with different types of spherical latex particles in glass jar by a magnetic stirrer at high speed for 30 minutes at room temperature.

Exp	Latex	Latex (mL)	Filler dispersion	Filler %	Stability
NC1	PS26	10	MJ3	2.85	stable
NC2	PS26	10	MJ2	2.85	stable
NC3	PS26	10	MJ1	2.85	stable
NC4	PS26	10	MJ9	2.85	stable
NC5	Latex A	15	MJ22	2.30	unstable
NC6	Latex A	15	MJ18	2.30	unstable
NC7	Latex A	15	MJ14	2.30	unstable
NC8	Latex A	15	MJ13	2.30	stable
NC9	Latex B	5.0	MJ18	0.42	stable
NC10	Latex B	5.0	MJ19	0.42	stable

Aqueous dispersions of MWCNTs2 (MJ3, MJ2, MJ1 and MJ9) were used as fillers for the latex PS-26 to form stable aqueous dispersion nanocomposites NC1, NC2,

NC3 and NC4 respectively as shown in photographic image 20. The SEM images of the nanocomposites are shown in figure 21.

Fig.20. Photograph of the CNTs-Latex nanocomposite in water of NC1, NC2, NC3 and NC4.

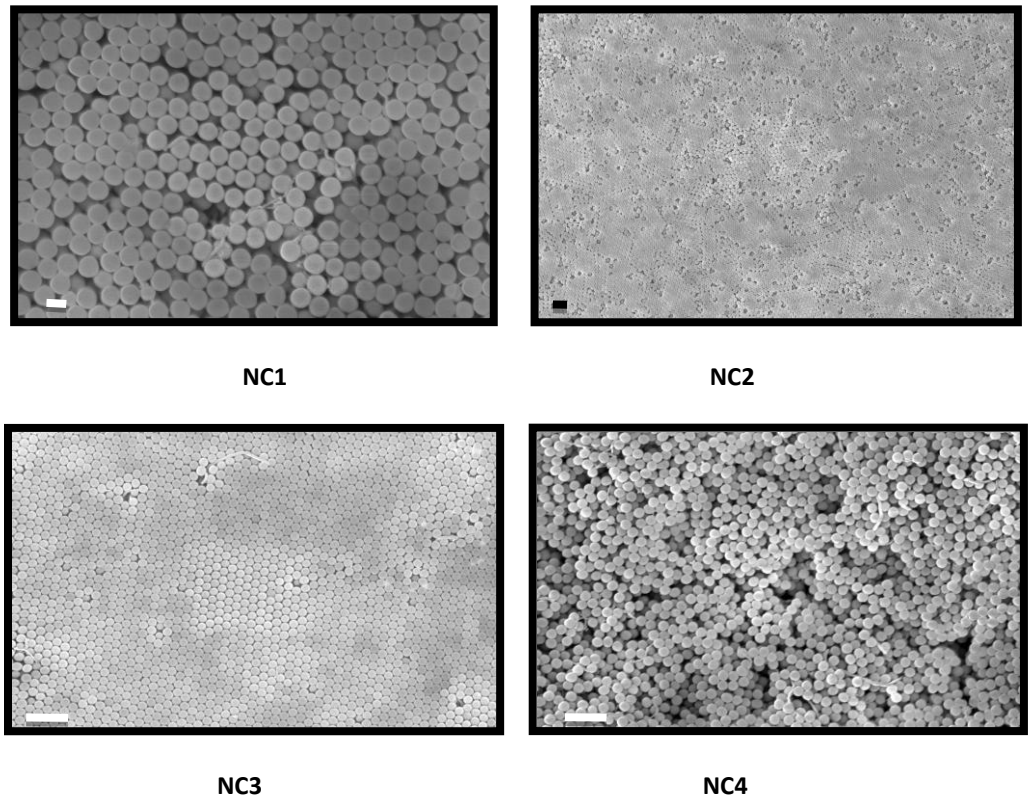

Fig.21.SEM images of nanocomposites of NC1, NC2, NC3 and NC4. Scale bar in NC1 is 200 nm, and in the rest of the images is 1.0 μm.

The SEM images of the four nanocomposites show that the MWCNTs2 are well distributed through the latex particles. It was also noticed that the filler aqueous dispersion of MWCNTs2 that stabilized with spherical hairy (core-shell) particles, which mixed with the spherical particles PS-26 to form the nanocomposites NC2 and

NC3 led to the formation of very well ordered colloidal particle arrays, in contrast to NC1 and NC4 which were mixed with aqueous MWCNTs2 dispersion that stabilized with hairy Janus particles. These nanocomposites do not form arrays like those formed in NC2 and NC3. A possible reason for this is the non-spherical Janus particles distract the ordering of the spherical particles as it has dumbbell shape morphology. The Cryo-TEM was used to visualize the nanocomposite in its aqueous state as showed in figure 22.

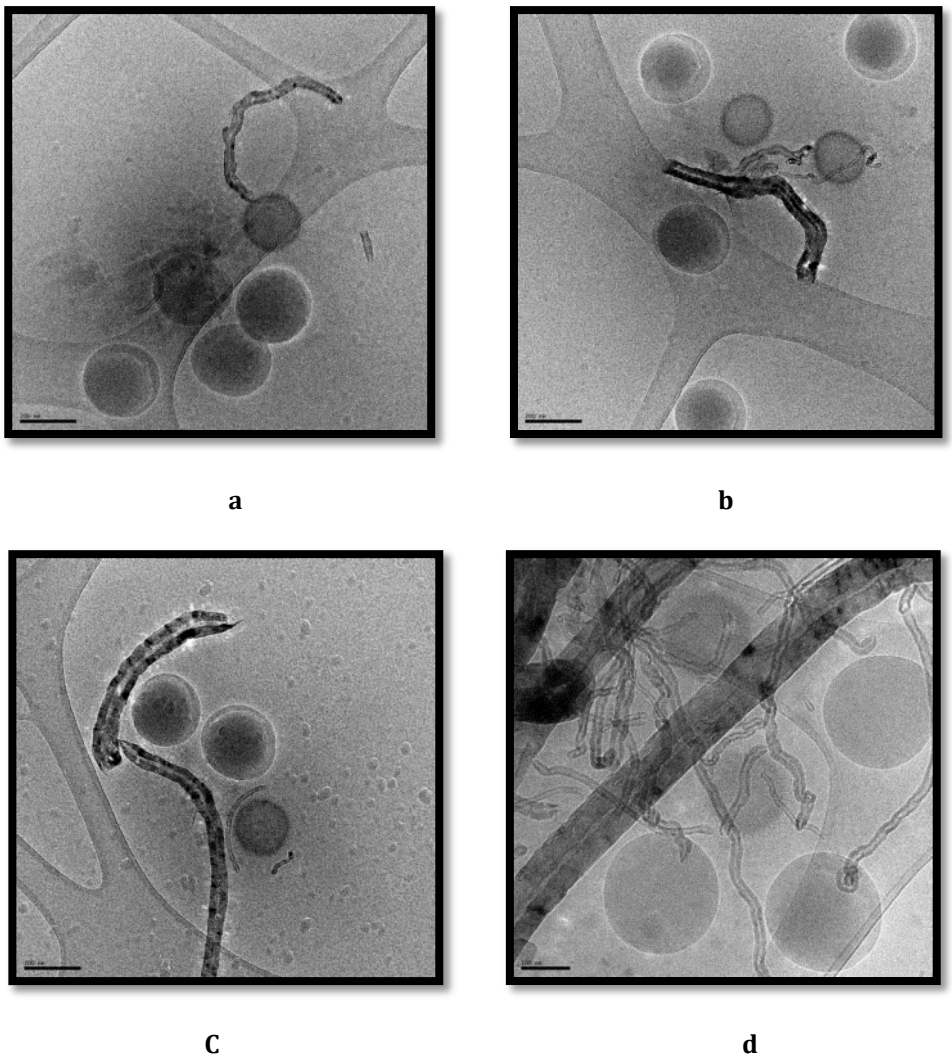

Fig.22. Cryo-TEM images of (NC2) nanocomposites. Scale bar in (a), (b) and (c) is 200 nm, and is 100 nm in (d).

Nanocomposite NC2, which is mixed with MWCNTs2 filler stabilized by visible hairy (core-shell) latex particles SET-171 containing poly(sodium styrene sulfonate),

was visualized by Cryo-TEM; the Cryo-TEM images of NC2 are shown in figure 22. The Cryo-TEM image shows that the hairy latex (SET-171) gathers or holds the MWCNTs2 and disperses them through the spherical latex particles PS-26, and this moreover indicates that the brushes are the key factor in achieving and stabilizing the MWCNTs2 dispersion.

Conversely, when the CNTs aqueous dispersions that showed only short term stability were used as filler for the spherical soap free PMMA–PBA (latex A) particles, the formed nanocomposites did not form a homogenous mixture and the MWCNTs2 just phase separated, as in the case of the nanocomposites NC5, NC6 and NC7. However, when the MWCNTs2 dispersed with SET-111 (MJ13 dispersion), which shows long term dispersion stability used as a filler for PMMA-PBA soap-free latex particles, the formed nanocomposite had a homogenous mixture and stable dispersion as nanocomposite NC8. Photographs of the nanocomposites NC5, NC6, NC7 and NC8 are shown in figure 23.

Fig.23. Photograph of the CNTs-Latex nanocomposites in water of NC5, NC6, NC7 and NC8.

The Cryo-TEM image of the nanocomposite NC8 is shown in figure 24. The Cryo-TEM image shows that the MWCNTs2 adheres selectively to the SET-111 which gathers and holds the MWCNTs2 through the PMMA-PBA spherical latex particles;

this is also evidence that the brushes on the surface of the latex particles are the major cause of the dispersion of MWCNTs2.

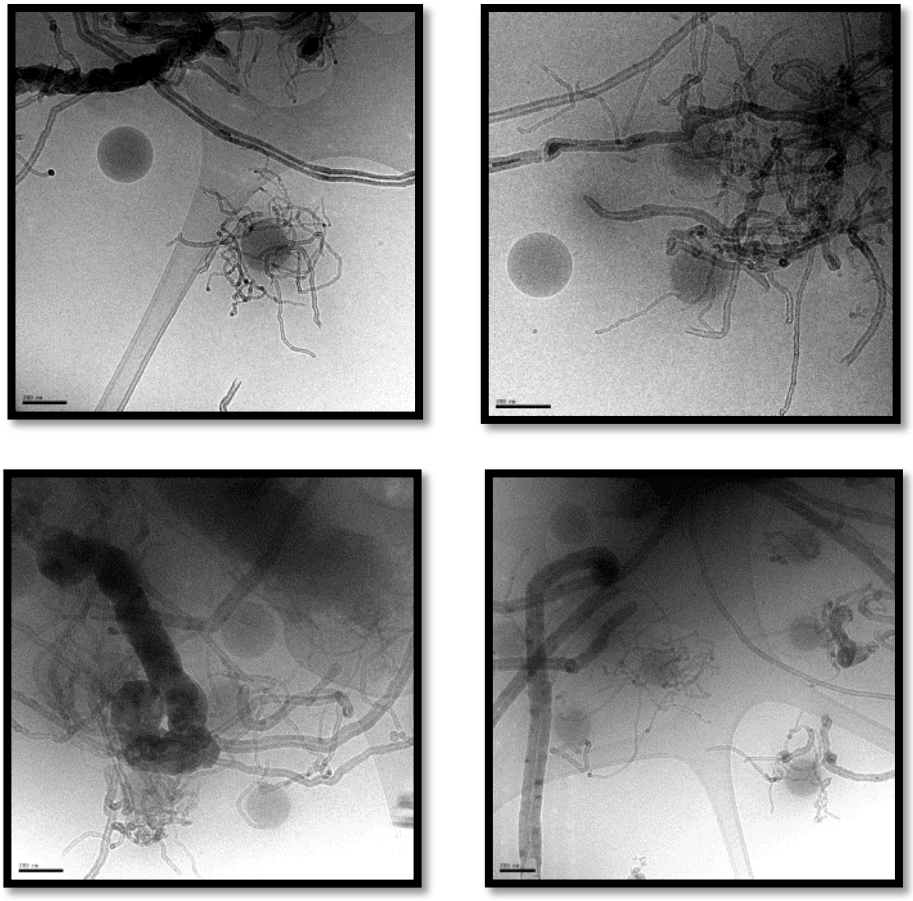

Fig.24. Cryo-TEM images of Nanocomposite NC8. Scale bar in all images is 200 nm.

Commercial latex consisting of poly(Styrene-BA-AA) (latex B) which contains a surfactant was also used as a matrix to form a nanocomposite with non-long term dispersions of carbon nanotubes MJ18 and MJ19 to form the nanocomposites NC9 and NC10 respectively. Both nanocomposites show very good dispersion and homogeneity as shown in figure 25. The reason behind the formation of good dispersion, even when the non-long term CNTs dispersions were used as filler, is the presence of the surfactant in the commercial latex, which works to stabilize the CNTs.

Fig.25. Photograph of the CNTs-Latex nanocomposites in water of NC9 and NC10**.**

7.2.5. Conclusion

The usage of different types of complex latex particles, including spherical particles, hairy core-shell particles, hairy Janus particles and non-hairy Janus particles, as aqueous phase stabilizers for carbon nanotubes (CNTs) was investigated.

The normal anionic spherical latex particles are not good for the stabilization of the CNTs, therefore an adjustment to the surface properties of the latex particles to have more complex particles is essential to compel those particles to interact with the CNTs. Based on this, when complex particles were used an interaction was observed; for instance it was observed that hairy Janus particles with short or long poly(sodium styrene sulfonate) or poly(sulfo propyl methacrylate) brushes are good aqueous phase stabilizers for multi-walled carbon nanotubes (MWCNTs) for short term stability (1 month) - after that the MWCNTs begin to flocculate and sediment.

The Cryo-TEM images suggest that the strong interaction of poly(sodium styrene sulfonate) brushes with the MWCNTs is the possible reason for the stabilization. However, the hairy core-shell particle with poly(sodium styrene sulfonate) brushes is very good stabilizer for MWCNTs for even long term stability (1year), and this is a result of the absence of the hydrophobic domains in this type of hairy particle, where

the attractive forces among them lead to flocculation and sedimentation of MWCNTs. Hairy Janus particles with cationic brushes are also good for only short term stability. And when hairy Janus particles with non-ionic brushes of poly(PEGMEA) were used, short term stability was also observed with a huge amount of CNTs foam generated.

In the case of hairy Janus particles with poly(NIPAM) brushes, a long term stability was also observed, and that is not the case when hairy Janus particles with poly(2-hydroxy ethyl acryalet) were used, which is only provide short term stability for the aqueous dispersion of MWCNTs. Conversely, when non-hairy Janus particles were used, a direct phase separation was observed, as in the case of spherical anionic latex particles. This indicates that the presence of polymer brushes is essential to provide stability for MWCNTs.

The stable aqueous dispersions of MWCNTs that were stabilized by complex latex particles were used as filler with less than a 3% ratio of MWCNTs to the latex matrix to form nanocomposite dispersions. Three types of spherical latex particle were used as the matrix; soap-free cross-linked poly(styrene), soap-free copolymer of 40% methyl methacrylate-60% butyl acrylate, and commercial copolymer latex of (styrene-butyl acrylate-acrylic acid) latex that contains on ordinary surfactant. The nanocomposites show a very good distribution of MWCNTs through the latex matrix.

7.3 Pickering stabilization using complex latex particle morphologies

7.3.1. Summary

Several types of complex latex particles with different morphologies synthesized in absolutely soap-free conditions, and their use as Pickering stabilizers, were investigated using two immiscible liquids. Dodecane, hexadecane and paraffin wax were used as the oil phases and water as the polar phase. It was observed that ionic particles, whatever their morphology (spherical, hairy, patchy hairy, hairy Janus and non-hairy Janus particles) were strongly hydrophilic and tended to remain in the water phase; however; non-ionic particles, whatever their morphology, tended to form stable Pickering emulsions. We propose that there are two main factors for forming stable Pickering emulsions: the presence of non-ionic polymer brushes on the surface of the latex particles, as in the case of hairy latex with brushes, e.g. poly(*N*, *N*-dimethyl acrylamide) and poly(PEGMEA) brushes, and the amphiphilic nature of hairy Janus particles.

7.3.2. Introduction

The term Pickering emulsion refers to an emulsion system (*e.g.* oil droplets dispersed in water) stabilized by solid particles adhered to the liquid-liquid interface, in contrast to conventional stabilization methods which involve the use of surfactants. Pickering used this method following early work in this area by Ramsden [17, 18]. In conventional emulsions, stabilization by normal low molecular weight surfactants is driven by the fact that the surfactant molecules in aqueous solution tend to adsorb at the interface in the form of a monolayer [19]. This adsorbed surfactant declines the overall surface energy and provides colloidal stability to the emulsion, preventing for instance the latex particles from flocculating and

coagulating. The most applicable surfactant is an anionic surfactant, which has a long hydrophobic tail (for example a C_{12} hydrocarbon chain) and a small hydrophilic head including sulfate or carboxylate groups. In the case of an oil/water emulsion, stability is gained by the presence of negative charges on the surface of the oil droplets as a result of the adsorption of surfactant molecules. Consequently, the oil droplets repel each other via electrostatic repulsion and stable oil droplets are formed this process known as electrostatic stabilization.

In Pickering emulsions, stabilization arises from the fact that the solid particles partially wet the two phases (oil and water) and are positioned at the interface, thereby lowering the overall interfacial energy. Once a Pickering emulsion is established, the adhesion of these particles on an interface such as oil/water is remarkably strong. As a result, the adhesion of the particles is generally irreversible with energies several magnitudes greater than the thermal energy (k_BT) [20]. There are several parameters that influence the adhesion of particles to the oil/water interface, such as the type of oil (its surface tension) and the contact angle $\phi^{o/w}$, whereby hydrophilic particles tend to have a lower contact angle and therefore an (o/w) emulsion forms; for more hydrophobic particles, the contact angle will be greater as an (w/o) emulsion forms [21]. Several types of particles with different chemical compositions and shapes have been investigated in the literature. In particular, silica particles have been used frequently. These researches have shown that by altering the silica particle's hydrophilicity and by varying the relative volume fraction of water and oil, dramatic phase inversion of the emulsion occurs [22, 23]. Laponite clay, which does not have a spherical shape, but is rather discotic, has also been used as a Pickering stabilizer [20]. Pickering emulsions are frequently applied in the food, cosmetic, petrochemical and oil-refining industries. The formation of supracolloidal

structures using the liquid-liquid or liquid-gas interface-driven assembly of solid particles is an important area of research, such as the synthesis of hollow supracolloidal structures via the assembly of poly(styrene) particles at the interface of emulsion droplets. These were coined as colloidsomes by Dinsmore *et al*. [24].

One interesting application of a particle-stabilized emulsion is to use the particles as stabilizing agents during dispersion polymerizations such as (emulsion, miniemulsion and suspension) in order to prevent the coalescence and coagulation of the monomer droplets and polymer colloidal particles formed by polymerization. In emulsion polymerization, Müller *et al*, used disk-shaped amphiphilic Janus particles as stabilizers [25]. They observed that the use of Janus particles led to strong, stable, colloidal latex particles with long-term stability. This was attributed to the dual function of the Janus particles that used the electrostatic effect derived from the hydrophilic part of the amphiphilic particle and the high adsorption energy derived from the Pickering effect. In suspension polymerization, hydroxyapatite and calcium carbonates were used as Pickering stabilizers with conventional surfactants consisting of sodium dodecyl benzene sulfonate (SDBS) and poly(vinyl pyrrolidone) (PVP) [26]. This work experienced some difficulties in the stabilization of the suspension by the SDBS system; this was attributed to the slow absorption of surfactant molecules on the surface of the Pickering particles. However, when PVP was used, a stable suspension was obtained. Pickering mini-emulsion polymerization has been studied by utilizing laponite clay as the stabilizing agent, and sodium chloride was used to induce instability in the clay, causing it to flocculate on the monomer droplets and polymer particles. The latex prepared by this process was initially stable, but after long-term storage, phase separation occurred. The latter was prevented after removal of the NaCl by dialysis. The kinetics of the polymerization

showed some retardation at the middle stage of conversion [20]. In this part of this chapter, the synthesized complex particles in chapters 4,5 and 6 (spherical particles, hairy particles, hairy Janus particles and non-hairy Janus particles) are investigated to be used as Pickering agents to form stable Pickering emulsions for different types of immiscible liquids.

7.3.3. Experimental

7.3.3.1 Materials

Dodecane (99%) (Sigma-Aldrich), hexadecane (99%) (Sigma-Aldrich), and paraffin wax (chunks) with melting point 54-56C° (Aldrich), complex latex particles which are synthesized in chapters 4, 5 and 6.

7.3.3.2 Apparatus

A Leica DM2500M optical microscope was used; the scale bars of the optical microscope images were calibrated using the Image J program.

7.3.3.3 Formation of the Pickering emulsion

The general procedure to form a Pickering emulsion was the following: 1.0 mL of dodecane or hexadecane was placed inside a glass vial, and then 2.0 mL of the latex dispersion was mixed with the oil phase for 1 minute by simple hand shaking at room temperature. In the case of the formation of the wax Pickering emulsion, 3.0 mL of the latex dispersion was mixed with 0.2 g of paraffin wax inside a glass vial, then placed inside an oil bath at 85°C until all the wax transformed into the liquid state. The glass vial was closed and the mixture was mixed by simple hand shaking for 1 minute; the flocculated unstable wax was removed from the dispersion by filtration.

7.3.4. Results and discussion

This section will be divided into several parts, depending on the type of complex particles used as Pickering stabilizers for different types of hydrophobic oil with water. Three types of hydrophobic oil were used: dodecane with the chemical formula $C_{12}H_{26}$ and a density of 0.75 g.cm^{-3} at 25°C, hexadecane with the chemical formula $C_{16}H_{34}$ and a density of 0.77 g.cm^{-3} at 25°C, and paraffin wax which has a melting point at 55°C.

7.3.4.1 Spherical and hairy particles as Pickering stabilizers

Table 6 shows the conditions and the outcome stability of the formed Pickering emulsion. In the beginning, simple anionic spherical PS-24 particles made by soap-free emulsion polymerization with batch addition of inimer was used as a control experiment (see chapter 2). These anionic particles were mixed with dodecane by simple hand shaking for 1 minute; complete phase separation occurred directly, which indicates that these particles are hydrophilic and tend to remain in the water phase.

This type of anionic hydrophilic particle can be induced to assemble at the oil water interface by destabilizing them in water by the addition of an electrolyte to minimize the electrostatic repulsion. This leads the particles to collects at the interface of the oil in water emulsion as can be seen in Table 6 and Figure 26. Stable dodecane oil in water emulsion with various droplet sizes from 20 to 200 µm was formed upon the addition of the electrolyte.

Table.6. Ingredients used to form a Pickering emulsion using spherical, hairy particles and an ordinary surfactant (SDS) by simple hand shaking for 1 minute at room temperature.

Latex	Oil	Particle morphology	Stability of the emulsion
PS-24 (2.0 mL)	Dodecane (1.0 mL)	Spherical particles	Phase separation
PS-24 (1.0 mL) + (1.0) of 0.1M NaCl	Dodecane (1.0 mL)	Spherical particles	Stable Pickering emulsion
SET-110 (2.0 mL)	Dodecane (1.0 mL)	Hairy Latex with Poly(NaSS) brushes	Phase separation
SET-82 (2.0 mL)	Dodecane (1.0 mL)	Hairy Latex with Poly(NIPAM) brushes	Stable Pickering emulsion
SDS (0.15%) (2.0mL)	Dodecane (1.0 mL)	Sodium dodecyl sulfate	Stable Pickering emulsion

For the purpose of comparison, an ordinary surfactant, sodium dodecyl sulfate (SDS), was used to form stable dodecane droplets dispersed in water with various droplet sizes from 20 to 200 µm, as shown in Figure 26. Based on these results, an investigation was initiated to utilize our synthesized particles with different complex surface morphologies and surface properties as Pickering stabilizers without the addition of an electrolyte.

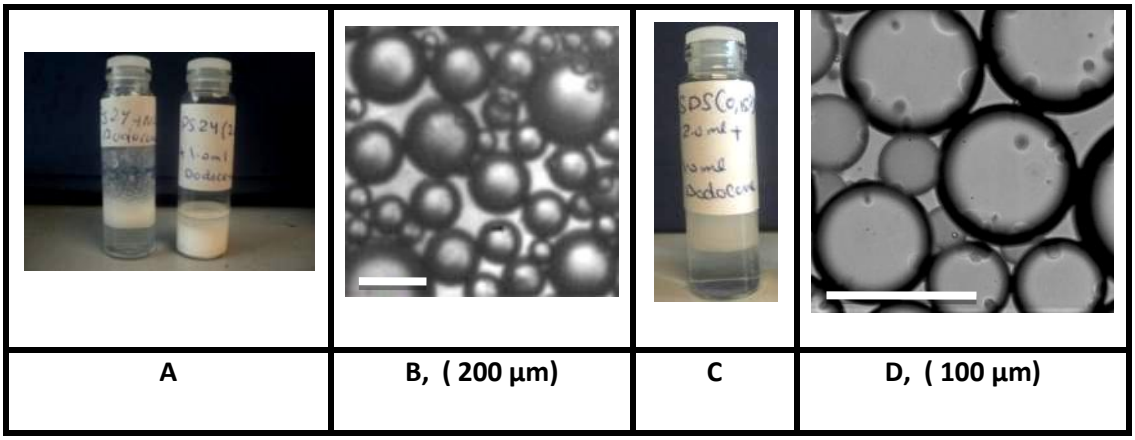

A	B, (200 µm)	C	D, (100 µm)

Fig.26. (A) Photograph of the obtained Pickering emulsion using PS24 latex as the Pickering stabilizer. In the image on the right, the latex (PS24) was used alone, and on the left an electrolyte (NaCl) was added. **(B)** Optical photograph image of the Pickering emulsion that formed upon the addition of the electrolyte (the scale bar is 200 µm). **(C)** Photograph of the Pickering emulsion that formed using SDS (0.15%). **(D)** Photograph of the Pickering emulsion that formed using SDS (the scale bar is 100 µm).

Some of those complex particles were hairy latex particles with different types of polymer brushes, for example the hairy latex particles SET-82 and SET-110. SET-82 is a hairy latex particle with poly(NIPAM) brushes; this hairy latex, when mixed with dodecane for 1 minute by simple hand shaking led to the formation of a stable Pickering emulsion with various dodecane droplets from 20-200 µm as shown in Figure 27.

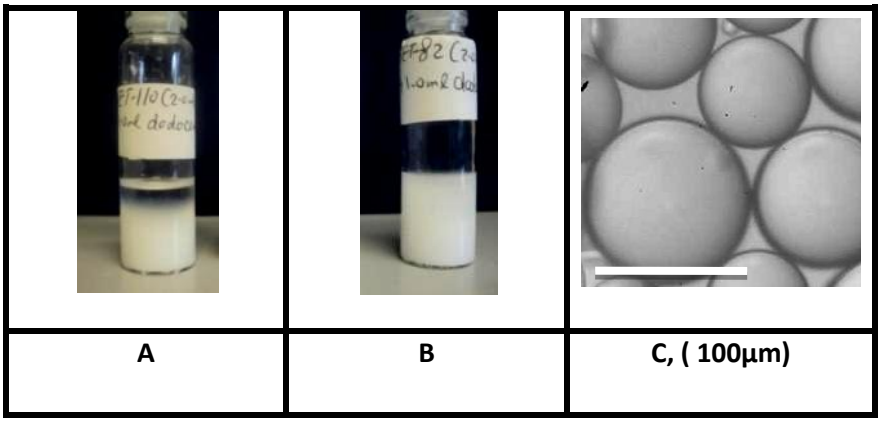

Fig.27.(A) Photograph of the phase separation formed using SET-110 hairy latex as the Pickering stabilizer. **(B)** Photograph of the Pickering emulsion that formed using SET-82 hairy latex. **(C)** Photograph of dodecane droplets stabilized by hairy latex SET-82. The scale bar is 100 µm.

In contrast, when latex SET-110, a hairy latex particle with poly(NaSS) brushes, was used as a Pickering stabilizer, direct phase separation occurred as was the case with spherical anionic latex PS-24 particles.

This indicates that the poly(NaSS) brushes have a high hydrophilic character which tends to keep the latex particles in the water phase. These results also show that the presence of poly(NIPAM) brushes on the surface of latex particles alters the surface activity of the latex particles and gives the particles a strong non-ionic character; as a result, SET-82 latex particles wet both phases to form a Pickering emulsion.

7.3.4.2 Patchy-hairy particles as Pickering stabilizers

Patchy particles are particles with a complex surface which contain multiple phases and polymer brushes with an anisotropic character. Examples of this type of particle are triplets, quartets, raspberry and popcorn morphologies (see chapters 5 and 6). Table 7 shows the different types of patchy particles and their use as Pickering stabilizers.

Table.7. Ingredients used to form Pickering emulsions using different patchy hairy particles by simple hand shaking for 1 minute at room temperature.

Latex	Oil	Particle morphology	Stability of the emulsion
SW-115 (2.0 mL)	Dodecane (1.0 mL)	Triplet with poly(NIPAM) brushes.	Stable Pickering emulsion.
SW-116 (1.0 mL)	Hexadecane (1.0 mL)	Quartet with poly(NIPAM) brushes.	Particles assembled at interface.
SW-182 (1.0 mL)	Hexadecane (1.0 mL)	Raspberry with poly(MAETAC) brushes.	Phase separation
SET-93 (2.0 mL)	Dodecane (1.0 mL)	Triplet and quartet with poly(NIPAM) brushes..	Stable Pickering emulsion.
SW-166 (2.0 mL)	Dodecane (1.0 mL)	Popcorn with poly(NIPAM) brushes.	Stable Pickering emulsion.
SW-167 (2.0 mL)	Dodecane (1.0 mL)	Popcorn with poly(SPMA) brushes.	Stable Pickering emulsion.

The triplet particles SW-115 and SET-93 contain three phases with a sandwich structure, whereby the poly(NIPAM) brushes are found in the middle of this triplet particle. The other two domains are hydrophobic cross-linked poly(styrene), which gives these triplet particles an anisotropic character. SW-115 latex particles are able to form Pickering emulsions with various dodecane droplet shapes (spherical and non-spherical) and sizes from 20 to 400 μm, and SET-93 latex particles are able to form spherical dodecane particles with different sizes from 20 to 200 μm, as can be seen in Figure 28 . The surface activity of SW-115 and SET-93 could be attributed to two factors: the anisotropic structure of the particles which make them amphiphilic,

and the presence of non-ionic poly(NIPAM) brushes which have been observed to be active as stabilizing agents, as in the case of spherical hairy particles in latex SET-82.

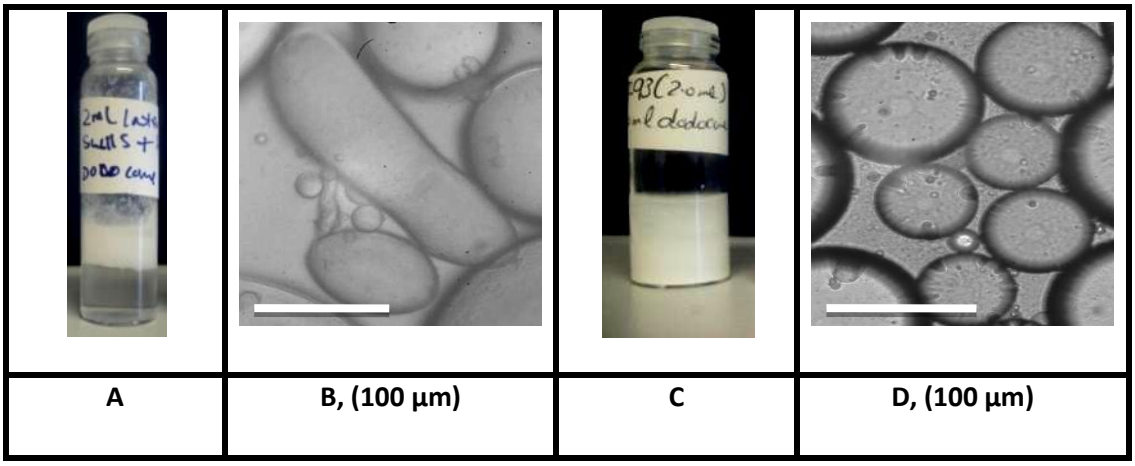

A	B, (100 µm)	C	D, (100 µm)

Fig.28. (A) Photograph of the Pickering emulsion that formed using SW-115 patchy particles with poly(NIPAM) brushes, **(B)** Photograph of dodecane droplets stabilized by SW-115 (the scale bar is 100 µm). **(C)** Photograph of the Pickering emulsion that formed using SET-93 patchy particles with poly(NIPAM) brushes, **(D)** Photograph of dodecane droplets stabilized by SET-93 (the scale bar is 100 µm).

Moreover, quartet latex particles which contain three hydrophobic domains and one hydrophilic domain with poly(NIPAM) brushes (SW-116) are also able to form stable Pickering emulsions with various hexadecane droplet sizes from 20 to 200 µm.

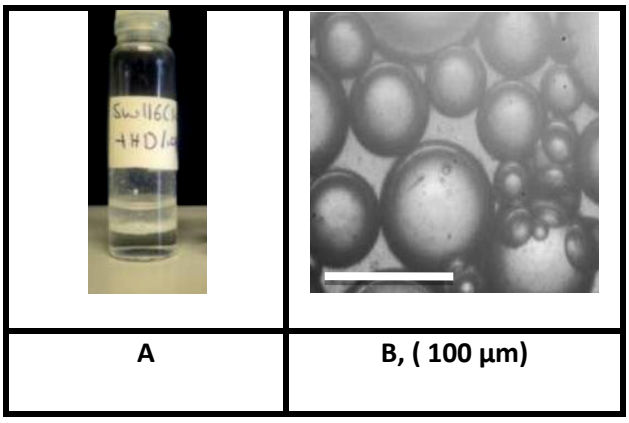

A	B, (100 µm)

Fig.29. (A) Photograph of the assembly of SW-116 latex particles at the interface between the hexadecane and water bulk phases. **(B)** Photograph of hexadecane droplets stabilized using SW-116 patchy particles with poly(NIPAM) brushes (the scale bar is 100 µm).

However, one day after the emulsification, the quartet particles tend to adhere to the interface between the bulk phases, as shown in Figure 29. The behavior of this latex particle (SW-116) could be attributed to the low colloidal stability of this latex as a result of the presence of three large hydrophobic domains which endow these particles with hydrophobic character. Moreover, the detachment of these particles from the hexadecane droplets/water interface was induced, but the presence of the poly(NIPAM) brushes prevented them from going completely to the hexadecane phase, but caused them to remain rather at the interface between the water and hexadecane bulk phases.

Two patchy particles with popcorn morphology (multiple hydrophobic domains; more than four but less than ten on the surface of patchy particles) were used. The latex particles SW-166, a popcorn particle with poly(NIPAM) brushes, and SW-167, with poly(sulfo propyl methacrylate) [poly(3-SPMA)] brushes, were able to form stable Pickering emulsions with spherical dodecane droplets (with various sizes from 20 to 200 µm) dispersed in the water phase as shown in Figures 30.

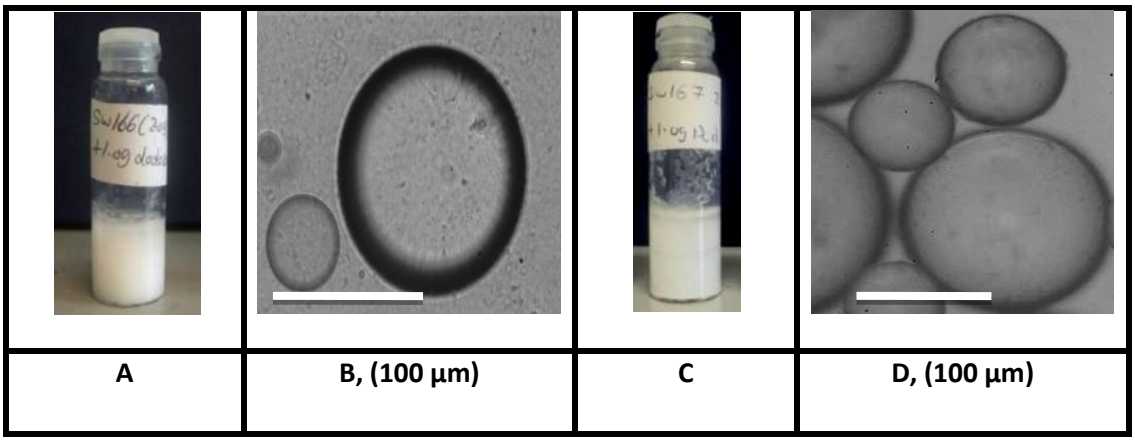

A	B, (100 µm)	C	D, (100 µm)

Fig.30. (A) Photograph of the Pickering emulsion that formed using SW-166 patchy particles with poly(NIPAM) brushes. **(B)** Photograph of dodecane droplets stabilized by SW-166 (the scale bar is 100 µm). **(C)** Photograph of the Pickering emulsion that formed using SW-167 patchy particles with poly(SPMA) brushes. **(D)** Photograph of dodecane droplets stabilized by SW-167 (the scale bar is 100 µm).

In the case of SW-166, the stabilization was observed to be stronger than in the case of SW-167. This was attributed to the presence of non-ionic poly(NIPAM) brushes in SW-166, in contrast to SW-167 which contains ionic (anionic) poly(SPMA) brushes; these allow the particles to partially wet the oil phase, which makes this Pickering emulsion weaker than in the case of SW-166. This behavior was also further demonstrated when raspberry particles (more than ten small hydrophobic domains) with cationic brushes (SW-182) were used as a Pickering stabilizer; direct and complete phase separation occurred after mixing the two bulk phases with SW-182 latex particles as shown in Figure 31.

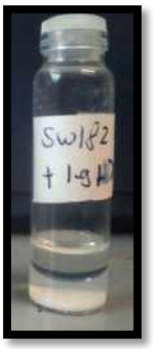

Fig.31. Photograph of the phase separation that occurred when patchy particles (SW-182) with poly[2-methacryloyloxy) ethyl]-trimethyl ammonium chloride] (MAETAC) brushes were used.

The latex particles remained and sedimented in the water phase. This confirmed the presence of ionic polymer (polyelectrolyte) brushes on the surface of patchy particles which make them more likely to stay in the water phase. In contrast, the presence of non-ionic polymer brushes on the surface of patchy particles makes them surface active and good Pickering stabilizing agents.

7.3.4.3 Hairy-Janus particles as Pickering stabilizers

Hairy Janus particles are dumbbell shaped latex particles with two different domains. Table 8 shows the ingredients used to form Pickering emulsions with different hairy Janus particles.

Table.8. Ingredients used to form the Pickering emulsions using different hairy Janus particles by simple hand shaking for 1 minute at room temperature.

Latex	Oil	Particle morphology	Stability of the emulsion
SET-150 (1.0 mL)	Hexadecane (1.0 mL)	Dumbbell with poly(2-HEA) brushes	Stable Pickering emulsion
SET-151 (2.0 mL)	Dodecane (1.0 mL)	Dumbbell with poly(MAETAC) brushes	Phase separation
SET-152 (2.0 mL)	Dodecane (1.0 mL)	Dumbbell with poly(NIPAM) brushes	Stable Pickering emulsion
SET-153 (2.0 mL)	Dodecane (1.0 mL)	Dumbbell with poly(PEGMEA) brushes	Stable Pickering emulsion
SET-160 (2.0 mL)	Dodecane (1.0 mL)	Dumbbell with poly(NDMA) brushes	Stable Pickering emulsion
SET-149 (2.0 mL)	Dodecane (1.0 mL)	Dumbbell with poly(NaSS) brushes	Phase separation
SET-162 (1.0 mL)	Dodecane (1.0 mL)	Dumbbell with poly(PEGMEA) brushes	Stable Pickering emulsion
SET-163 (2.0 mL)	Dodecane (1.0 mL)	Dumbbell with poly(SPMA) brushes	Phase separation
SET-155 (1.0 mL)	Hexadecane (1.0 mL)	Dumbbell with poly(NaSS) brushes	Phase separation

It has been observed that, in general, hairy Janus particles with non-ionic polymer brushes are able to form stable Pickering emulsions with long-term stability as shown in Figure 32.

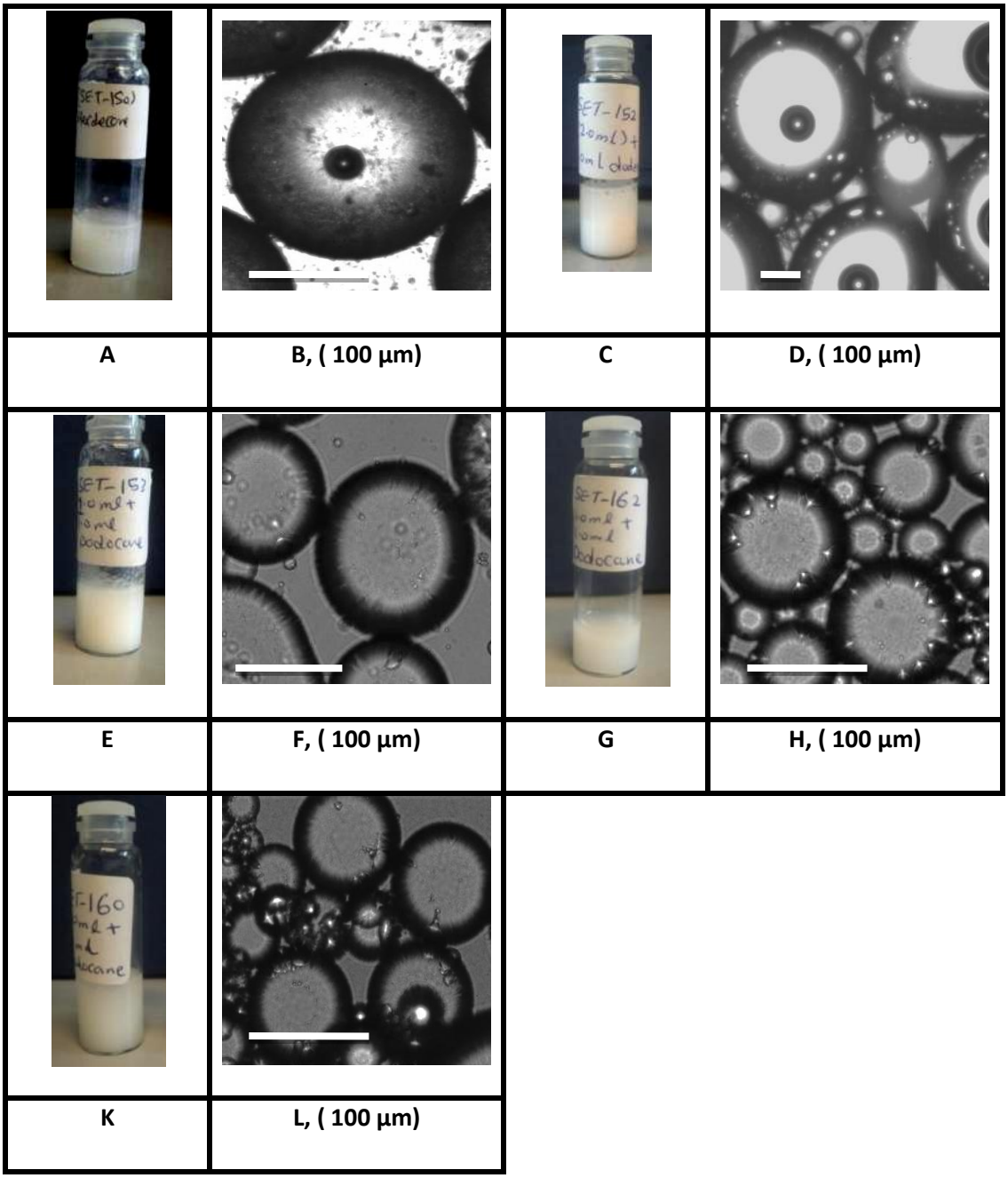

Fig.32. (A) Photograph of the Pickering emulsion that formed using SET-150 hairy Janus particles with poly(2-HEA) brushes. **(B)** Photograph of hexadecane droplets stabilized by SET-150 (the scale bar is 100 µm). **(C)** Photograph of the Pickering emulsion that formed using SET-152 hairy Janus particles with poly(NIPAM) brushes. **(D)** Photograph of dodecane droplets stabilized by SET-152 (the scale bar is 100 µm). **(E)** Photograph of the Pickering emulsion that formed using SET-153 hairy Janus particles with poly(PEGMEA) brushes. **(F)** Photograph of dodecane droplets stabilized by SET-153 (the scale bar is 100 µm). **(G)** Photograph of the Pickering emulsion that formed using SET-162 hairy Janus particles with poly(PEGMEA) brushes.**(H)** Photograph of dodecane droplets stabilized by SET-162 (the scale bar is 100 µm). **(K)** Photograph of the Pickering emulsion that formed using SET-160 hairy Janus particles with poly(NDMA) brushes. **(L)** Photograph of dodecane droplets stabilized by SET-160 (the scale bar is 100 µm).

In the case of hairy Janus particles with ionic polymer brushes poly(electrolyte), whether anionic or cationic, an instantaneous phase separation occurred as shown in Figure 33.

A **B** **C** **D**

Fig.33. (A) Photograph of the phase separation of the emulsion using SET-149 anionic hairy Janus particles with poly(NaSS) brushes. **(B)** Photograph of the phase separation of the emulsion using SET-155 hairy Janus particles with poly(NaSS) brushes. **(C)** Photograph of the phase separation of the emulsion using (SET-163) hairy Janus particles with anionic poly(SPMA) brushes. **(D)** Photograph of the phase separation of the emulsion using SET-151 hairy Janus particles with cationic poly(MAETAC) brushes.

This confirms that the presence of ionic polymer brushes on the surface of the particles confers a more hydrophilic character, without considering the different morphologies of the particles (core-shell hairy particles, patchy hairy particles or even dumbbell Janus particles), consequently those ionic hairy particles prefer to remain in the water phase.

7.3.4.4 Non-hairy Janus particles as Pickering Stabilizers

Non-hairy Janus particles are dumbbell particles with one hydrophobic domain which is cross-linked-poly(styrene), and another hydrophilic domain which is (cross-linked- poly(styrene) that contains ionic moieties of a copolymer of styrene sulfonate with styrene, and the sulfate end group which comes from the KPS initiator. In addition, a copolymer of styrene with a functional monomer (inimer) which has

some hydrophilic character. Three types of non-hairy Janus particles have been investigated: normal spherical anionic surface latex particles, e.g. PS-18, snowman dumbbell particles such as latexes SW-281 and SW-300, as well as dumbbell particles such as latexes SW-291, SW-290 and SW-295. Table 9 shows the ingredients used to form Pickering emulsions with different types of non-hairy Janus particles, followed by Figure 34 which shows the formed emulsions after the mixing.

Table.9. Ingredients used to form Pickering emulsions using different non-hairy Janus particles by simple hand shaking for 1 minute at room temperature.

Latex	Oil	Particle morphology	Stability of the emulsion
SW-281 (2.0 mL)	Dodecane (1.0 mL)	Snowman Janus particles	Phase separation
PS-18 (2.0 mL)	Dodecane (1.0 mL)	Spherical	Phase separation
SW-291 (2.0 mL)	Dodecane (1.0 mL)	Dumbbell Janus particles	Phase separation+ small droplets
SW-295 (2.0 mL)	Dodecane (1.0 mL)	Dumbbell Janus particles	Phase separation+ large droplets
SW-290 (2.0 mL)	Dodecane (1.0 mL)	Dumbbell Janus particles	Phase separation+ large droplets
SW-300 (2.0 mL)	Dodecane (1.0 mL)	Snowman Janus particles	Phase separation

Fig.34. Photograph of the emulsions formed after mixing non-hairy Janus particles with dodecane; following from left to right, PS18, SW-291, SW-300, SW-295 and SW-290.

In the case of PS-18, this latex had anionic moieties on the surface that caused the particles to remain preferentially in the water phase; the same pattern was also observed in the case of snowman shaped non-hairy Janus particles (SW-281 and

SW-300). More than 60% of these particles gained anionic moieties which made them more hydrophilic, although the particles were amphiphilic. In the case of dumbbell Janus particles (SW-290, SW-291 and SW-295), these particles had close to a 50% hydrophilic domain and a 50% hydrophobic domain.

Therefore, they had a different HLB balance compared to snowman shaped particles. It was observed that those particles tended to form stable Pickering emulsions, but with very large stable water droplets dispersed in dodecane. This confirms that increasing the ratio between the hydrophobic and hydrophilic domains to be equal to unity in non-hairy Janus particles should increase their surface activity and allow them to adhere to the interface between the two immiscible liquids. This also verifies that the hydrophobic domain is essential to endow particles with surface active properties.

7.3.4.5. Janus particles as Pickering stabilizers for paraffin wax

The purpose of the formation of Pickering emulsions with paraffin wax is divided into three goals: first, to confirm the activity of the complex particles that provide very good Pickering emulsions with dodecane or hexadecane; second, to visualize how these particles assemble or orient at the interface between the two immiscible liquids (wax and water). Since the stable wax droplets will be solidified after cooling below the melting point of paraffin wax (55-56°C), the particles will be trapped at the interface between the wax and water and will not tumble.

It is expected that the hydrophobic domain will be oriented toward the wax phase and the hydrophilic domains toward the water phase. The third goal was to assess whether the orientation of the particles could be characterized directly by normal dry SEM. Four systems were tested, including hairy Janus particles with poly(NDMA)

brushes in the case of latex SET-160, hairy Janus particles with poly(PEGMEA) brushes in the case of latex SET-162, non-hairy dumbbell Janus particles in the case of SW-291 and the common surfactant SDS for the purposes of comparison. Table 10 shows the ingredients used to form the paraffin wax in water Pickering emulsion

Table.10. Ingredients used to form a paraffin wax Pickering emulsion using different Janus particles by simple hand shaking for 1 minute.

Latex	Oil	Particle morphology	Stability of the emulsion
SET-160 (3.0 mL)	Paraffin wax (0.2 g)	Dumbbell with poly(NDMA) brushes	Stable Pickering emulsion + phase separation
SET-162 (3.0 mL)	Paraffin wax (0.2 g)	Dumbbell with poly(PEGMEA) brushes	Stable Pickering emulsion + phase separation
SW-291 (3.0 mL)	Paraffin wax (0.2 g)	Dumbbell Janus particles	Phase separation
SDS (0.15%) (2.0 mL)	Paraffin wax (0.2 g)	----------	Phase separation + Pickering emulsion

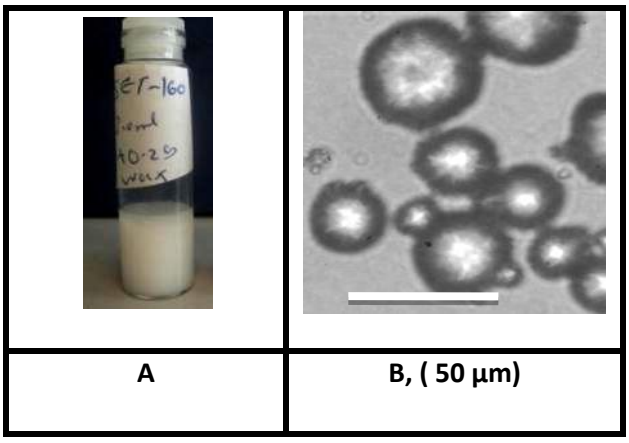

A **B, (50 µm)**

Fig.35. (A) Photograph of the wax in water Pickering emulsion that formed using SET-160 hairy Janus particles with poly(NDMA) brushes. **(B)** Photograph of wax particles stabilized by SET-160 (the scale bar is 50 µm).

SET-160 hairy Janus particles containing poly(NDMA) brushes produced a stable Pickering emulsion of wax in water with various sizes of wax particles from 1.0 µm to 50 µm as shown in Figure 35. For a further close-up of how these particles oriented around the wax particles, SEM images were taken as shown in Figure 36.

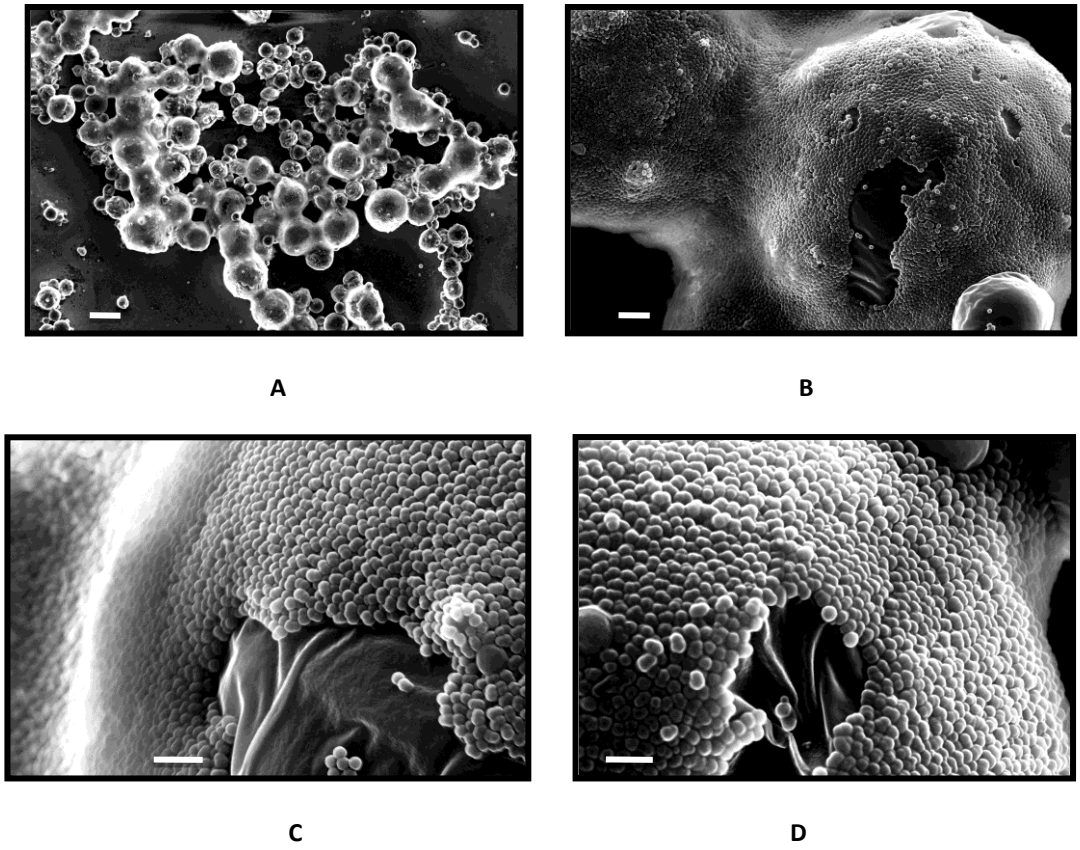

Fig.36. SEM images of paraffin wax particles stabilized using SET-160 hairy Janus particles with poly(NDMA) brushes. Scale bar as the following (A, 20 µm), (B, 2 µm), (C, 1 µm), (D, 1 µm).

It can be concluded from the SEM images that the SET-160 hairy Janus particles tended to form closely pack monolayers around the wax particles, which is the main reason for the formation of stable wax particles.

Taking into consideration that non-hairy Janus particles (SW-291) did not form a stable Pickering emulsion with wax, the poly(NDMA) brushes clearly play a major role in the formation of a stable Pickering emulsion with wax in addition to the presence of the hydrophobic domain, which in some cases in the SEM images appears to be trapped inside the wax phase. This may indicate the amphiphilic nature of the particles which would reinforce the formation of a stable wax Pickering emulsion. Various wax particle sizes from 1.0 µm to 20 µm were formed when the common surfactant SDS was used in order to compare with the wax particles that formed with the complex latex particles as shown in the SEM images in Figure 37.

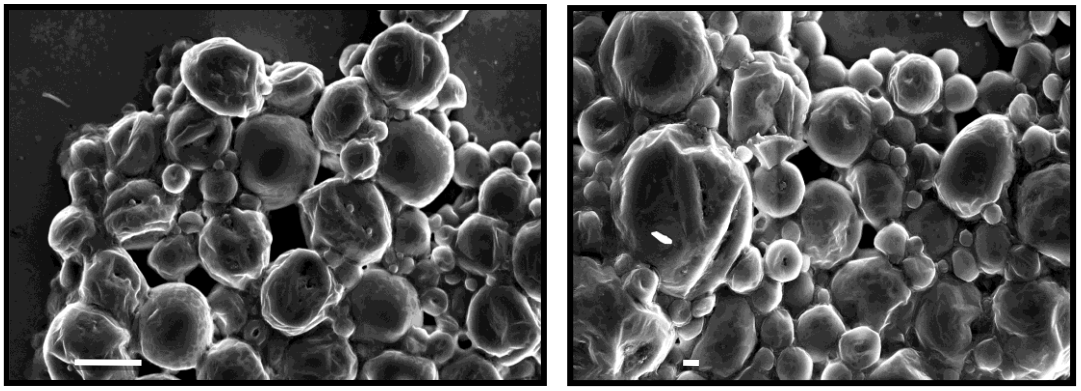

A B

Fig.37. SEM images of paraffin wax particles stabilized by using SDS as surfactant. Scale bar as the following (A, 10µm), (B, 2µm).

Hairy Janus particles (SET-162) containing poly(PEGMEA) brushes seemed to function as a very good Pickering stabilizer for paraffin wax particles dispersed in the water phase as shown in Figure 38.

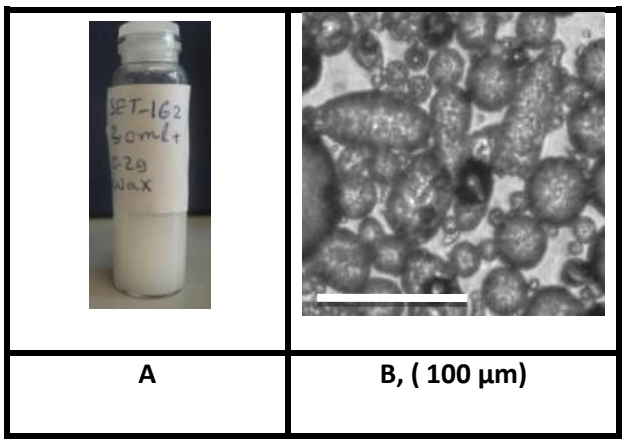

Fig.38. (A) Photograph of the wax in water Pickering emulsion that formed using SET-162 hairy Janus particles with poly(PEGMEA) brushes. **(B)** Photograph of wax particles stabilized by SET-162 (the scale bar is 100 µm).

Various wax particle sizes were formed from 1.0 µm to 50 µm. The SEM images in Figure 39, show the formation of monolayers of SET-162 on the surface of the wax particles, with most of the particles oriented on the surface of the wax particle by both domains, the hydrophobic domain and the hydrophilic domain, in addition to some cases where the hydrophobic domain was immersed inside the wax phase.

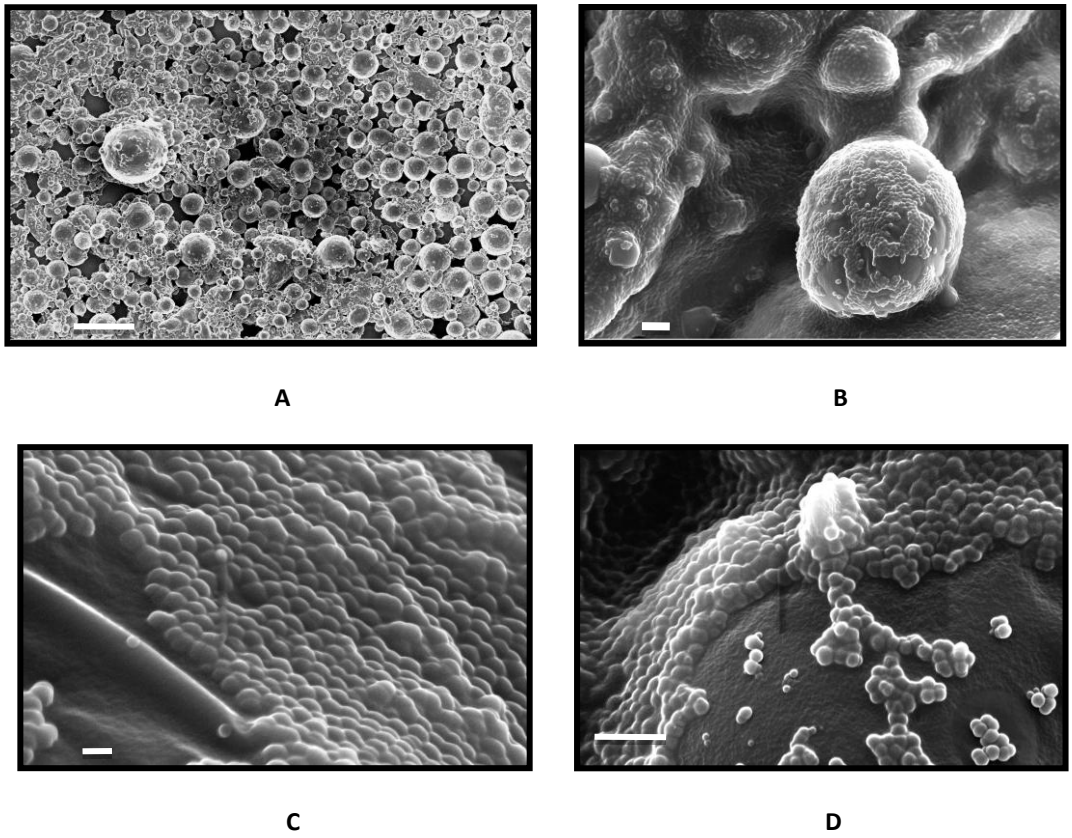

Fig.39. SEM images of paraffin wax particles stabilized by using SET-162 hairy Janus particles with poly(PEGMEA) brushes. Scale bar as the following (A, 100 µm), (B, 1µm), (C, 0.2 µm), (D, 1 µm).

7.3.5 Conclusion

Several types of complex latex particles with different morphologies synthesized in absolutely soap-free conditions and their applications as Pickering stabilizers were investigated for two immiscible liquids. Dodecane, hexadecane and paraffin wax were used as the oil phases and the water as the polar phase. It was observed that ionic particles, whatever their morphology (spherical, hairy, hairy patchy, hairy Janus and non-hairy Janus particles) were strongly hydrophilic and tended to remain in the water phase; however, the non-ionic particles, whatever their morphologies, tended to form stable Pickering emulsions. It is proposed that there are two main factors that form stable Pickering emulsions: the presence of non-ionic polymer brushes on the surface of the latex particles as is the case with hairy latex particles

carrying poly(*N*,*N*-dimethyl acrylamide) or poly(PEGMEA) brushes, and the amphiphilic nature of hairy Janus particles.

7.4. Directed Self-assembly of Janus particles

7.4.1. Summary

The directed self-assembly of non-hairy dumbbell Janus latex particles and hairy dumbbell Janus latex particles was investigated. The self-assembly was induced by changing the ionic strength of the latex aqueous medium by the addition of an electrolyte. In the case of non-hairy dumbbell latex Janus particles, the electrolyte concentration required to decrease the zeta potential of the latex to below -25 mV is 0.1M, with a slight increase in the particle size; above this concentration a massive increase in the particle size was observed which indicates that a typical coagulation of the latex particles was occurring. However, the spherical and snowman non-hairy Janus latex particles require a higher concentration of the electrolyte, above 0.2M, to decrease the zeta potential to below -25 mV with a slight increase in the particle size and this indicates that the larger hydrophilic domain is the more stable latex. This also highlights that in the case of the dumbbell non-hairy Janus particles the responsible factor for the destabilization of the latex and self-assembly is the bigger hydrophobic domain in those particles. The Cryo-TEM images of the dumbbell non-hairy Janus particles suggest that more than 70% of the interactions among the particles are head to head (hydrophobic–hydrophobic domain interactions) and the remaining interactions are either head to tail or tail to tail. In the case of hairy Janus particles, it was observed that, due to the low solid concentration of these Janus latexes and the presence of the brushes which function as another source for the colloidal stability via steric stabilization alongside the existence electrostatic

repulsion stabilization, these Janus hairy particles required very high concentration of NaCl concentration, usually above 1.5M, which is 15 times as high as the salt concentration used in the case of non-hairy Janus particles. This restricts the visualization of the assembly by Cryo-TEM due to the high salt concentration in the sample.

7.4.2. Introduction

Janus particles with two different hemispheres (in our case one hemisphere is hydrophobic and the other hydrophilic) could be utilized to mimic the behaviour of a simple surfactant to self-assemble into clusters to form a colloidal superstructure, consequently the Janus particles are the building blocks to form that structure. Janus particles will not only have a repulsive force among themselves by means of electrostatic repulsion, as in the case of isotropic ionic colloidal stable particles, but also hydrophobic attractive forces which induce the self-assembly of Janus particles in water, whereby the hydrophobic domains will be the core and the hydrophilic side forms the shell of the cluster in order to minimize the interaction between the hydrophobic domains and water. Since these opposite forces present among the Janus particles, one of these forces has to be minimized; this is the repulsive force in order to maximize the hydrophobic attractive interaction to induce the self-assembly. Steve Granick and co-workers assembled 1.0 μm poly(styrene) amphiphilic particles by the addition of electrolyte (KNO_3) to form clusters and a worm-like structure by further increase of electrolyte concentration [27], but one could suggest that normal ionic isotropic particles when treated with electrolyte lead to clustering and aggregation. But their aggregation and clustering is not controllable, and leads to sedimentation or flocculation; conversely the Janus particles will lead to the formation of stable clusters as a result of a hydrophilic repulsive force (electrostatic

or steric) if the gravitational forces that come into play to sediment these particles is low. With Janus magnetite particles (5.0 nm) in which one hemisphere contains poly(acrylic acid) and the other hemisphere contains either poly(styrene sulfonate) or poly(NIPAM), upon decreasing the pH in the case of poly(styrene sulfonate), and increasing the temperature in the case of poly(NIPMA) leads to these Janus particles clustering with a hydrodynamic diameter of 80-100 nm [28,29]. The self-assembly of the Janus particles can be studied by measuring their hydrodynamic diameter under variation of the pH and temperature by utilizing dynamic light scattering (DLS) and Cryo-TEM. Steve Granick and co-workers also indicate that the critical design rule to make Janus particles self-assemble is that the range of interparticle interaction among the particles (hydrophobic attraction and electrostatic or steric repulsion) must be short relative to particle size, and that the interaction must be reversible. By applying that principle, they are able to induce self-assembly of 1.0 μm poly(styrene) Janus particles, wherein one hemisphere contains fluorescent sulfate negatively charged (hydrophilic side) and the other contains titanium and gold thin film (hydrophobic side). Upon addition of salt (NaCl) with a concentration of 0.0038M, the Janus particles assemble to form clusters, and with a further increase in the NaCl solution to 0.0050M the Janus particles assemble into longer helical clusters [30]. The same research group self-assembled triblock Janus particles which were made from 1.0 μm negatively charged fluorescent poly(styrene) latex particles; the two hydrophobic patches were made by glancing angle deposition of titanium and gold thin films, and followed by the deposition of a self–assembled monolayer of n-octadecanethiol. The self-assembly of these triblock Janus particles was induced by adding 0.0035M NaCl solution to screen electrostatic repulsion and allowing self-assembly via short range hydrophobic attraction [31].

7.4.3. Experimental

The self-assembly of non-hairy Janus particles was studied by determining the concentration of (NaCl) that should be added to destabilize the latex in order to induce the self-assembly. This was monitored by DLS, whereby 1.0 mL from the stock latex dispersion was mixed with 5.0 mL of pure water, and then 0.5 mL from that newly formed dispersion was mixed with 0.50 mL of the aqueous solution of NaCl electrolyte. The dispersion was sonicated for 2.0 minutes prior to the measurement by DLS. After determining the concentration of the electrolyte that gives low zeta potential and after the particle size began to rise as a result of the self-assembly, Cryo-TEM images were taken for the latex wherein 0.5 mL of the 0.1M NaCl solution was mixed with 0.5 mL of the stock latex dispersion. In the case of the hairy Janus particles 0.5 mL of stock latex dispersion was mixed with 11.0 mL of water, and 0.5 mL from the newly prepared emulsion was mixed with 0.5 mL of NaCl solution or with 0.5 mL of different pH solutions at room temperature.

7.4.4. Results and discussion

The directed self-assembly was studied for two major types of Janus particle: non-hairy and hairy. The non-hairy Janus particle is a dumbbell cross-linked particle with an anisotropic surface whereby one side is hydrophilic, containing on its surface a copolymer of sodium styrene sulfonate with styrene and divinylbenzene. In addition to that copolymer, the KPS was used as initiator; this makes the surface contain a negative charge at medium and high pH. The hydrophilic domain also contains a copolymer of 2-methacryloxyethyl-2-bromoisobutyrate. On the other hand, the hydrophobic domain contains a copolymer of styrene and divinylbenzene with AIBN as initiator; based on that, the Janus non-hairy particle is amphiphilic,

whereby one domain is hydrophilic (ionic) with negative charge and the other domain is hydrophobic.

In order to induce the self-assembly of these kinds of Janus particle, the electrostatic repulsion present in the hydrophilic domain should be minimized to create suitable conditions for increasing the short range hydrophobic Van der Waals attraction among the hydrophobic domains to form the cluster. The core of the cluster is the hydrophobic domain and the shell is the hydrophilic domain, and this mimics the structure of ordinary surfactant when the concentration of the surfactant in water is over the critical micelles concentration (CMC). These non-hairy Janus Particles are long term colloidal stable, therefore an external stimulus has to be used to induce the self-assembly, as in the case of an amphiphilic copolymer where co-solvent has to be added to induce the aggregate structure. Taking inspiration from Steve Granick's earlier work where he used an electrolyte aqueous solution to induce the self-assembly of Janus particles that contain a negatively charged hydrophilic side and hydrophobic domain to form clusters of Janus particles, in our work, the Janus particles attain dumbbell (peanut) shaped particles which makes a massive difference in how these types of Janus particles could be assembled. A simulation of how these types of Janus particle assembled was studied by our group [32]. So in this section, the self-assembly of the non-hairy Janus particles is studied by initially determining the concentration of electrolyte that should be used to induce the self-assembly without causing the Janus particles to undergo the normal coagulation through lack of colloidal stability.

The particle size and zeta potential of the non-hairy Janus latex particles were monitored by DLS as a function of the electrolyte concentration. After determining the suitable electrolyte concentration, Cryo-TEM images were taken at that

concentration to visualize the interaction among the Janus particles. We expected hydrophobic domain attraction to be the predominant interactions among the non-hairy Janus particles. Five non-hairy Janus particles were studied: SW-290, SW-295, SW-296, SW-297, and SW-300. The first non-hairy Janus particle studied was SW-290; this is a dumbbell shape particle with an anisotropic surface wherein 57.2% of the surface is hydrophilic and 42.8% is hydrophobic, the total solid of that dispersion is 1.76%. Figure 40 shows the particle size, PDI (particle size distribution) and zeta potential of SW-290 as a function of the NaCl aqueous solution concentration.

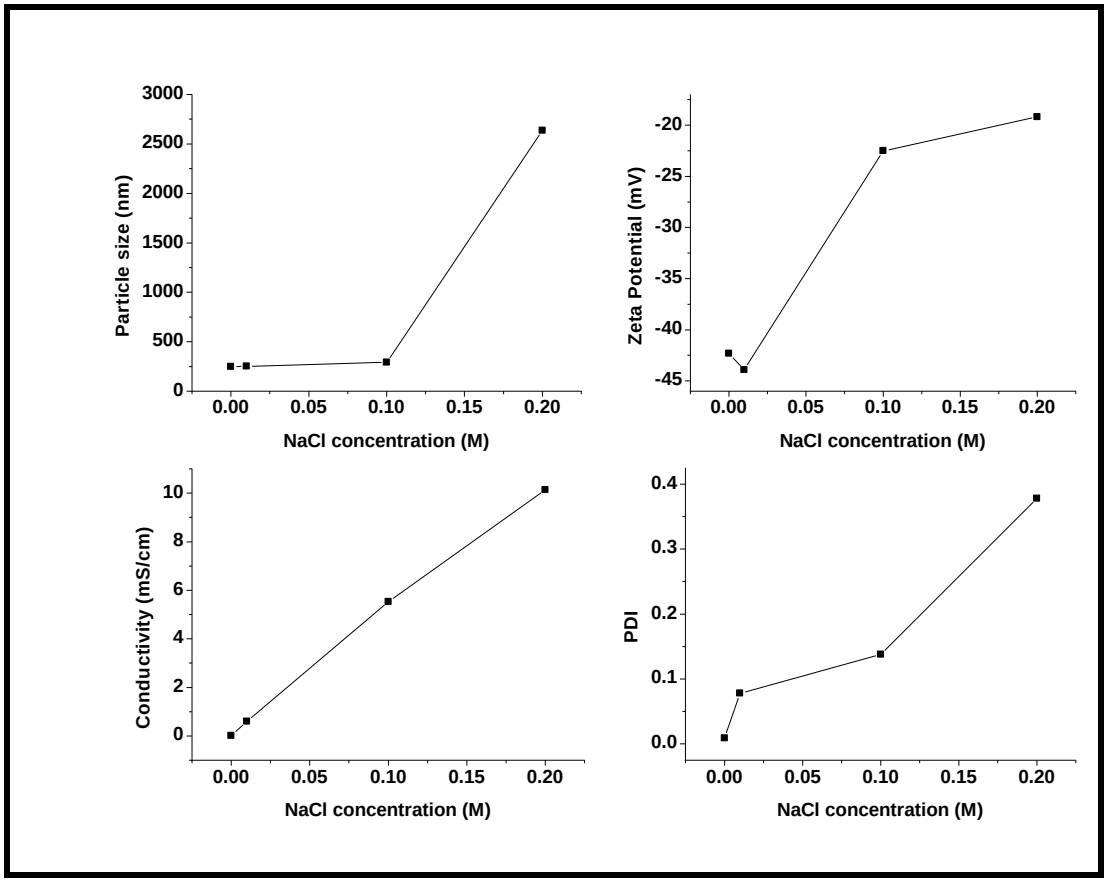

Fig.40. Particle size, PDI and zeta potential of the non-hairy Janus particles SW-290 as a function of NaCl aqueous solution concentration.

From the graphs, the zeta potential of the Janus particles before the addition of the electrolyte was (-42.5 mV) and this indicates the very good colloidal stability of

these Janus particles; after adding a very low electrolyte concentration, the zeta potential increased to (-45 mV) with similar particle size to that before the addition of the electrolyte, but with 0.1M NaCl concentration a significant decrease in the zeta potential was observed to (-22 mV) with a slight increase in the particle size and the PDI. With a further increment of the electrolyte concentration to 0.2M, the particle size was increased massively to above 2.5 µm, with an additional decrease in the zeta potential to be less than (-20 mV); the conductivity against electrolyte concentration graph was shown to prove the accurate increase of the electrolyte concentration to validate the results obtained. It can be concluded from the graphs that the suitable concentration to study the structures and the interactions among the Janus particles under the Cryo-TEM is 0.1M, which provides lower zeta potential and slightly increased particle size, which is perhaps caused by the formation of clusters owing to the attraction among the hydrophobic domains, and that concentration does not cause coagulation of the Janus particles. An example of the Cryo-TEM images of SW-290 without the addition of an electrolyte is shown in Figure 41, and after the addition of 0.1M of NaCl electrolyte in Figure 42. After analysing the Cryo-TEM images by manual counting the different particle interactions (whether head to head, head to tail, or tail to tail), it was observed that in case of the Janus particles (SW-290) without the addition of an electrolyte from a total of 156 interactions, there are 55.7% is head to head interactions and the remaining 44.3% are either head to tail or tail to tail. This indicates that there is already hydrophobic attraction among the Janus particles SW-290 even before the addition of the electrolyte. And after the addition of 0.1M NaCl aqueous solution, the head to head interactions increased to 71% out of the total 150 interactions and

the other 29% is either head to tail or tail to tail; besides that some cluster structures were also formed.

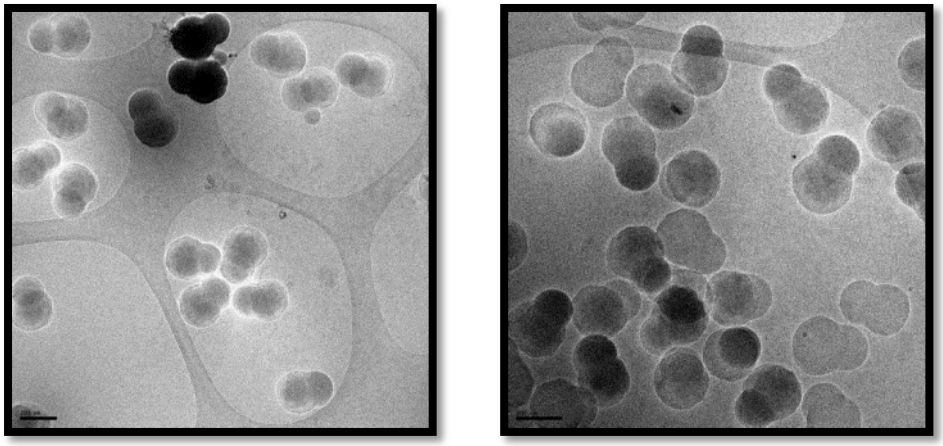

Fig.41. Cryo-TEM images of the non-hairy Janus particles SW-290 before the addition of an electrolyte. Scale bar in both images is 200 nm.

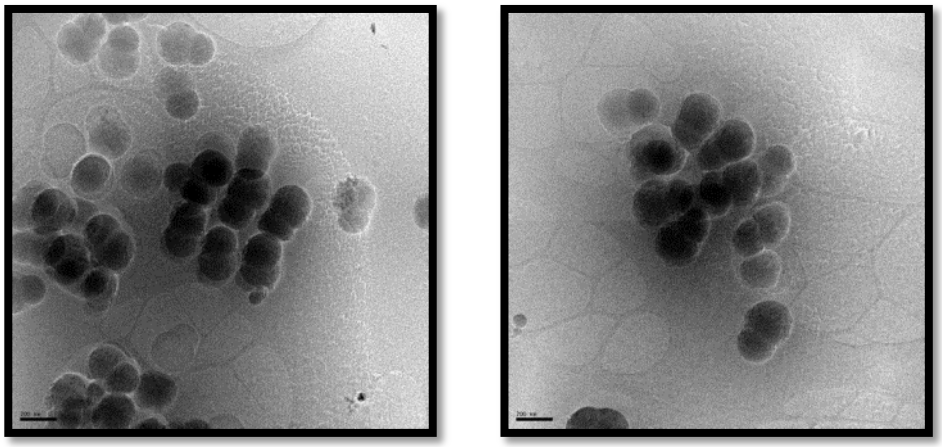

Fig.42. Cryo-TEM images of some clusters that are formed due to the hydrophobic attractions among the hydrophobic heads of non-hairy Janus particles SW-290 after addition of 0.1M of NaCl solution. Scale bar in both images is 200 nm.

This 15% increase in the head to head interactions (hydrophobic attractions) indicates that the addition of the NaCl electrolyte led to minimization of the electrostatic repulsion among the Janus particles by decreasing the electrical double layers. Based on this, a directed self-assembly of Janus particles leads to the hydrophobic domain (the head) minimizing its contact with water by sticking to the other hydrophobic domain, and the addition of the electrolyte leads to the distances between the non-hairy Janus particles to decrease due to the minimization of the

repulsive forces, which increases the percentage of hydrophobic interactions. Another non-hairy Janus particle (SW-295) was also studied to compare it with the results obtained with SW-290; SW-295 is a dumbbell anisotropic particle with a surface consisting of a 51.7% hydrophilic domain and a 48.3% hydrophobic domain; the hydrophobic domain ratio in SW-295 is a little higher than in SW-290. The total solid of SW-295 dispersion is 1.82%. The Janus particles SW-295 behave quite similarly to SW-290 as a function of NaCl concentration (see Figure 43), whereby a slight increase in the particle size and particle size distribution were observed when the latex was treated with 0.1M NaCl solution, and the zeta potential decreased to become below -20 mV, which is lower than that observed in SW-290.

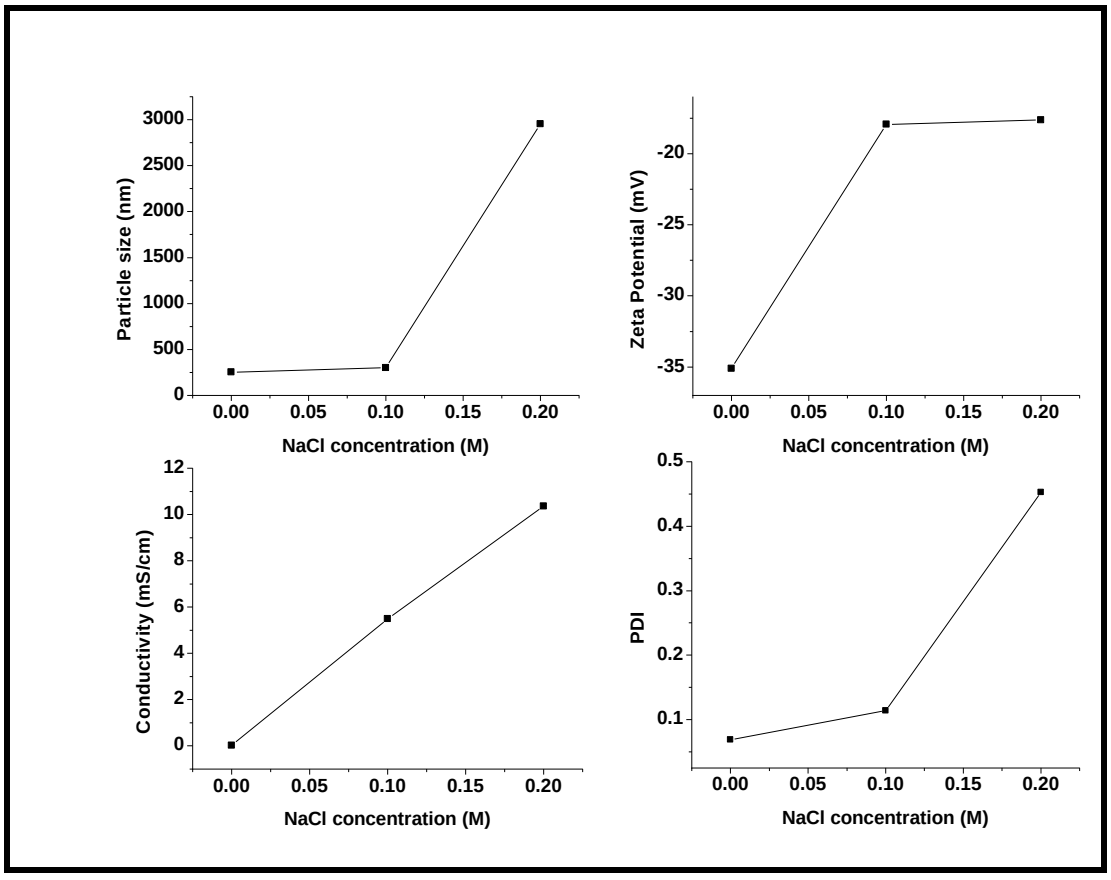

Fig.43. Particle size, PDI and zeta potential of the non-hairy Janus particles SW-295 as a function of the NaCl aqueous solution concentration.

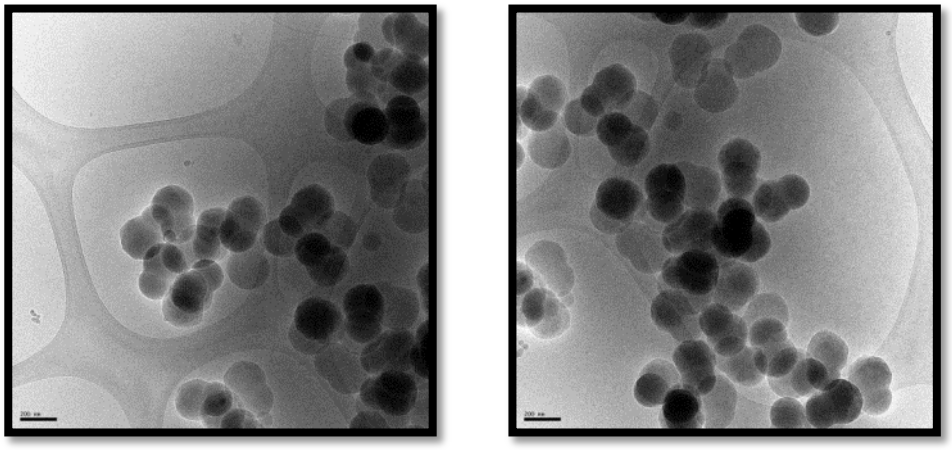

Fig.44. Cryo-TEM images of the non-hairy Janus particles SW-295 before the addition of an electrolyte. Scale bar in both images is 200 nm.

As with SW-290, the higher NaCl solution leads to coagulation of the latex wherein the particle size becomes over 2.5µm. Based on this, Cryo-TEM images were taken when the latex was treated with a 0.1M NaCl solution. The Cryo-TEM images were taken for SW-295 before the addition of an electrolyte, and after analyzing the 133 interactions among the SW-295 Janus particles, it was observed that 69% of those interactions were head to head interactions and the remaining 31% head to tail or tail to tail interactions. This indicates that the hydrophobic attractions among the hydrophobic heads are already established, which is clear in the Cryo-TEM images in figure 44, where some clusters are already formed that consist of triplet and quartet individual Janus particles. After the addition of the 0.1NaCl solution, it was observed that 74% of the 282 interactions observed in the Cryo-TEM images are head to head interactions and the other 26% are either head to tail or tail to tail; this demonstrates that the hydrophobic attractions are slightly increased by the addition of the 0.1M of the electrolyte. A sample of the Cryo-TEM images of SW-295 after treating with NaCl is shown in Figure 45. The hydrophobic attraction in SW-295 is higher than that observed in SW-290, and this could be attributed to two factors: the

slightly higher solid concentration of SW-295 compared to SW-290, and the slightly higher ratio of the hydrophobic domain of SW-295 compared to SW-290.

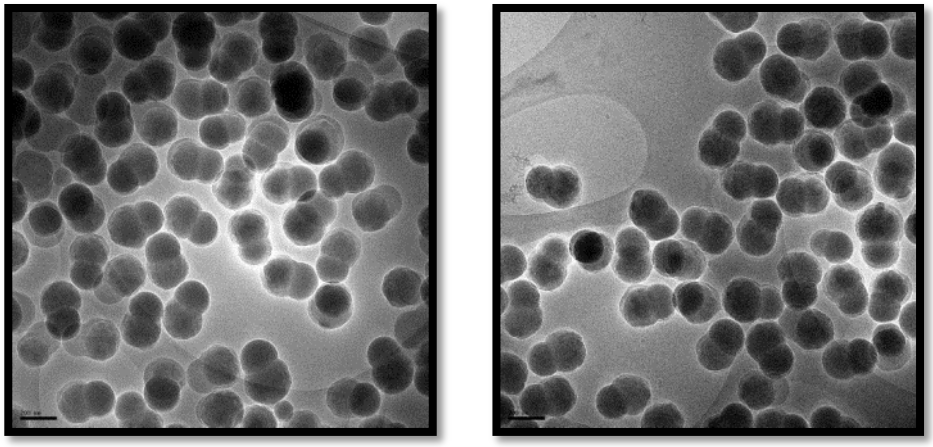

Fig.45. Cryo-TEM images of particles SW-295 after addition of 0.1M of NaCl solution. Scale bar in both images is 200 nm.

The self-assembly of another non-hairy Janus particle (SW-296) was also investigated. SW-296 has a solid concentration of 2.2%; the particles are anisotropic with a 54.21% hydrophilic domain and a 45.78% hydrophobic domain. A similar trend in these particles was observed after treating them with different NaCl aqueous solutions (see Figure 46), wherein a slight increase in the particle size was observed and massive decrease in the zeta potential to (-22.5 mV) when the latex was again treated with the 0.1M concentration of NaCl. As with the previous latexes, a higher concentration of NaCl solution (0.2M) led to coagulation of the latex, as that observed by the huge increase in the particle size and particle size distribution.

The Cryo-TEM images of SW-296 after treating with 0.1M of NaCl aqueous solution is shown in Figure 47 After analysing the Cryo-TEM images, it was observed that 68% of 95 interactions among the Janus particles are head to head interactions and the remaining 32% interactions are head to tail or tail to tail. The lower percentage of the head to head interactions (hydrophobic attractions) might be

due to the presence of small spherical particles (secondary nucleation) which were generated during the formation of the Janus particles and the lower ratio of the hydrophobic domain of the Janus SW-296 particles compared to SW-295 although there is the high solid concentration of SW-296.

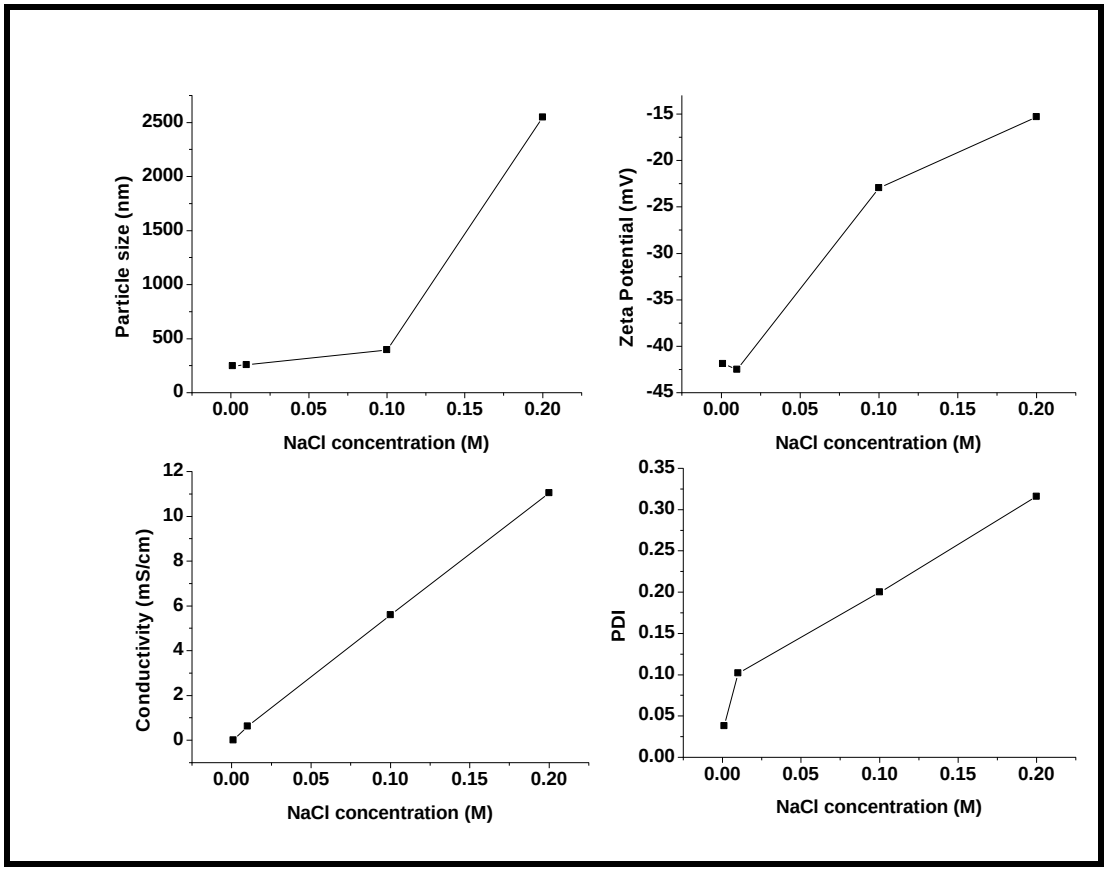

Fig.46. Particle size, PDI and zeta potential of the non-hairy Janus particles SW-296 as a function of NaCl aqueous solution concentration.

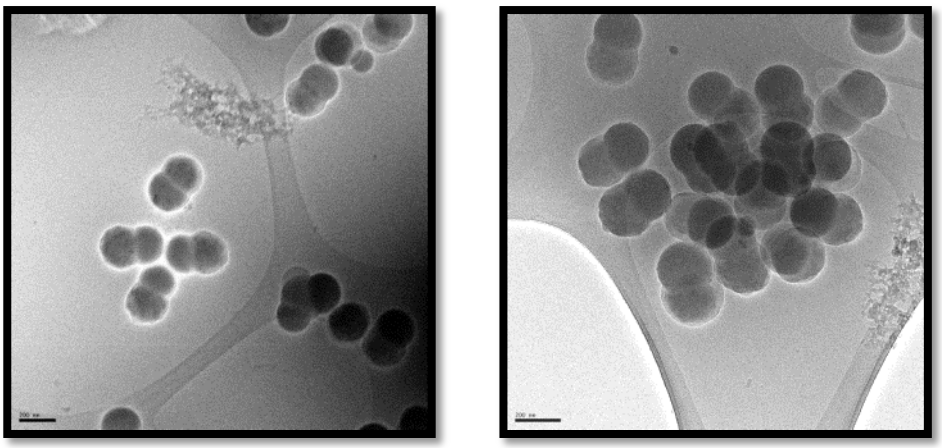

Fig.47. Cryo-TEM images of SW-296 particles after addition of 0.1M of NaCl solution. Scale bar in both images is 200 nm.

Further study was performed on another non-hairy Janus particle, (SW-297); this latex has dumbbell shaped anisotropic particles with a 52.49% hydrophilic domain and a 47.5% hydrophobic domain, the solid concentration of (SW-297) is 1.7%. The behaviour of these latex particles against various NaCl concentrations is shown in Figure 48. It was found that a slight increase in electrolyte concentration (0.01M NaCl) led to a slight increase in particle size (from 250 nm to 320 nm) and in the particle size distribution.

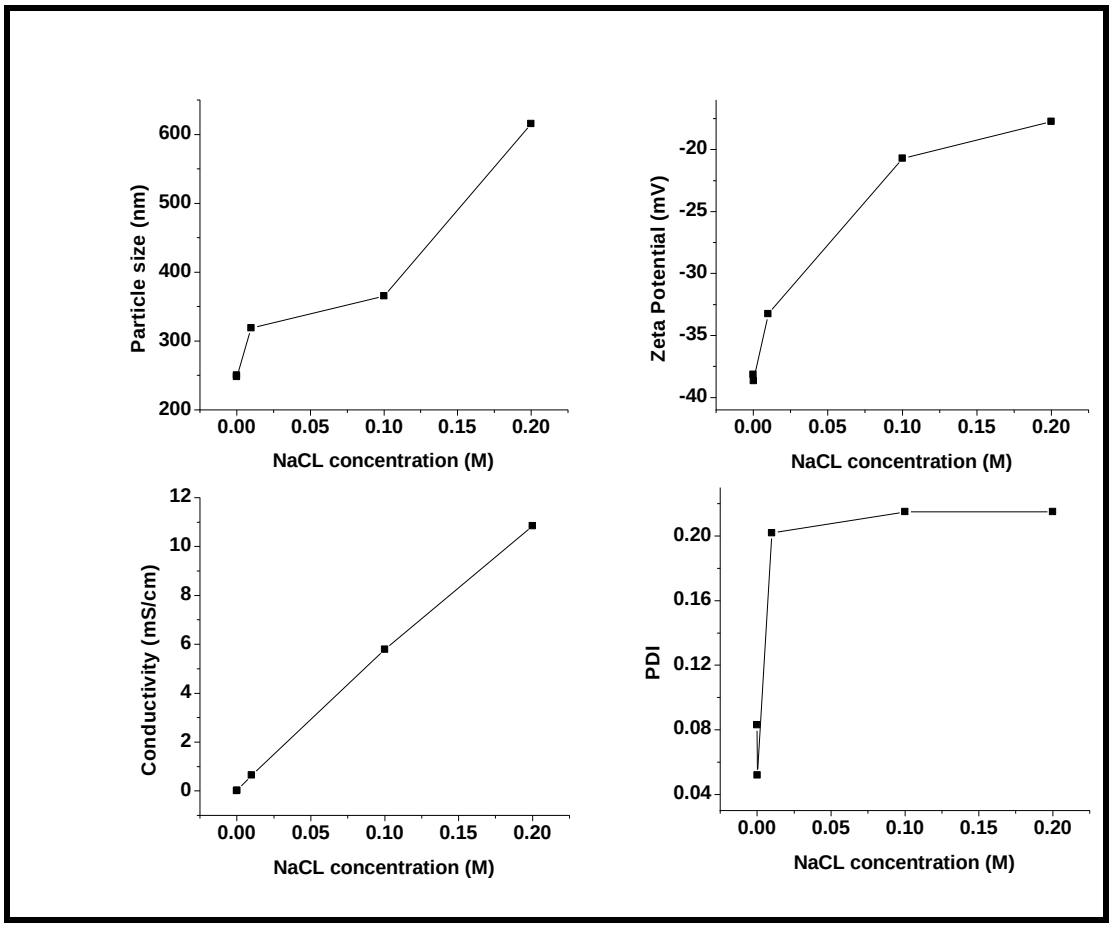

Fig.48. Particle size, PDI and zeta potential of the non-hairy Janus particles SW-297 as a function of NaCl aqueous solution concentration.

The zeta potential dropped to (-32 mV), and when the (SW-297) latex was treated with the typical electrolyte concentration that induced self-assembly in the previous cases, 0.1M, the particle size further increased to 350 nm, with a massive increase in the particle size distribution. The zeta potential dropped to (-20 mV), and as usual

when the concentration of the electrolyte was increased to 0.2M, the latex particle size was further increased, but in this case did not exceed 1.0 μm. The Cryo-TEM images of SW-297 when treated with 0.1M NaCl are shown in Figure 49.

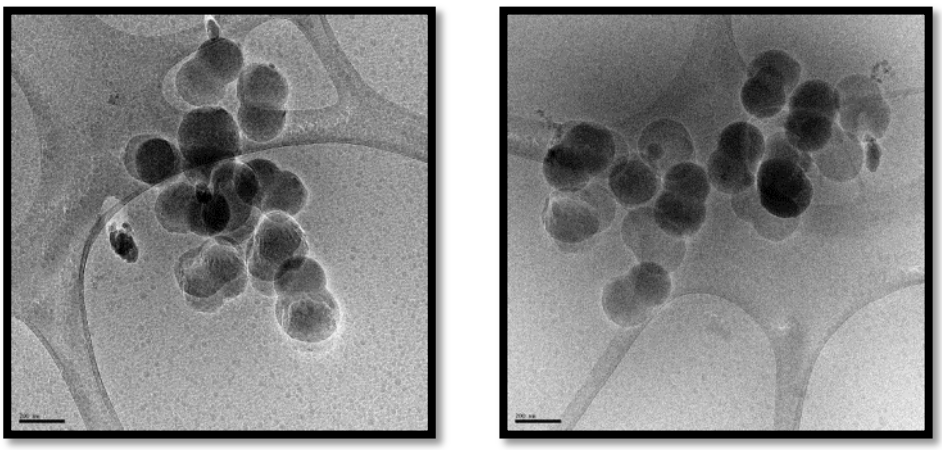

Fig.49. Cryo-TEM images of particles SW-297 after the addition of 0.1M of NaCl solution. Scale bar in both images is 200 nm.

After analyzing the Cryo-TEM images of SW-297, it was observed that out of 137 interactions that occurred among the Janus particles, 69.3% were head to head interactions and the other 30.6% were head to tail or tail to tail. This confirms that the hydrophobic heads of Janus particles tend to minimize their contact with water by sticking with other hydrophobic heads to form clusters which lead to the particle size and particle size distribution to increase. The Cryo-TEM images show some clusters of the Janus particles SW-297.

Finally, for the purpose of comparison, non-hairy Janus particles with snowman shape (SW-300) were studied. This latex is different from the other latex in the ratio of the amphiphilicity, wherein the hydrophilic domain represents 66.3% of the particle surface and the hydrophobic domain only 33.7%, which is the lowest hydrophobic area in contrast to the other studied latexes. We expected that this latex

would require more electrolyte concentration to induce self-assembly, and this was indeed the case, as can be concluded from Figure 50 below.

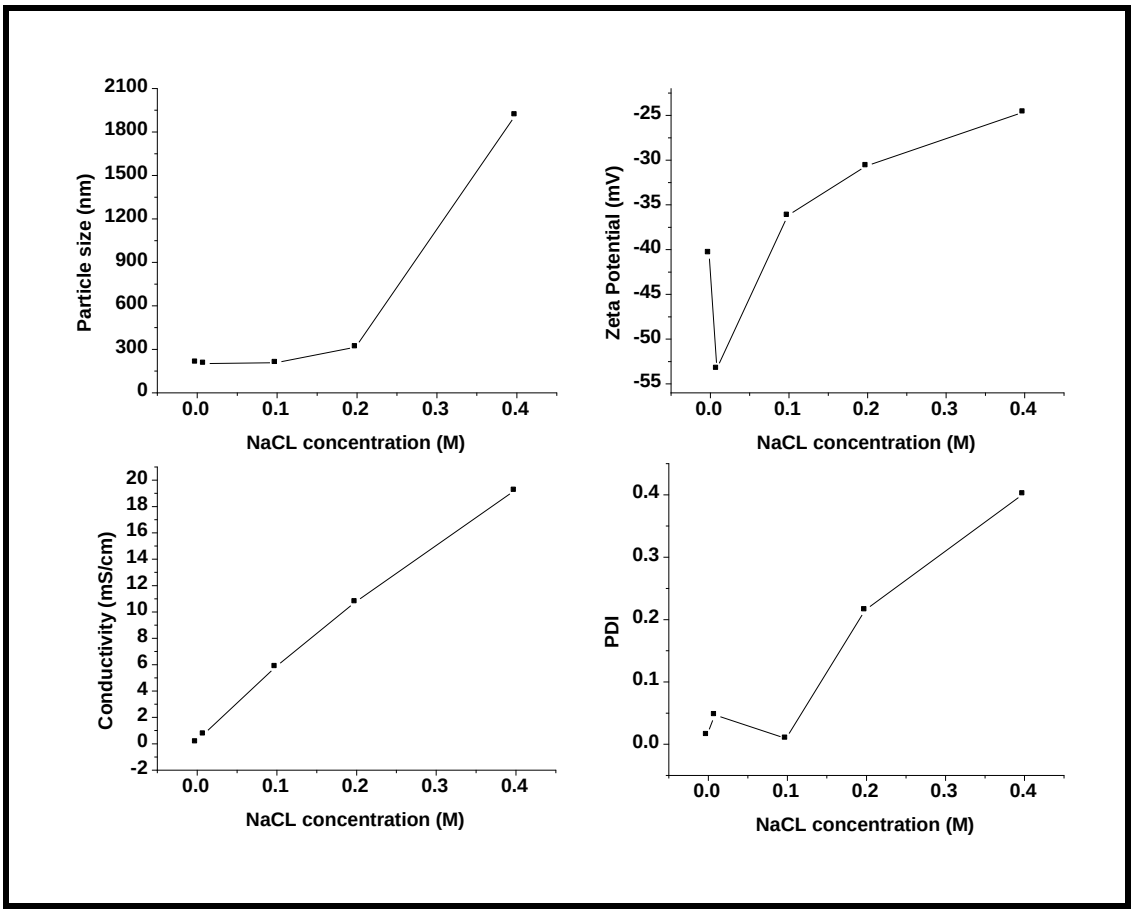

Fig.50. Particle size, PDI and zeta potential of the non-hairy Janus particles SW-300 as a function of NaCl aqueous solution concentration.

When the latex SW-300 was treated with 0.1M NaCl, the zeta potential just decreased to (-35 mV) which means the latex was still stable, owing to the smaller ratio of the hydrophobic domain; and even when it was treated with 0.2M NaCl there was a very slight increase in the particle size with a small decrease in the zeta potential to (-30 mV). This implies that in the previous cases the responsibility for the increase in the particle size and the decline in the zeta potential lies with the higher ratio of the hydrophobic domain, which lead to the individual Janus particles being attracted to each other via hydrophobic attractions to form different types of

clusters based on the number of individual building blocks (Janus particles) used to make them.

Conversely, quite similar behaviour to that of SW-300 was also observed with normal anionic spherical latex (PS24), as higher NaCl concentration is required to minimize the electrostatic repulsion among the particles, whereby 0.4M of NaCl is used to decrease the zeta potential of the latex particles to around (-25 mV), as shown in figure 5. This also proves that the hydrophobic domain plays a major role in the destabilization and formation of clusters.

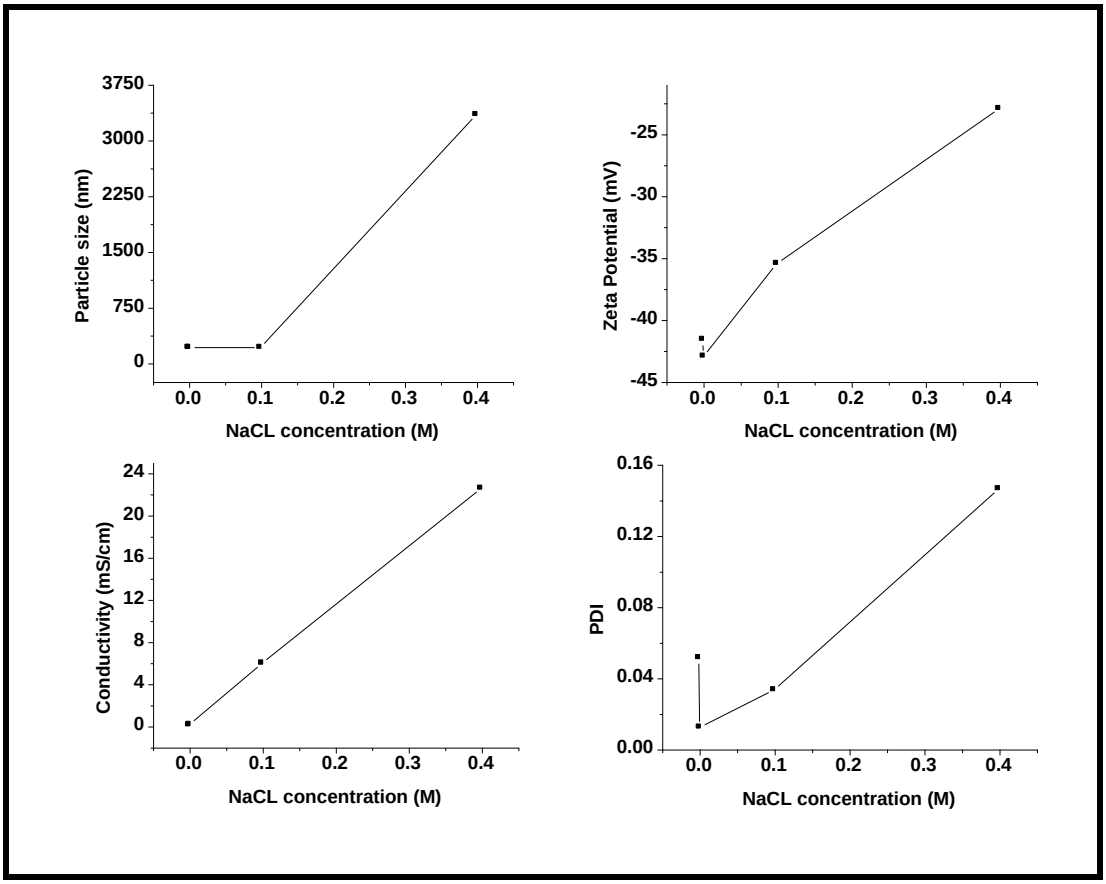

Fig.51. Particle size, PDI and zeta potential of normal spherical particles PS24 as a function of NaCl aqueous solution concentration.

In the case of hairy Janus particles, it was observed that, owing to the low solid concentration of these Janus latexes and the presence of the brushes, which work as another source for colloidal stability via steric stabilization alongside the existing

electrostatic repulsion stabilization, these Janus particles required a very high concentration of NaCl, usually above 1.5M. This higher concentration of electrolyte in this case has to fulfil two functions simultaneously: firstly to minimize the charges (negative or positive) in the surface of the Janus particles, and secondly to shrink the brushes, as in the case of poly(electrolyte) brushes. The high salt concentration in the sample restricted the visualization of the assembly of hairy Janus particles by Cryo-TEM.

7.4.5. Conclusion

The directed self-assembly of non-hairy and hairy dumbbell latex Janus particles was investigated. Self-assembly was induced by changing the ionic strength of the latex aqueous medium by the addition of an electrolyte. Decreasing the electrostatic or steric repulsion among the Janus particles lead them to be close to each other and then the Van der Waals attractive forces will predominate and cause the particles to group together to form clusters, wherein the core of the cluster is made up of the hydrophobic domains and the shell is made up of the hydrophilic domains, which function to stabilize the cluster via the remaining electrostatic and steric repulsion forces present in the Janus particles. In the case of non-hairy dumbbell latex Janus particles, the required electrolyte concentration to decrease the zeta potential of the latex to be below -25 mV is 0.1M, with a slight increase in the particle size. Above this concentration a massive increase in the particle size was observed, which indicated that a typical coagulation of the latex particles was occurring. However, the spherical and snowman non hairy latex Janus particles require a higher concentration of electrolyte, above 0.2M, to decrease the zeta potential to below -25 mV, with a slight increase in the particle size and this indicates that the bigger hydrophilic domain is the more stable latex, and also highlights that in the case of the dumbbell

non-hairy Janus particles the factor responsible for the destabilization of the latex and self-assembly is the bigger hydrophobic domain in those particles. The Cryo-TEM images of the dumbbell non-hairy Janus particles suggest that more than 70% of the interactions among the particles are head to head (hydrophobic–hydrophobic domain interactions) and the remaining interactions are either head to tail or tail to tail. This indicates that the particles assemble in various sizes clusters by their hydrophobic heads to minimize their contact with water and the clusters are stabilized by the remaining electrostatic repulsion among the hydrophilic domains. In case of hairy Janus particles, it was observed that due to the low solid concentration of these Janus latexes and the presence of the brushes which function as another source for the colloidal stability via steric stabilization alongside the existent electrostatic repulsion stabilization, these Janus particles require a very high concentration of NaCl concentration, usually above 1.5M, which is 15 times higher than the salt concentration that is used in case of non-hairy Janus particles and that restricts the visualization of the assembly by Cryo-TEM due to the high salt concentration in the sample.

7.5. References

1- Ma, P.-C.; Siddiqui, N. A.; Marom, G.; Kim, J.-K. *Composites, Part A.* **2010**,*41A*, 1345-1367.

2- Salvetat-Delmotte, J.-P.; Rubio, A. *Carbon.* **2002**, *40*, 1729-1734.

3- Yang, D. J.; Wang, S. G.; Zhang, Q.; Sellin, P. J.; Chen, G. *Physics Letters A.* **2004**, *329*, 207-213.

4- Kyrylyuk, A. V.; Hermant, M. C.; Schilling, T.; Klumperman, B.; Koning, C. E.; van der Schoot, P. *Nat Nano.* **2011**, *6*, 364-369.

5- Peng, M.; Li, D.; Chen, Y.; Zheng, Q. *Macromol. Rapid Commun.* **2006**, *27*, 859-864.

6- Grossiord, N.; Loos, J.; Regev, O.; Koning, C. E. *Chem. Mater*. **2006**, *18*, 1089-1099.

7- Wu, T.-M.; Chen, E.-C. *Compos. Sci. Technol.* **2008**, *68*, 2254-2259.

8- Park, E. J.; Hong, S.; Park, D. W.; Shim, S. E. *Colloid Polym. Sci.* **2010**,*288*, 47-53.

9- Antonietti, M.; Shen, Y.; Nakanishi, T.; Manuelian, M.; Campbell, R.; Gwee, L.; Elabd, Y. A.; Tambe, N.; Crombez, R.; Texter, J. *ACS Appl. Mater. Interfaces*. **2010**, *2*, 649-653.

10- Stankovich, S.; Piner, R. D.; Chen, X.; Wu, N.; Nguyen, S. T.; Ruoff, R. S. *J. Mater. Chem.* **2006**, *16*, 155-158.

11- Moore, V. C.; Strano, M. S.; Haroz, E. H.; Hauge, R. H.; Smalley, R. E.; Schmidt, J.; Talmon, Y. *Nano Letters*. **2003**, *3*, 1379-1382.

12- Bonaccorso, F. *International Journal of Photoenergy*. **2010**.

13- Tkalya, E.; Ghislandi, M.; Alekseev, A.; Koning, C.; Loos, J. *J. Mater. Chem.***2010**, *20*, 3035-3039.

14- Patole, A. S.; Patole, S. P.; Yoo, J.-B.; Ahn, J.-H.; Kim, T.-H. *J. Polym. Sci., Part B: Polym. Phys.* **2009**, *47*, 1523-1529.

15- Woo,D.; Kim,B.; Lee,S. *J.Korea-Australia Rheology*.**2009**,*21*,185-191.

16- Zhu, J.; Yudasaka, M.; Zhang, M.; Iijima, S. *J. Phys. Chem. B.* **2004**, *108*, 11317-11320.

17- Pickering, S. U. *J. Chem. Soc. Trans.* **1907**, *91*, 2001-2021.

18- Ramsden, W. *Proc. Royal Soc.* **1903**, *72*, 156-64

19- Hiemenze, P.C. *Principles of colloid and surface chemistry.* **1986**, *2nd ed.*

20- Bon, S. A. F.; Colver, P. J. *Langmuir* .**2007**, *23*, 8316-8322.

21- Vignati, E.; Piazza, R.; Lockhart, T. P. *Langmuir* .**2003**, *19*, 6650-6656.

22- Midmore, B. R. *Colloids Surf, A.* **1998**, *132*, 257-265.

23- Binks, B. P.; Lumsdon, S. O. *Langmuir* .**2000**, *16*, 2539-2547.

24- Dinsmore, A. D.; Hsu Ming, F.; Nikolaides, M. G.; Marquez, M.; Bausch, A. R.; Weitz, D. A. *Science* .**2002**, *298*, 1006-1009.

25- Walther, A.; Hoffmann, M.; Mueller, A. H. E. *Angew. Chem., Int. Ed.* **2008**, *47*, 711-714.

26- Wolters, D.; Meyer-Zaika, W.; Bandermann, F. *Macromol. Mater. Eng.* **2001**, *286*, 94-106.

27- Hong, L.; Cacciuto, A.; Luijten, E.; Granick, S. *Langmuir* .**2008**, *24*, 621-625.

28- Isojima, T.; Lattuada, M.; Vander Sande, J. B.; Hatton, T. A. *ACS Nano* .**2008**, *2*, 1799-1806.

29- Lattuada, M.; Hatton, T. A. *J. Am. Chem. Soc.* **2007**, *129*, 12878-12889.

30- Chen, Q.; Whitmer, J. K.; Jiang, S.; Bae, S. C.; Luijten, E.; Granick, S. *Science*.**2011**, 331, 199-202.

31- Chen, Q.; Bae, S. C.; Granick, S.*Nature*.**2011**, *469*, 381-384.

32- Whitelam, S.; Bon, S. A. F. *J. Chem. Phys.***2010**, *132*, 074901/1-074901/8

Chapter 8: Final Conclusion, Future work and summary of whole achievement

We can now return to scheme 1.4.1 which was presented in Chapter 1 as shown below.

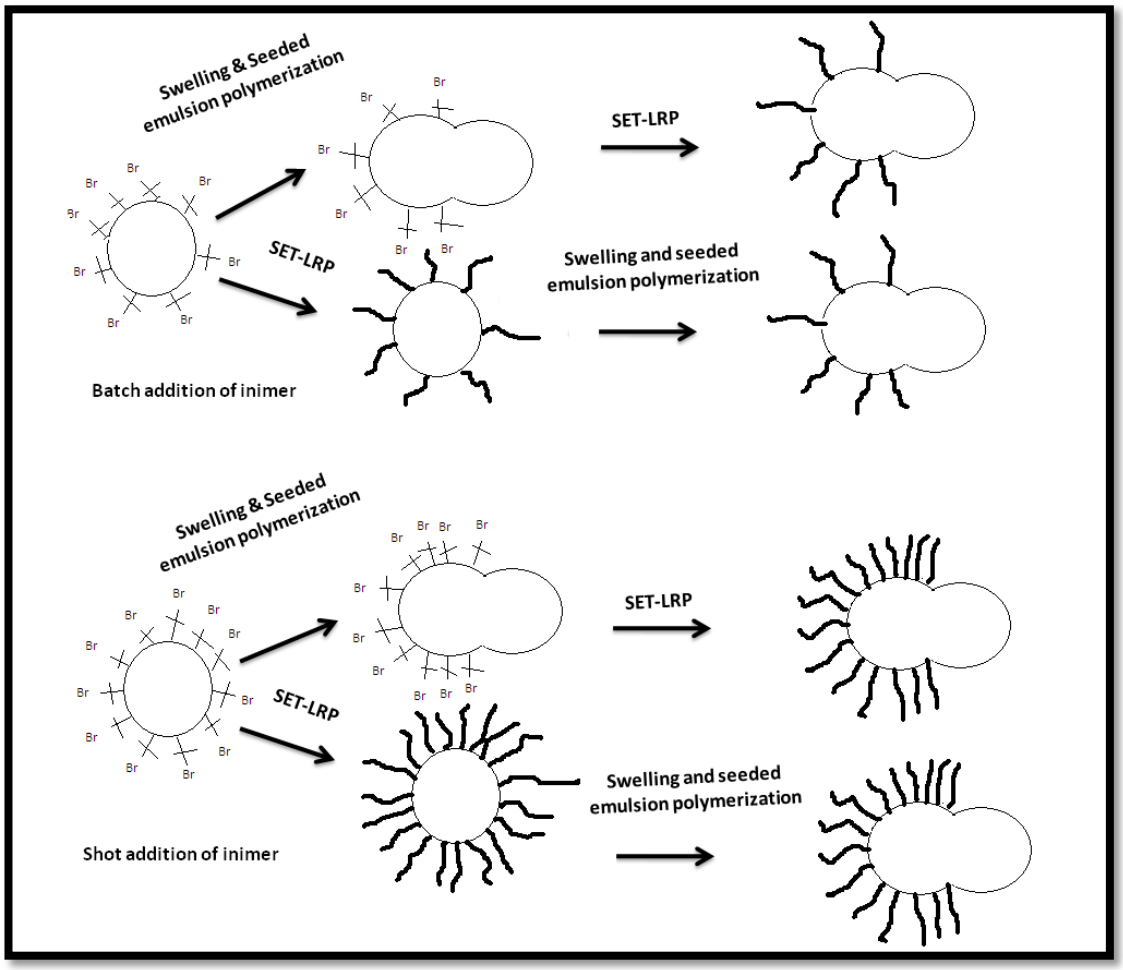

Scheme.1.4.1. Proposed method to fabricate hairy dumbbell shape Janus Particles by utilisation of both seeded emulsion polymerisation and SET-LRP.

We find that the effective synthetic pathway to make Janus hairy dumbbell particles is reproducible; we start the synthesis with precursor poly(styrene) latex particles made by the shot addition method and lightly cross-linked with 1.9 to 3.0 wt % DVB. The direct entropic phase separation from these latex particles leads to the formation of only one new domain with dumbbell shape morphology. The swelling

ratio used is between 2.0 and 4.0, and low DVB concentration in the swelling step (between 0.15-1.0 wt %) with AIBN as initiator. The formation of hydrophilic polymer brushes by SET-LRP resulted in the synthesis of hairy Janus particles with sup-micrometer diameter. The reasons behind the utilisation of the aforementioned conditions is attributed to the shot addition method making the surface of precursor particles more hydrophilic, which makes the surface hydrophilicity of the precursor particles greater; this makes the new domain stand independent from the original seed domain, which is not the case for the batch addition method where the separated domain wets the original seed domain by covering the *tert*-bromine functional group.

The hydrophilic polymer brushes are hard to visualise by the batch addition method as low *tert*-bromine functional groups concentration on the surface of latex particles. The formed brushes have another conformation, instead of stretched brushes toward the water phase as in case of shot addition, as a result of the high density of the formed brushes leading to repulsion among brushes.

Besides the shot addition method, the low crosslinked density in the original seed particles plays a crucial role in inducing only one domain. This increases the absorption of the monomer inside the latex particles and reduces the force of squeezing of the swollen monomer allowing induction of only one domain. The new domain size can be controlled by varying the concentration of DVB in the swelling step and the swelling ratio between the monomer and latex particles; a higher DVB concentration and low swelling ratio lead to snow-man particle morphology, and lower DVB concentration and high swelling ratio lead to dumbbell particle morphology.

The entropic phase separation from hairy latex made by both the batch and shot addition method with various crosslinked densities leads usually to the formation of raspberry and popcorn morphologies and with some limited isolated cases they are able to form snowman or dumbbell hairy Janus particles which are non-reproducible.

During the chemical modification of the precursor and the dumbbell particles by hydrophilic polymer brushes via SET-LRP, it was found that SET-LRP is an efficient way to grow polymer brushes from the surface of both particles made by either the shot or batch addition method. In particular Poly(sodium styrene sulfonate) brushes grown from the surface of the latex particles (precursor or dumbbell) made by the shot addition method, analysed in the aqueous phase by Cryo-TEM, can be visualised as extending arms from the surface of the latex particles. The length of the polymer brushes can be controlled by the addition of a water soluble ATRP initiator to produce shorter polymer brushes.

The rate of SET-LRP was ultrafast and can be reduced by the addition of more deactivator $CuBr_2$. The polymer formed after SET-LRP is not an ideal controlled radical polymerisation as it is performed in water. This leads to a broader molecular weight distribution. Although the control is poor, SET-LRP has significant commercial feasibility as polymer brushes can be formed from latex particles by utilising Cu(0) wire as a catalyst alone, which can be easily isolated from the polymerisation vessel and utilised again in many polymerisations.

With regard to the applications of synthesised particles, this was studied in three different systems as follows: Aqueous stabilizer for MWCNTs, Pickering stabilizer, and their self-assembly upon the addition of electrolyte.

Hairy core-shell particles with poly(sodium styrene sulfonate) brushes are a good stabilizer for MWCNTs in aqueous dispersion leading to longer stability (1 year); the Cryo-TEM images suggest that the strong interaction between the poly(sodium styrene sulfonate) brushes and the MWCNTs is the possible reason for the stabilisation.

It was observed that non-ionic particles, whatever their morphology (hairy spherical-core-shell, hairy patchy, hairy Janus), tend to form stable Pickering emulsions. It is proposed that there are two main factors in forming stable Pickering emulsions: the presence of non-ionic polymer brushes on the surface of the latex particles, e.g. poly(*N*,*N*-dimethyl acrylamide) and poly(PEGMEA), and the amphiphilic nature of hairy Janus particles.

The interaction among the non-hairy dumbbell Janus particles in water upon the addition of the electrolyte was investigated (self-assembly). The Cryo-TEM images of the dumbbell non-hairy Janus particles suggest that more than 70% of the interactions among the particles are head to head (hydrophobic–hydrophobic domain interactions) and the remaining interactions are either head to tail or tail to tail, which means the electrostatic repulsion reduces upon addition of an electrolyte; the particles tend to minimise the water contact via short range Van der Waal hydrophobic attractions.

Future work:

It is recommended to cover these areas:

1- Study the possibility of scaling up the synthesis of the dumbbell-shape latex particles instead of using the 30 mL glass vial and the rotating oven to large reactor which will enhance productivity.

2- Addition of the (inimer) after complete monomer conversion of the soap-free emulsion polymerisation with only a small amount of styrene and DVB. This will have two effects: (i) prevent the secondary nucleation; (ii) increase the hydrophilicity of the surface of the latex particles, which will enhance the phase separation toward one new domain only, as well as enhancing the visibility of the grown polymer brushes.

3- Study the usage of the new ATRP inimer to validate the results and their effect in both SET-LRP and phase separation after swelling and seeded emulsion polymerisation.

4- Study the effect of the usage of the new (surfmer) instead of sodium styrene sulfonate, in both the particle size of the precursor latex particles and the phase separation after swelling and seeded emulsion polymerisation.

5- Study the effect of the usage of the new oil soluble initiator during swelling and seeded emulsion polymerisation as this will have an effect on the kinetic of the phase separation.

6- Optimise the required time to induce the new hydrophobic domain via phase separation, instead of the 48 hour process.

7- Employ new methods to characterise the polymer brush on the surface of the latex particles, such as DSC (Differential Scanning Calorimeter), elemental analysis and liquid phase AFM.

8- Vary the length of the polymer brushes by changing the concentration of the sacrificial initiator.

9- Study the adsorption of the label on the hairy side of the Janus particles, such as small inorganic nanoparticles (below 50 nm).

10- Study the effect of adding ordinary surfactants in the swelling and seeded emulsion polymerisation step, and also study their effect on the visualisation of the polymer brushes.

11- Study the change in the conformation of the polymer brushes by cryo-TEM upon the usage of a stimulus such as the addition of the electrolyte.

12- Study the swelling and seeded emulsion polymerisation of the hairy Janus dumbbell shaped particles; this may result in novel new latex particle morphology.

13- Study the swelling and seeded emulsion polymerisation of the dumbbell particles; this may result in control triplet and quarter hairy Janus particles.

14- More studies have to be conducted, to use the hairy latex particles with poly(sodium styrene sulfonate) brushes to stabilise the SWCNTs (single walled carbone nanotubes) in water, as this was an excellent stabiliser in the case of stabilisation of MWCNTs (multi walled carbone nanotubes).

15- Measure the conductivity and mechanical properties of the nanocomposite (latex+ CNTs filler) film, and compare it with the film that does not contain the CNTs filler.

16- Conduct more studies on the visualisation and how the non-ionic hairy Janus particles self-assemble at the interface between two immiscible liquids, such as the usage of the Cryo-SEM for this purpose.

Summary of whole achievement:

1- The targeted hairy-Janus particles with dumbbell shape were synthesised successfully by three steps: (i) formation of monodispersed precursor latex

particles that contain ATRP initiator moieties via soap free emulsion polymerisation; (ii) swelling of the precursor latex particles by monomer mixture and oil soluble initator for 24 h inside tumbling oven which tumbles the sample at a speed of 30 rpm at room temperature, and then heating the sample to start the polymerisation and induce the phase separation; (iii) selective surface initiated polymerisation of water soluble monomer by SET-LRP to grow hydrophilic polymer brushes from one domain of the dumbbell particles.

2- Shot addition of the inimer during the soap-free emulsion polymerisation offers dense polymer brushes and promotes the phase separation.

3- Cryo-TEM is able to characterise and visualise the formed polymer brushes, in particular poly(sodium styrene sulfonate).

4- The length of the polymer brushes can be controlled by addition of the sacrificial ATRP initiator.

5- Polymer brushes can be formed from latex particles by utilising Cu(0) wire as a catalyst alone by SET-LRP, which can be easily isolated from the polymerisation vessel and utilised again in many polymerisations. This makes the process commercially feasible.

6- Cross-link density in the precursor latex particles, DVB concentration in the swelling step, and the swelling ratio between the latex particles and monomer, play a significant role in obtaining the required dumbbell shape latex particles.

7- Hairy latex particles with poly(sodium styrene sulfonate) are able to form stable MWCNTs dispersion in water. This arises as a result of the strong

interaction between the MWCNTs and poly(sodium styrene sulfonate) brushes.

8- (Hairy-core-shell, hairy-patchy, hairy-Janus) particles with non-ionic hydrophilic polymer brushes tend to form stable Pickering emulsions.

9- The interactions among the non-hairy dumbbell Janus particles show that more than 70% of the interactions among the particles are head to head (hydrophobic–hydrophobic domain interactions) and the remaining interactions are either head to tail or tail to tail.